A DFT Guided/Experimental Approach to Asymmetric Allylation and Phase-Transfer Catalysis

Roya Mirabdolbaghi, M.Sc.

Department of Chemistry

A dissertation submitted in partial fulfilment of the

requirements for the degree of

Doctor of Philosophy

Faculty of Mathematics and Science, Brock University

St. Catharines, Ontario

Abstract

The Dudding group is interested in the application of Density Functional Theory (DFT) in developing asymmetric methodologies, and thus the focus of this dissertation will be on the integration of these approaches. Several interrelated subsets of computer aided design and implementation in catalysis have been addressed during the course of these studies. The first of the aims rested upon the advancement of methodologies for the synthesis of biological active $C_{(1)}$-chiral 3-methylene-indan-1-ols, which in practice lead to the use of a sequential asymmetric Yamamoto-Sakurai-Hosomi allylation/Mizoroki Heck reaction sequence. An important aspect of this work was the utilization of *ortho*-substituted arylaldehyde reagents which are known to be a problematic class of substrates for existing asymmetric allylation approaches. The second phase of my research program lead to the further development of asymmetric allylation methods using *o*-arylaldehyde substrates for synthesis of chiral $C_{(3)}$-substituted phthalides. Apart from the *de novo* design of these chemistries *in silico*, which notably utilized water-tolerant, inexpensive, and relatively environmental benign indium metal, this work represented the first computational study of a stereoselective indium-mediated process. Following from these discoveries was the advent of a related, yet catalytic, Ag(I)-catalyzed approach for preparing $C_{(3)}$-substituted phthalides that from a practical standpoint was complementary in many ways. Not only did this new methodology build upon my earlier work with the integrated (experimental/computational) use of the Ag(I)-catalyzed asymmetric methods in synthesis, it provided fundamental insight arrived at through DFT calculations, regarding the Yamamoto-Sakurai-Hosomi allylation. The development of ligands for unprecedented asymmetric Lewis base catalysis, especially asymmetric allylations using

silver and indium metals, followed as a natural extension from these earlier discoveries. To this end, forthcoming as well was the advancement of a family of disubstituted (*N*-cyclopropenium guanidine/*N*-imidazoliumyl substituted cyclopropenylimine) nitrogen adducts that has provided fundamental insight into chemical bonding and offered an unprecedented class of phase transfer catalysts (PTC) having far-reaching potential. Salient features of these disubstituted nitrogen species is unprecedented finding of a cyclopropenium based C-H•••π_{aryl} interaction, as well, the presence of a highly dissociated anion projected them to serve as a catalyst promoting fluorination reactions. Attracted by the timely development of these disubstituted nitrogen adducts my last studies as a PhD scholar has addressed the utility of one of the synthesized disubstituted nitrogen adducts as a valuable catalyst for benzylation of the Schiff base *N*-diphenyl methylene glycine ethyl ester. Additionally, the catalyst was applied for benzylic fluorination, emerging from this exploration was successful fluorination of benzyl bromide and its derivatives in high yields. A notable feature of this protocol is column-free purification of the product and recovery of the catalyst to use in a further reaction sequence.

Acknowledgements

First and foremost, I would like to express my special appreciation and thanks to my supervisor, Professor Travis Dudding, for affording me the opportunity to work in a young research group as his first doctoral student. He patiently provided the invaluable encouragement, wise advice, and meticulous comments necessary for me to proceed through the doctoral program and complete my dissertation. Alongside of his strong and supportive advice he has always given me great freedom to pursue independent work.

Grateful thanks to my advisory committee, Professors Costa Metallinos, and Theocharis Stamatatos for their guidance and helpful suggestions. I owe my deepest gratitude to Professors Stuart Rothstein for his generous support and insightful comments as a former member of my advisory committee and candidacy examination. Professor Georgii Nikonov and Professor Tony Yan are graciously thanked for their participation in my candidacy examination.

I would like to thank Tim Jones and Razvan Simionescu for their help with collection and providing technical service of nuclear magnetic resonance, mass spectrometry, and infra red spectroscopy. Many thanks must be extended to Professor Costa Metallinos and Joshni John for the use and collection of HPLC data.

I would like to thank all of the past and present members of the Dudding group for creating a workplace of enjoyment and warmth; especially to Keivan Taban, a former member of Dudding group, who was always there to offer his best advice when I had any questions regarding computational chemistry. As well, I would like to thank my friends all around the world.

I gratefully acknowledge the Queen Elizabeth II and J. Stephen Hartman scholarship for financial support.

Words cannot express how grateful I am to my family, their love provided me inspiration and driving force, without their support finishing this journey was not possible.

Table of Contents

List of Schemes

List of Figures

List of Tables

Abbreviations

AIBN	azobisisobutyronitrile
AIM	atoms in molecules
AO	atomic orbital
aq	aqueous
B3LYP	Becke 3-parameter (exchange), Lee, Yang, Parr
BCP	bond critical point
BIMA	bis(*N*,*N*'-dialkylimidazolium)amides
BINAP	2,2'-bis(diphenylphosphino)-1,1'-binaphthyl
BINOL	1,1'-Bi-2-naphthol
Bn	benzyl
BP86	Becke and Perdew 86 correlation functional
Bu	butyl
C	concentration
CAB	chiral acyloxy borane
calcd	calculated
CDP	carbodiphosphorane
DBNE	*N*,*N*-dibutylnorephedrine
DFT	Density Functional Theory
$^{d}Ipc_2BCl$	(-)-*B*-chlorodiisopinocomphenylborane
DMAP	4-dimethylaminopyridine
DMF	dimethylformamide
DOS	diversity oriented synthesis
ee	enantiomeric excess
equiv.	equivalents
FMO	Frontier Molecule Orbital
HMO	Hückel Molecular Orbital
HMPA	hexamethylphosphoric triamide
HOMO	highest occupied molecular orbital
HPLC	high pressure liquid chromatography
IEFPCM	integral equation formalism polarizable continuum model
IR	infrared
KHMDS	potassium bis(trimethylsilyl)amide
LanL2DZ	Los Alamos national laboratory 2-double-z
LUMO	lowest unoccupied molecular orbital
m	meta
Me	methyl
MO	molecular orbital
n	normal
NAO	natural atomic orbitals
nbd	norbornadiene
NBS	*N*-bromosuccinimide
NHC	*N*-heterocyclic carbene
NICS	nucleus-independent chemical shift
NMR	Nuclear magnetic resonance

o	ortho
OTf	trifluoromethanesulfonate
p	para
PA	proton affinity
Pd_2dba_3	tris(dibenzylideneacetone)dipalladium
PET	positron-emission tomography
PHCP	P-heterocyclic carbodiphosphorane
PM-BOX	phosphinoylmethylbisoxazoline
Pr	propyl
PTC	phase transfer catalysis
p-Tol-BINAP	2,2′-bis(di-*p*-tolylphosphino)-1,1′-binaphthyl
py	pyridine
rt.	room temperature
s	secondary
SDD	Stuttgart/Dresden
STC	sequential tandem catalysis
t	tertiary
TBAF	tetra-*n*-butylammonium fluoride
TDA	tris(dimethylamino)cyclopropenylium
TFA	trifluoroacetic acid
THF	tetrahydrofuran
TMS	trimethylsilyl
TS	transition state
TZVP	triple zeta for valence electrons plus polarization function
v	volt

1. Introduction

1.1. Enantioselective Allylation of Aldehydes

1.1.1. Historical

The formation of carbon-carbon bonds is of crucial importance throughout organic synthesis. The reactions, in which a carbon-carbon bond is formed, are of great interest as they allow for the production of many chemicals, such as pharmaceuticals and plastics. Consequently a number of approaches to construct carbon-carbon bonds have been developed, including the aldol reaction, Diels-Alder reaction, Heck reaction, Michael reaction, and Wittig reaction to name a few.[1] One of the most commonly implemented strategies to form carbon-carbon bonds is allylation which involves the nucleophilic addition of an allylic reagent to a carbonyl derivative. Allylation reactions are especially advantageous in chemistry because, along with the formation of a new carbon-carbon bond, a new functionality (*i.e.*, alcohol) may also be introduced. Moreover, subsequent manipulations of the allylic moiety can lead to further synthetic alterations, ultimately allowing for a greater range of products to be produced.[2]

It is well known that enantioselective synthesis plays a key role in organic chemistry, especially in pharmaceuticals, fine chemical, and material science industries. As such, enantioselective synthesis is of great importance, allowing the synthesis of pure enantiomers from achiral substrates. This however is not always achieved without complications, making the process formidable and challenging. To accomplish the asymmetric version of an allylation reaction, employment of organometallic allyl reagents and chiral metal-ligand complexes are routinely used.[3] Notably, these processes can often times allow for high levels

of stereochemical induction, due to the creation of a chiral environment near the reaction center originating from the chiral ligand.

Catalysts used for enantioselective allylations can be subdivided into three general types; chiral Lewis acids, chiral Lewis bases, and chiral bifunctional (Lewis acid-Lewis base) catalysts. Although many enantioselective allylations catalyzed by chiral Lewis acids exist, the addition of allyltrimethylsilane or allyltributylstannane to an aldehyde stands out as the most common example.[2] In this reaction, the Lewis acid renders the aldehyde more electrophilic upon binding which in turn activates the carbonyl for nucleophilic attack. Accordingly, Lewis acid allylation using allyltrimethylsilane and allyltributylstannane will be discussed in detail throughout the following section.[2]

Allylation, catalyzed by chiral Lewis acids can lead to high enantioselectivities, however the related diasteromeric reactions such as crotylations are more limited in scope due to the flexibility of the transition state structures involved in these processes.[1] To address this problem, Lewis base catalyzed addition of allyltrichlorosilane to aldehydes has been developed. Fundamentally, Lewis base promoted additions of allyl reagents differ from those of Lewis acids catalyzed processes and as a result they have provided new catalytic methodologies.[2]

Accordingly, in response to the problems associated with regio- and stereoselective preparation of homoallylic alcohols under Lewis acid catalyzed conditions, Kobayashi *et al.* have applied Lewis base catalyzed approaches for the synthesis of homoallylic alcohols **3** *via* organosilicon intermediates. More specifically, target compound **3** was prepared from an array of aldehydes **2** and readily available allyltrichlorosilane (**1**). It was determined that DMF was the optimal solvent choice and that superior levels of regio- and stereoselection

obtained at 0 °C. A particular interesting feature of this work was that the solvent DMF served a dual role in that it also acted as a catalyst for this reaction, thus forgoing the need for the addition of an external catalyst source (Scheme 1).[4]

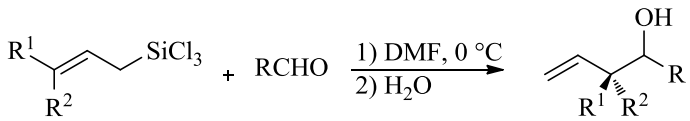

1 **2** **3**

1a	$R^1 = H$	$R^2 = H$	$R = PhC_2H_4$	yield = 90%	syn/anti = ---
1b	$R^1 = CH_3$	$R^2 = H$	R = Ph	88	3:97
1c	$R^1 = H$	$R^2 = CH_3$	R = Ph	89	99:1
1d	$R^1 = CH_3$	$R^2 = CH_3$	$R = C_6H_{11}$	89	---

Scheme 1. Reaction of allyltrichlorosilanes with aldehydes.

Among the many interesting aspects of this reaction was the finding that sterically hindered allyltrichlorosilane species, such as prenyltrichlorosilane, afforded the corresponding homoallylic alcohol products with high yield and most notably carbon-carbon bond formation occurred only at the γ-position of the allyltrichlorosilanes as opposed to α-position. Moreover, the reaction of either (*Z*)- or (*E*)-allyltrichlorosilanes with benzaldehde afforded the respective *syn*- and *anti*-homoallylic alcohols with high levels of diastereoselectivity (99:1 and 3:97) , respectively. As for the selection of DMF this choice was arrived at after screening the effect of several different solvents on the overall yield of the reaction. When DCM, acetonitrile, benzene, ether and THF were used, only trace amounts of products were obtained, whereas it was found that DMF was essential for quantitative yield formation, delivering 82-97% yield. One exception to this was the moderate yield obtained using hexamethylphosphoric triamide (HMPA). To further test the effect of solvent on this reaction, solvents providing low yields were mixed with DMF or HMPA as a co-solvent, resulting in moderate to high product formation. To rationalize this

transformation, Kobayashi *et al.* proposed the transient existence of a hypervalent silicate as a key intermediate leading to product formation (Scheme 2). This became evident based on the ^{29}Si NMR of (*Z*)-crotyltrichlorosilane. The ^{29}Si NMR signal for the reaction in DMF was observed at -170 ppm, however, in other solvents the peak occurred at approximately 6 ppm. This supports the notion that DMF facilitates the generation of a hypervalent organosilicate through coordination of the silicon atom allowing for smooth progression of the reaction. The later arising from the electron withdrawing chlorine groups, which increase the Lewis acidity of the Si atom, in turn facilitating the reaction *via* a Zimmerman-Traxler[5] transition state. Concomitantly, the hypervalent silicon atom donates electron density to the allyl π-systems (s-p conjugation), thus increasing the nucleophilicity of the allyl component. Consistent with this reasoning, six-membered cyclic transition states **5a** and **5b** have been proposed for the reaction of (*Z*)-crotyltrichlorosilane **4a** and (*E*)-crotyltrichlorosilane **4b**, respectively, with aldehydes to afford *syn*- and *anti*-products **6a** and **6b** (Scheme 2). Accordingly, these and related transition states models have served as valuable conceptual

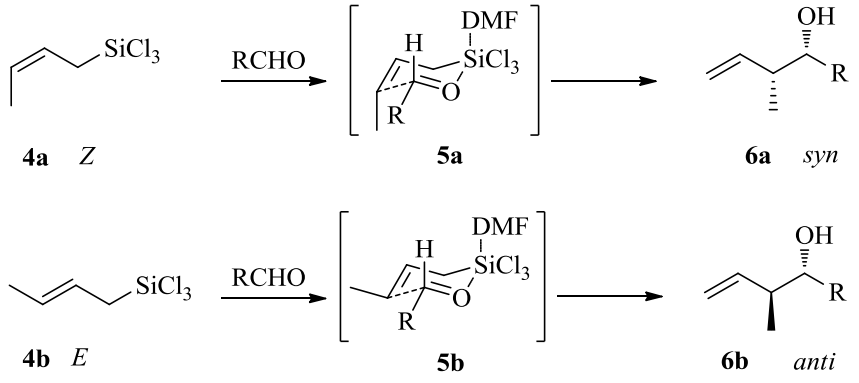

Scheme 2. Proposed six-membered cyclic transition states of hypervalent organosilicate.

templates for rationalizing the high diastereoselectivity of Lewis base catalyzed allylation reactions.[4] At the same time, Denmark and coworkers reported the first method for the asymmetric allylation of aldehydes with chiral Lewis bases.[6] More specifically, the asymmetric allylation of benzaldehyde (**8**) with allyltrichlorosilane (**7**) to afforded **9** in moderate ee = 56-63% was realized through optimization studies using different phosphoramides. Among the tested phosphoramides, the highest enantioselectivity were obtained using phosphramide **10a** and **10b** (Scheme 3). To extend this, the addition of (*Z*)- and (*E*)-crotyltrichlorosilane to benzaldehyde in presence of **10b** provided the syn- and *anti*-products, with 60 and 68% ee, respectively; the ratio of diastereoselectivity was 98:2.[6]

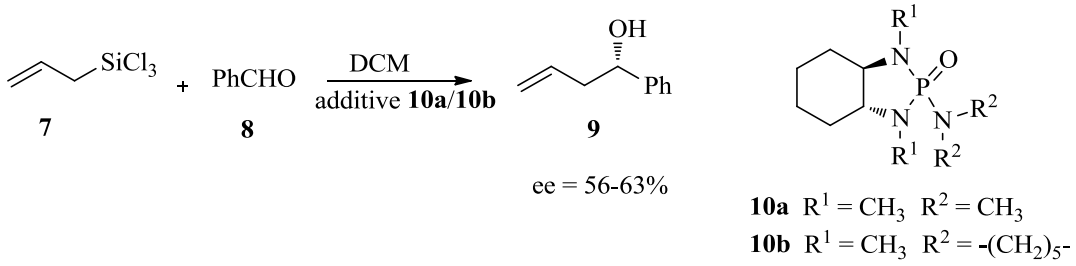

Scheme 3. Allylation of benzaldehyde using allyltrichlorosilane and additives.

Several years after Denmark's work, Rowlands *et al.*, building upon these concepts, reported the first example of a chiral sulfoxide Lewis base catalyzed allylation of a benzaldehyde with allyltrichlorosilane.[7] The reaction of benzaldehyde (**12)** and allyltrichlorosilane (**11)** in the presence of the sulfoxide catalysts **13a-c** were investigated (Scheme 4). The sulfoxide **13b** afforded homoallylic alcohol **14a** in good yield and moderate ee. However the *tert*-butylsulfoxide **13c**, due to the steric bulk, can not coordinate with the silane. In this case no product was obtained.

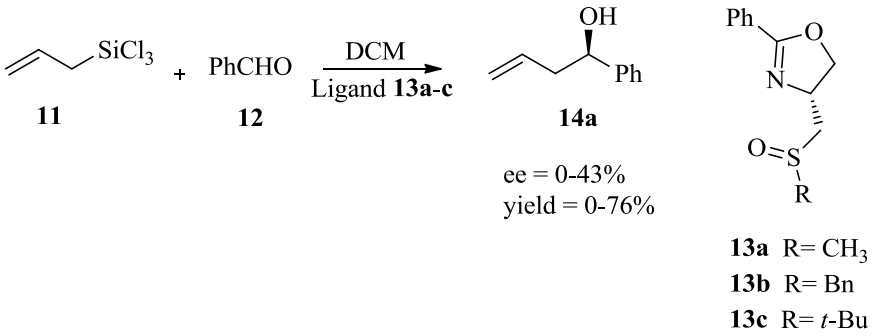

Scheme 4. Allylation of benzaldehyde using allyltrichlorosilane in presence of sulfoxides ligand.

In bifunctional Lewis acid-Lewis base-catalyzed allylation reactions, dual activation occurs. That is, the Lewis acid activates the carbonyl group, while the Lewis base activates the nucleophile. In this context, Yamamoto *et al.*[8] have used bifunctional bisoxazoline-metal complexes as catalysts for enantioselective allylations of aldehydes with allyltrichlorosilane. Emerging from this work was the finding that 10 mol% phosphinoylmethylbisoxazoline (PM-BOX) **15a** provided the best results in the reaction of benzaldehyde (**12**) with allyltrichlorosilane (**11**). Reactions carried out in THF afforded the corresponding homoallylic alcohol **14b** in 76% yield and 86% ee. To show the effects of phosphine oxide (acting as a Lewis base) on product yield and enantioselectivity, the reaction was catalyzed by benzhydrylmethylbisoxazoline-ZnI_2 complex **15b**, which afforded the product in only 4% yield and 13% *ee*. It was postulated that this was caused by the absence of phosphine oxide as a Lewis base. In addition, the interaction between the diphenylphosphinyl moiety and allyltrichlorosilane was supported by a shift in the ^{31}P NMR spectrum of the PM-BOX-ZnI_2 complex from 29.9 ppm to 44.5 ppm, in the presence of an equimolar mixture of the complex and allylsilane.[8]

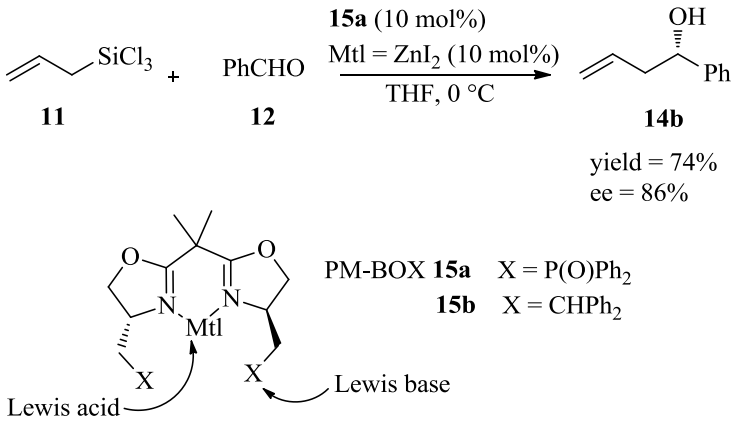

Scheme 5. Enantioselective allylation of aldehyde catalyzed by bifunctional Zn (II)-bisoxazoline complexes.

1.1.1.1. Lewis acid Catalyzed Addition of Allylic Silanes to Aldehydes

Allylsilanes are an interesting class of synthetic reagents, due to the presence of a nucleophilic double bond having latent reactivity which allows for allyl transfer to reactive electrophiles, such as carbonyl derivatives. In 1976, Sakurai and Hosomi, in a pioneering discovery, reported that the allylation of carbonyl compounds with allyltrimethylsilane was catalyzed by titanium tetrachloride.[9,10]

Building upon this work, two years later they found that tetra-*n*-butylammonium fluoride (TBAF) resulted in the cleavage of allyl-silicon bond of allylsilanes to produce an allylic anion species that added to carbonyl compounds to afford homoallylic alcohol products after hydrolysis of silyl ether intermediates.[11] Today, the Sakurai-Hosomi reaction is well-known, and is often used for transforming carbonyl compounds to homoallylic alcohols and by many is considered to be a complementary allylation approach to classic allyl Grignard reactions.

1.1.1.1.1. Mechanism

In general, allylsilanes such as **16** react with an electrophile to produce intermediate cation **17**, which is stabilized through overlap of the Si-C bonding orbital with the empty *p* orbital of the cation (Scheme 6). Although, allyl **18** forms by loss of the silyl group, there is not strong evidence to support the formation of a free intermediate cation.[12]

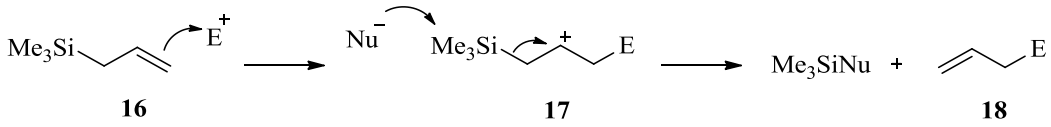

Scheme 6. Reaction of allylsilane with electrophile.

In the case of stereoselective allylations of aldehydes using chiral ligand based metal complexes the reaction outcome has been shown to depend on the orientation of the aldehyde with respect to the chiral complex. In this regard several studies have investigated the effect of Lewis acids on the rate and level of stereochemical induction of allylation reactions.[2]

In 1971, Corey proposed that in the complex $C_6H_5CHO{\bullet}BF_3$ (**19**) the B─F and formyl hydrogen prefer an eclipsed conformation, due to a weak interaction between the acidic formyl hydrogen and the electron rich co-planar fluorine (Figure 1). The weakness of this hydrogen bond is reasonable, given the distance of H---F is 2.35 Å which is less than the sum of the van der Waals radii of H (1.20 Å) and F (1.47 Å) is consistent with the interaction between H and F. [13]

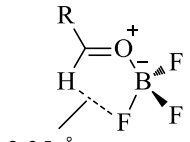

19

Figure 1. Proposed hydrogen bonding in the complex of $C_6H_5CHO \bullet BF_3$.

Supporting this interaction, Bottoni *et al.* investigated the mechanism of the Sakurai reaction, using acetaldehyde with allylsilane and BH_2F with DFT calculations. Revealed from these calculations was that synclinal addition of allyl moiety to the aldehyde *via* the eight-membered cyclic transition state assemblies **20a** and **20b** were the most energetically favorable modes of addition (8.03 and 7.12 kcal mol^{-1}, respectively), Figure 2.[14]

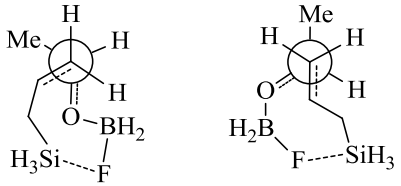

20a **20b**

Figure 2. Transition states of the Sakurai reaction of the acetaldehyde with allylsilane and BH_2F.

1.1.1.1.2. Hypervalent Silicon as a Reactive Site in Bond-Forming Processes

Organosilicon compounds find widespread use in a number of synthetic organic transformations, due to their intrinsic chemical reactivity which is closely tied to the ability of silicon to form five and six coordinate hypervalent species. Interestingly, associated with ability of silicon to form hypervalent complexes is the perhaps counter-intuitive, yet synthetic useful, aspect that silicon becomes progressively more electropositive with increasing valence, while the coordinated ligands become more electronegative. (Figure 3). Consequently, the Lewis acidity of the silicon increases, while the nucleophilicity of the

substituents increases in moving from tetra-, penta-, to hexavalency at silicon. Associated with this is an elongation of Si-L bonds, which formally places excessive negative charge on the L groups, thus increasing the capability of L group to transfer to an acceptor.[15] From a historical point it is noteworthy that the extraordinary chemical reactivity of hypervalent silicon was, and continues to be, a controversial subject among chemists and thus is of interest from a fundamental standpoint and correspondingly remains an active area of study.

Based on the Jensen-proposed criteria, all Lewis acid-base interactions could be classified according to the character of the interacting orbitals.[16] More specifically, as suggested the combination of three distinct types of acceptor orbitals with three different kinds of donor orbitals would produce nine categories of bonding interactions which in total would define all possible Lewis acid-base interactions (Table 1).

Table 1. Jensen's orbital analysis of molecular interactions.

Donor	Acceptor		
	n*	σ*	π*
n	n– n*	n– σ*	n– π*
σ	σ – n*	σ – σ*	σ– π*
π	π – n*	π – σ*	π – π*

However, in terms of catalysis only three interactions out of nine are significant; these include: 1) interactions between nonbonding electron pairs and antibonding orbitals with p character (n–π* interactions), 2) interactions between nonbonding electron pairs and antibonding orbitals with s character (n– σ* interactions), and 3) interactions between nonbonding electron pairs and vacant nonbonding orbitals (n–n* interactions).

Among these interactions, the largest and most known interaction in Lewis base catalysis is n– π* which often is incorrectly termed "nucleophilic catalysis". In these three types of interactions, the nonbonding electron pair of a Lewis base interacts with a π* orbital of an unsaturated functional group acceptor such as alkynes, alkenes, carbonyls, etc. As for the other two less-well known types of interactions, n– σ* and n–n*, they are equally important in catalysis. In general, n– σ* interactions are found in a large number of bonding modes, including organometallic reagents derived from main-group elements in a hypervalent bonding state. On the other hand, n–n* interactions involve a specific group of Lewis acid acceptors, such as borane or other Group 13 elements, which are capable of expanding their coordination sphere through "hypervalency". In this context, the reactivity of hypervalent species can be understood by Gutmann's empirical analysis[17], which asserts that when an acid-base adduct forms, overall electron density at the acceptor moiety decreases while that of the donor increases. However, the electron density on the atoms that constitute the acceptor fragments may not be equal distributed (Scheme 7).

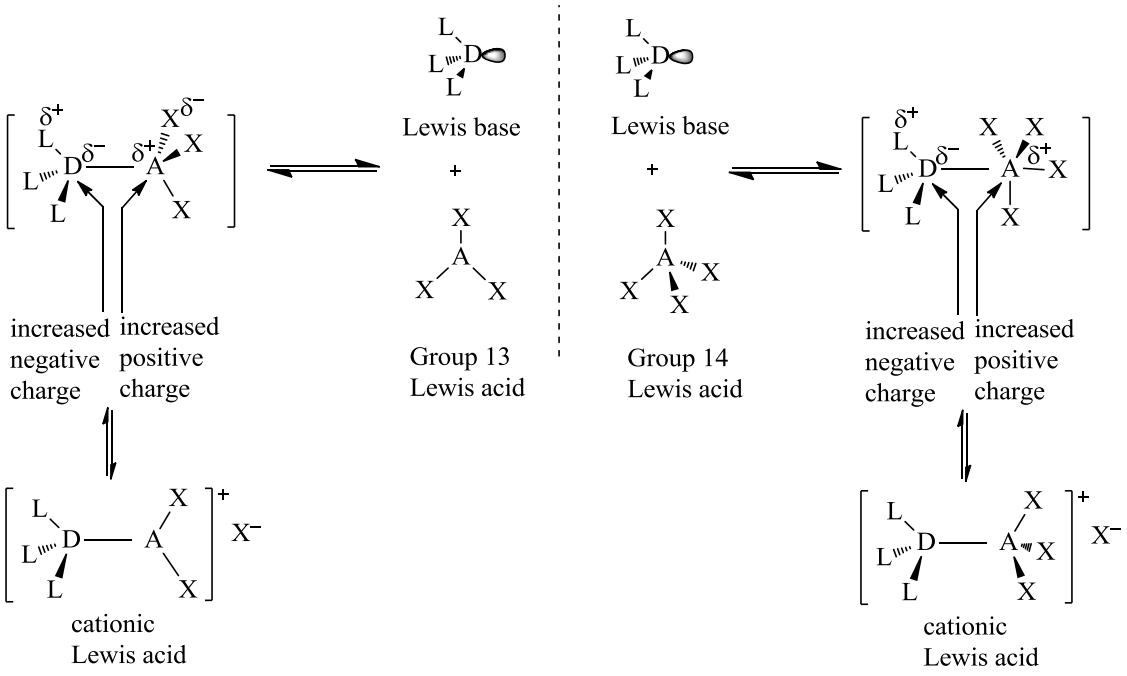

Scheme 7. Lewis acid-base complexation and resulting electronic redistribution.

Gutmann's bonding analysis comprises four rules of molecular adduct formation: "1) the smaller the intramolecular distance between the donor (D) and the acceptor (A), the greater the induced lengthening of the peripheral bonds (A–X), 2) the longer the bond between D and A, the greater the degree of polarization of electron density across that bond, 3) as the coordination number of an atom increases, so do the lengths of all the bonds originating from that coordination center, and 4) the bonds adjacent to D and A will either contract or elongate to compensate for the changes in electron density at D and A".[18] There is an upshot from Gutmann's fourth rule regarding charge density variations which states: "although a donor–acceptor interaction will result in a net acceptor species, it will, in the case of polyatomic species, actually lead to a net increase or "pileup" of electron density at the donor atom of the donor species and to a net decrease or "spillover" of electron density at the acceptor atom of the acceptor species. This results from the accompanying changes in the

intramolecular charge distribution induced by the primary donor–acceptor interaction. These disperse the net change in electron density among all the atoms and in so doing, overcompensate for the initial changes induced at the donor and acceptor atoms. This result is important as it contradicts the usual assumption of organic chemists that the net changes in formal charges remain localized on the donor and acceptor atoms."[18]

In this regard, extensive computational studies on donor-acceptor complexes have been executed in the Group 14 elements. For example, Mulliken charges at the silicon atom of the series SiF_4^-, SiF_5^-, and SiF_6^- are +1.19, +1.14, and +2.12 while for $SiCl_4^-$ $SiCl_5^-$ and $SiCl_6^-$ are +0.178, +0.279, and +0.539, respectively.[18] These results show the binding of a Lewis base (Cl^- and F^-) renders formally negative charged adducts. However, positive charge character increases on the acceptor silicon atom.

Similar to transition-metal complexes, formation of compounds in main-group elements which break the Langmuir-Lewis octet rule was originally explained by incorporation of d orbitals (such as 3d for silicon). As the hybridization of silicon changes from sp^3 (**A**, tetravalent) to sp^3d (**B**, pentavalent) to sp^3d^2 (**C**, hexavalent) there is a loss of s-character and with it a decrease in electron density at silicon (Figure 3). However, silicon is

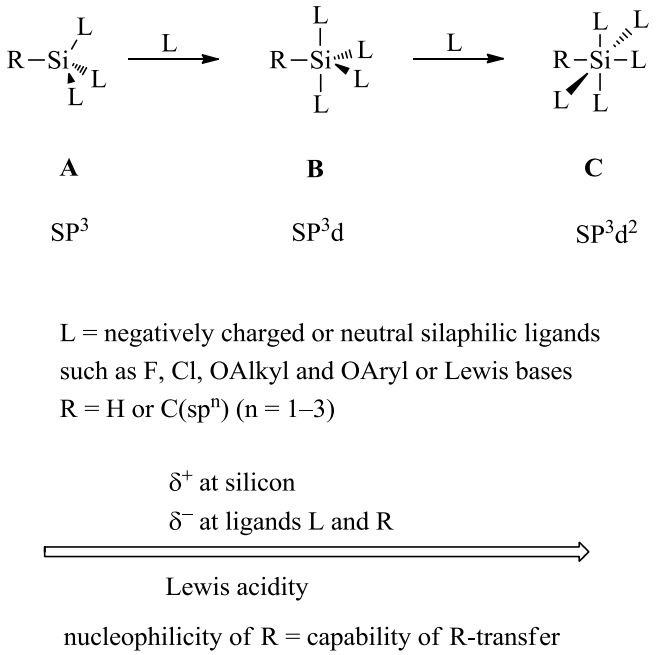

Figure 3. Valency and electron density at silicon in organosilicon compounds (charges at silicon have been omitted for the sake of clarity).

not a transition metal and the 3d orbitals on silicon are too diffuse to participate in bond formation. As such, the hypervalency of silicon was proposed to arise from formation of an electron-rich three-center four electron (3c-4e) bonding motif involving a silicon based 3p orbital.

Usually, consistent with the outer-shell octet rule, silicon with four other atoms forms SiL_4 compounds. In these compounds, central silicon atom has sp^3 hybridizaton and the molecules have a tetrahedral geometry (Figure 4). To expand to a pentacoordinate silicon complex (SiL_5), engagement of a p orbital in hypervalent three-center four-electron is necessary. To do so, central silicon atom employs sp^2 hybridization and the molecules have trigonal bipyramidal geometry. As well, formation of hexacoordinate complex (SiL_6) with octahedral geometry needs employment of a second p orbital. Given the fact that the proportion of "s-character" in hybrid orbitals increases while moving from sp^3, sp^2, and sp

hybridization, the energy of the hybrid orbitals are involved in covalent bond decrease[18] (Figure 4).

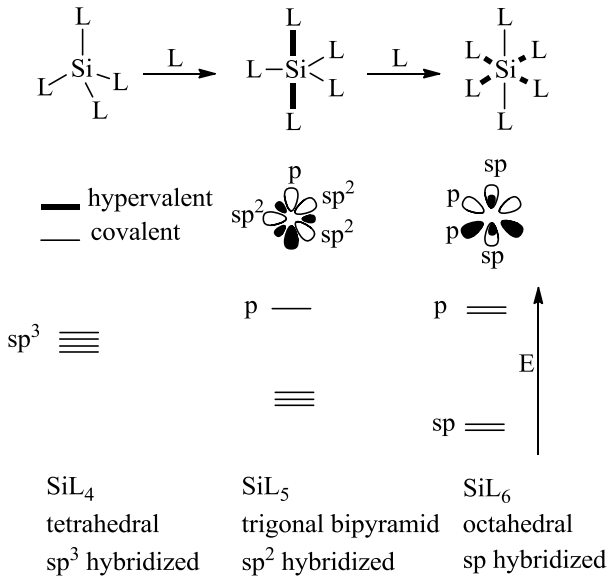

Figure 4. Silicon complexes hybridization and orbital picture.

As shown in figure 5, three molecular orbitals (MOs) are formed from a combination of three atomic orbitals (AOs). A pair of hybrid orbitals is created by mixing the filled σ orbital of the acceptor with the filled n orbital of the donor. There is a node at the central atom and the electron density localizes at the peripheral atoms in the HOMO of the hybrid orbital. As such, in the adduct, both electrophilic and nucleophilic character can be created at different atoms. While the strength of donor element increases, the polarization and the energy gap between the Ψ^1 and Ψ^2 orbital increases which as it is shown in Scheme 7 can lead to ionization and creation of a cationic species. Accordingly, Gutmann's four rules explain the changes in bond order and the polarization of electron density in the 3c-4e hybrids. Consistent with this interpretation, X-ray crystallographic methods show the bond lengths of the axial and equatorial fluorine atoms in SiF_5^- are 1.646 Å and 1.579 Å,

respectively, indicating a significant difference. Also, in SiF_5^- the formal bond order of the 3c-4e hybrid is 0.75.[18]

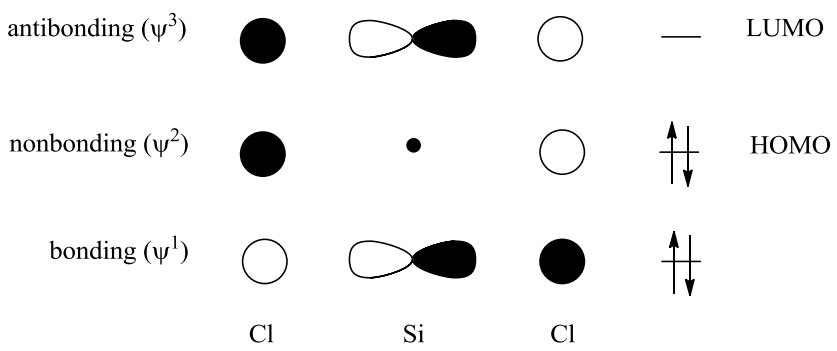

Figure 5. Molecular orbital diagram of three-center-four-electron hybrids.

In summary, the extracoordination or so-called hypervalency is thought to derive from the occurrence of donor-acceptor interactions n–σ* (Si-L) between the filled σ orbital of the acceptor with the filled n orbital of the donor. Accordingly, as the hybridization of silicon changes from sp^3 (tetravalent) to sp^2 (pentavalent) to sp (hexavalent) there is a loss of s-character and with it the energy of the hybrid orbitals that involve in covalent bond decrease.

1.1.1.2. Silver/BINAP-Catalyzed Allylation Reactions

Many examples of chiral Lewis acids have been reported for the chemo-, regio-, enantio- and diastereoselective allylation of carbonyl compounds, which have allowed for the synthesis of numerous chiral natural products, medicinal useful compounds, and value-added materials. Among these approaches the Sakurai-Hosomi allylation has maintained a steadfast place as a go-to reaction as it is robust in nature, operationally simple, and provides predictable patterns of stereochemical induction. In this regard, in 1991, Yamamoto *et al.*[19] reported the first example of catalytic asymmetric allylation of aldehydes with allylsilanes

using a chiral acyloxy borane complex (CAB) as a catalyst to furnish homoallylic alcohols in moderate to high enantiomeric excess (55-90%). Moreover, catalytic asymmetric reaction methodologies mediated by chiral Ag(I)-complexes, have provided chemists with a rich portfolio of C–C bond-forming strategies over the last two-decades. More specifically, the Ag(I)-catalyzed asymmetric Sakurai-Hosomi allylation methodologies of Yamamoto *et al.* have found considerable use in key synthetic steps leading to chiral homoallylic alcohols. For instance, they reported the first example of a (*R*)-*p*-Tol-BINAP•AgF (*p*-tol-BINAP = 2,2'-bis(di-*p*-tolylphosphino)-1,1'-binaphthyl) catalyzed asymmetric addition of allyl trimethoxysilanes (**19**) to aldehydes **12**, to produce homoallylic alcohols **14b**. This transformation was made possible by activation of the trimethoxysilanes by the fluoride ion of the catalyst. Optimal conditions were obtained using allyltrimethoxysilane (1.5 eq.) in the presence of the chiral Ag^{I}-based catalyst prepared from (*R*)-*p*-Tol-BINAP (6 mol%) and AgF (10 mol%), by keeping the reaction temperature at -20 °C and use of MeOH as solvent (Scheme 8).[20]

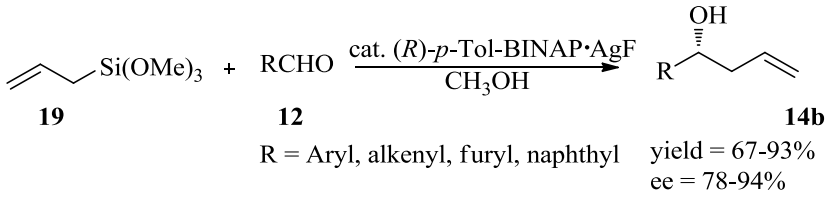

Scheme 8. Allylation of aldehyde with allyltrimethoxysilanes catalyzed by(*R*)-*p*-Tol-BINAP•AgF.

Further, Yamamoto *et al.* reported the allylation of benzaldehyde (**12)** with *E*-enriched crotyltrimethoxysilane (*E*/*Z* = 83/17) (**20**) in presence of (*R*)-BINAP•AgF in MeOH at -20 to -25 °C.[20] These conditions allowed for the exclusive formation of γ products **21a** and **21b**, with an *anti*/*syn* ratio of 92/8. The use of (*Z*)-crotyltrimethoxysilane (*E*/*Z*<1/99) or

a 1/1 mixture of (*E*)-and (*Z*)-crotyltrimethoxysilane afforded similar results, highlighting the high *anti* selectivity of this reaction, irrespective of the configuration of the crotylsilane (Scheme 9).

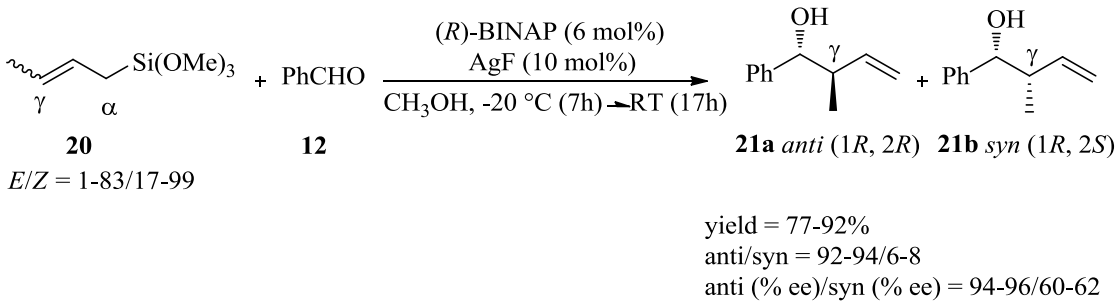

Scheme 9. Allylation of (*E*)-and (*Z*)- crotyltrimethoxysilane with benzaldehyde catalyzed by (*R*)-BINAP•AgF.

From NMR spectroscopic data, Yamamoto *et al.* proposed the existence of a six-membered cyclic transition state, **22a** or **22b**, in which BINAP was coordinated to silver to account for the observed stereoselectivity of the products (Figure 6). The ^{13}C NMR spectra of the reaction of crotyltimethoxysilane with a 1/1 mixture of (*R*)-BINAP•AgF and DMF in CH_3OD at room temperature provided additional support for this mechanistic hypothesis based on the observed appearance of $(CH_3O)_3SiF$ as it was reasoned that transmetalation occurred during the catalytic cycle resulting in the formation of a transient crotylsilver species. Accordingly, to account for stereoselective formation of the major *anti*-homoallylic alcohol products via proposed transition state **22a**, regardless whether the (*Z*)- or (*E*)-crotyl reagents were employed, it was suggested that under the reaction conditions the *in situ* derived (*Z*)-crotylsilver species isomerized to the corresponding (*E*)- isomer.[20]

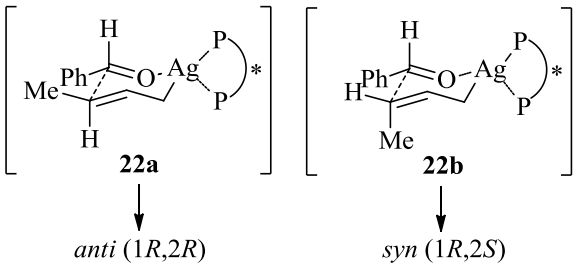

Figure 6. Proposed cyclic transition-state structures **22a** and **22b**.

The Ag^{I}-catalyzed asymmetric Sakurai-Hosomi allylation methodologies of Yamamoto *et al.* have also found considerable use by other groups as key synthetic routes to chiral homoallylic alcohols.[20] For instance, Rodríguez-García *et al*. employed Yamamoto's (*R*)-*p*-tol-BINAP•Ag^{I}OTf catalyzed allylation approach as a pivotal disconnection in the reported synthesis of the antifungal agents (–)-*trans*-pterocarpin (**23**) and the corresponding epimer (–)-*cis*-pterocarpin.[21] Similarly, Kanai, Shibasaki, and co-workers in a route to the natural antibiotic fostriecin (**24a**) and 8-*epi*-fostriecin (**24b**) employed a (*R*)-*p*-tol-BINAP•Ag^{I}F catalyzed allylation as a strategic stereochemical setting step (Figure 7).[22]

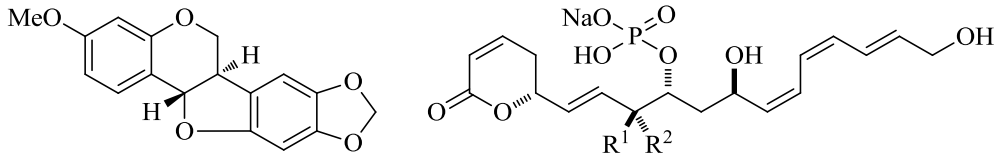

23

24a R^1 = Me, R^2 = OH
24b R^1 = OH, R^2 = Me

Figure 7. Structure of (–)-*trans*-Pterocarpin (**23**), Fostriecin (**24a**) and 8-*epi*-Fostriecin (**24b**).

1.1.1.3. Allylation of *ortho*-Substituted Arylaldehydes

In general, *ortho*-substituted arylaldehydes are a class of compounds affording poor levels of stereoinduction when applying most known catalytic asymmetric allylation approaches. As a showcase of this trend, Kotora *et al.* reported the addition of

allyltrichlorosilane to variously substituted benzaldehydes, catalyzed by (*S*)-(-)-bipyridine *N*,*N'*-dioxide **25** (Figure 8), in order to obtain the corresponding (*R*)-homoallylic alcohol products. More specifically, it was found that the reaction of benzaldehyde afforded the product in 80% ee, whereas with substituted derivatives decreasing levels of *ee* were found as substituents were placed closer to carbonyl group, implying sterics effect were a major factor responsible for this erosion in ee. Also, using the same reaction conditions *p*-MeO, *m*-MeO, and *o*-MeO afforded *ee* of 87, 80, and 67%, respectively. Similarly, the use of *p*-Cl, *m*-Cl, and *o*-Cl substituted benzaldehdyes provided the corresponding homoallylic alcohols with ee of 71, 70, and 65%.[23] Having observed a related finding Singaram and coworkers[24] prepared a variety of substituted homoallylic alcohols using an indium mediated allylation protocol of arylaldehydes; achieving this with the use of In^0, allyl bromide, pyridine and (+)-(1*S*,2*R*)-2-amino-1,2-diphenylethanol as a chiral ligand. As reported the use of benzaldehyde provided product in 93% ee, while *o*-Me and *o*-Cl substituted benzaldehydes afforded homoallylic alcohols of lower enantiopurity in 88% and 78% ee.

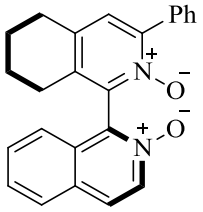

25

Figure 8. Chiral (*S*)-(-)-bipyridine *N*,*N'*-dioxide.

1.1.1.4. Indium-mediated Allylation Reaction

During the last century, organometallic reagents have played a central role in the organic chemistry, but never more so than today. Organometallic reagents prepared from

main group metals, such as lithium and magnesium are amongst some of the most popular metals for organic reagents. Though these reagents offer a broad range of applications, the preparation and handling of these reagents is difficult due to the sensitivity of these species to moisture and air. Moreover, the poor functional group compatibility such as seen with carbonyl and hydroxyl groups has set limitations to the applications of these reagents in organic synthesis. To get around these obstacles, organoindium reagents emerged with the expressed purpose of increasing the prospective applications that organo-metal species could accommodate. Today, indium is regarded as an important element in organic synthesis due to the low toxicity, high functional group compatibility, and its tolerance to air and moisture. However, apart from a small handful of reactions, indium remains almost foreign in the field of asymmetric catalysis.[25] Some success has been made when incorporating indium into allylation reactions. These transformations are able to proceed smoothly with very mild conditions, affording homoallylic alcohols. In this respect, in 1988, Butsugan *et al*. reported the first indium-mediated allylation reaction using indium powder (1.5 equiv), allyl iodide (1.5 equiv), and benzaldehyde (1 equiv) in DMF to provide the corresponding homoallylic alcohol in 87% yield.[26] Although some strides were made in the area, it would be over 10 years until the first asymmetric version of indium-mediated allylation of benzaldehyde was discovered by Loh *et al.* Using cinchonidine as the chiral promoter, an excess of allyl bromide (6 equiv) and a 3:1 THF/hexane mixed solvent, the corresponding (*R*)-homoallylic alcohol was obtained in 73% yield and 75% ee. This method is applicable to various allyl bromides and aldehydes to give good yield coupled with moderate to high selectivities. Another advantage of this method is that the chiral promoter is inexpensive and commercially available. Though this reaction has many useful prospective applications, the

mechanistic nature of the allyl indium chiral promoter complex is still ambiguous.[27] Extending the appeal of In, Singaram and co-workers reported a similar method for the enantioselective allylation of aldehydes using two-fold excess of allyl bromide, in contrast to the six-fold called for in the Loh report. Furthering their findings, various limonene-based amino alcohols (2 equiv), metallic indium (2 equiv), as well as a large excess of allyl bromide were also used. This strategy had poor success until stoichiometric amounts of pyridine were added, increasing both yield and enantiomeric excess of the product. Although this addition did allow quantitative product formation, the asymmetric induction did not exceed more than 40%. To boost the ee of the product, a myriad of commercially available amino alcohols were screened. It was found that (1*S*,2*R*)-(+)-2-amino-1,2-diphenylethanol **27** was the most effective chiral promoter found for the allylation of arylaldehyde **26**, resulting in the homoallyl alcohol **28**, in up to 97% conversion and 93% ee (Scheme 10). Singram *et al*. also identified the important role of pyridine in this transformation in order to obtain high level of inversion and ee. It was found that the amino alcohol ligand could be recovered through a simple acid-base extraction to use in another reaction sequence.[28]

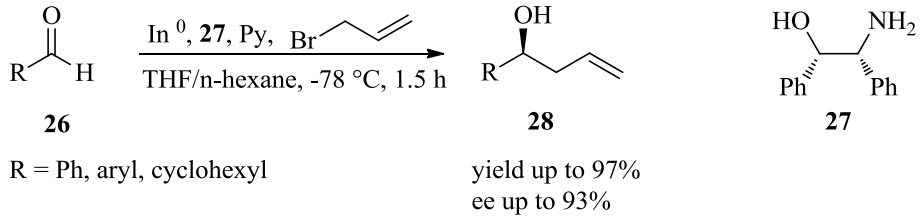

Scheme 10. Enantioselective allylation of arylaldehydes using **27** as a chiral promotor.

The use of indium and commercially available chiral promoters has provided enantioselective allylation of both aromatic and aliphatic aldehydes in moderate to high

enantiomeric excess and respectable yield. However the nature of the allyl indium chiral promoter complex and the reaction mechanism has not been completely elucidated to date.

1.1.1.5. Synthesis of $C_{(3)}$-Chiral Substituted Phthalides

$C_{(3)}$-Chiral substituted phthalides, are a widely distributed structural motif found within a number of biologically active natural products and medicinally important pharmaceuticals. One such compound is the *Sporotrichum laxum* metabolite spirolaxine, (**29**) (Figure 9) produced by a fungi belong to the genera *Sporotrichum* and *Phanerochaete*, possessing specific activity against the microaerophilic Gram-negative bacterium *Helicobacter pylori*. The spirolaxine **29** compounds are useful for the treatment of gastroduodenal disorders and in the prevention of gastric cancer. The family of compounds has been the target of many recent total syntheses, owing to the desirable applications of these compounds. Spirolaxines CJ-12,954 (**30**) and CJ-13,014 (**31**) are reported to lower cholesterol activity, and interestingly also exhibit cytotoxicity against endothelial (BMEC and Huvec) and tumor (LoVo, HL60) cell lines (Figure 9).[29,30,31] Moreover, Kittakoop *et al.*[32] have recently isolated a phthalide containing the natural product Colletorialide (**32**), from a culture of *Colletotrichum* sp. CRI53502. This remarkable compound possesses oxygen radical absorbance capacity against peroxy radicals. In experimental testing, the phthalide **32** has shown potent antioxidant activity. A final example is (*S*)-3-*n*-butylphthalide (**33**), obtained from the *Apium* seed extract. This compound has recognized potential as a treatment for strokes and remarkably as a pretreatment for Parkinson disease (PD).[33-36]

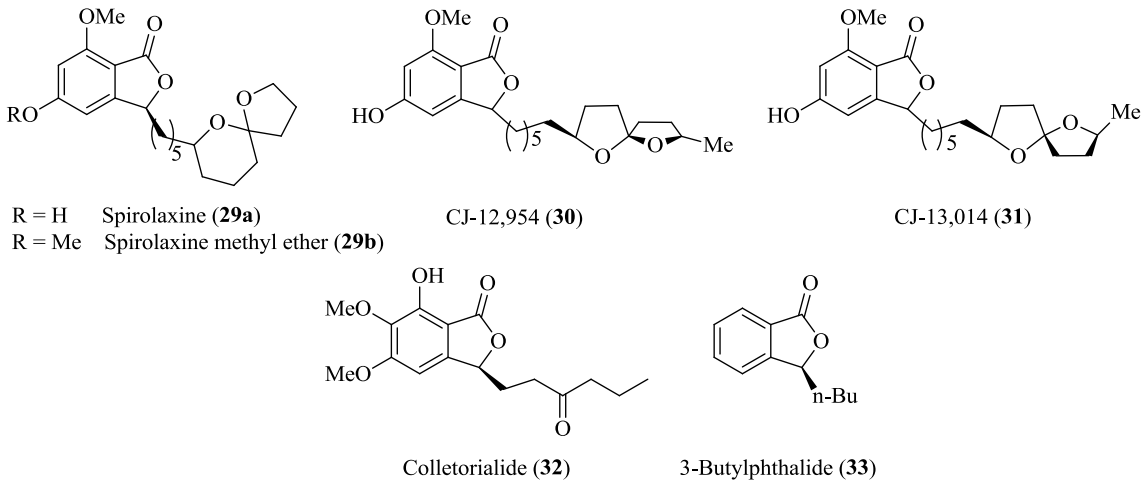

Figure 9. Examples of natural products containing $C_{(3)}$-chiral substituted phthalides.

Not surprisingly, the impressive range of applications of these phthalides has prompted organic chemists to develop novel and efficient methods for their synthesis. In 1990, Noyori reported the first catalytic enantioselective synthesis of phthalide **35**, accomplished through the asymmetric hydrogenation of ethyl *o*-acetylbenzoate **34** in ethanol with 0.4 mol% of the (*S*)-BINAP-Ru catalyst at 100 atm and 35 °C for 7 days (Scheme 11).[37]

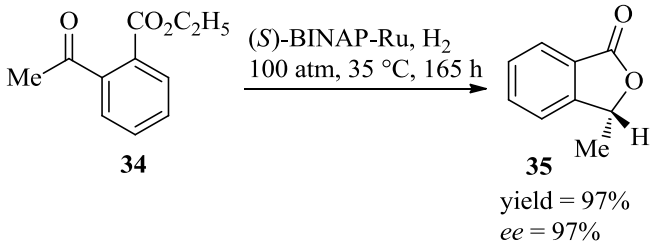

Scheme 11. Enantioselective synthesis of phthalide *via* asymmetric hydrogenation.

A year after, Soai *et al.* published a catalytic enantioselective synthesis of 3-alkylphthalides **41** using *N*,*N*-dibutylnorephedrine (DBNE) **42** as a chiral catalyst. Their

synthesis started with the reaction of 2-bromobenzaldehyde **36** with alkylzinc **37** (2 equiv) in presence of DBNE **42** (0.2 equiv). The resulting alcohol **38** with 90% ee was treated with *n*-BuLi and *N*,*N*-dimethylformamide to afford benzaldehyde **39** and lactol **40** in 82% yield. Consequent oxidation of **39** and **40** with silver oxide produced the desired product **41** (Scheme 12).[38]

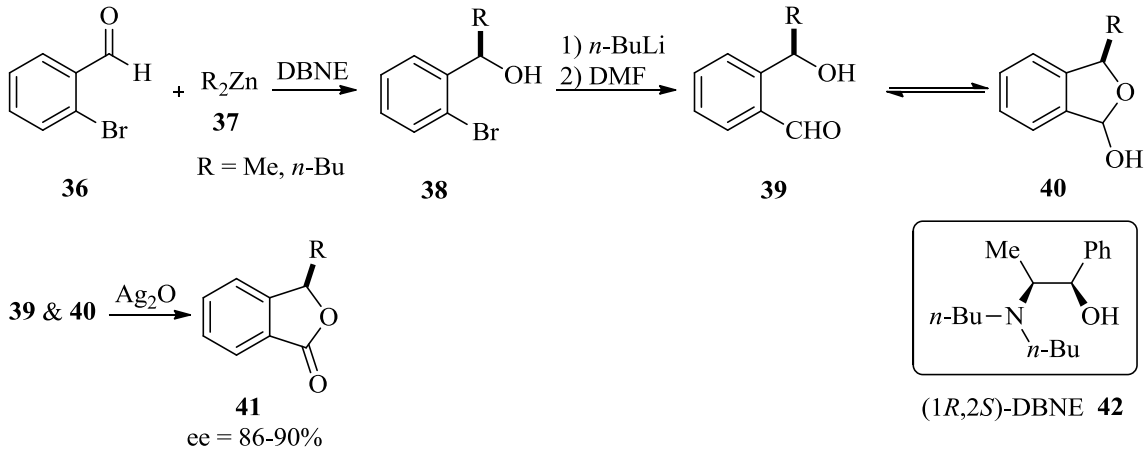

Scheme 12. Enantioselective synthesis of chiral 3-substituted phthalide catalyzed with (1*R*,2*S*)-DBNE.

Further development continued until 1996, when a similar but more convenient synthesis than Noyori's approach of chiral 3-alkylphthalides **46** was reported by Brown *et al.*, *via* asymmetric reduction of *o*-acetylbenzoate **43** with (-)-*B*-chlorodiisopinocomphenylborane ($^{d}Ipc_2BCl$) **44** in diethyl ether at -25 °C for 8 h. Following workup of the resulting borane **45** with diethanolamine, produced chiral 3-alkylphthalide **46** with an ee of up to 99% (Scheme 13).[39]

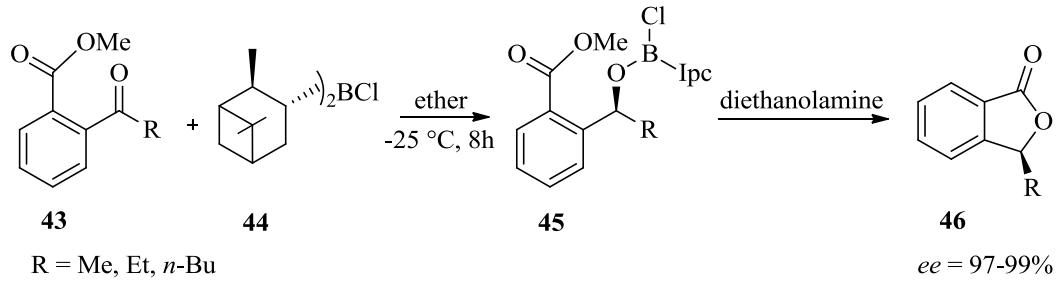

43 **44** **45** **46**

R = Me, Et, *n*-Bu

ee = 97-99%

Scheme 13. Asymmetric synthesis of 3-substituted phthalide *via* intermolecular asymmetric reduction.

The first enantioselective total synthesis of spirolaxine methyl ether **29b**, was attempted by Brimble *et al*. This strategy linked 5,7-dimethoxy phthalide **51** with the 6,5-spiroacetal group, leading to the product formation. The (3*R*)-stereochemistry of phthalide **51** was built on enantioselective allylation of 3,5-dimethoxybenzaldehyde **47** with titianium (+)-BINOL (1,1'-Bi-2-naphthol) to afford the (*R*)-homoallylic alcohol **48** in 78% yield and 86% ee. In order to allow the subsequent installation of the phthalide functionality, regioselective bromination of the aromatic ring was performed using *N*-bromosuccinimide (NBS) to provide the bromide compound **49**. Conversion of alcohol functionality to diethylcarbamate **50** followed by lithium-halogen exchange and intramolecular lactonization produced phthalide **51** (Scheme 14).[33]

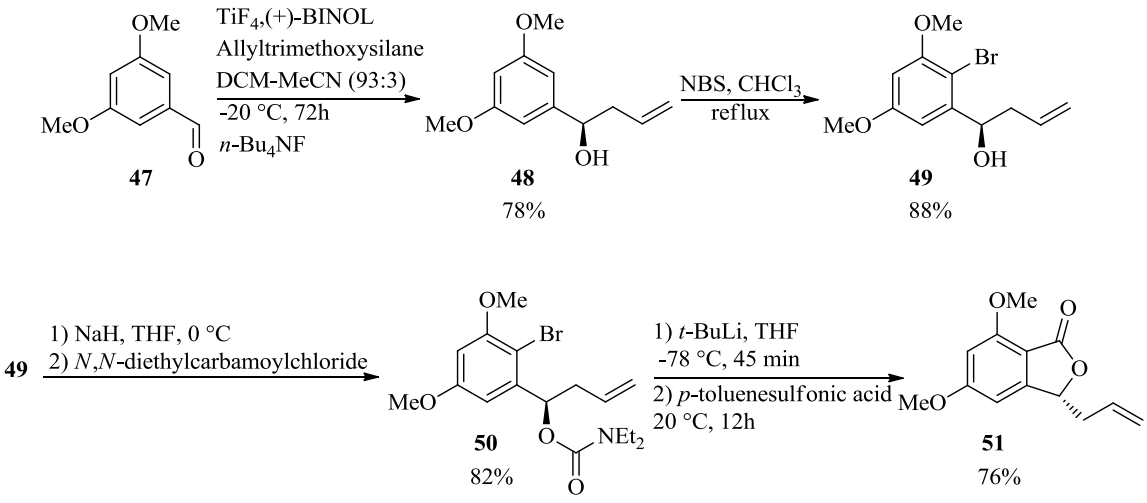

Scheme 14. Enantioselective synthesis of 5,7-dimethoxy $C_{(3)}$-chiral substituted phthalide.

Seeking the various bioactivities of phthalide natural products, Dong and coworkers synthesized phthalide **54** *via* hydroacylation of 2-ketobenzaldehyde **52** using a Rh catalyst and Duanphos **55** as the ligand. They envisioned transition state **53** for this transformation, finding that the reactivity and asymmetric induction are highly dependent on the choice of counterion. The selectivity for hydroacylation over decarbonylation increased with use of counterions that displayed a stronger coordination with Rh (Scheme 15). The reaction of 2-ketobenzaldehyde **52** (R = Me) with 10 mol% catalyst, using Cl^- as a counterion gave 97% yield, 97% *ee* within 3 days; though it was found that the addition of $AgNO_3$ reduced the reaction time to a single day. This was due to the reduced tendency of NO_3^- to coordinate with Rh, maintaining yield and *ee*.[40]

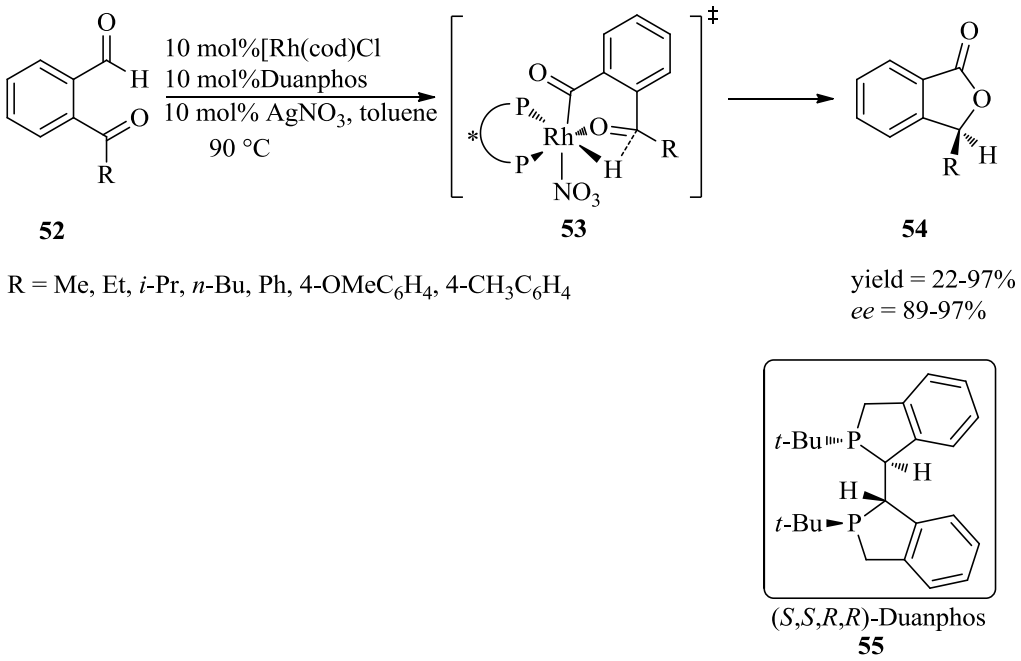

Scheme 15. Intramolecular hydroacylation of various ketones.

1.1.1.6. Synthesis of $C_{(1)}$-Chiral 3-methylene-indan-1-ols

Chiral indanol products are key substructures within a number of biologically active compounds. For instance, the A and B rings of Anisatin, a biologically active component of fruit obtained from the Japanese star anise, are derived from a chiral indanol template. Recent syntheses of Anisatin have hinged upon the use of a chiral indanols.[41] In 2006, Smith *et al*. disclosed the use of a cyclic carbamate substituted indane motif as a side chain of HIV-1 protease inhibitors.[42] Likewise, alkylidene indanes have been employed in diversity oriented synthesis (DOS) as published by Kesavan *et al*. in 2007.[43] Another example of the versatility of chiral indanols is their use in the preparation of dopamine reuptake blockers, for the treatment of addicts suffering cocaine abuse.[44]

Meanwhile the use of palladium catalyzed reactions such as the Heck reaction, Suzuki-Miyaura, Stille, Hiyama, Kumada, Negishi, and Buchwald-Hartwig cross-coupling have emerged as a powerful set of chemical transformation in recent years . Having

contributed to these developments is palladium functional group tolerance which has allowed for its use in numerous natural product syntheses, industry, and production of value-added compounds. Taking advantage of the compatibility of palladium with carbonyl groups, the racemate of benzocyclopentenol **60** was synthesis by Griff *et al*. utilizing a non-phosphine-containing palladacycle **57** as a catalyst and allene **58** as a precursor to a π-allyl species (Scheme 16).

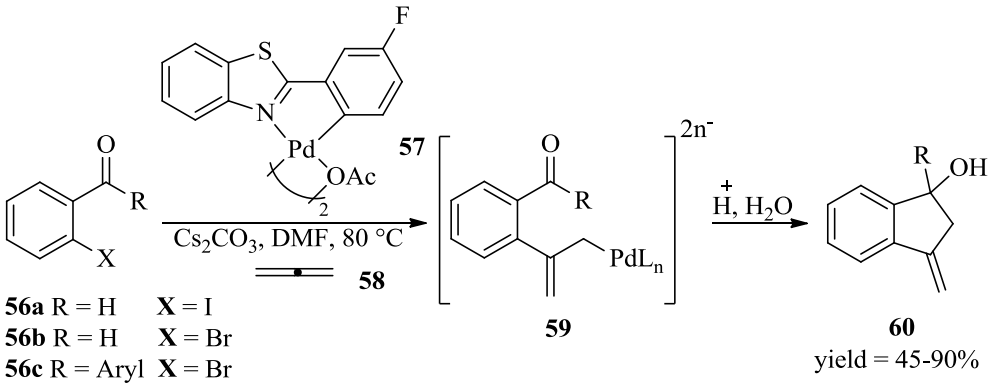

Scheme 16. Palladium catalyzed synthesis of 3-methylene-indan-1-ols *via* nucleophilic cyclization.

Using 2-iodobenzaldehyde, 2-bromobenzaldehyde, and 2-bromo arylalkyl ketones **56a-c**, as starting reagents with allene in DMF at 80 °C in presence of **57** (2 mol%) and Cs_2CO_3 (2 equiv), products **60** were obtained *via* the formation of an intermediate **59**. Consistent with oxidative addition in the mechanism of this process it was found that 2-iodo aldehyde **56a** was more reactive than bromoaldehyde **56b**. The key step in this reaction as shown in Scheme 17 is formation of anionic η^3-and η^1 –species **62a** and **62b** by coordination of carbonate anions to Pd^{II}. Further, it is postulated that bond shift of η^1 –species **62b** could happen due to the ability of carbonate as a mono- or hemilabile bidentate ligand, as depicted in **65** or **66**. Regarding the catalyst recycling (i.e. reduction of Pd^{II} to Pd^0), it was assumed that use of DMF as a solvent contains formate impurities, or this impurities could be

generated *in situ*, reacting with Pd^{II} to afford HPdX which in turn converted to Pd^{0} by a base.[45]

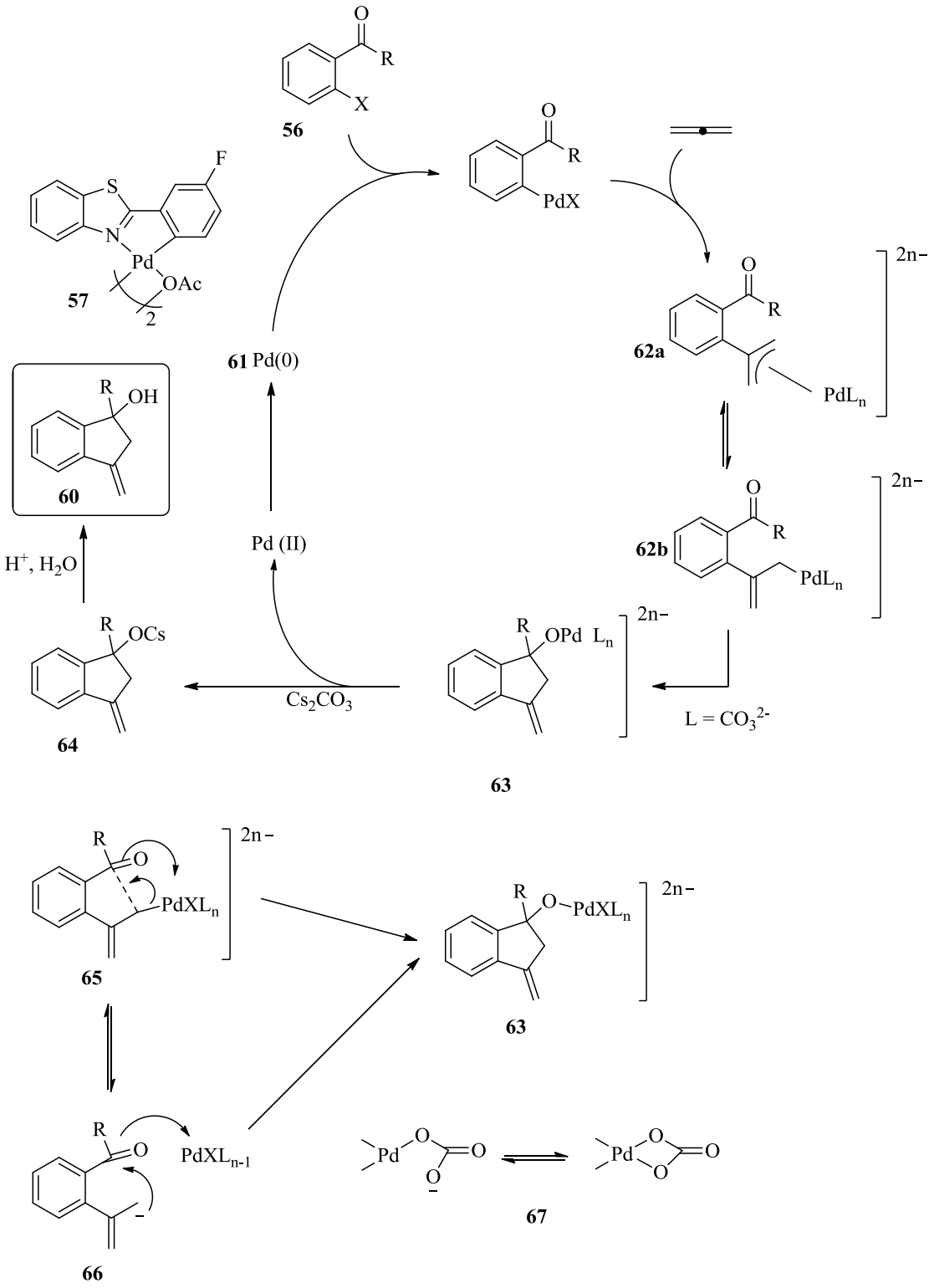

Scheme 17. Catalytic cycle for synthesis of 3-methylene-indan-1-ols *via* nucleophilic cyclization.

In this context, Schmalz and coworkers, in 2009, reported a domino allylstannylation /Heck reaction for the synthesis of 3-methylene-indan-1-ols **70** using 2-iodo and 2-bromobenzaldehydes with allyltributylstannane (2 equiv) in the presence of 1 mol% of [$PdCl_2$(dppf)] with DMF as solvent to give racemate **70**. Relating to the mechanism of this conversion, it was proposed that oxidative addition of a [L_2Pd^0] species into the C –X bond of aldehyde **68** produced an *ortho*-palladated intermediate **69**. A salient structural feature of **69** was the Lewis acid activation of the carbonyl group by the palladium (II) center of the derived *ortho*-palladacycle which promoted allylstannylation. Apart from the mechanism of this domino reaction sequence it is notable that it proceeded under neutral conditions due to the use of alkoxystannane, acting as a base equivalent in a Heck-type reaction (Scheme 18).[46]

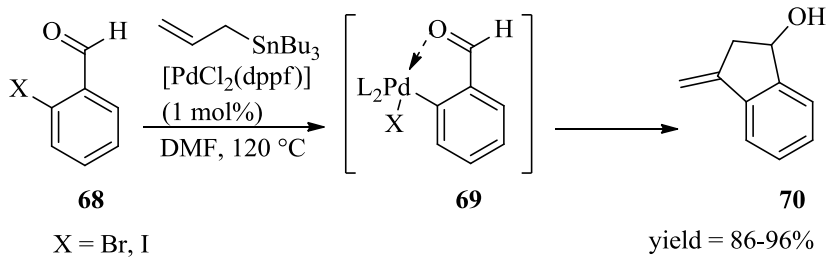

Scheme 18. Synthesis of 3-methylene-indan-1-ols through a domino allylstannylation/Heck reaction.

Two years later, in an attempt to perform the transformation in an enantioselective fashion, Schmalz *et al*. used various chiral ligands **74-78** at the palladium center (Figure 10). [47] The reaction of benzaldehyde **71a** and **71b** was carried out with two equivalents of allyltributylstannane **73** in DMF at 80 °C, in the presence of 2 mol% of tris(dibenzylideneacetone)dipalladium(0) (Pd_2dba_3) as a source for palladium (0) and 3 mol% of a chiral ligand **74-78** (Scheme 19). In the first set of experiments, (*R*)-BINAP **74a**, as well as two of its derivatives, **74b** and **74c,** were investigated. The best selectivity (50% for X = I

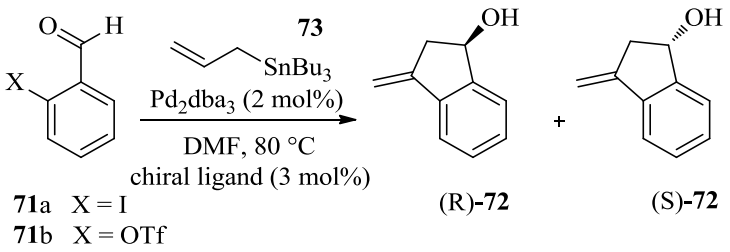

Scheme 19. Asymmetric synthesis of 3-methylene-indan-1-ols through a domino allylstannylation/Heck reaction.

and 48% for X = OTf) was obtained using the parent ligand **74a**, showing that the more sterically hindered BINAP derivatives **74b** and **74c** induced less enantioselectivity (Figure 10). Thus, as a second set of chiral ligands, Taddol-derived phosphine-phosphite ligands **75 a-e** were tested; in which ligand **75e** performed best in terms of yield although the product (*R*)-**72** was produced with low 54% enantioselectivity. As a continuation of the study, biphenyl-derived diphosphanes**76a-e** were used which gave similar results. Lastly, they tested catalysts derived from ferrocene-based ligands (R_p)-(*S*)-Josiphos (**77**) and (S_p)-(*S*)-Taniaphos (**78**) and Pd(0) which provided the desired product (*R*)-**72** with 96% and 70% ee form substrates **71a** and **71b** with up to 67% yield, respectively. Applying the catalyst derived from ligand **X** and Pd(0) and substrate **71a** the product was afforded in 46% ee and 66% yield.

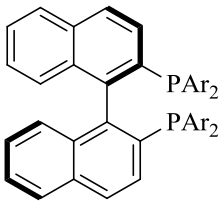

74a Ar = Ph
74b Ar = 3,5-xylyl
74c Ar = 4-tolyl

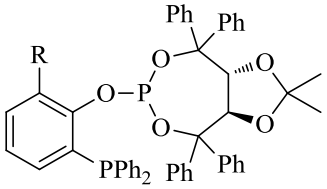

75a R = H
75b R = Me
75c R = *i*-Pr
75d R = *t*-Bu
75e R = Ph

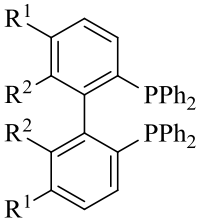

76a $R^1 = R^2 = OCH_2O$
76b $R^1 = R^2 = OC_2H_4O$
76c R^1 = H; R^2 = OCOCy
76d R^1 = H; R^2 = MeO
76e R^1 = Cl; R^2 = MeO

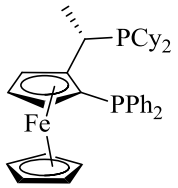

77 (R_p) -(*S*)-Josiphos

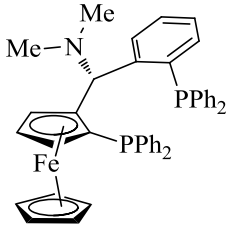

78 (S_p)-(*S*)-Taniaphos

Figure 10. Chiral ligands tested in the asymmetric domino allylstannylation/Heck reaction.

Taken together the work of Schmalz has allowed for the racemic synthesis of 3-substituted-indan-1-ols using palladium as a catalyst. Moreover, these same authors have advanced synthetic methodology for the preparation of C_1-chiral 3-methylene-indan-1-ols using palladium and chiral ligands based catalyst. As it stands however, a major limitation of their work was the substrate scope as only two starting compounds, *ortho*-iodo- and *ortho*-trifluoromethanesulfonate benzaldehyde, were addressed which afforded product in high and moderate ee, respectively.

1.2. Carbene-Stabilized N^{I}-Centered Cations

1.2.1. Historical

1.2.1.1. The Carbene

Carbenes are generally considered to be short-lived, highly reactive intermediates, with a broad range of applications in synthetic chemistry.[48] It was not until 1954, through the efforts of Doering *et al.,* that carbenes were introduced into the field of organic synthesis.[49] At that time, synthesis of carbenes was achieved by reacting chloroform with cyclohexene in the presence of potassium *t*-butoxide to afford 7,7-dichlorobicyclo[4.1.0]heptane, thus producing the first known example of a carbene in organic chemistry.[50] Accordingly, this breakthrough by Doering *et al.* paved the way for a new branch of organic chemistry where carbenes would play a fundamental role in new exploratory studies over the next 50 years. One such achievement in this field took place in 1964 when Fisher *et al.* characterized the first transition-metal complex of a carbene by binding methoxymethylcarbene to $W(CO)_5$.[51] Later, in 1975, Schrock reported the first transition metal methylene complexes of $Ta(\eta^5\text{-}C_5H_5)_2(CH_3)(CH_2)$ and some other members of this alkylidene family. Significantly, the Schrock's methylene ligand has moderate nucleophilic character, which is in strong contrast with the electrophilic character of Fisher-type carbene ligands.[52] Following these successes, in 1991, Arduengo *et al*. prepared the first crystalline carbene which opened up a new forefront of carbene chemistry that continues to receive an enormous amount of attention from researchers.[53] More specifically, the stable crystalline carbene 1,3-di-1-adamantylimidazol-2-ylidene (an example of a *N*-heterocyclic carbenes, NHCs) **80** was prepared as colourless crystals with sufficient kinetic and thermodynamic stability for isolation and characterization. The NHC **80** was obtained from deprotonation of

bis(adamantyl)imidazolium chloride **79** in THF at room temperature with sodium hydride in the presence of catalytic amounts of dimethyl sulfoxide anion (Scheme 20).[54]

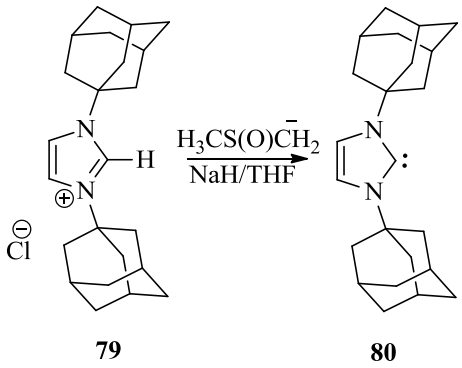

79 **80**

Scheme 20. Synthesis of 1,3-di-1-adamantylimidazol-2-ylidene.

It deserves mention that Bertrand *et al.*, in 1985, were able to isolate stable phosphanylcarbenes; however, at that time it had not been identified that these compounds contained a divalent carbon (*i.e.*, carbenes).[55] In addition, Schubert and coworkers, five years earlier in 1980, reported a number of cyclic carbodiphosphoranes that to date remain the only known examples of such compounds. The synthesis of these carbodiphosphoranes was achieved through the quaternization of methylenebis(diphenylphosphane) (**81**) with α,ω-dihaloalkanes (**82a-c**) to afford the respective bisphosphonium salts **83a-c,** which were subsequently converted to carbodiphosphoranes **84a-c** in variable yields by mild dehydrohalogenation using methylenetrimethylphosphorane in THF *via* a double transylidation mechanism (Scheme 21). Their experiments showed that product **84c** was stable; however, **84b** decomposed at 35 °C, and **84a** was even less stable decomposing at 20 °C within a few hours. Schubert and coworkers also found compound **84b** had a P = C = P bond angle of 117 °, which is the smallest known of all carbodiphosphoranes. Extending this, X-ray crystallographic data showed that the P = C bond distances of the P = C = P motif were

equivalent, within the expected range of 1.645 Å to 1.653 Å. Because **84b** had an angle less than 120 ° between the P=C=P atoms, it was rationalized that such strain would increase the probability that the molecule would decompose. Further, compound **84a** had an even smaller respective bond angle, thus by comparison making it even more labile as confirmed by experiment.[56]

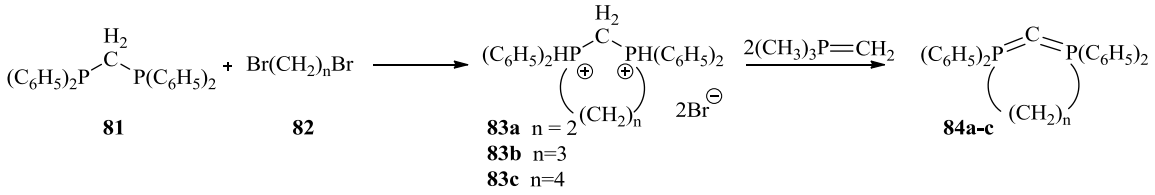

Scheme 21. Synthesis of ring-strained carbodiphosphoranes.

Several years after these discoveries, Baceiredo *et al.* described carbodiphosphoranes as a compound with two cumulated ylide functionalities, in which two negative charges reside on the central divalent carbon (II), stabilized by two phosphonio groups. Because of the very strong nucleophilicity associated with this group of compounds, originating from their bent structure, they can serve as potential electron-rich carbon-centered ligands. In view of this rationale Baceiredo *et al.* prepared and subsequently investigated the ability of structurally related P-heterocyclic carbodiphosphorane (PHCD) **85b** (Figure 11) to function as a ligand by coordinating $[\{PdCl(allyl)_2\}_2]$, $[\{RhCl(nbd)_2\}_2]$(nbd=norbornadiene), and $[\{RhCl(CO)_2\}_2]$ in THF at room temperature, which to their delight, quantitatively yielded the corresponding Pd^{II} and Rh^{I} complexes. In contrast, however, no complexation was observed when the more sterically hindered ligand **85a** was used.[57]

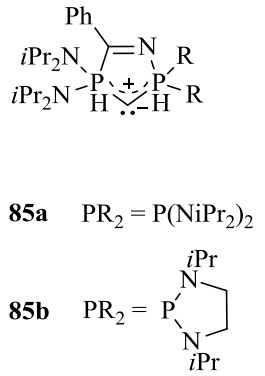

Figure 11. P-heterocyclic carbodiphosphorane (PHCP).

It is interesting to note that while Baceiredo *et al.* described these compounds as containing a central divalent carbon (II) the work of Frenking *et al.* one year later suggested that the central divalent carbon of carbodiphosphoranes, which he termed CDPs **86**, had a formal oxidation state of zero (i.e., divalent carbon (0)).[59]

According to Frenking this divalent carbon (0) possesses two electron lone pairs, which in free molecules do not participate in chemical bonding (Figure 12). Using both theoretical and experimental evidence, Frenking *et al.* showed that similar to carbenes, CDPs have a divalent carbon atom. They differ however in that in CDPs, the carbon-phosphorus bonds are phosphor-carbon donor-acceptor interactions, but in carbenes, the carbon-carbon bonds come from electron-sharing.[59]

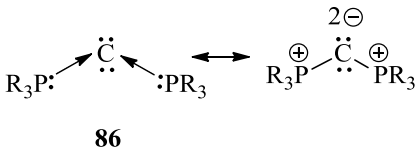

86

Figure 12. Two resonance forms of carbodiphosphoranes; donor-acceptor interactions (left), Lewis structure (right).

The novel features of CDPs included donor-acceptor interactions as well as the presence of two electron lone pairs at the central carbon atom, yielding a high proton affinity

(PA). Theoretical calculations suggest that depending on the CDPs substituent, the PA of the CDPs could be altered. Notably, it was predicted that changing the substitution of **87** and **88** to afford CDPs such as **87a-c** and **88a-c** would provide congeners having larger PA than previously reported NHCs (**89**) and guanidine base **90** (Figure 13).[59]

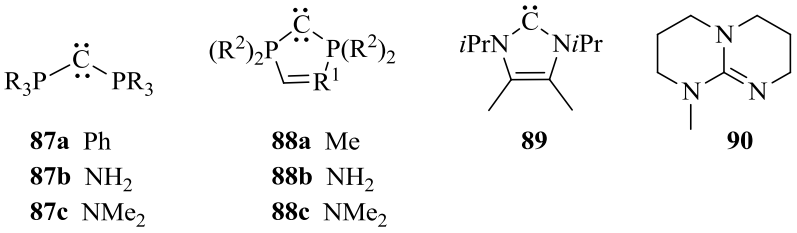

87a Ph
87b NH_2
87c NMe_2

88a Me
88b NH_2
88c NMe_2

89

90

Figure 13. Carbodiphosphoranes (**87**), P-heterocyclic carbodiphosphoranes (**88**), NHCs (**89**), guanidine base (**90**).

Poli *et al.* [58] isolated $[Ph_3PCH_2PPh_3][FeCl_4]_2$ from the interaction of a solution of $FeCl_3$ and PPh_3 in $CHCl_3$ with air. The X-ray analysis from a single crystal has been reported. Accordingly, Frenking *et al*. suggested the predicted PA of the dication $[\mathbf{87a}(H)_2]^{2+}$ is consistant with experimental observation.[59] Moreover, they synthesized another dicoordinated CDP complex from the treatment of readily available $[(PPh_3)_3CH][BF_4]$ which contains the trication $[(\mathbf{87a}H)_2Ag]^{3+}$.

Thus, it was concluded that carbodiphosphoranes are carbon (0) compounds with two electron lone pairs at the central carbon atom. Having this property causes an extremely high proton affinity which can be utilized for synthesizing compounds such as dication $[(PPh_3)_2CH_2]^{2+}$ and the trication $[\{(PPh_3)_2CH\}_2Ag]^{3+}$.

1.2.1.2. Structure of Carbenes

During the last few decades, carbenes have gained considerable attention and through exploration of their related reactivity, carbenes have become a major area of research. Carbenes are divalent carbon compounds containing a total of six electrons in the valence shell; however two of these electrons are nonbonding. These two electrons can exist in two separate spin-states. The electrons can have parallel spins, known as the triplet state, or can have antiparallel spins, resulting in a singlet state. In the triplet ground state, the carbene unit is linear, suggesting a sp-hybridized carbon center, possessing two degenerate p (p_x and p_y) orbitals (Figure 14). Deviating from this, singlet state carbenes are not linear, but instead bent. Correspondingly, singlet state carbenes are sp^2-hybridized with two non-degenerate orbitals. In the singlet state, the p_y orbital resides almost unchanged in comparison with the triplet state, called p_π, whereas the p_x orbital gains some 's' character and become lower in energy and therefore more stable. The central carbon of carbenes and the two covalently bonded atoms flanking the central carbon exist in one plane which contains the σ-orbital, while the orbital perpendicular to this plane is assigned as a p-orbital. It is indicative of the σ-orbital to have 's' character making it more stable than the p-orbital. In general, most carbenes are not linear; therefore occur primarily in the singlet state, lowering their energy.[49]

Figure 14 depicts the energy configuration of both a triplet and singlet state carbene, which includes the configuration $\sigma^1 p_\pi^1$, σ^2, and p_π^2. When electron spins in σ^2, and p_π^2 configurations are paired, the singlet state is formed. Extending this, when the electron spins are antiparallel and in different orbitals, the singlet state is produced. This is the defining factor for determining the framework configuration of a carbene.[49]

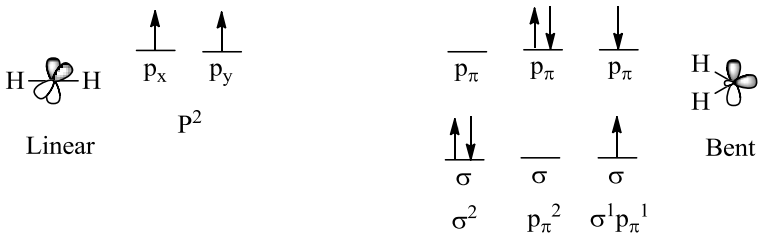

Figure 14. Electronic configuration of linear and bent methylene.

1.2.1.3. Cyclopropenylium Ions

In general, cations are accepted as an electron deficient species with a positive charge. One exception to this convention is tris(dialkylamino) substituted cyclopropenylium cations, which are electron rich systems, making them novel compounds. In contrast to aromatic systems with six or more electrons, cyclopropenylium cations are three membered ring systems containing two π-electrons, delocalized over three 2p orbitals. These structures are the smallest examples of aromatic systems that satisfy Hückel's rules. The first preparation of this small aromatic ring derivative occurred in 1957, when Breslow reported the synthesis of 1,2,3-triphenyl-2-cyclopropene carboxylic acid nitrile (**91a**) from reaction of diphenylacetylene with phenyldiazoacetonitrile (Figure 15).[60] Treatment of **91a** with boron trifluoride etherate and a trace of water produced 1,2,3-triphenylcyclopropenyl fluoroborate (**91b**) contaminated with the hydroxyfluoroborate (**91c**).

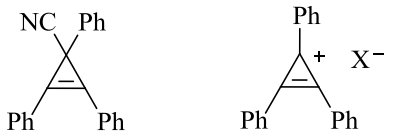

91a **91b** X = BF_4
91c X = BF_3OH

Figure 15. 1,2,3-triphenyl-2-cyclopropene carboxylic acid nitrile (**91a)** and corresponding **c**yclopropenyl cations.

Although this molecule has inherent strain due to the small ring size, it is known to be thermodynamically stable owing to Hückel aromaticity. Since 1957, several derivatives of the cyclopropenylium cations have been synthesized. An example of this was documented by Yoshida *et al.*, who reported a method for the synthesis of a triaminocyclopropenyl cation system. Here, the amino group has a much stronger electron donation π-conjugative effect than the electron withdrawing σ-inductive effect, increasing the overall stability. A secondary amine was used as a protic nucleophile and mixed together with tetrachloropropene **92**, afforded the desired product **93** in a quantitative yield (Scheme 22). The advantage of the resulting aminocyclopropenyl perchlorates was their stability to water, even at elevated temperature when compared to the related trichloro- and triphenylcyclopropenyl perchlorates.[61]

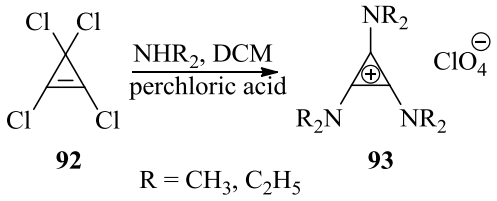

Scheme 22. Synthesis of triaminocyclopropenyl cation system.

Extending the research of Yoshida *et al.*, Weiss and coworkers found that the transamination reaction of trichlorocyclopropenylium hexachloroantimonate (**94**•$SbCl_6^-$) can be controlled through variation of temperature and stoichiometry of the trimethylsilyldialkylamines to afford a series of $SbCl_6^-$ salts: dimethylaminodichloro-(**95)**, bis(dimethylamino)chloro-(**96**), and tris(dimethylamino)cyclopropenylium cations (**97**) (Scheme 23).[62]

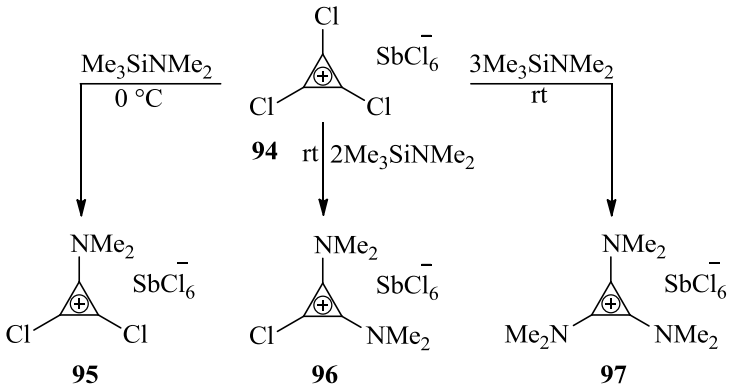

Scheme 23. Synthesis of dimethylaminodichloro-, bis(dimethylamino)chloro-, and tris(dimethylamino)cyclopropenylium cations.

Although there are several reports for the generation and isolation of organic radical cations, very little is known about mono radical dications. Generation of mono radical dications involves removal of an electron from a positively charged precursor, possessing a relatively high energy of highest occupied molecular orbital (HOMO). If the HOMO is low in energy, it becomes difficult to abstract an electron, producing the dication. However, Weiss *et al*. showed that trisamino cyclopropenium ions **98** are exception to this rule (Figure 16). According to the Hückel Molecular Orbital (HMO) approximation, the HOMO of **98**

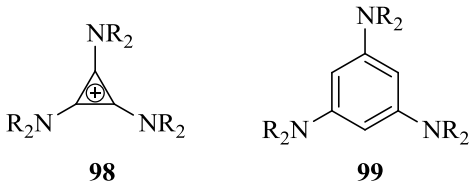

Figure 16. Comparison of trisamino cyclopropenium with neutral trisamino benzene.

falls within the same energy range of the degenerate HOMOs of neutral compound **99**, known as an electron rich and highly oxidizable compound (Figure 16). Through the

comparison of these two compounds, Weiss *et al*. were able to postulate **98**'s qualities; aiding in the first synthetic approach towards stable tris(dialkylamino)cyclopropenium radical dications. This approach involved a two-step reaction: synthesis of tris(dialkylamino)cyclopropenium chlorides **100**, followed by oxidation of the anhydrous solution of salt **100** with $SbCl_5$. The resulting product was radical dication **101**, described as brick-red microcrystals in 90% yield (Scheme 24).These radical dications are stable for several hours in atmospheric conditions, however over several weeks gradual decomposition was found. The NMR spectra of **101** showed broadened peaks, due to the unpaired electron. Addition of Zn to these solutions removed the characteristic red colour affiliated with the radical dication species, and yielded the NMR spectra of the parent compound **100**.[63] Later,

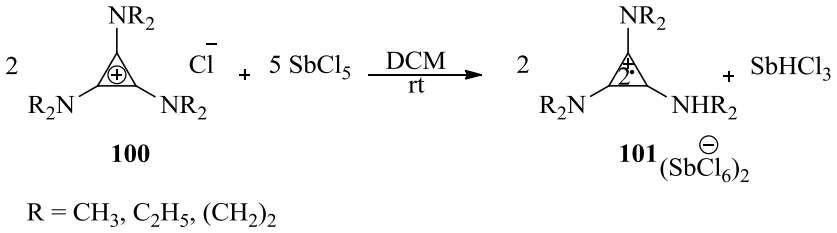

Scheme 24. Formation of radical dication.

Weiss *et al*. combined tris(dimethylamino)cyclopropenylium (TDA) cation with the donor chloride ion. In spite of the opposing charges of these ions, the oxidation potential ($E_{1/2}$) values were almost the same, about 1.4 v (vs Ag/AgCl; 0.1 N NEt_4Cl/CH_3CN) for both the TDA cation and the chloride ion. The orbital repulsion of the two ions would be maximum at the point of maximum electrostatic attraction. Since the interacting orbitals have the same local symmetry, the repulsion can be attributed to the HOMO/HOMO interaction (Figure 17). In contrast with other salt like halides, TDA halides have a lower tendency to form inner ion

pairs in dipolar aprotic solvents. Therefore, the TDA halides are possibly potential source of naked halide ions.[64]

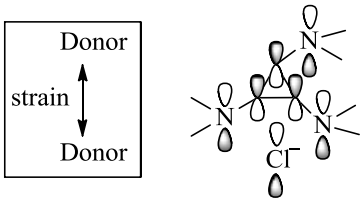

Figure 17. Interacting orbitals involved in the HOMO/HOMO interaction between TDA and Cl^-.

Although great strides have been made towards a better understanding of carbene chemistry over the past two decades, many pitfalls have to be overcome to achieve a more complete apprehending. It was thought for many years that singlet carbenes could only be isolated if at least one π-donor heteroatom was bonded directly to the carbene center, compensating for the inherent electron deficiency of the carbene. For example in diaminocarbenes, there is a push, push mesomeric pull, pull inductive substitution pattern that stabilizes the carbene. The electron deficiency of carbenes can be reduced by the donation of the two nitrogen lone pairs, all the while; the lone pair of carbene is stabilized by the inductive effect of two electronegative nitrogen atoms. However, the idea that a carbene should have at least one π-donor heteroatom for isolation has been shown to not necessarily be true. Bertrand *et al.* reported the preparation of (diisopropylamino)cyclopropenylidene **103**, boasting stability at room temperature as well as a carbene center that is not stabilized by adjacent π-donor hetero atoms. The carbene **103** was obtained through the reaction of cyclopropenium tetraphenylborate **102** with potassium bis(trimethylsilyl)amide (KHMDS) at

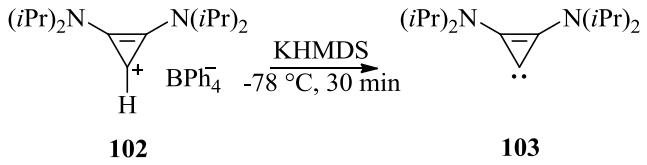

102 **103**

Scheme 25. Synthesis of bis(diidopropylamino)cyclopropenylidene.

-78 °C, for half an hour (Scheme 25).[65] After this time, the ^{13}C NMR signals at 99 and 133 ppm, corresponding to the ring carbons of **102** were disappeared; however new signal appeared at 185 and 159 ppm which predicted for **103**. The interaction of the nitrogen lone pairs with the π system of the ring was proven through X-ray diffraction, in which the amino groups of cyclopropenylidene **103**, and cationic precursor **102**, are close to a coplanar geometry. Cyclopropenylidene **103** has a singlet ground state due to angular constraint and is stabilized through interaction of the nitrogen lone pairs with the π system of the ring.[65]

1.2.1.4. Divalent Nitrogen (I)

The low oxidation state of nitrogen as a main group element alongside carbon, phosphorus, and so on, has involved as an intensively investigated field of chemistry due to the novelty associated with the unusual chemical environment. In general atomic nitrogen possesses five valence electrons. In most organic compounds, nitrogen uses three electrons to form bonds with neighboring atoms, reserving the remaining two electrons to form a lone pair. Similarly, carbon is normally found as a tetravalent atom; however, it can deviate from this in certain situations. Some common examples of this alteration of orbitals include carbon monoxide, carbenes, and isonitriles; this flexibility extends carbon's versatility throughout chemistry. Continuing this concept, carbodicarbenes **104** and **105** (Figure 18) illustrate two separate carbenes or a carbene and a phosphine, ligated to a central zerovalent carbon. **104** and **105** have been synthesized by Fürstner *et al.*,[66] and later used as a model by Alcarazo *et*

al.[67] They envisioned that the central carbon could be replaced by an isoelectronic N^+ fragment to produce a cation such as **106** (Figure 18). However, the nitrogen with positive charge which has been introduced in the systems can prevent interaction with metal centers. Therefore to neutralize the positive charge on the nitrogen a subsequent structural change

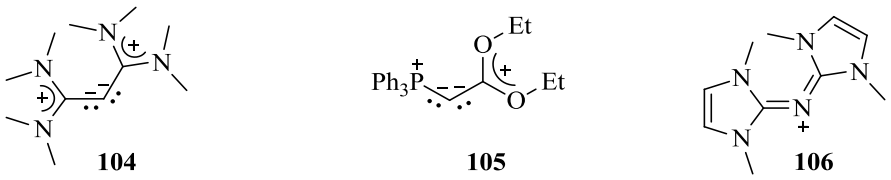

Figure 18. Representative structures of carbodicarbenes **104**, **105**, and bis(carbene)iminium cations **106**.

was needed. To bring this structure to light, Alcarazo *et al.*[67] synthesized compound **110** (Scheme 26), starting with the mesitylation of readily available chlorocyclopropenium salts **107** with mesitylamine to give amine **108**. This was followed by deprotonating with KH (or KHMDS), giving the desired product in two mesomeric form of **109** and **109′**. To evaluate

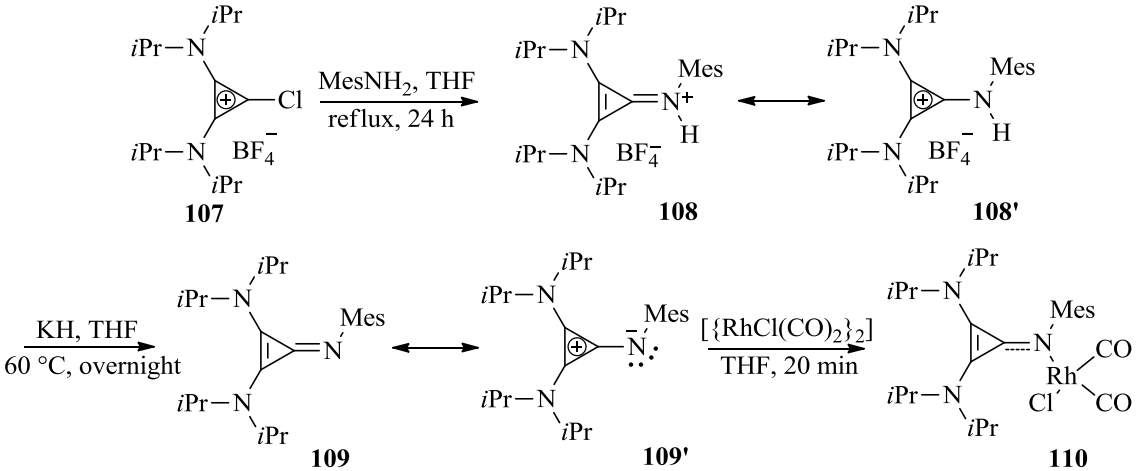

Scheme 26. Synthesis of complex of [RhCl(CO)$_2$•**109**].

the donor ability of this ligand, the complex of **110** was prepared by reacting **109/109′** with [{RhCl(CO)$_2$}$_2$]. The X-ray structure revealed that in the free ligand, the mesomeric structure **109** has more contribution than **109′**. However, after coordination to rhodium, the bond distance between the nitrogen (I) and carbon of cyclopropenyl elongated; allowing for the cyclopropenyl system to return to its aromatic state. This cyclopropenyl moiety can be considered as an electron source. The cyclopropenyl loses aromaticity in the free ligand due to donation of the π-electron density by imino nitrogen. However, as nitrogen coordinates to Rh, electron density transfers to the metal and cyclopropenyl moiety compensates the positive charge on the nitrogen and regain aromaticity. As such, the calculated total negative charge on the nitrogen atom remained constant. To explore the characterization of this novel structure, the properties of the bonds were investigated using DFT calculations at BP86(RI)/TZVP level. The results generated from the frontier orbitals show that the HOMO and HOMO-1 correspond to π- and σ-type lone-pair orbitals and maximum coefficients reside at the central nitrogen atom. This finding suggests the nitrogen of compound **109** as a divalent nitrogen(I). Having two available lone pairs localized on the nitrogen conducted the study of reactivity and coordination property of the compound **109**. As such, **109** was reacted with both a soft Lewis acid [AuCl(Me$_2$S)] and a hard Lewis acid B(C$_6$F$_5$)$_3$, affording metal complex **111** and **112** respectively, in good yield (Figure 19).[67]

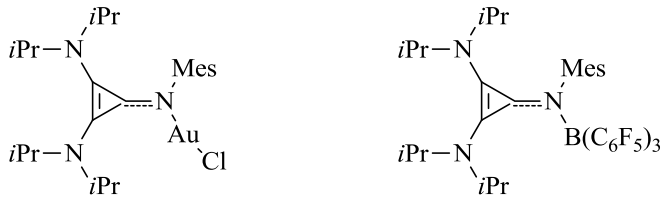

Figure 19. Coordination of compound **109** with AuCl and $B(C_6F_5)_3$.

Three years after the synthesis and characterization of **109**, Alcarazo *et al.*[68] isolated compound **114** from the reaction of readily available chlorocyclopropenium tetrafluoroborate **113** with $KN(SiMe_3)_2$ in THF. X-ray diffraction analysis confirmed the presence of a central nitrogen atom bridging two cyclopropenyl moieties (Scheme 27). Compound **114** was further described as an intermediate between two mesomeric forms: an *N*-cyclopropenium cyclopropenylimine **114a** and N^+ cation **114b**, stabilized by the donation of two cyclopropenylydene moieties simultaneously. The formal oxidation state of the

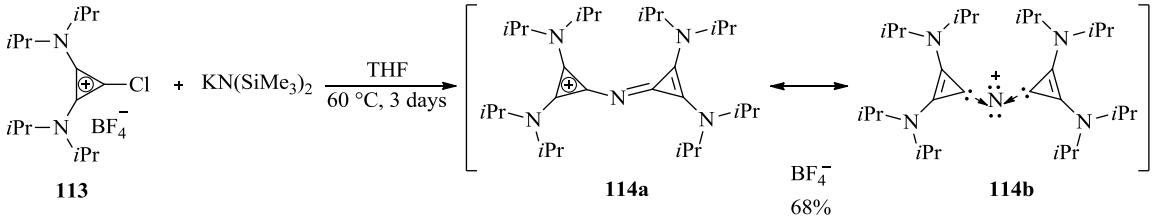

Scheme 27. Synthesis of two mesomeric forms of **114a** and **114b**.

nitrogen atom in compound **114** is +1 and as such, this atom is electron rich. Cyclic voltammetry experiments illustrate two reversible one-electron oxidations at $E_{1/2}$ = -0.407 and -1.046 V, versus Fc^+/Fc which confirms nitrogen is an electron rich atom in compound **114**. In addition, protonation of the nitrogen in compound **114** could be carried out with

strong Brønsted acids, such as HBF_4 or $HGaCl_4$. This finding suggests that the cyclopropenylidine moiety acts as an ancillary ligand. As expansion of this work, two equivalents of **113** were reacted with $PhN(SiMe_3)_2$ to afford the salts **115** (Scheme 28).[68]

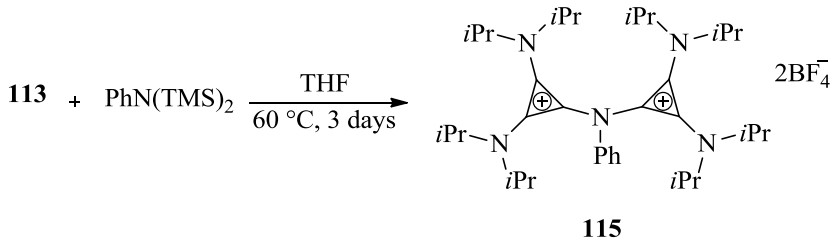

Scheme 28. Synthesis of bis(cyclopropenium) substituted amines.

The central divalent nitrogen (I) possesses two lone pairs and stabilized by cyclopropenylidene substituents in a trigonal planar geometry, has an unusual chemical environment. It has been envisioned that this class of compounds have potential to use in coordination chemistry and catalysis, however specific applications in this area of research are still under investigation.

1.2.1.5. Application of Divalent N(I) Complexes as a Phase-Transfer Catalyst (PTC)

Phase transfer catalyst (PTC) compounds are catalysts which allow the migration of a reactant from one phase to another phase. Generally ionic reactants are soluble in an aqueous phase and insoluble in organic phase. In heterogenous two- phase system, phase transfer catalysts cause or accelerate the reaction between the ionic reactants, and the substrate soluble in the organic phase. The catalyst possesses a lipophilic cation which allows it to reside in the organic phase. The reagent, as an anionic species in the form of lipophilic counterion, introduces itself into the organic phase continuously. Phase-transfer catalysis is attractive for industrial applications due to the low cost, operational simplicity, and

commercial availability. To have a sustainable catalyst, the lipophilic cation portion of the catalyst should be stable in the basic/nucleophilic reaction conditions. However, most organic cations suffer from a lack of stability in concentrated aqueous alkali hydroxide solutions, or in the presence of strong nucleophiles, especially at high temperature. As such, there is growing interest in the development of stable organic cations in the field of Phase-transfer catalysis.[69]

In 1991, Schwesinger *et al.*[70] reported a stable and easily accessible phosphazenium fluoride **118**•F^- as a source of naked fluoride ions in THF solutions (Scheme 29). The synthesis started with the reaction of PCl_5 with NH_4Cl to give salt **116**. Subsequent addition of dimethylamine and $NaBF_4$ afforded **118**•BF_4^-. Also, hexamethylphosphoric triamide (HMPA) and salt of **117** were formed as a by-product. It was found that peralkylated cation **118** showed much higher stability towards nucleophiles than conventional organic cations.

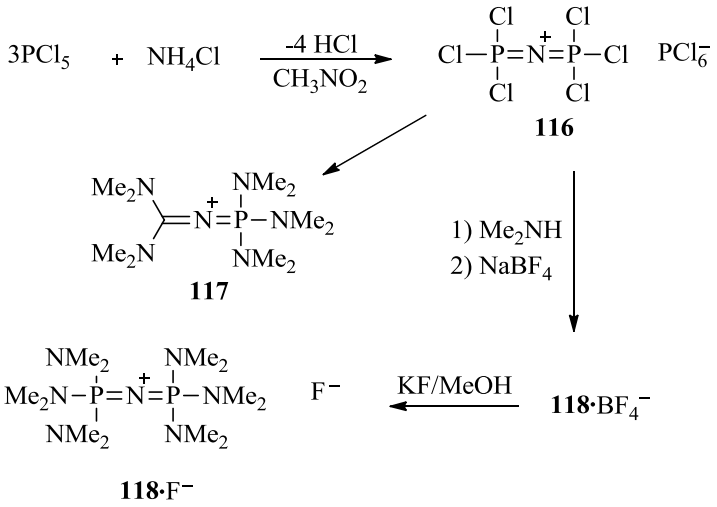

Scheme 29. Synthesis of phosphazenium fluoride salt **118**•F^-.

The commercially available tetrakis{[tris(dimethylamino)phosphoranyliden] amino}phosphonium fluoride (P_5-phosphazenium cation, Figure 20) has been used for the production of high-quality polymeric materials on an industrial scale. The cation stability of

the P_5 cation requires a high molecular weight for delocalization of the positive charge through the network containing P and N atoms. Drawing upon the known similarity of N-heterocyclic carbenes (NHC) and phosphines, both considered to be strong σ-donors yet poor back-bonding π-acceptors, Lyapkalo *et al.*[71] in 2009, prepared a series of bis(*N*,*N*'-dialkylimidazolium)amides (BIMA) **123a-c** from tetraalkylimidazolin-2-ylidene precursors **120a-c.** These were derived from 1,3-dialkyl-4,5-dimethyl-1H-imidazole-2(3H)-thiones **119a-c**. Conversion of **120a-c** to **121a-c** using C_2Cl_6 and **120a-c** to **122a-c** employing Me_3CN_3, NH_4BF_4 was carried out. KF-mediated coupling of the two salts of **121a-c** and corresponding derivatives **122a-c** afforded BIMA salts **123a-c** (Scheme 30). Interestingly, there was no explicit mention in the aforementioned report that the prepared phase-transfer catalyst was conformed to be a divalent N(I) complexes (e.g., N(I)(←:L)$_2$) (L = NHC; *N*,*N*'-dialkyl-4,5-dimethylimidazol-2-ylidenes).

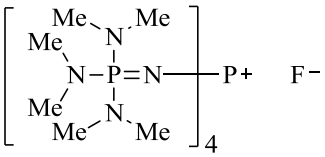

Figure 20. Structure of tetrakis{[tris(dimethylamino)phosphoranyliden] amino}phosphonium fluoride**.**

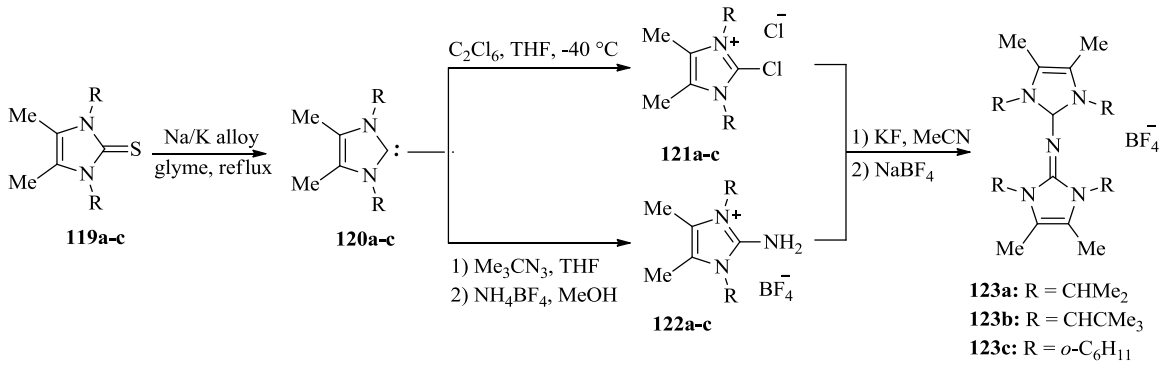

Scheme 30. Synthesis of the BIMA salts.

The hydrolytic cleavage of **123a** gave the imidazolinone derivatives **124** and **125** (Scheme 31). In the rate-limiting step, OH^- attacked the carbon center of **123a**, which in turn dearomatized the imidazolium ring. As such, an enhancement in the activation barrier resulted in an increased base resistance. Table 2 shows the half-lives of the organic cations

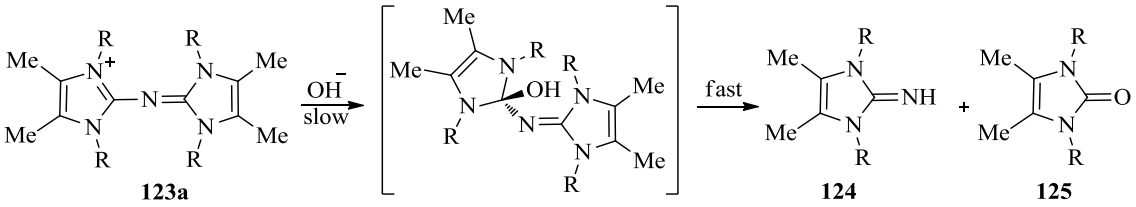

Scheme 31. Hydrolytic cleavage of the BIMA cation.

123a-c while vigorously stirred and refluxed, in a biphasic mixture of PhCl/50% aqueous KOH. The neopentyl-substituted cation **123b** displayed the most stability in the BIMA series. The stability of BIMA cations can be explained by the distribution of the positive charge throughout aromatic imidazolium moiety.[71]

Table 2. Half-lives of the organic cation **123a**. Condition: vigorously stirred biphasic mixture of PhCl/50% aqueous KOH, reflux (115 °C inner temperature, 145 °C oil-bath temperature).

Entry	Compound	Reaction time [h]	Conversion [%]	$t_{½}$ [h]
1	**123a**.BF_4	24	42	31
2	**123b**.BF_4	48	trace	Stable
3	**123c**.BF_4	21	33	36

Furthermore, additional steric protection is produced by the presence of bulky *N*-alkyl groups, as well as a decrease in Hofmann degradation due to the low charge density on the endocyclic nitrogen atoms. This was especially true in the case of the tetraneopentyl cation

123b. The synthesized imidazolium cations **123a-c** were stable in basic conditions at elevated temperature. The stability of the compound **123a-c** can be attributed to the distribution of positive charge through the aromatic imidazolium moiety. In addition, bulky *N*-alkyl groups on the nitrogen of imidazolium moiety provide higher stability due to steric hinderance. Overall, the possibility of Hofmann degredation was strongly diminished due to the aforementioned stability of the synthesized imidazolium cations. The stability of these cations paved the way for their application as a phase-transfer catalyst under harsh reaction conditions.[71]

Building upon Lyapkalo *et al.*, Tan and co-workers[72] worked with bicyclic guanidines, containing five nitrogen atoms in conjugation, as chiral Brønsted base catalysts for enantioselective reactions. They rationalized that the basicity of conjugated penta-nitrogen systems can be greater than guanidine. As such, they recently reported a number of structurally related C_2-symmetric chiral catalysts **129** that were christened Pentanidium (Scheme 32). It was found that Pentanidium was as an excellent phase-transfer catalyst and had successful application in catalytic enantioselective Michael addition reactions. The synthesis of pentanidium chloride **129a** started from commercially available (S,S)-diphenyldiamineoethane **126**, which, with simple manipulations, gives imidazoline salt **127**. Subsequent conversion of salt **127** to imine **128** and condensation of **127** and **128** afforded pentanidium chloride **129** (Scheme 32). Using the catalyst **129a-e** as a chiral phase-transfer

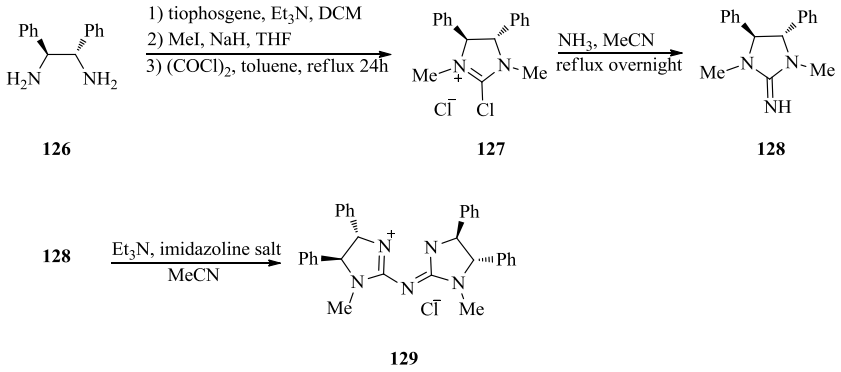

Scheme 32. Preparation of Pentanidium chloride **129**.

catalyst for Michael addition reactions of *tert*-butyl glycinate-benzophenone Schiff base **130** with various *α,β*-unsaturated acceptors **131a-f**, afforded products **132a- f**, with ee of up to 97% (Scheme 33). In addition, the same conditions were used for reactions of Schiff base

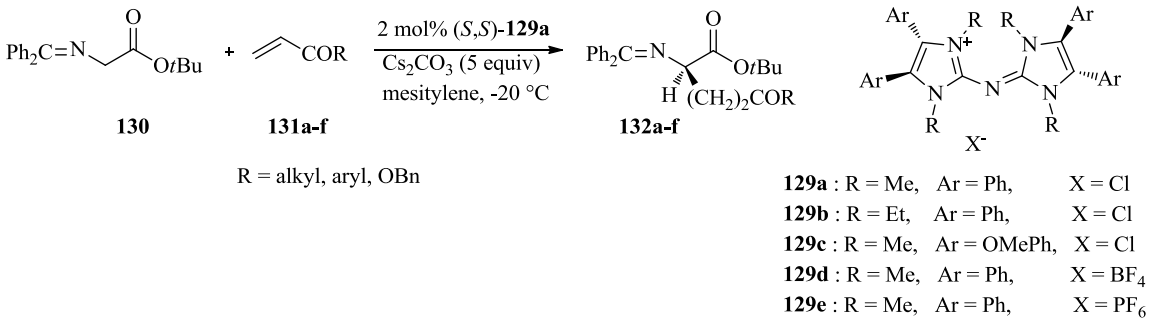

Scheme 33. Michael addition of *tert*-butyl glycinate-benzophenone Schiff base to various a,b-unsaturated acceptors.

133 with chalcones **134a-f** which led to adducts **135a-f** as a single diastereomer and ee up to 94% (Scheme 34). The developed chiral pentanidium exhibited potential applications as a phase-transfer catalyst and employing the catalyst in Michael addition reaction led to high diastereo- and enantioselectivity.[72]

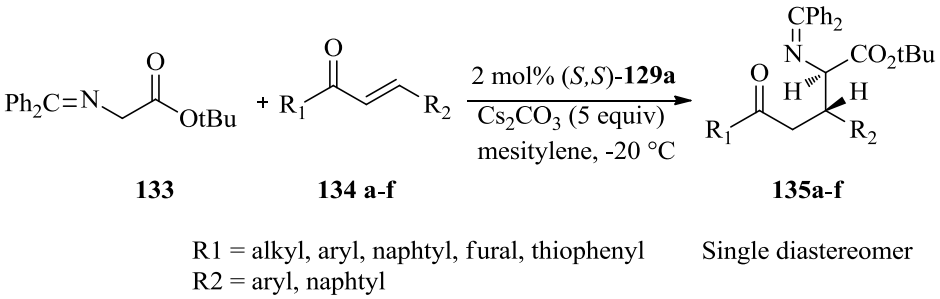

Scheme 34. Michael addition of *tert*-butyl glycinate-benzophenone Schiff base to various chalcones acceptors.

1.3. Fluorination

1.3.1. Historical

Fluorine is the lightest halogen and the most electronegative element. Although fluorine is the 13th most abundant element within the earth's crust,[73] only 21 biologically-synthesized natural products containing fluorine have been identified. Notwithstanding, a large number of fluorine containing compounds are known to possess biological activity and are useful in medical applications, including pharmaceuticals, and ^{18}F-labeled compounds used for positron-emission tomography (PET, a powerful, noninvasive tool for the in vivo, three-dimensional imaging of physiological structures and processes). Not surprisingly, at least one fluorine atom is present in *ca*. 20% of all pharmaceuticals and *ca*. 40% of all agrochemicals.[74-78] Accordingly, the development of methods for introducing fluorine into organic molecules has gained considerable traction in the past decade as fluorine is known to impart useful physicochemical properties, such as improved solubility, bioavailability, lipophilicity, and metabolic stability compared with non-fluorinated analogues. Historically, one of the most common protocols for incorporating fluorine into organic molecules has been the well-known Balz-Schiemann reaction. One classic example of this reaction involves the

thermal decomposition of aromatic diazonium tetrafluoroborates (**137**), which can be obtained from the reaction of aniline **136** with nitrous acid, affording aromatic fluorides **138** (Scheme 35).[1] Another conventional method is the halogen exchange (Halex) reaction of

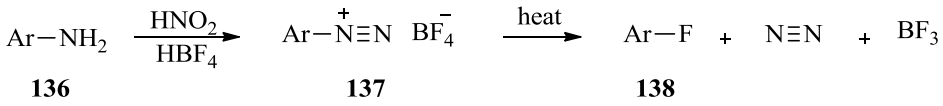

Scheme 35. Fuorination of aryl diazonium salts with HBF_4 (Balz–Schiemann reaction).

activated aryl halides, which for instance was reported to afford fluorinated product **141** in 91% yield from intermediate **140** which was prepared from **139** with metal fluorides (Scheme 36). A major limitation of this approach, however, was the use of spray-dried KF and a high-boiling point polar aprotic solvent, such as sulfolane. Factors that, in practice complicated matters, but through the use of a phase-transfer catalysts, improved the solubility of the fluoride ion were overcome rendering the approach effective.[79]

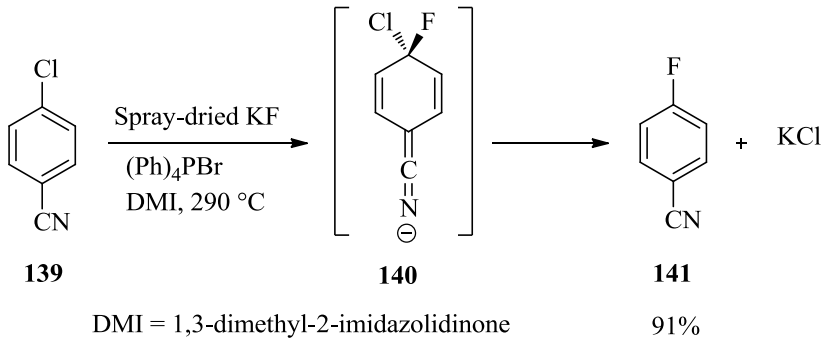

Scheme 36. A classic Halex reaction.

Though an isolated example, it deserves mention that the requirement of high temperatures and activated substrates has limited Halex reaction as a general protocol. Nevertheless, to overcome this limitation a number of transition-metal-mediated aromatic

$C(sp^2)$–F bond forming reactions have been developed. However, the methods for formation of $C(sp^3)$–F bond still remain limited. The present protocols for synthesis of alkyl fluorides involve nucleophilic or electrophilic substitution reactions or radical fluorintion.[80] Among these methods for the introduction of fluorine, the most commonly method is nucleophilic substitution of aliphatic halides or sulfonates by fluoride. Frequently, alkali metal fluoride was used as a nucleophilic component towards halides or sulfonates, however, this reaction required high temperature, or long reaction time to overcome the low solubility and reactivity of the reagent.[81] The focus of the following sections would be on the use of (PTC) to promote nucleophilic substitution of aliphatic halides or sulfonates by fluoride ion.

1.3.1.1. Reaction of Alkyl Halides and Methanesulfonates with Potassium Fouoride in the Presence of Phase Transfer Catalysts.

In a heterogenous system, in the presence of phase-transfer catalyst, unassociated halide ions can be obtained. In these systems, anionic reagents continuously transfer from an aqueous to an organic phase by means of organic cations. Anions would be reactive, in the case of the poor solvation and low energy of interaction with the cation. In 1974, Montanari *et al.*[82] reported displacement of primary or secondary alkyl chloride and alkyl bromides by fluorine under vigorously stirring at 100-160 °C with a saturated aqueous solution of potassium fluoride and catalytic amounts of hexadecyltributylphosphonium bromide. Reaction of 1-chloroalkane in presence of 5 mol of potassium fluoride at 160 °C in 6-8 h afforded alkyl fluorides in 80% yield and olefins as well as primary alcohols as a by-products. The same results were obtained by using 1.5 mol potassium fluoride with longer reaction times, approximately 16 h. When reaction was conducted at lower temperatures

(110-120 °C) after 8-10 h only 25-30% conversion was happened, even the use of an excess of potassium fluoride did not change the percentage of conversion. However, benzyl chloride was converted to the corresponding fluoride at 120 °C after 7 h in high yield. The conversion of secondary halo derivatives was noticeably slower, and elimination products predominated over substitution products. The ratio of elimination products to substitution products increased as the temperature was elevated. In 1984, Cox *et al*.[83] reacted anhydrous tetrabutylammonium fluoride (TBAF) with a halo- or tosyl- substituted organic compounds such as allylic, benzylic, primary, secondary, and tertiary which afforded corresponding fluoro compounds with 48-98% yield. Significantly, these reactions were conducted at low temperatures between 25-40 °C and short reaction times of 0.1 to 8 h. In the case of 2-bromooctane and 2-octyl tosylate, elimination of HBr and TsOH predominated rather than fluorination due to the fact that anhydrous TBAF can behave as a potent base rather than as a nucleophile. However, hydrolysis of the substrate halide or tosylate, such as benzyl bromide, chlorotriphenylmethane, or 1-bromooctane, to the corresponding alcohol was a significant side reaction. The alcohol products likely were formed by the remaining traces of moisture in the reagent. Moreover, the reaction of anhydrous TBAF with (-)-2-octyltosylate yielded (+)-2-fluorooctane in good yield and 100% optical purity. Based on the comparison of the value and sign of the specific rotation of resulting (+)-2-fluorooctane with the previously reported,[84] the discussed fluorination reaction proceeds *via* an S_N2 mechanism. In this context, and considering the higher leaving group ability of triflates compare to halides, mesylates, or tosylates, Shin *et al*. [85] investigated the reactivity of triflates in presence of fluoride ion species which are less nucleophilic compared to TBAF. As such, the basicity of fluoride would be reduced and the formation of the elimination side product would be

minimized. Therefore, the reaction of triflate **142** (figure 21) with tetrabutylammonium fluoride (TBAF), bifluoride (TBABF), dihydrogen-trifluoride (TBADTF), and hydrogen fluoride pyridine complex, which are less nucleophilic and less basic in character, were tested. The best result was obtained by using an *in situ* formed solution of triflate **142** in dichloromethane with TBABF. Formation of the elimination product under these conditions was only 3%, while the use of TBAF gave 28% elimination product in the same reaction condition. The same level of elimination product formed using less basic dihydrogen trifluoride, however, high quantity of unidentified by-product yielded. With the least basic hydrogen fluoride pyridine complex, only decomposition of **142** was obtained. In addition, a

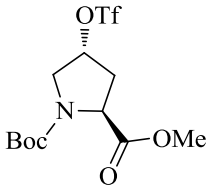

142

Figure 21. Stucture of proline **142.**

number of primary alcohols such as **143** were tested under the condition shown in Scheme 37, to afford the fluorinated products of **145** through intermediates **144** with up to 92% yield in 1h. For secondary acyclic alcohols, the elimination reaction was happened in the range of between 7 to 46%. In addition, having ester or lactone group at α position to hydroxyl groups gave excellent yields.[85]

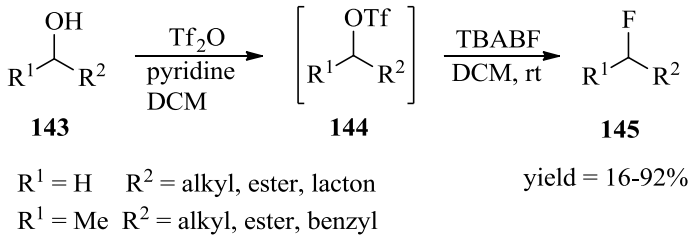

Scheme 37. Nucleophilic fluorination of triflates substrates.

A new type of phase-transfer catalysis was introduced by Makosza *el al.* [86] in which fluoride anions transfer to the organic phase in the form of potassium difluorotinorgano-stannate. Initially, in these reactions triorganotin fluorides in presence of solid KF form hypervalent difluorotinorganostannate anions. Subsequently, ion exchange with tetraalkylammonium (TAA) salts Q^+X^- produce liphophilic ion-pairs of the difluorotinorganostannate with TAA cations. These ion-pairs transfer to organic phase and react with R–X to afford R–F and triorganotin fluoride. Reaction of resulting triorganotin fluoride with KF reproduces difluorotinorganostannate to participate in another reaction sequence (Scheme 38). Notably, they found that fluorination of alkyl halides in sulfolane

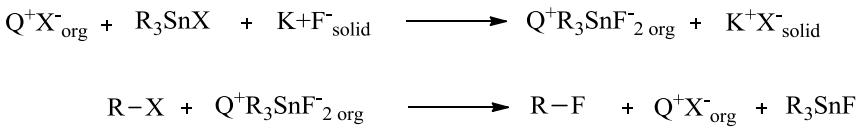

Scheme 38. Fluorination of alkyl halide using hypervalent difluorotriorganostannate.

proceeded without Q^+X^- , it means that R_3SnX promoted the reaction by itself. As a result, hypervalent anion $R_3SnF^-_2K^+$ should be sufficiently soluble in the solvent to react with R–X. Accordingly, they presented new concept of PTC in which complexation of reacting anion with appropriate catalyst produce lipophilic anions. The solubility of the potassium salts of these liphphilic anions are sufficient for transferring to the organic phase. The reaction of the

complexed anion in organic phase liberates catalyst, which in turn forms a new complexed anion (Scheme 39). Makosza *el al*. tested triphenyltin fluoride for fluorination of benzyl

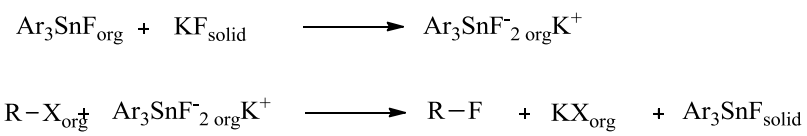

Scheme 39. Fluorination of alkyl halide using potassium difluorotriarylstannate.

bromide in different solvent systems and it was found that sulfolane and DMF gave 54% while acetonitrile afforded only 3% yield. As it is shown in Table 3 alkyl –mesylates, –tosylate, and -halide gave fluorination products with 70-100% yield determined by GLC.[86]

Table 3. Fluorination of alkyl -mesylates and –tosylate with triphenyltin fluoride in different solvent systems.

R–X	Solvent	Temperature (°C)	Time (h)	Yield[a] (%) of R–F
$PhCH_2Br$	Mix[b]	95	24	100
$PhCOCH_2Br$	Sulf	85	4	92
$PhCOCH_2Br$	Mix	95	4	70
n-$C_8H_{17}OMs$	Sulf[c]	105	24	90
2-$C_8H_{17}OTs$	Sulf	85	48	80
4-$NO_2Ph(OMs)CHCH_3$	Mix	95	8	85

[a] Yield determined by GLC.
[b] Mix-sulfolane+acetonitrile, 1:2.
[c] Sulfolane.

1.3.1.2. The Role of the Solvent in Nucleophilic Fluorination

The solubility of fluoride ion even in highly polar aprotic solvents such as dimethyl sulfoxide (DMSO) is low due to the high ratio of charge/volume of fluoride ion. It has been show that the free fluoride ion is very reactive and performs both S_N2 and E2 reactions. For secondary halides the E2 process is predominant and this limits use of nucleophilic fluorination of secondary halides. In addition, in less solvating media elimination reactions become more important. In an aprotic solvent, if fluoride ion could be associated with some molecules of water, the reactivity of the fluoride ions decreases which in turn would lead to higher ratio of S_N2 to E2 products. The reactivity (i.e. nucleophilicity or basicity) of the anions with localized and/or less polarizable charge would be more affected with the hydration.[87]

The tendency of fluoride to interact with protic solvents leading in strong hydrogen bond is well-known.[87] As such, Landini *et al*.[87] studied the effect of hydration on both nucleophilicity and basicity of lipophilic quaternary ammonium fluorides in low polar solvents. They reacted $hexyl_4N^+F^-\bullet nH_2O$ with *n*-octyl methanesulfonate in chlorobenzene, where *n* is ranging from 0 to 8.5. It was found that reactivity of fluoride diminished by a factor of 10^3 as the hydration increased. This shows that clusters of $F^-(H_2O)_n$ have been formed due to the strong fluoride-water interaction energy. Therefore, fluoride ion becomes less reactive and the ratio of S_N2 process versus E2 increased. The same results were obtained by Albanese *et al*.[88] from the reaction of $Bu_4N^+F^-\bullet nH_2O$ with 1-bromooctane in acetonitrile or without solvent. They found that the ratio of S_N2 process versus E2 increases with n value, yield reached to 91% at 80 °C after 2 h where *n* = 5. However, in the reaction of 2-bromooctane, the hydrated fluoride is less selective and gave 30-40% yield. Accordingly, it has been suggested that the reaction must proceed through a hydrated transition state as depicted in Figure 22.[89]

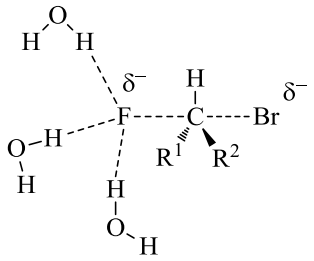

Figure 22. Model for the hydrated fluoride ion reaction.

It is well-known that in nucleophilic displacement, polar aprotic solvents such as acetonitrile and dimethylformamide (DMF) are better than protic solvents.[90] That is due to the solvation of the cations in polar aprotic solvents which increases the nucleophilicity of the anion; in protic solvents the interaction between the anions and partial positive charge of

protic solvents renders a reduction in nucleophilicity. In this context, Chi *et al.*[90] used nonpolar, protic tertiary alcohols as a reaction media for the nucleophilic fluorination with alkali metal fluoride. They tested fluorination of mesylate **146** with 3 equiv of CsF in CH_3CN, DMF, 1,4-dioxane, and benzene, the naphthalene product **147a** was obtained in very low yields, with alcohol **147b** and alkene **147c** as byproducts (Scheme 40). However, when the reaction was conducted in *t*-BuOH, fluoroalkane **147a** was produced within 6 h in high yield (92%) with small amounts of the ether byproduct **147d**. The RbF and KF were less reactive for fluorination in *tert*-alcohol media, with RbF afforded 76% and KF gave trace of the product. It was found that sterictlly hindered *tert*-amyl alcohol was the best solvent among the alcohols that were tested for this reaction. Using *tert*-amyl alcohol gave the fluoroalkane **147a** in 94% yield and reduced reaction time of 2.5 h at 90 °C.

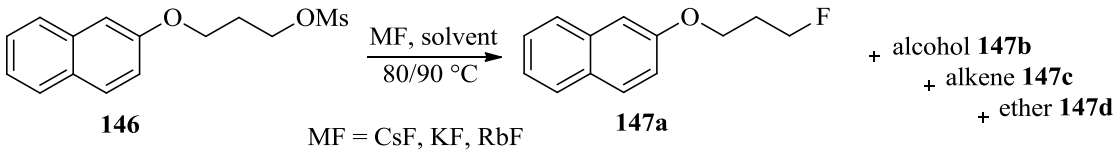

Scheme 40. Fluorination of mesylate **146** with metal fluorides.

Given the utility of fluorine in pharmaceuticals, agrochemicals, materials, and tracers for positron emission tomography, it is not a surprise that this element always attracted attention of the chemists. In this regards, traditionally, alkali metal fluorides have been used for the fluorination of the corresponding alkyl sulfonate or halides. However, fluorination with alkali metal fluorides requires harsh conditions due to the low solubility and nucleophilicity of the fluoride source in organic solvents. Furthermore, to improve the fluorination reaction, "naked" fluoride ion which is weakly associated with cations or solvent molecules was used. A number of phase-transfer catalysts such as crown ether and

quaternary ammonium fluoride derivatives have been introduced to increase the nucleophilicity and solubility of fluoride ions in organic solvent, accelerating the nucleophilic displacement. However, further research is essential to develop more practical and general fluorination reactions.

2. Results and Discussions

2.1. Synthesis of Biologically Active Compounds.

2.1.1. $C_{(1)}$-Chiral 3-methylene-indan-1-ols.

The Lewis acid-catalyzed Sakurai-Hosomi allylation and palladium-catalyzed Mizoroki-Heck cross-coupling reactions represent two of the most powerful and widely utilized C–C bond forming reactions in the field of synthesis. Moreover, with the ever increasing demand for highly-optically enriched materials, such as agrochemicals and chiral pharmaceuticals, it is noteworthy that asymmetric versions of the Heck and Sakurai reactions have also been developed.

As for the above advancements, the (*R*)- and (*S*)-BINAP•$Ag^{I}F$ catalyzed asymmetric Sakurai-Hosomi-Yamamoto allylation reaction is considered as being one of the most effective means for preparing chiral homoallylic alcohols.[20] It is also noteworthy that a number of other synthetically useful procedures for carrying out the catalytic enantioselective allylation of carbonyls have been reported, including those by Denmark, Schaus, and Keck.[3,91,92] Likewise, the asymmetric Mizoroki-Heck reaction has been well studied over the last three decades and notably several methodologies for constructing chiral quaternary centers have been developed.[93]

Accordingly, we was attracted by the potential development of an annulative $Ag^{I}F$ and $Pd^{II}Cl_2$-catalyzed asymmetric Sakurai-Hosomi/Mizoroki-Heck reaction sequence for the synthesis of biologically active $C_{(1)}$-chiral 3-methylene-indan-1-ol products **148a** (Scheme 41).

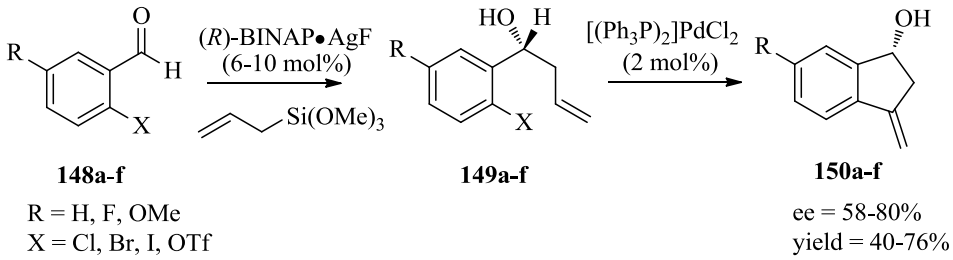

Scheme 41. Synthesis of $C_{(1)}$-chiral 3-methylene-indan-1-ols derivatives *via* a sequential (*R*)-BINAP•$Ag^{I}F$ catalyzed allylation/$(Ph_3P)_2Pd^{II}Cl_2$ Heck alkenylation reaction.

The hypothesis at the outset of this work was that a sequential, or possibly concurrent, pair of catalytic reaction cycles that are shown in Figure 23 would provide routine access to optically enriched products such as **150a-f**. As for the mechanistic elements of this catalytic event, Cycle 1 corresponds to a Sakurai-Hosomi-Yamamoto allylation that establishes $C_{(1)}$-chirality *via* the formation of homoallylic alcohol **149a**. In Cycle 2, **149a** undergoes a 5-*exo*-trig ring closing Mizoroki-Heck reaction to afford enantioenriched **150a**.

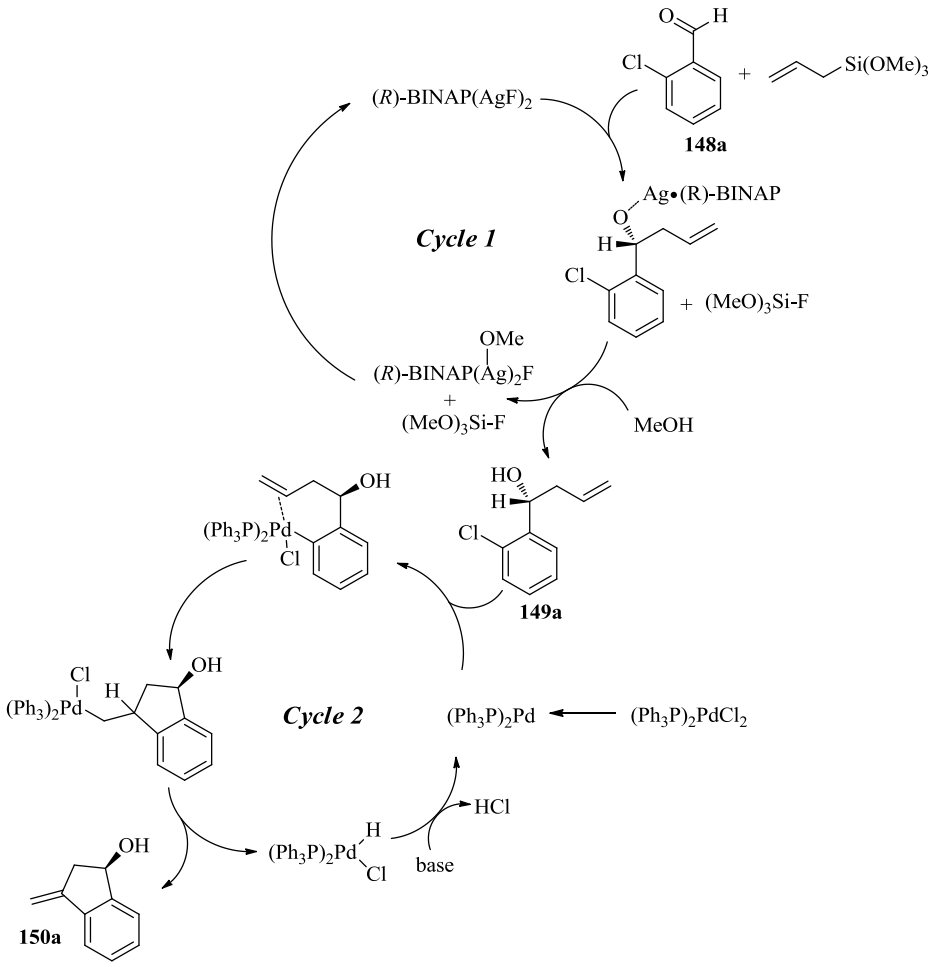

Figure 23. Proposed catalytic cycle for formation of $C_{(1)}$-chiral 3-methylene-indan-1-ols.

With this mechanistic proposal in mind, a one-pot concurrent tandem catalysis (CTC) reaction using 2-chlorobenzaldehyde (**148a**) (1.0 eq), allyltrimethoxysilane (1.8 eq) and (*R*)-BINAP•$Ag^{I}F$ (6-10 mol %) and $(Ph_3P)_2Pd^{II}Cl_2$ (2 mol%) in MeOH was attempted that only afforded an intractable mixture of products.

Nevertheless, it was felt confident that the envisioned reaction sequence could be achieved. As such, a subsequent reaction utilizing sequential tandem catalysis (STC) conditions afforded the targeted $C_{(1)}$-chiral indanol product **150a** with moderate ee = 68% in 45% yield (Table 4, Entry 1). Having found this to be the optimal set of reaction conditions

we then set out to explore the substrate scope of this reaction. The more sterically demanding and electron deficient substrate *o*-bromobenzaldehyde (**148b**) resulted in the formation of **150b** in slightly higher ee than **148a** (Table 4, Entry 2 vs 1). This result was unexpected, as in general, marked erosion in enantioselectivity is observed when *o*-substituted arylaldehydes are used in catalytic asymmetric allylations. The sterically more demanding *o*-iodobenzaldehyde substrate **148c** was then reacted which afforded the desired indanol **150a** with even higher ee (Table 4, entry 3). In order to explore this trend further we tested the sterically demanding *o*-trifluoromethylsulfonylated substrate **148d**. Under these reaction conditions no reaction occurred and only starting material and decomposition products were obtained (Table 4, Entry 4). Further exploration of the reaction scope demonstrated that electron-rich 2-bromo-5-methoxybenzaldehdye **148e** afforded **150e** of comparable ee to **150a** (Table 4, Entry 5). In contrast, the use of the electron-deficient 2-bromo-5-fluorobenzaldehyde **148f** resulted in a dramatic decrease in product ee (Table 4, Entry 6).

Table 4. Sequential (*R*)-BINAP•$Ag^{I}F$ catalyzed allylation[a]/$(Ph_3P)_2Pd^{II}Cl_2$ Heck alkenylation [b] reaction of functionally different electrophilic aldehydes.

		Step 1		Step 2				
Entry	Substrate	Intermediate	Yield [b] (%)	T (°C)	t (h)	Product	Yield [c] (%)	ee [d] (%)
1	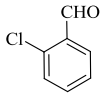 **148a**	**149a**	91	100 130	48 24	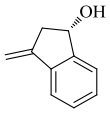 **150a**	0 45	-- [e] 68
2	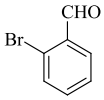 **148b**	**149b**	80	100	24	**150a**	73	75
3	 **148c**	**149c**	81	100	12	**150a**	64	80
4	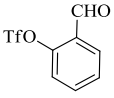 **148d**	**149d**	0				--	--
5	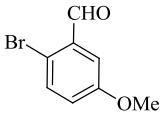 **148e**	**149e**	64	100	24	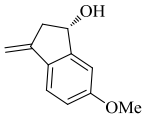 **150e**	76	74
6	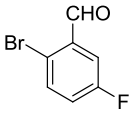 **148f**	**149f**	67	100 130	48 24	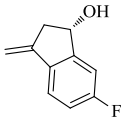 **150f**	0 40	-- 58

Reaction conditions: [a] (*R*)-BINAP•$Ag^{I}F$ (6-10 mol%), MeOH, -20 °C, 4h. [b] $(Ph_3P)_2Pd^{II}Cl_2$ (2 mol%), DMF. [c] Yields of isolated products after flash chromatography. [d] Enantiomeric excess was determined by HPLC analysis (OD-H). [e] (--) Not applicable.

As a working model transition state **TS1** (Figure 24, X = Cl, Br, I) was proposed to account for the increase in product ee as a function of halogen size (see Entries 1-3, Table 4). **TS1** not only accounts for the increase in product ee observed herein, but also offers a rationale for the enantioselectivity in the Sakurai-Hosomi-Yamamoto allylation reaction. This last point is noteworthy as the precise mechanism for the asymmetric (*R*)- or (*S*)-BINAP•$Ag^{I}F$ Sakurai-Hosomi-Yamamoto allylation reaction is poorly understood at this time.

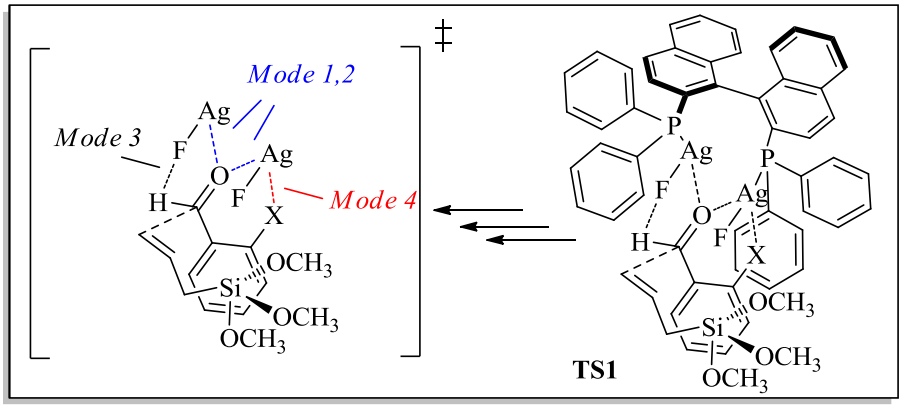

Figure 24. Proposed transition state model **TS1**.

TS1 possesses four energetically favorable binding interactions which reduce to (1) a bifurcated mode (Modes 1 and 2) of aldehyde activation, (2) a conformational reinforcing aldehyde based C–H•••F interaction (Mode 3), and (3) an aryl C–X•••Ag (X = Cl, Br, I) agostic interaction or Ag•••halogen coordination (Mode 4) (Figure 23). Based upon this model it is surmised that the greater level of enantioselectivity found with increasing *o*-aryl halogen size originates from the better donor-acceptor coordinating ability of larger halogens with silver (i.e., mode 4). The strengthening of this C–X•••Ag interaction with growing halogen size results in better (*re*)-stereofacial selectivity in the following order I > Br > Cl, as

a result of increasing transition state stabilization. It is presumed that other non-stereoselective modes of addition do not appreciably benefit from this interaction.

In this work, a dual metal-catalyzed methodology for the synthesis of biological active C_1-chiral 3-methylene-indan-1-ols (ee $\leq$ 80%) was used that hinges upon the sequential use of a Yamamoto's asymmetric Sakurai-Hosomi allylation reaction and a Mizoroki-Heck reaction. Notably, this procedure benefits from the use of various *o*-substituted arylaldehydes, allyltrimethoxysilane and catalytic amounts of (*R*)-BINAP•$Ag^{I}F$ (6-10 mol %) and $(Ph_3P)_2Pd^{II}Cl_2$ (2 mol%).

2.1.2. DFT-Directed Approach to $C_{(3)}$-Chiral Functionalized Phthalides *via* Indium-Mediated Allylative/Transesterification.

The ability of a catalyst or single reagent to promote a desired cascade of reaction events in a single-reaction flask with high enantioselectivity in useful yields represents an efficient strategy for assembling complex synthetic targets, such as natural products. In this context, we were attracted by the possibility of employing a chiral indium reagent or catalyst as a resource for preparing optically enriched, value added, chemicals and/or synthetic precursors of natural products. Driving this interest was the low toxicity, functional group compatibility, and tolerance to air and moisture of inidium which remains underutilized in synthesis at this time (especially in the field of asymmetric catalysis), apart from a few notable examples.[94-96,27] To this end, the development of an enantioselective, indium-mediated, synthetic approach to $C_{(3)}$-chiral substituted phthalides, which are a widely distributed structural motif within a number of biologically active natural products and medicinally important pharmaceuticals, appeared an ideal challenge.

Given the therapeutic properties of $C_{(3)}$-chiral substituted phthalides it is perhaps not surprising that a number of efficient synthetic routes to optically enriched $C_{(3)}$-chiral

phthalides have been reported.[97] Nevertheless, there remains a pressing need for synthetic routes to $C_{(3)}$-chiral phthalides, as the majority of the reported approaches are limited in substrate scope, use expensive and/or toxic rare earth transition-metals, and provide low levels of enantioselectivity.

Fully aware of these limitations, we were drawn towards the possibility of developing a more robust and synthetically efficient strategy for preparing optically enriched $C_{(3)}$-chiral phthalides. Accordingly, we describe here a target-oriented assembly of chiral $C_{(3)}$-substituted phthalides *via* the orchestrated use of rational forethought (*i.e.*, **D**ensity **F**unctional **T**heory (DFT) calculations) in prelude to experimental practice. Notably, this work has also provided, (1) theoretical models for rationalizing the enantioinduction of the reactions, (2) the ligand component used was easily recoverable after the reaction.

At the outset of this work, with the goal of developing an In-mediated protocol for preparing $C_{(3)}$-chiral phthalides, using a reaction scenario such as that outlined in Scheme 42 was envisioned. In this mechanistic proposal, a highly reactive In-allyl species, **154**, is generated *in situ* from **153**, inexpensive indium metal, and allyl bromide (Step 1). Intermediate **154** then reacts with methyl-2-formylbenzoate **151** (Step 2) to give allyl intermediate **155**, which subsequently undergoes a dual In-metal/pyridinium salt (pyr-H^+), catalyzed intramolecular transesterification to afford (*R*)-3-allylisobenzofuran-1(3*H*)-one **152** (step 3). However, due to the frequently observed erosion in the enantioselectivity of catalytic asymmetric allylations of *ortho*-substituted substrates,[23,24,95,98] we were concerned if this process would in fact impart enantioselectivity. For this reason, in keeping with our philosophy of utilizing computation to augment experimental development, we initially turned to DFT calculations to discern to what, if any, extent this process would afford

enantioselection. Thus working under the assumption that allylation was the (*R*)- *vs.* (*S*)-enantioselective determining step of this reaction, the addition of **154** to **151** was modeled using the Gaussian 09 suite of programs at the B3LYP/LanL2DZ level of theory with the IEFPCM dielectric continuum solvation model and the default parameters for THF (ε = 7.6).

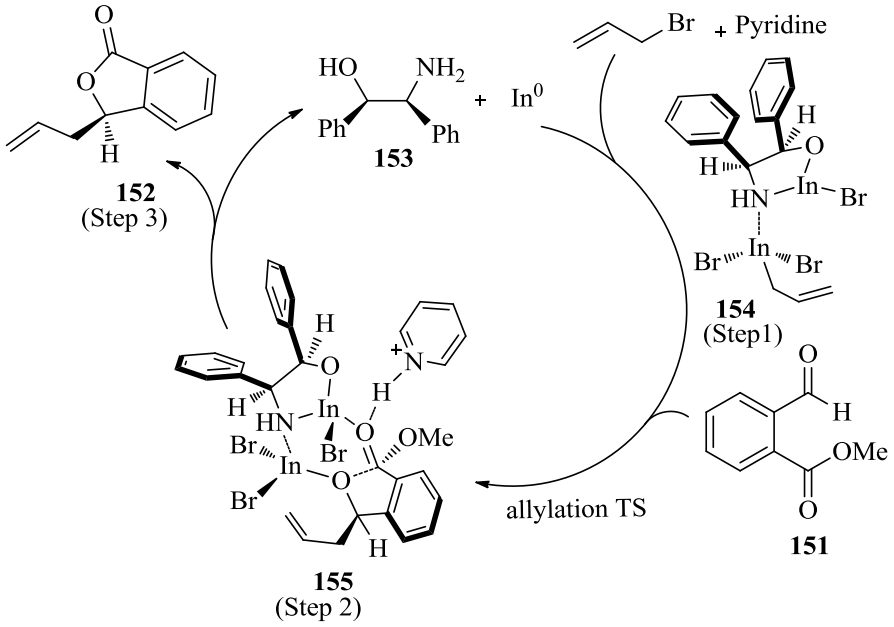

Scheme 42. Envisioned mechanistic cycle for the synthesis of $C_{(3)}$-substituted phthalides.

Surfacing from these calculations were a number of insightful features with respect to the first-order saddle points, (*R*)-**TS1** and (*S*)-**TS2**, governing the (*R*)- *vs.* (*S*)- enantioselective allylation (Figure 25). A particularly dominant feature of these transition states was the presence of a bidentate mode of (LUMO-lowering) aldehdye activation by the two In-metal centers ($In_{(1)}$•••$O_{(1)}$ and $In_{(2)}$•••$O_{(1)}$), which interestingly, due to geometric constraints, only occurred in the two lowest transition structures, (*R*)-**TS1** and (*S*)-**TS2**. A second notable feature of these two transition structures is that the $In_{(1)}$-metal center resides within the plane of the 5-membered ring system containing the *N*- and *O*-atoms of the ligand, while, the $In_{(2)}$-metal center resides below the plane of this same 5-membered ring system and *trans* to the

bulky phenyl substituents of the ligand. Geometrically, this in plane/below the plane relationship of the two In-metals with respect to the sterically bulky vicinal phenyl groups of the ligand component in (*R*)-**TS1** and (*S*)-**TS2**, shields the top face of these structures, forcing allylation to take place on the bottom face in a synclinal manner *via* a chair-like transition state.

Importantly, these structural differences reduce the activation barrier for *re*-stereofacial addition by 2.15 kcal/mol with respect to the *si*-stereofacial mode of addition ($\Delta G^{\ddagger}$ = 4.13 (*re*-addition, (*R*)-**TS1**) *vs.* 6.28 kcal/mol (*si*-addition, (*S*)-**TS1**), which translates to 98% enantioselectivity, agreeing well with experiment (*vide infra*). The specific origin of this enantiofacial selectivity appears to result from the presence of a shorter $In_{(1)}\bullet\bullet\bullet O_{(1)}$ distance in (*R*)-**TS1** (d = 2.11 Å) *vs.* (*S*)-**TS2** (d = 2.19 Å), and increased Pitzer and Baeyer strain in (*S*)-**TS2**. This strain is attributed to the half-chair transition state assembly for allylation in (*S*)-**TS2**, while in (*R*)-**TS1**, allylation proceeds through a less strained, chair-type transition state see figure 25 (red colored atoms).

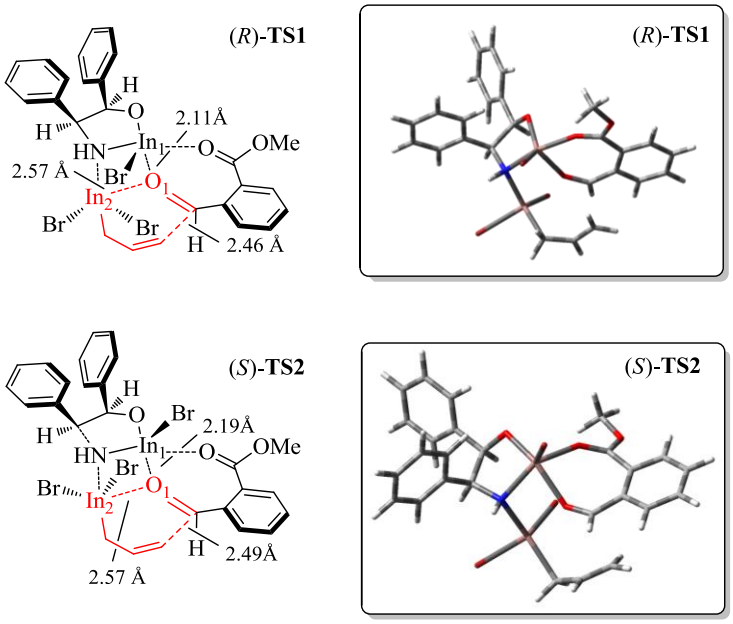

Figure 25. DFT (B3LYP/LanL2DZ) computed enantioselective transition states (*R*)-**TS1** and (*S*)-**TS2**.

Charged with this insight as a proof of concept, our efforts then turned towards the experimental realization of the rationally designed $C_{(3)}$-chiral phthalide forming reaction sequence. In this vein, methyl 2-formyl-benzoate **151a** was prepared from the reaction of 2-formyl benzoic acid **153a** and methyl iodide (Scheme 43). Later, methyl 2-formylbenzoate

153a $R^2 = H$
153b $R^2 = OCH_3$
153c $R^2 = NO_2$
153d $R^2 = Br$
153e $R^2 = HNCOOCH_2CH(CH_3)_2$
153f $R^2 = Ph$

151a-f

Scheme 43. Synthesis of methyl 2-formylbenzoate **151a-f.**

151a (1 eq) was reacted with allyl bromide (2 eq), indium powder (2 eq), (1*R*, 2*S*)-(-)-2-amino-1,2-diphenylethanol (2 eq), and anhydrous pyridine (2 eq) in THF at -78°C, which to our delight, as predicted, afforded **152a** in a respectable 80% ee (Scheme 44, Table 5, entry 1).

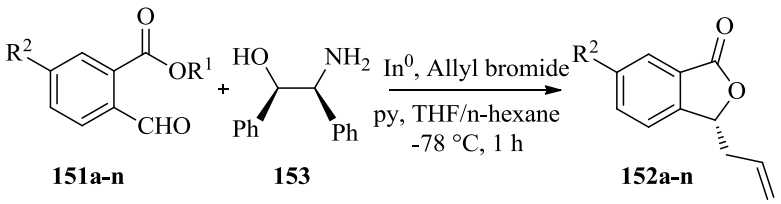

R^1 = CH_3, C_2H_5, CH_2Ph, C_5H_{11}, C_6H_{13}, $C_{12}H_{25}$, $CH(CH_3)_2$, $C(CH_3)_3$, solid support
R^2 = H, OCH_3, NO_2, Br, isobutyl-CO_2NH, Ph

Scheme 44. Synthesis of $C_{(3)}$-Chiral Functionalized Phthalides *via* indium-mediated enantioselective allylation/intramolecular transestrification

Encouraged by this result a more extensive scan of the substrate scope of this reaction was then explored. Substrate methyl 2-formyl-5-methoxybenzoate (**151b)** was synthesized by reaction of 5-methoxybenzoic acid (**154**) with formaldehyde in acidic conditions to afford phthalide **155b** (Scheme 45). Subsequent bromination of phthalide **155b** gave resulting

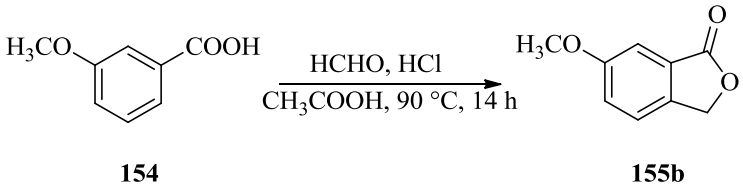

Scheme 45. Synthesis of 6-methoxyphthalide.

product of **156b** which was in turn hydrolyzed to 2-formyl-5-benzoic acid (**153b)** (Scheme 46), following methylation produced **151b** (Scheme 43). Arising from the

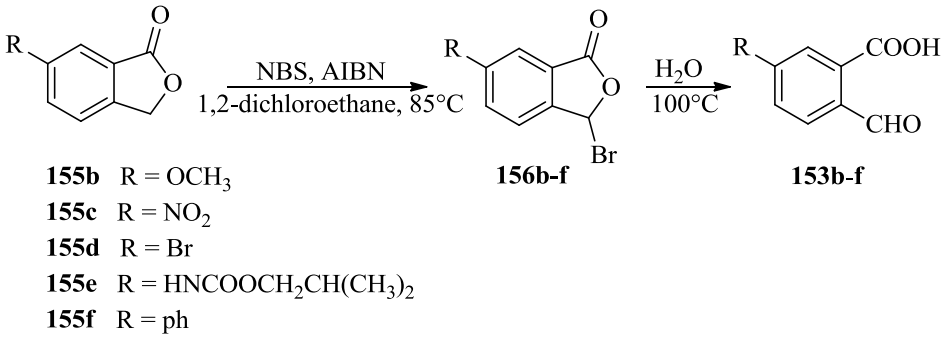

Scheme 46. General procedure for conversion of phthalide **155b-f** to methyl 2-formyl benzoate **153b-f**.

reaction of electron-rich substrate (methyl 2-formyl-5-methoxybenzoate) **151b**, phthalide **152b** was isolated in comparable ee to that of **152a** (Table 5, entry 1, 2). In the next step, phthalide (**157)** was reacted with a mixture of nitric acid and sulfuric acid to obtain 6-nitrophthalide (**155c)** (Scheme 47). General procedure for conversion of phthalide **155c** to

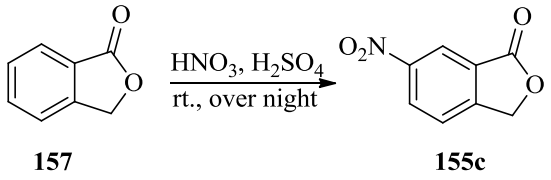

Scheme 47. Synthesis of 6-nitrophthalide.

methyl 2-formyl benzoate **151c** was followed (Scheme 46 and 43). Disappointingly, however, the electron deficient methyl 2-formyl-5-nitrobenzoate substrate (**151c**) resulted in a dramatic decrease in product ee (Table 5, entry 3). Alternatively, 6-bromophthalide (**155d**) was prepared from the reaction of phthalide **157** with *N*-bromosuccinimide (NBS) in presence of TFA and sulfuric acid (Scheme 48), following the general procedure converted **155d** to the desired compound of **151d** (Scheme 46 and 43). Moreover, to synthesize

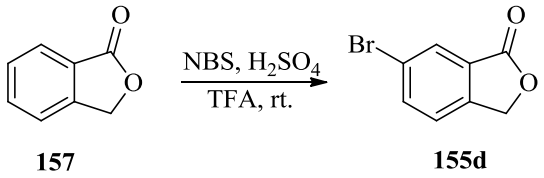

Scheme 48. Synthesis of 6-bromophthalide.

carbamate 5-substituted **155e**, 6-nitrophthalide **155c** was reduced to the corresponding amine **158**, following protection of resulting amine afforded phthalide **155e**. Subsequent conversion of **155e** to **151e** was carried out following the general procedure (Scheme 46 and 43).

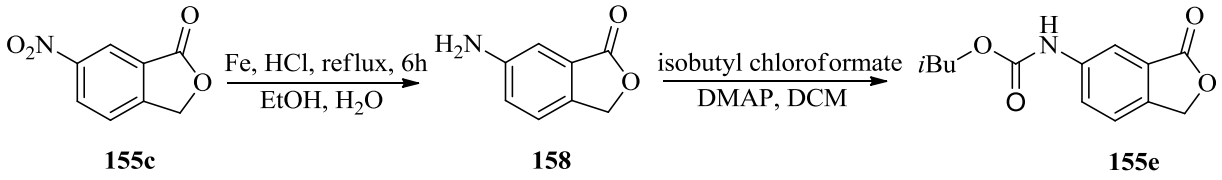

Scheme 49. Synthesis of 6-carbamatephthalide **155e**.

Additionally, Suzuki coupling of 6-bromophthalide **155d** with phenylboronic acid and palladium as a catalyst afforded phthalide **155f** (Scheme 50). Subsequent bromination,

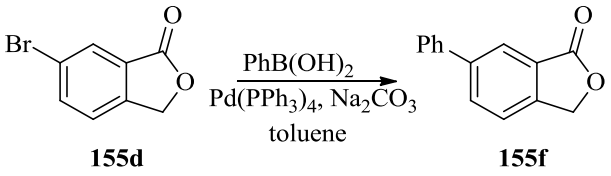

Scheme 50. Synthesis of 6-phenylphthalide **155f**.

hydrolysis, and methylation of phthalide **155f** resulted in product **151f** (Scheme 46 and 43). Having bromo, carbamate, and phenyl 5-substituted phthalide substrates **151d-f** in hand, the

described enantioselective allylation/transesetification was carried out. The resulting phthalides afforded moderate ee, which is somewhat interesting considering the electronic and structural differences existing between these substrates (Table 5, entries 4-6).

Then, the dependence of this reaction on the chain length and steric bulk of the ester group was examined. Substrates **151g-m** were prepared from the reaction of 2-formylbenzoic acid **153a** with the corresponding alkyl halide under the conditions that has been shown in

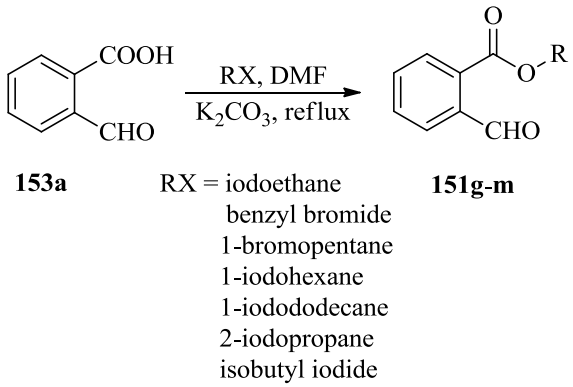

Scheme 51. Synthesis of alkyl 2-formyl benzoate **151g-m.**

Scheme 51. The resulting trends indicated an increase in ee with diminishing *n*-alkyl carbon chain length (Table 4, entries 7-11). It is believed these results may originate from substrate aggregation and potential micelle formation. With respect to changes in steric bulk of the ester group, it was found that increased branching led to erosion of ee. For instance, isopropyl 2-formylbenzoate, **151l,** afforded the product in 64% ee, whereas with *tert*-butyl 2-formylbenzoate, **151m**, no reaction occurred (Table 4, entry 12, 13). Lastly, to investigate the effect of performing the reaction on a solid support, Merrifield resin bound 2-formylbenzoic acid **151n**, was prepared from the reaction of 2-formylbenzoic acid **153a** and Merrifield resin in basic condition (Scheme 52). The reaction of **151n** under the described

allylation/transesterification conditions disappointingly only afforded racemic phthalide **152a** (Table 5, entry 14).

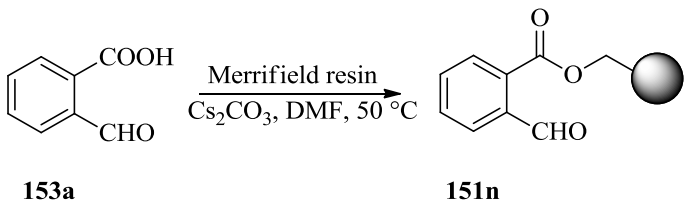

153a **151n**

Scheme 52. Synthesis of Merrifield resin bound 2-formylbenzoic acid.

Table 5. Indium-mediated enantioselective allylation[a]/intramolecular transesterification of functionalized aldehydes.

entry	Substrate	R^1	R^2	product	yield (%)[b]	ee (%)[c]
1	**151a**	CH_3	H	**152a**	77	80
2	**151b**	CH_3	OCH_3	**152b**	67	77
3	**151c**	CH_3	NO_2	**152c**	68	45
4	**151d**	CH_3	Br	**152d**	69	69
5	**151e**	CH_3	isobutylCO_2NH	**152e**	65	69
6	**151f**	CH_3	Ph	**152f**	67	68
7	**151g**	C_2H_5	H	**152a**	62	79
8	**151h**	CH_2Ph	H	**152a**	58	76
9	**151i**	C_5H_{11}	H	**152a**	60	71
10	**151j**	C_6H_{13}	H	**152a**	55	65
11	**151k**	$C_{12}H_{25}$	H	**152a**	57	50
12	**151l**	$CH(CH_3)_2$	H	**152a**	78	64
13	**151m**	$C(CH_3)_3$	H	--	0	--[d]
14	**151n**	[e]Solid support	H	**152a**	52	0

[a] Allyl bromide, indium powder, (1*R*, 2*S*)-(-)-2-amino-1,2-diphenylethanol and anhydrous pyridine in THF at -78 °C. [b] Yields of isolated products after flash chromatography. [c] Enantiomeric excess was determined by HPLC analysis. [d](--) Not applicable. [e]Merrifield resin was used.

At that stage, we set out to determine the absolute stereochemistry of the prepared phthalides by synthesizing an analogue, for which the absolute stereochemistry had already been established. Benzaldehyde appeared to be a suitable substrate for achieving this goal, assuming our mechanism was correct, and racemization did not occur under the reaction conditions. Applying the same conditions used throughout this work, we reacted benzaldehyde (**159**) with allyl bromide and obtained the (*R*)-enantiomer, **160** (Scheme 53),

the identification of which was determined by comparing the direction of the optical rotation $[\alpha]^{20}_{D} = +37$ (c = 1, $CHCl_3$) with those previously reported by several groups.[99,100]

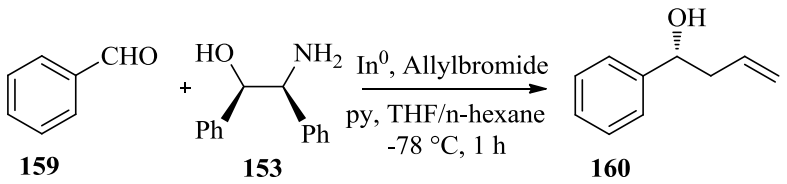

Scheme 53. Synthesis of (*R*)-1-phenylbut-3-en-1-ol *via* an indium-mediated enantioselective allylation reaction.

Finally, as a last mechanistic probe we set out to determine the catalytic role of indium and the *in situ* generated pyridinium salt (pyr-H^+), on the transesterification step of this reaction. In order to do this, modeling of the corresponding transition states for $C_{(3)}$-chiral phthalide forming ring closure, both in the presence ((*R*)-**TS3** and (*S*)-**TS4**) and absence ((*R*)-**TS5** and (S)-**TS6**) of pyr-H^+ and the indium bound complex generated from allylation was performed (Figure 26). Encouragingly, the results were consistent with our initial mechanistic premise, in that the indium and pyr-H^+ catalyzed transition states were energetically favored over the control transition states in which no catalyst was present. The free energies of activation for transesterification in presence of indium and pyr-H^+ were 5.8 kcal/mol ((*R*)-**TS3**) and 4.5 kcal/mol ((*S*)-**TS4**), while those for the uncatalyzed ring closure were 31.4 kcal/mol and 37.5 kcal/mol for (*R*)-**TS5** and (*S*)-**TS6** respectively.

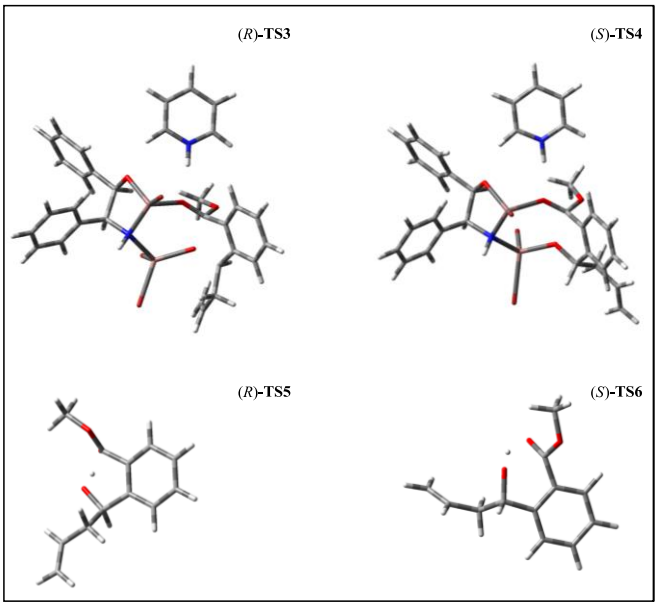

Figure 26. The free energies of activation for transesterification in presence of indium and pyr-H^+ ((*R*)-**TS3**), ((*S*)-**TS4**), and uncatalyzed ring closure (*R*)-**TS5** and (*S*)-**TS6**.

Furthermore, to experimentally substantiate this theoretical model, we carried out four separate, representative, intermolecular reactions between 2-propanol and methyl phenylacetate (conditions A-D), (see experimental section for details). Under conditions A wherein no indium species or pyr-H^+ were present, product formation was not observed by ^{1}H NMR after 6 h, while in the presence of $InBr_3$ (derived *in situ* from Br_2 and In) a notable rate enhancement was observed, and the reaction had gone to ~40% completion after 6 h (conditions B). Similarly, when pyridinium salt pyr-H^+ (conditions C) was employed as the sole catalyst, a marked rate enhancement was again observed. However, when the reaction was performed in the dual catalytic presence of In/Br_2 and pyr-H^+, only an intractable formation of by-products resulted. It would thus appear that further investigation is warranted to better understand the reactivity in the presence of both of these catalytic entities.

Taken together we have disclosed here an In-promoted one-pot allylation/intramolecular transesterification sequence and accompanying DFT rationale of

stereoselection that provides enantioenriched $C_{(3)}$-functionalized chiral phthalides (**152a-f**). Notably, as well this work presents the first example of a DFT-drafted stereochemical model for rationalizing the observed enantioselectivity of indium-mediated allylation reaction, to the best of my knowledge. Moreover, an interesting dependence of the ee of this reaction upon the steric size and chain length of the ester appendage undergoing transesterification during this reaction dynamic was revealed.

2.1.3. Synthesis of Chiral $C_{(3)}$-Functionalized Phthalides *via* a Ag(I)-Catalyzed Allylation/Transesterification Sequence

As it was discussed in section 2.1.1, an overlooked strength of the Ag(I)-catalyzed allylation procedures in terms of their operational compatibility with *ortho*-substituted arylaldehydes discovered, which are typically considered to be challenging substrates for the majority of existing catalytic asymmetric allylation approaches. More specifically, while developing synthetic methodology for preparing $C_{(1)}$-chiral 3-methylene-indan-1-ols, it was found that under the Ag(I)-catalyzed allylation conditions of Yamamoto, *ortho*-halogenated benzaldehydes provided chiral homoallylic alcohol intermediates with respectable levels of enantiomeric excess (ee). In following up upon this advancement, and continuing our ongoing interest in developing catalytic asymmetric methodologies for preparing biologically important structural motifs found in natural products and pharmaceuticals, our interest turned to catalytic synthesis of chiral $C_{(3)}$-substituted phthalides. Based on our stoichiometric In-mediated methodology which was discussed in section 2.1.2, it was reasoned that the development of a mechanistically similar catalytic approach for producing $C_{(3)}$-chiral phthalides would be of synthetic value. However, we were somewhat concerned as to the viability of this approach considering the aforementioned challenges associated with the use

of *ortho*-substituted aryladehydes as substrates. Regardless, we were delighted to find that under the reported Sakurai-Hosomi allylation conditions of Yamamoto *et al.*, allyltrimethoxysilane reacted with methyl 2-formyl benzoate (**151a**) in the presence of (*R*)-BINAP•$Ag^{I}F$ (6-10 mol %) to afford the $C_{(3)}$-substituted phthalide **152a** in 71% ee (Table 6, entry 1). Encouraged by this result to further explore the scope of this reaction a range of substituted methyl 2-formyl benzoates (**151b-m**) were then reacted.

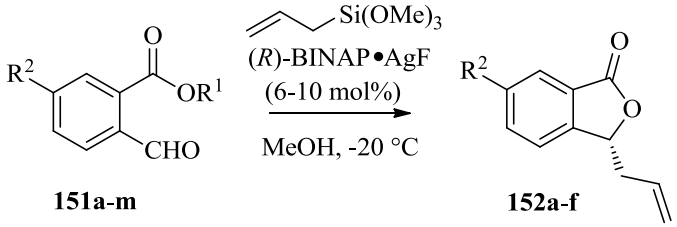

Scheme 54. Synthesis of chiral $C_{(3)}$-functionalized phthalides *via* a Ag(I)-catalyzed asymmetric Sakurai-Hosomi allylation/transesterification.

Table 6. A Ag(I)-Catalyzed asymmetric Sakurai-Hosomi allylation/transesterification of functionalized aldehydes.

entry	Substrate	R^1	R^2	t [h]	Product	yield [b] (%)	ee[c] (%)
1	**151a**	CH_3	H	5	**152a**	68	71
2	**151d**	CH_3	Br	5	**152d**	57	39
3	**151c**	CH_3	NO_2	5	**152c**	52	33
4	**151e**	CH_3	Isobutyl-CO_2NH	5	**152e**	65	43
5	**151f**	CH_3	Ph	5	**152f**	67	61
6	**151b**	CH_3	OCH_3	5	**152b**	55	86
7	**151g**	C_2H_5	H	5	**152a**	58	80
8	**151h**	C_6H_{13}	H	4	**152a**	73	86
9	**151i**	$C_{12}H_{25}$	H	4	**152a**	70	86
10	**151j**	CH_2Ph	H	10	**152a**	54	63
11	**151k**	$CH(CH_3)_2$	H	10	--	0	--[d]
12	**151l**	$C(CH_3)_3$	H	10	--	0	--
13	**151m**	[e]Solid support	H	10	**152a**	68	76

[a]Allyl trimethoxysilane, (*R*)-BINAP•AgF (6-10 mol%), in MeOH, -20 °C. [b] Yields of isolated products after flash chromatography. [c] Enantiomeric excess was determined by HPLC analysis.[d] Not applicable.[e] Merrifield resin was used.

More specifically, the reaction of **151d** having an inductively withdrawing/resonance donating *para*-bromo substituent had a negative impact upon the reaction as the target phthalide **152d** was generated with a low level of enantioinduction (Table 6, entry 2). Similarly, the incorporation of an electron withdrawing *para*-nitro substituent, which introduced the added complication of potential catalyst binding, afforded the targeted

phthalide **152c** in low ee (Table 6, entry 3). Likewise, the reaction of the electron deficient *para*-carbamate substituted substrate **151e** lead to erosion in product ee (Table 6, entry 4).

Having identified the limitations of this reaction towards the use of electron deficient substrates, the more electron rich *para*-phenyl **151f** was reacted, which generated phthalide **152f** with respectable yield in 61% ee (Table 6, entry 5). More encouraging, however, was the subsequent finding that the electron rich substrate methyl 2-formyl-5-methoxybenzoate (**151b**) afforded phthalide **152b** with even higher ee (Table 6, entry 6).

At that stage, in shifting our investigation from an analysis of what effect the aryl substitution had upon this reaction the *n*-alkyl chain length of the starting 2-formylbenzoate was systematic elongated. In this vein, the ethyl ester functionalized **151g** was reacted which surprisingly afforded **152a** with respectable ee, despite the slightly more sterically demanding nature of this substrate (Table 6, entry 7). Intrigued by this finding, hexyl-2-formylbenzoate (**151h**) was then subjected to the reaction conditions to afford **152a** in the highest ee yet (Table 6, entry 8). Notably, the ee of phthalide **152a** derived from **151h** was almost the same as the homoallylic alcohol **160** obtained from the reaction of benzaldehyde (**159**) (ee = 87%, Scheme 55), which according to the proposed reaction cycle of Figure 27 (*vide infra*), implies that once the stereochemical setting allylation step had occurred there was no erosion in ee and the bulky *ortho*-ester group of **151h** had no deleterious effect upon the reaction outcome.

To further explore this interesting trend between the steric size of *n*-alkyl ester chain length of the substrate and product ee, the dodecyl derivative **151i** was then reacted to afford phthalide **152a** with the same ee as that obtained from **151h** (Table 6, entry 9). As to the origin of this interesting dependency of the *n*-alkyl chain length of the substrate upon the

enantioinduction of this reaction, it was thought that micelle aggregation effects played a decided role in this respect.

In branching out from an analysis of the *n*-alkyl chain length of the starting substrate, benzyl-2-formylbenzoate (**151j**) was reacted to provide **152a** in moderate 63% ee (Table 6, entry 10). The influence of further branching at the α-carbon of the ester group was probed next. To this end, the *iso*-propyl and *t*-butyl 2-formyl-benzoates **151k** and **151l** were reacted, which as non-events only afforded unreacted starting materials (Table 6, entry 11, 12). In drawing upon the foreseeable use of our reaction methodology within the context of "split-and-pool", "parallel synthesis" or other combinatorial based solid-support approaches the reaction of the Merrifield resin bound **151m** was investigated.[101] Eventfully, much to our liking the desired phthalide was afforded in 76% ee, despite the heterogenous nature of this reaction (Table 6, entry 13). Furthermore, from an experimental standpoint it is noteworthy that the desired phthalide is freed from the solid support by transesterification, thus alleviating the need for post-allylation cleavage of the product from the solid support.

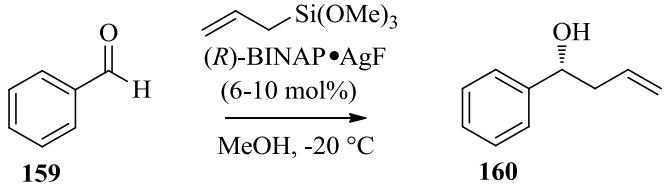

159 **160**

Scheme 55. Yamamoto-Sakurai-Hosomi allylation of benzaldehyde.

Taking into consideration the above results, the mechanistic cycle depicted in Figure 27, was tentatively proposed. According to this posit a short-lived complex **GS1** is initially formed from methyl 2-formylbenzoate (**151a**), allyltrimethoxysilane, and the catalyst, wherein the allyltrimethoxysilane reagent resides at the periphery of the inner coordination

sphere containing the directly bound catalyst and aldehyde assembly. From **GS1**, a fluoride assisted transmetalation occurs to form a highly reactive Ag-allyl species that rapidly undergoes enantioselective allylation *via* **TS7** in a *re*-stereofacial C–C bond-forming process that provides the Ag-alkoxy bound intermediate **GS2**. Thereafter, an intramolecular transesterification (likely Ag-facilitated) follows to afford (*R*)-3-allylisobenzofuran-1(3H)-one (**152a**), tetramethoxysilane and in turnover the catalyst for another productive cycle.

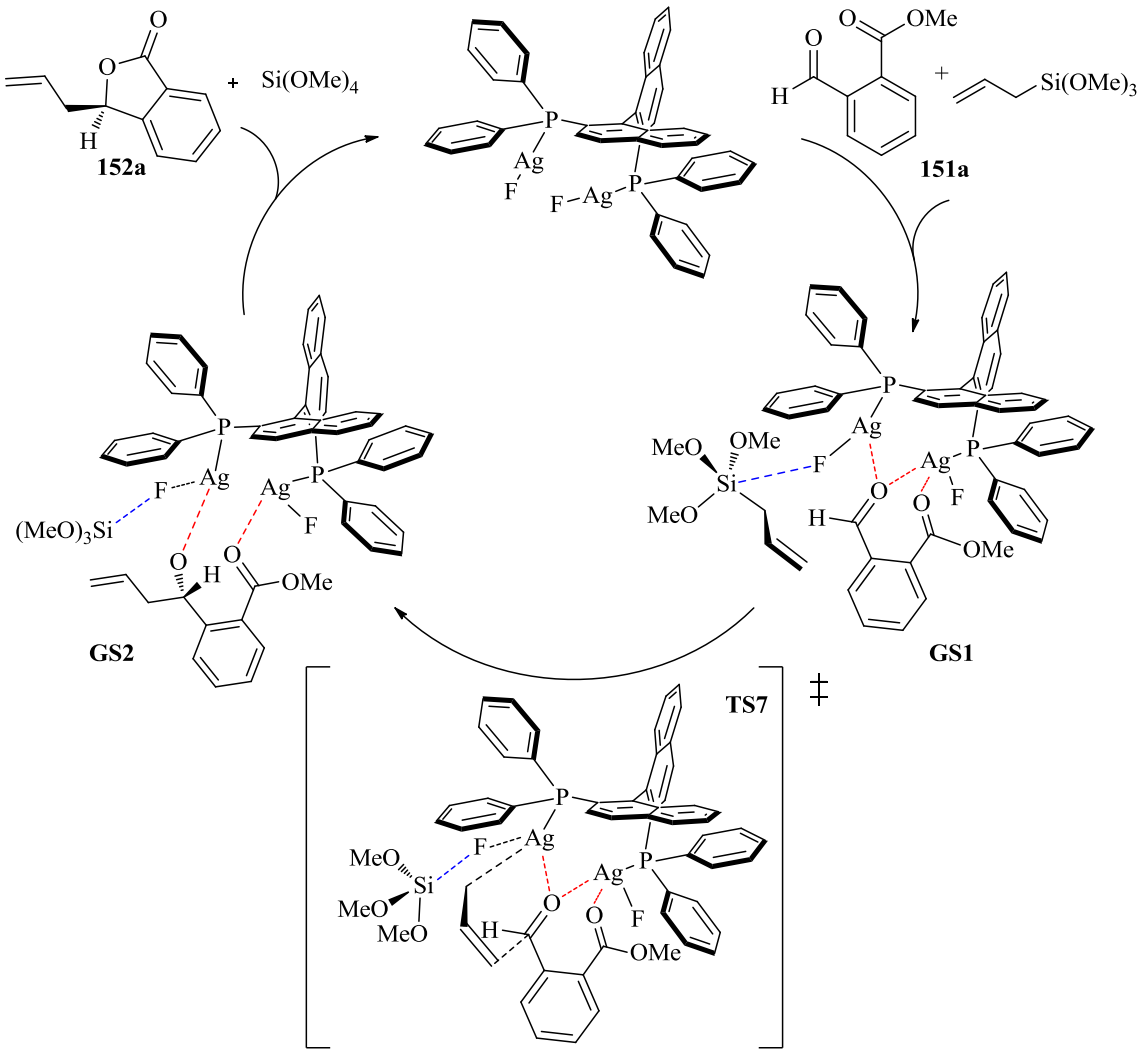

Figure 27. Envisioned Mechanistic Cycle for the Synthesis of Chiral $C_{(3)}$-Substituted Phthalides.

In this work as outlined above a unique synthetic entry-point to chiral $C_{(3)}$-phthalides has been described that relies upon the use of Yamamoto's variant of the Sakurai-Hosomi reaction and allows for the synthesis of structural motifs found throughout many biologically active compounds. A second unique feature of this reaction is that it utilizes *ortho*-substituted aldehydes which in general are known to afford poor levels of stereoinduction when applying most of the catalytic asymmetric allylation technologies reported to date. As well, the

counterintuitive finding that a marked improvement in product ee occurred, up to a point, upon elongation of the *n*-alkyl chain (R^1, up to n = 6; R^2 = H) of the starting alkyl 2-formylbenzoate employed was discovered.[102]

2.2. A Class of Phase-Transfer Catalyst (PTC): Synthesis and Applications

2.2.1. Synthesis of a Class of Phase-Transfer Catalyst with Interionic Strain: Insight into the Bonding of Disubstituted N- vs Carbene-Stabilized N^I-Centered Cations.

The chemistry of low-valent Group 14 based complexes, such as the so-called ylidones L: → E ← :L (L: = donor, E = C – Pb), has seen a bourgeoning level of interest in the last decade, due to their peculiar electronic structures and unique reactivity, which has led to recent controversy.[103-110] Emerging from the study of these complexes, has been the non-intuitive, yet chemically relevant view that the acceptor atom (E) retains its valence electrons in the form of two lone pairs and the two ligands are coordinated through dative donor-acceptor interactions.

On the other hand, p-block (Group 15) donor-acceptor ylidone complexes have received far less attention and only recently have studies related to these systems begun to surface. In this regard, Alcarazo, Frenking, and others have reported divalent nitrogen species that are formally isoelectronic with carbodicarbenes. Moreover, several computational and experimental reports have appeared in which these compounds were depicted as possessing dative bonding character.[111-117] Although questionable, this bonding scenario corresponds to a carbene stabilized N-centered cation such as L: → N^I ← :L.

Intrigued by the recent reports of carbene stabilized N^I centered complexes, as well as our interest in catalysis we were drawn towards the possibility of preparing structurally related complexes for applications in synthesis. As outlined in Scheme 56, Chloro-1,3-

dimethylimidazolinium chloride (DMC) (**162**) was synthesized from reaction of the commercially available 1,3-dimethyl-2-imidazolidinone (**161**) with oxalyl chloride. Subsequently, the DMC salt in presence of ammonia gas and basifying afforded free guanidine **163**. The desired product of **168**•Cl^- was prepared as a bench stable solid from guanidine **163** and tetrachlorocyclopropene (**167**), which is a commercially available reagent that can also be synthesized from the reaction of trichloroethylene (**164**) and sodium trichloroacetate (**165**) followed by the reaction of the resulting product with potassium hydroxide (Scheme 56).[118]

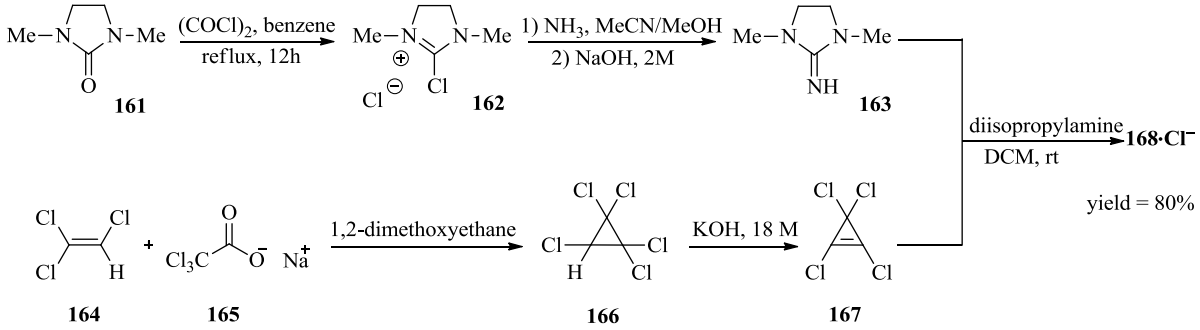

Scheme 56. Synthesis of **168**•Cl^-.

Given cation **168** embodies what can be viewed as a divalent N^I adduct, coordinated by two different well-known carbenes (*i.e.*, NHC and cyclopropenylidene carbene ligands), it offers insight into the bonding of so-called nitrogen centered low-valent complexes. In this regard, a salient feature of **168** are the mesomeric forms that may be invoked to describe the bonding in the parent cation: (1) a heteroleptic donor–acceptor complex of an imidazole-based NHC and cyclopropenylidene stabilized N^I-cation **168a**; (2) a *N*-cyclopropenium guanidine **168b**; (3) a imidazoliumyl *N*-cyclopropenylimine **168c**; (4) imidazoliumyl *N*-cyclopropenium **168d**, etc. (Figure 28).

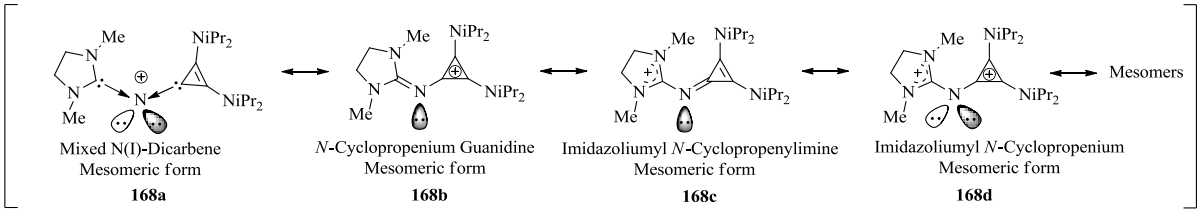

Figure 28. Mesomeric forms of **168**•Cl^-.

Based on Bharatam's *in silico* findings[114-117] related to structurally similar N^I complexes which were predicted to coordinate metals, the ligation of **168**•Cl^- to Au^I, and In^I were computed. Figure 29 shows geometry optimization of complex $\mathbf{168}^+$ with one and two AuCl or InI in which they bind in bridging nitrogen positions. The computed bond dissociation energies (BDEs) of complex $\mathbf{168}^+$ with AuCl and InI were -145.9 and 83.2 Kcal/mol respectively. Also, the second BDEs of $\mathbf{168}^+$•$(AuCl)_2$ and $\mathbf{168}^+$•$(InI)_2$ were 6.2 and 209.2 Kcal/mol, respectively, which is higher than the first BDE. In a structurally related compound, Bertrand suggested this is because the first AuCl or InI distorts the structure and makes it easier for the second AuCl or InI to bind.[119]

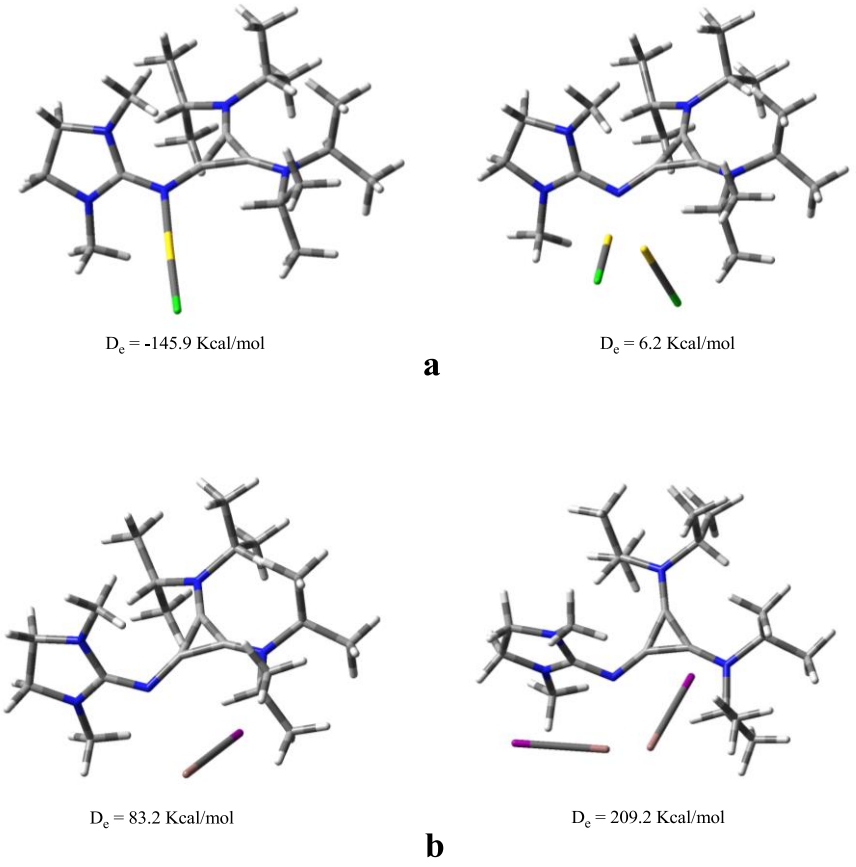

Figure 29. geometry optimization of complex **168**$^{+}$ with one and two AuCl (a) or InI (b) at B3LYP-D3/SDD and B3LYP/LanL2DZ level of theory respectively.

Having **168**•Cl^{-} in hand, and with the aim of applying **168** as a potential ligand for metal based catalysis, the coordination properties of **168**•Cl^{-} with a number of metals [*e.g.*, Ag^{I}, Au^{I}, In^{I}] was subsequently investigated. To this end, despite numerous failed attempts to isolate a *N*-ligated metal complex of **168**•Cl^{-}, we were able to obtain a single crystal of **168**•$AuCl_4^{-}$ suitable for X-ray diffraction, from a mixture of **168**•Cl^{-} and AuCl (Figure 30). Apparent from the X-ray structure of **168**•$AuCl_4^{-}$ was the noticeable displacement of the $AuCl_4^{-}$ anion at a N(3)•••Au(1) distance of 8.47Å.

A characteristic feature of **168**•$AuCl_4^-$ was the C(1)-N(3)-C(4) bond angle of 125°, as it was similar to that of carbones and consistent with Alcarazo's reported bis-cyclopropenium N^I-cations. Further telling were the N(3)-C(1) and N(3)-C(4) bond distances of 1.34(4) and 1.30(6) Å which were in line with partial double bond character. Also supporting partial double bond character were the computed Wiberg bond indices of 1.25 and 1.40, respectively, obtained from the DFT optimized X-ray coordinates of **168**•$AuCl_4^-$. As for the $AuCl_4^-$ counterion of **168**•$AuCl_4^-$ the calculated tetrahedrality based on the X-ray metrics provided a dihedral angle of 0.8°, supporting an almost perfect square planar geometry around Au^{III}.[120] Additionally, the *cis*- and *trans*-angles ranged from 88.8-91.1° and 179.3-179.6°, deviating only slightly from the values of 90° and 180° of an ideal square plane (Figure 30).

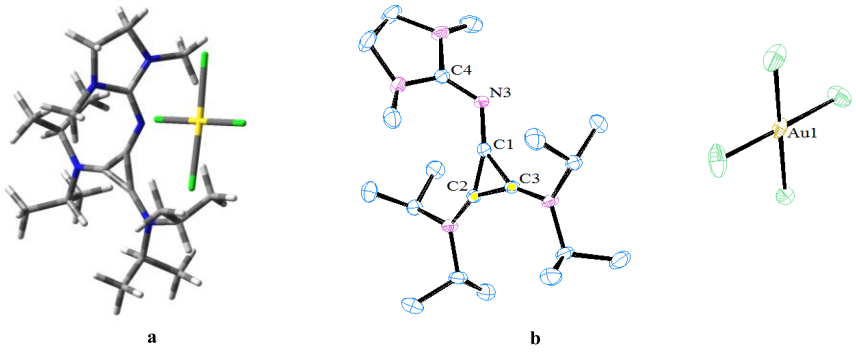

Figure 30. a) 3D optimized geometry of **168**•$AuCl_4^-$ at B3LYP/SDD. b) X-ray structure of **168**•$AuCl_4^-$ in the solid state (hydrogen atoms removed for clarity).

Meanwhile, the natural atomic orbital (NAO) charges of C(1), C(2), and C(3) ($\sum_{i=1}^{3} Ci = 0.714\ e$) suggest the presence of an aromatic cyclopropenium cation. Standing

in stark contrast to the affinity of **168**•Cl^- to bind metals, was the high negative partial charge of -0.649 *e* at the bridging N(3) atom.

Given the failure of **168**•Cl^- to bind Au, we turned to the Frontier Molecule Orbitals (FMOs) of this complex to gain a clearer understanding of its electron distribution. Apparent from the HOMO, was the presence of a pure π-type orbital at N(3) that shared an anti-bonding relationship with respect to the MO density of the two adjacent ring systems, while no orbital density was present on the $AuCl_4^-$ counterion. Further still, a detailed inspection of the lower lying HOMO−3 and HOMO−5, which are more stable than the HOMO (E = −6.68, −6.86 vs −5.62eV) and thus less available for bonding, revealed the presence of a small σ-type lone pair (Figure 31). On the other hand, the LUMO resided totally on the $AuCl_4^-$ counterion. In view of these trends, and the modest HOMO-LUMO gap of 2.09 ev of **168**•$AuCl_4^-$, as well as the negative partial charge of N(3), it would appear that N(3)-Au bond formation is in part disfavoured by sterics (Figure 30).

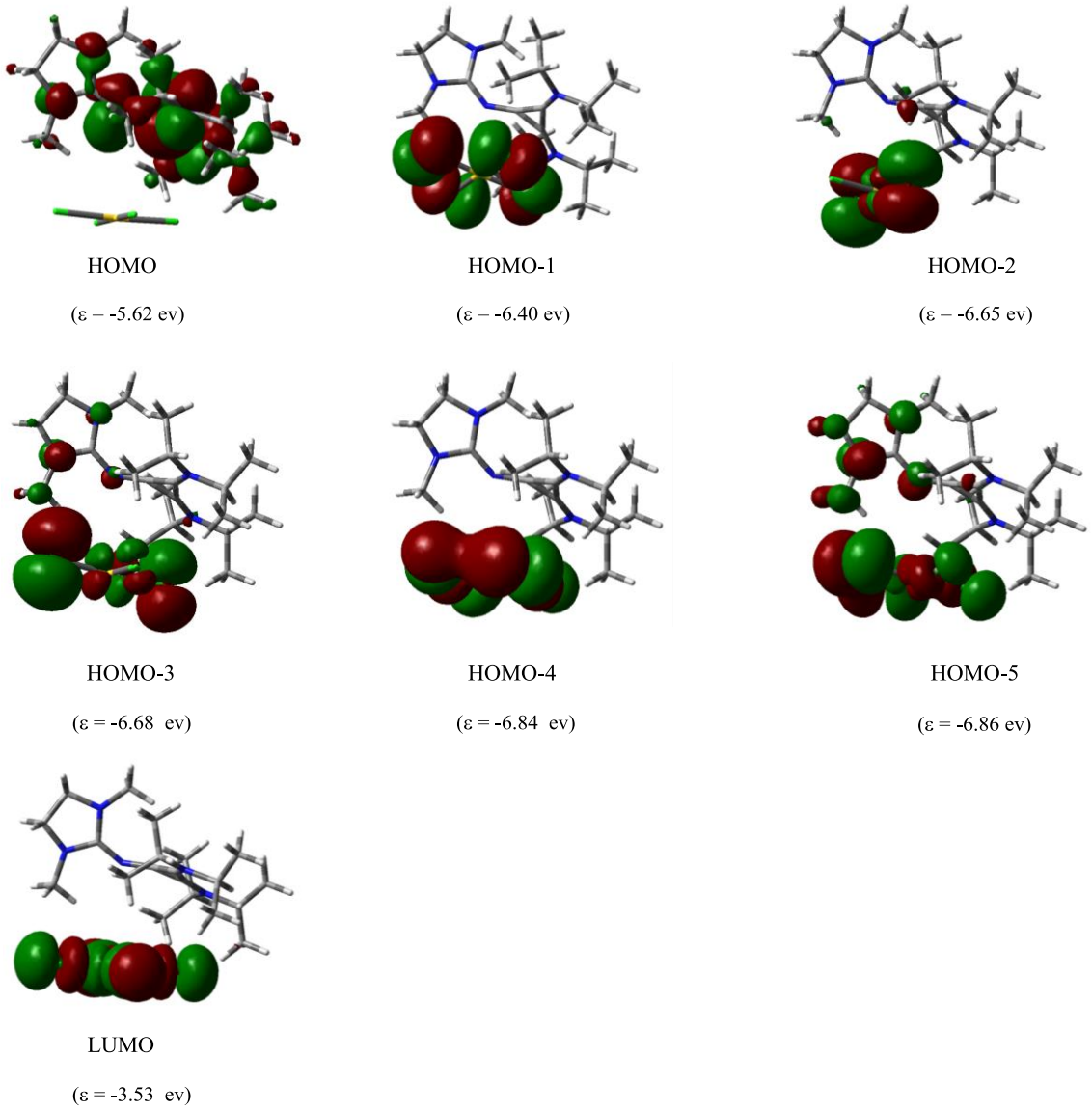

Figure 31. Plot of the HOMO, HOMO-1, HOMO-2, HOMO-3, HOMO-4, HOMO-5 and LUMO of **168**•$AuCl_4^-$. Orbital energies were computed at the B3LYP/SDD level of theory.

Taken that steric hindrance represented a potential obstacle of **168**•Cl^- to bind metals, the first and second proton affinity of **168**•Cl^- were computed which suggested 166.5 and 38.1 Kcal/mol respectively (Figure 32). Further, the protonation of **168**•Cl^- was attempted using trifluoroacetic acid (TFA). Accordingly, an excess of TFA was added to a solution of

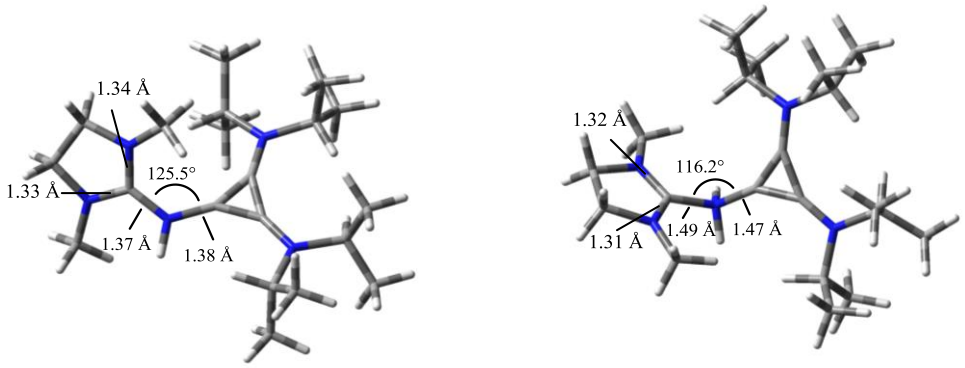

PA = 166.5 Kcal/mol PA = 38.1 Kcal/mol

Figure 32. First and second proton affinity of **168**•Cl^- at the B3LYP-D3/6-31G(d) level of theory.

168•Cl^- in DCM, after stirring for 1 h it was concentrated and the resulting solid recrystallized from DCM/Ether at -20 °C, affording X-ray quality crystals. Resulting was **168**•$(TFA)_3Cl^-$ which interestingly exhibited three ^{15}N NMR signals at δ = 120.96, 108.11, and 82.68 in comparison to 128.58, 105.50, and 81.28 ppm for the compound **168**•Cl^-. More enlightening, the X-ray structure of **168**•$(TFA)_3Cl^-$ revealed that the Cl^- resided far from the parent cation **168** at a remarkable separation distance of N(1)•••Cl(1) distance of 6.63 Å (Figure 33). A striking aspect of **168**•$(TFA)_3Cl^-$ was the presence of three associated TFA working in concert, two of which were directly H-bonded to the Cl^- anion and the third H-bonded to the other two TFAs. The decisive energetic factor for formation of this adduct, being the presence of a well-organized H-bonding framework capable of stabilizing the highly dissociated chloride anion. Contributing to the marked displacement of Cl^- anion (average C(12,13,20)•••Cl(1) distance = 7.98 Å) was cyclopropenylium based "ion pair strain" (*vide infra*), which ultimately displaces the Cl^- towards the adjacent heterocyclic ring system of cation **168**.

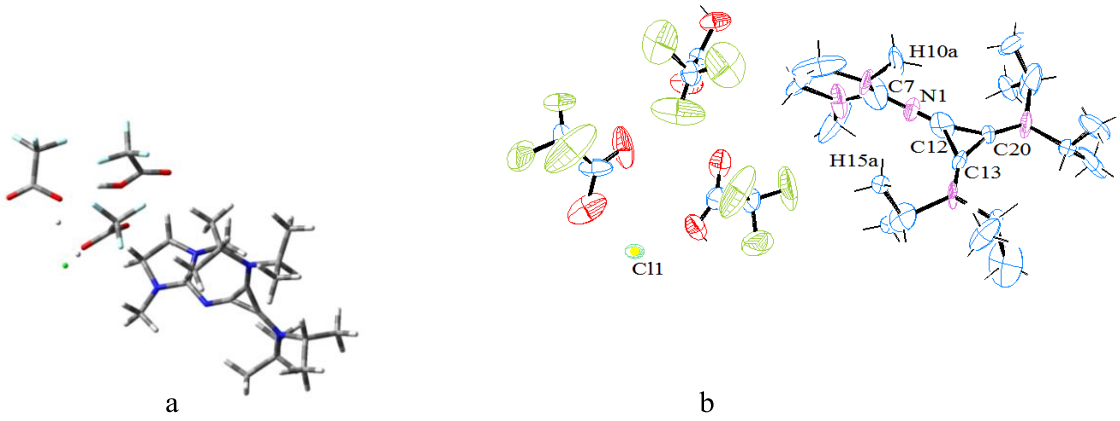

Figure 33. a) 3D Optimized geometry of **168**•$Cl(TFA)_3^-$ computed at the B3LYP/6-311G(d) level of theory. b) Molecular structure of **168**•$(TFA)_3Cl^-$.

Mirroring the X-ray parameters of **168**•$(TFA)_3Cl^-$ was the DFT optimized structure (Figure 33). As for perhaps the most salient bonding feature of computed **168**•$(TFA)_3Cl^-$, Wiberg bond indices provided nearly equivalent bond orders of 1.31 and 1.30 for N(1)–C(7) and N(1)–C(12), consistent with partial double bond character. Instructive as well was the insight gained from atoms in molecules (AIM) theory which supported the Wiberg bond order assignment of partial double bond character to N(1)–C(7) and N(1)–C(12) (Figure 34). More specifically, AIM analysis revealed that the N(1)–C(7) and N(1)–C(12) bonds were covalent in nature with a degree of π-bonding character based on the Laplacian ($\nabla^2\rho_{bcp}$) values of -0.246 and -0.271, electron densities (ρ_{bcp}) of 0.346 and 0.342, and the total electronic energies (H_{bcp}) -0.469 and -0.471 at the corresponding (3, -1) bond critical points (BCPs) defining these bonds, respectively.[121] Also diagnostic of partial π-bonding, were the calculated ellipticities (π) of 0.130 and 0.080 at these two BCPs, with the N(1)-C(7) bond having a greater degree of double bond character than that of N(1)-C(12), thus suggesting the bonding in **168**•$(TFA)_3Cl^-$ was more weighted towards mesomeric form **168b** (*vide supra*).

AIM analysis as well revealed the presence of a bond path between H(10a) and C(12) (ρ = 0.01, $\nabla^2\rho_{bcp}$ = 0.0094) with a (3, -1) BCP located closer to the atomic basin of H(10a),

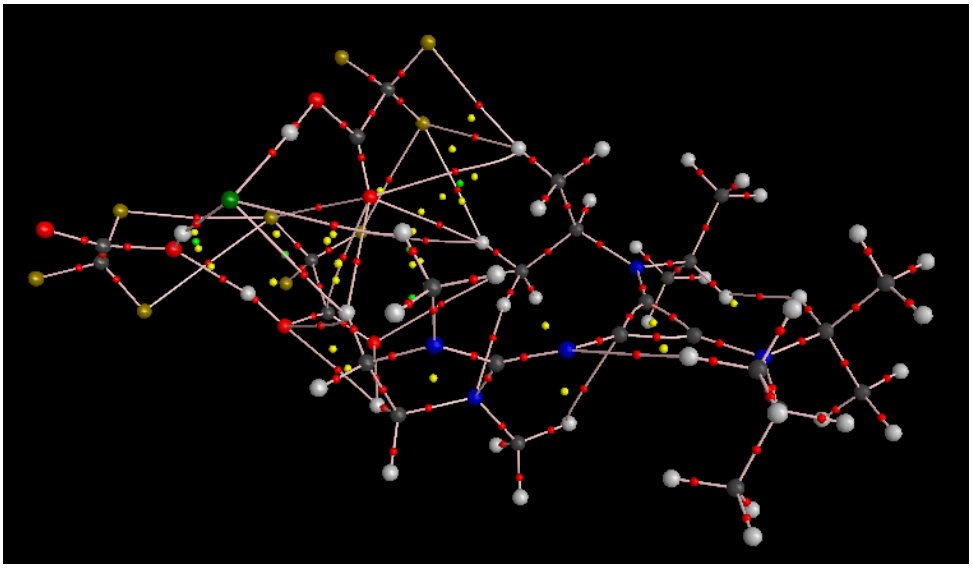

Figure 34. Computed AIM structure of **168**•$(TFA)_3Cl^-$.

suggesting the presence of an C-H(10a)•••π_{aryl} interaction (Figure 34). Furthermore, application of Schleyer's nucleus independent chemical shift (NICS) method indicated that the cyclopropenylium ring of **168**•$(TFA)_3Cl^-$ had appreciable aromatic character (NICS (0) = -30.5, NICS (-1) = 9.2, NICS (1) = -8.9), consistent with the existence of an C-H(10a)•••π_{aryl} interaction (Figure 35). Moreover, the summed NAO charges of C(1), C(2), and C(3) $(\sum_{i=1}^{3} Ci = 0.714\ e)$ supported the presence of an aromatic cyclopropeninium cation.

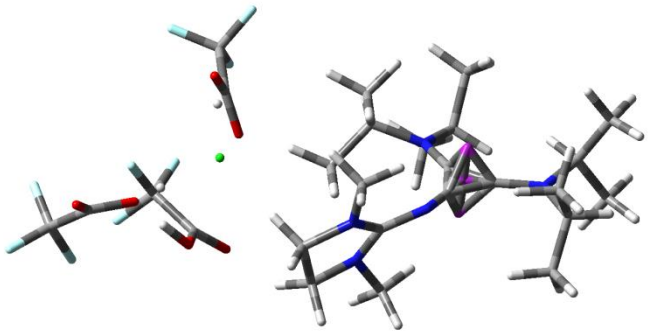

Figure 35. Schleyer's nucleus independent chemical shift (NICS) method of **168**•$(TFA)_3Cl^-$.

Given the importance of C-H•••π_{aryl} interactions in crystal packing,[122] structures of biological molecules,[123] molecular recognition processes[124] and as directing elements in asymmetric reactions,[125] it is notable that the involvement of a cyclopropenium ring system in such an interaction is unprecedented to the best of our knowledge. One last interaction of note was the presence of an apparent H-bond between the electron rich N(1) nitrogen and the H(15a) hydrogen of the imidazoline ring ($\rho = 0.0080$, $\nabla^2\rho_{bcp} = 0.0061$), as identified by a (3, -1) BCP.

Notably, due to donor-donor "ion pair strain" originating from a strong repulsive closed-shell interaction between the electron-rich anion and electron excessive cyclopropenylium ring of **168**•X (X = $AuCl_4^-$, $(TFA)_3Cl^-$, Cl^-) the anion of these compounds is high dissociated with the tell-tale signs of being a "naked anion",[64,126] providing an interesting feature for the design of PTC. Given this weak association of the lipophilic cation (**168**) with anions, ion pair **168**•Cl^- was applied to phase-transfer catalysis. To this end, the benzylation of Schiff base *N*-diphenyl methylene glycine ethyl ester **169** in the presence of **168**•Cl^- (1 mol%) under hydroxide-initiated PTC conditions[127] using an aqueous biphasic KOH (50%)/dichloromethane system, was carried out. Accordingly, we were pleased to find

that **168**•Cl^- promoted the reaction in 4 h at rt to afford product **170** in 85% yield (Scheme 49), whereas a control reaction without **168**•Cl^- gave unreacted starting material.

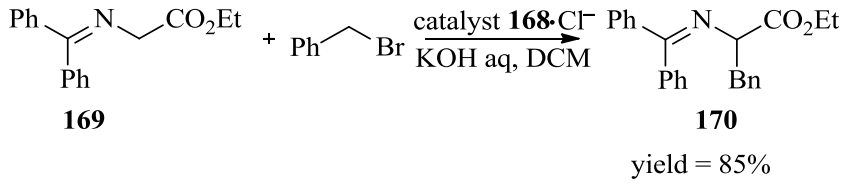

Scheme 57. Benzylation of Schiff base **169** using KOH aqueous-catalyst **168**•Cl^- phase-transfer conditions.

Notably, this transformation represents a promising entry in PTC.[128] Lastly, the relative stability of **168**•Cl^- to concentrated biphasic (50% KOH) PTC conditions deserves further mention as it along with the X-ray metrics of **168**•X, and DFT findings presented herein are more consistent with the two heterocyclic rings of cation **168** being covalently bonded as opposed to datively coordinated as carbene ligands to the central nitrogen. This point should be appreciated as it provides in many ways clarification regarding the current questionable views of bonding in *N*-centered cations.

In summary, a structural class of phase-transfer catalyst offering fundamental insight into the chemical bonding of *N*-centered cations vs. so-called divalent nitrogen(I) complexes was presented. A marked feature of these PTC was the presence of a highly dissociated anion resulting from interionic donor-donor "ion pair strain". Notably, this structural attribute provides a unique design element that as demonstrated allows for high catalytic activity. Emerging from DFT calculations was the finding that the central nitrogen had a measurable degree of negative charge and a significant amount of partial double bonding with respect to the adjacent ring systems, providing convincing evidence against divalent N^I character. Of

interest as well was the unprecedented finding of a C-H•••π_{aryl} interaction between the cyclopropeninium ring and a proximal hydrogen in these systems.

2.2.2. Fluorination of Benzyl Bromide and its Derivatives with Cesium Fluoride in The Presence of Phase Transfer Catalyst.

The construction of carbon-fluorine (C-F) bonds is of longstanding interest and continues to gain traction in both industry and academia as fluorine is known to impart desirable physiochemical properties to organic molecules. [74-78] Attesting to this fact is a *ca*. 40% of agrochemicals and *ca*. 20% of pharmaceuticals marketed currently, as well as an ever increasing fraction of drugs containing at least one fluorine atom. It is well known that the lipophilicity and metabolic stability of organic compounds can be adjusted by fluorine and trifluoromethyl substituents. In addition, they have effect on binding affinity and selectivity through non-covalent interactions of the aryl group. However, complex compounds having fluorine atoms at the benzylic position are challenging to prepare and accordingly, they are less studied.[129]

In section 2.2.1. development of a class of phase transfer catalysts with highly dissociated anion originated from interionic donor-donor "ion pair strain" was discussed. This interesting feature of the synthesized catalyst as well as highly demand for fluorination methodologies, especially metal-free approaches, inspired us to use catalyst **168**•Cl^- as a PTC in the fluorination reaction for benzylic fluorination. As a outset of the reaction, benzyl bromide (**171**) (1 equiv), potassium fluoride (4 equiv), and catalyst **168**•Cl^- was mixed in acetonitrile and refluxed (Scheme 58). The reaction was monitored with TLC during hours up to 48 h, however, no conversion was observed. Subsequently, to investigate the effect of solvent on the reaction outcome, polar protic, polar aprotic, and nonpolar solvents such as

methanol, THF, toluene, and acetonitrile were scanned, notwithstanding, fluorination reaction was failed. Given the failure of potassium fluoride to serve as a fluoride anion

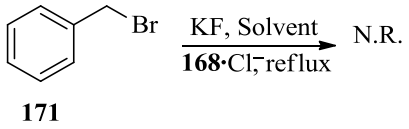

171

Solvent: methanol, THF, toluene, and acetonitrile

Scheme 58. Fluorination of benzyl bromide using KF and catalyst **168**•Cl^-.

source, we turned to the use of a moderately basic cesium fluoride. We were pleased to find using cesium fluoride in acetonitrile after 7 h reflux afforded benzyl fluoride with 94% yield. However, when the reaction of benzyl bromide was performed under the same conditions in absence of catalyst **168**•Cl^- only a trace amount of the fluorinated product was obtained (~5% yield). A salient feature of this protocol was the column-free purification of the product and recovery of the catalyst that could be used for subsequent reaction cycles with no apparent loss in catalytic reactivity (up to 5 cycles attempted); see the experimental section for details. Attesting to the reliability of this fluorination protocol as well was the reaction of several other substitution benzyl bromides which afforded the corresponding fluorinated adducts in high yields (Figure 36) see the experimental section for reaction conditions. It is additionally noteworthy that in comparison to anhydrous TBAF based fluorination of benzylic substrates the approach introduced herein affords higher yields and does not require prior reagent preparation.[83] Furthermore, when compared with the alternative use of semimolten mixtures of tetrabutylammonium bromide and alkali metal fluorides it deserves mention that fluorination with catalyst **168**•Cl^- could be achieved under much milder conditions.[130]

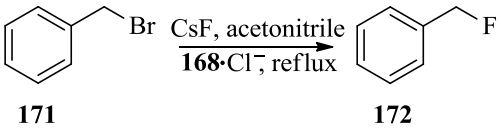

Scheme 59. Fluorination of benzyl bromide using CsF and catalyst **168**•Cl^-.

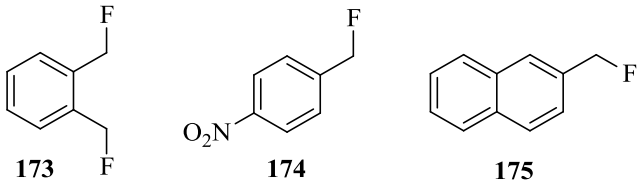

Figure 36. Examples of fluorination products derived from bromide substrates.

3. Conclusions & Future Works.

In this dissertation, synthesis of biologically active C_1-chiral 3-methylene-indan-1-ols (ee $\leq$ 80%) based on the sequential use of a Yamamoto's asymmetric Sakurai-Hosomi allylation reaction and a Mizoroki-Heck reaction was described. As well, an In-promoted one-pot allylation/intramolecular transesterification sequence and accompanying DFT rationale of stereoselection that provides enantioenriched $C_{(3)}$-functionalized chiral phthalides was disclosed. To the best of my knowledge, notably, this work presents the first example of a DFT-drafted stereochemical model for rationalizing the observed enantioselectivity of indium-mediated allylation reaction. Moreover, an interesting dependence of the ee of this reaction upon the steric size and chain length of the ester appendage undergoing transesterification during this reaction dynamic was revealed. Based on the developed stoichiometric In-mediated methodology, an enantioselective catalytic synthesis of chiral $C_{(3)}$-functionalized phthalides *via* a Ag(I)-catalyzed allylation/transesterification sequence was described.

Additionally, a structural class of phase-transfer catalysts offering fundamental insight into the chemical bonding of *N*-centered cations vs. so-called divalent nitrogen(I) complexes was presented. A marked feature of these PTC was the presence of a highly dissociated anion resulting from interionic donor-donor "ion pair strain". Notably, this structural attribute provides a unique design element that allows for high catalytic activity. Emerging from DFT calculations was the finding that the central nitrogen had a measurable degree of negative charge and a significant amount of partial double bonding with respect to the adjacent ring systems, providing convincing evidence against divalent N^I character. Of interest as well was

the unprecedented finding of a C-H•••π_{aryl} interaction between the cyclopropeninium ring and a proximal hydrogen in these systems.

Lastly, applications of synthesized phase-transfer catalysts in benzylation of the Schiff base *N*-diphenyl methylene glycine ethyl ester and also fluorination at the benzylic position were demonstrated.

Accordingly, ongoing efforts in our laboratory are focusing on other applications of the synthesized PTC in organic transformations. For instance, allylation of the aldehydes **167a** or ketones **176b** with allyltrimethylsilane **177a** or methallyltrimethylsilane **177b** in presence of **168**•Cl^- as a catalyst and cesium fluoride will be carried out to afford homoallylic alcohol **178** (Scheme 60). Having success in the symmetric allylation reaction, the enantioselective

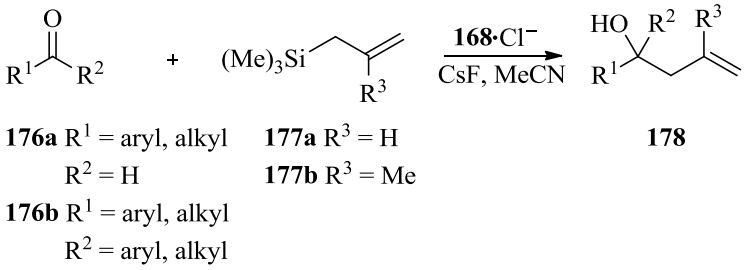

Scheme 60. Allylation of the aldehydes or ketones with allyltrimethylsilane or methallyltrimethylsilane using **168**•Cl^- as a catalyst.

variant of this transformation will be perform using chiral catalyst **184**•Cl^- which in turn can be synthesized from commercially available diamine **179** with simple manipulations (Scheme 61). Additionally, chiral catalyst **184**•Cl^- could also be used in asymmetric fluorination reactions.

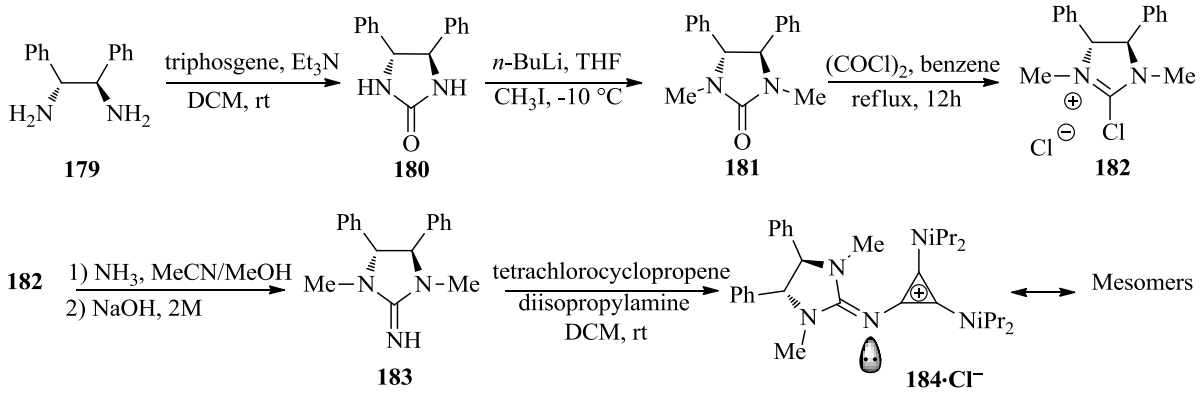

Scheme 61. Synthesis of chiral catalyst **184•**Cl^-.

4. Experimental Procedures

4.1. General information.

Materials were obtained from commercial suppliers (Sigma-Aldrich) and were used without further purification. Dry dichloromethane (DCM), tetrahydrofuran (THF), dimethylformamide (DMF), and toluene were obtained by Puresolv MD 5 purification system. All reactions were performed under an inert atmosphere. Reactions were monitored by thin layer chromatography (TLC) using TLC silica gel plates 60 F254, EMD Merck. Flash column chromatography was performed over Silicycle ultrapure silica gel (230-400 mesh). NMR spectra were obtained with a Bruker DPX-300 (^{1}H 300 MHz or ^{1}H 600 MHz, ^{13}C 75.5 MHz, ^{15}N 60.8 MHz, ^{19}F 292 MHz) in $CDCl_3$. The chemical shifts are reported as δ values (ppm) relative to tetramethylsilane for ^{1}H NMR, ^{13}C NMR, liquid ammmonia for ^{15}N NMR, and boron trifluoride etherate for ^{19}F NMR. Enantiomeric excess was measured on an Agilent 1100 series high pressure liquid chromatography (HPLC) with (OD-H or AS-H) column, wavelength = 245 nm. Mass spectra were obtained on an MSI/Kratos concept IS Mass spectrometer. Optical rotations were recorded on a Perkin Elmer 341 with sodium lamp polarimeter. FT-IR spectra were obtained on an ATI Mattson Research Series spectrometer using KBr discs/ solids mixed with KBr or Bruker Alph Platinum ATR using neat sample.

4.2. Synthesis of Biological Active $C_{(1)}$-Chiral 3-methylene-indan-1-ols.

4.2.1. The Typical Procedure for the Asymmetric Allylation of an Aldehyde With Allyltrimethoxysilane and (*R*)-BINAP•AgF as a Catalyst.

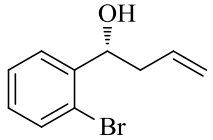

Synthesis of (*R*)-1-(2-bromophenyl)-3-buten-1-ol (149b). (Table 4, Entry 2). A mixture of AgF (32.9 mg, 0.26 mmol) and (*R*)-BINAP•AgF (99.6 mg, 0.16 mmol) was dissolved in anhydrous methanol (3 mL) under nitrogen

atmosphere with exclusion of direct light, and it was stirred at room temperature for 10 min. To the resulting solution were added dropwise 2-bromobenzaldehyde (264 μL, 2.6 mmol) and allyltrimethoxysilane (791 μL, 4.7 mmol) at -20°C. The mixture was stirred for 4 h at this temperature, and then treated with a mixture of 1N HCl (13 mL) and solid KF (1.3 g) at room temperature for 30 min. The resulting precipitate was filtered off, dried over Na_2SO_4 and concentrated under vacuum. The residual crude product was purified by column chromatography on silica gel with ethyl acetate/hexane (1:6) as eluent to afford the chiral homoallylic alcohol (469 mg, 2 mmol, 80% yield) as a colorless oil. ^{1}H NMR (300 MHz, $CDCl_3$): δ = 7.52-7.59 (m, 2H), 7.35 (td, *J* = 7.6 Hz, 1.0 Hz, 1H), 7.14 (td, *J* = 7.3 Hz, 1.8 Hz, 1H), 5.85-5.91 (m, 1H), 5.21-5.25 (m, 2H), 5.12 (dd, *J* = 8.5 Hz, 3.8 Hz, 1H), 2.62-2.65 (m, 2H), 2.35-2.43 (m, 1H); ^{13}C NMR (75.5 MHz, $CDCl_3$): δ = 141.3, 134.3, 131.1, 129.3, 128.4, 127.1, 127.0, 119.5, 69.6, 42.0. IR: 3361, 3073, 2909, 1637, 1466, 1466, 1022, 753. MS (EI) m/z 226 (M+); HRMS (EI): m/z calcd for $C_{10}H_{11}BrO$ (^{79}Br) (M+): 225.9993; found: 225.9993. Based upon the work of Hall *et al*.[99] we assigned the absolute configuration of the chiral homoallylic alcohol (*R*)-**149b** [entry 2, Table 4: $[\alpha]^{20}_D$ = +38.2 (c = 3.7, $CHCl_3$)] as (*R*)-configuration. Previously, Hall reported that chiral homoallylic alcohol (*R*)-**149b** had an optical rotation of $[\alpha]^{20}_D$ = +50.71 (c = 1.61, $CHCl_3$). The absolute configurations of the remaining chiral homoallylic alcohols (i.e., (*R*)-**149a**, (*R*)-**149c-f**) reported in the present work were assumed to be the same as (*R*)-**149b**.

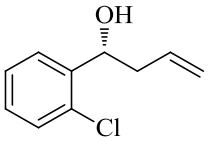

(*R*)-1-(2- chlorophenyl)-3-buten-1-ol, 149a. (Table 4, entry 1). ^{1}H NMR (300 MHz, $CDCl_3$): 7.35 (dd, *J* = 7.8 Hz, 1.6 Hz, 1H), 7.20-7.25 (m, 3H), 5.82-5.96 (m, 1H), 5.21-5.82 (m, 3H), 2.61-2.69 (m, 1H), 2.40-2.45 (m, 1H), δ = 2.30 (br, 1H); ^{13}C NMR (75.5 MHz, $CDCl_3$): δ = 141.3, 134.3, 131.7, 129.3, 128.4, 127.1, 127.0,

118.5, 69.6, 42.0; MS (EI) m/z 182 (M+). IR: 3349, 3072, 2910, 1639, 1471, 1436, 1032, 754. HRMS (EI): m/z calcd for $C_{10}H_{11}ClO$ (M+): 182.0498; found: 182.0498; $[\alpha]^{20}_D$ = +78.8 (c = 1.9, $CHCl_3$).

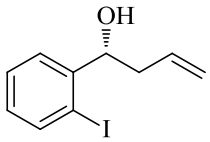

(*R*)-1-(2-iodophenyl)-3-buten-1-ol (149c). (Table 4, entry 3). ^{1}H NMR (300 MHz, $CDCl_3$): δ = 7.82 (dd, *J* = 7.8 Hz, 0.9 Hz, 1H), 7.54 (dd, *J* = 8.1 Hz, 0.8 Hz, 1H), 7.37 (td, *J* = 7.6 Hz, 0.5 Hz, 1H), 6.70 (td, *J* = 7.5 Hz, 1.5 Hz, 1H), 5.87-5.93 (m, 1H), 5.19-5.26 (m, 1H), 4.94 (dd, *J* = 8.6 Hz, 3.7 Hz, 1H), 2.38-2.66 (m, 1H), 2.28-2.35 (m, 2H); ^{13}C NMR (75.5 MHz, $CDCl_3$): δ = 145. 6, 139.3, 134.3, 129.21, 128.5, 127.1, 118.6, 97.5, 76.3, 42.2. IR: 3315, 3070, 2933, 1637, 1461, 1433, 1012, 747. MS (EI) m/z 274 (M+); HRMS (EI): m/z calcd for $C_{10}H_{11}IO$ (M+): 273.9855; found: 273.9855; $[\alpha]^{20}_D$= +54.8 (c = 1.6, $CHCl_3$).

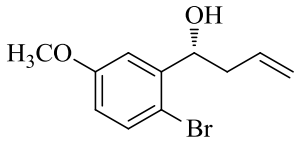

(***R*)-1-(2-bromo-5-methoxyphenyl)-3-buten-1-ol (149e).** (Table 4, entry 5): ^{1}H NMR (300 MHz, $CDCl_3$): δ = 7.71 (dd, *J* = 8.9 Hz, 3.1 Hz, 1H), 7.27(d, *J* = 8.1, 1H), 7.14 (d, *J* = 3.0 Hz, 1H), 5.84-5.97 (m, 1H), 5.19-5.25 (m, 2H), 5.04-5.08 (m, 1H), 3.83 (s, 3H), 2.62-2.68 (m, 1H), 2.37-2.39 (m, 2H); ^{13}C NMR (75.5 MHz, $CDCl_3$): δ = 164.9, 161.6, 146.1, 146.0, 120.0, 117.0, 116.7, 115.7, 115.4, 72.5, 42.8. IR: 3391, 3074, 2835, 1692, 1466, 1440, 1015, 755. MS (EI) m/z 256 (M+); HRMS (EI): m/z calcd for $C_{11}H_{13}BrO_2$ (^{79}Br) (M+): 256.0099; found: 256.0099; $[\alpha]^{20}_D$ = +2.3 (c = 2, $CHCl_3$).

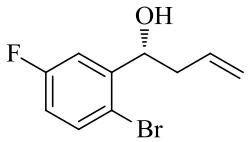

(*R*)-1-(2-bromo-5-fluorophenyl)-3-buten-1-ol (149f). (Table 4, entry 6): ^{1}H NMR (300 MHz, $CDCl_3$): δ = 7.47 (dd, *J* = 8.7 Hz, 5.3 Hz, 1H), 7.31 (dd, *J* = 9.7 Hz, 3.0 Hz, 1H), 6.88 (td, *J* = 8.1 Hz, 3.1 Hz, 1H), 5.83-5.90 (m, 1H), 5.19-5.24 (m, 2H), 5.02-5.07 (m, 1H), 2.60-2.67 (m, 1H), 2.31-2.40 (m, 2H); ^{13}C NMR (75.5 MHz, $CDCl_3$): δ = 164.1, 160.8, 145.3, 145.2, 133.9, 119.2, 116.2, 114.6, 71.7, 42.0. IR:

3286, 3081, 2934, 1642, 1461, 1427, 1027, 767. MS (EI) m/z 244 (M+); HRMS (EI): m/z calcd for $C_{10}H_{10}BrFO$ (^{79}Br) (M+): 243.9899; found: 243.9899; $[\alpha]^{20}_D$ = +65.6 (c = 0.7, $CHCl_3$).

4.2.2. Typical Procedure for Alkenylation of Chiral Homoallylic Alcohol with Catalytic Amount of $(Ph_3P)_2Pd^{II}Cl_2$.

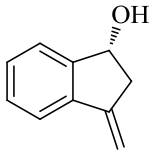

Synthesis of (*R*)-3-methylene-2,3-dihydro-1H-inden-1-ol (150a). (in Table 4, entry 2). To a mixture of (*R*)-1-(2-bromophenyl)-3-buten-1-ol (385.9 mg, 1.7 mmol), bis(triphenylphosphine)-palladium(II) chloride (23.8 mg, 0.034 mmol), potassium carbonate (469.9 mg, 3.4 mmol), and DMF (3 mL) were added under a nitrogen atmosphere followed by 2 drops of hydrazine by syringe. The mixture was heated at 100°C for 24h. The resulting mixture was filtered off and it was diluted with ether and washed with water. The ether layer was dried over Na_2SO_4 and concentrated. The residual crude product was purified by column chromatography on silica gel with pentane/ether (1:4) as the eluent to afford the chiral (*R*)-3-methylene-2,3-dihydro-1H-inden-1-ol (180 mg, 1.2 mmol, 73% yield) as a colorless oil. ^{1}H NMR: (300 MHz, $CDCl_3$): δ = 7.49-7.57 (m, 2H), 7.28-7.38 (m, 2H), 5.55 (t, *J* = 2.3 Hz, 1H), 5.27-5.34 (m, 1H), 5.12 (t, *J* = 1.9 Hz, 1H), 3.18-3.28 (m, 1H), 2.66-2.73 (m, 1H), 1.82 (d, *J* = 7.3 Hz, 1H); ^{13}C NMR (75.5 MHz, $CDCl_3$): δ = 147.1, 146.5, 140.2, 128.9, 128.6, 125.2, 120.6, 104.1, 73.1, 42.4. IR: 3296, 3080, 2920, 1639. MS (EI) m/z 146 (M+); HRMS (EI): m/z calcd for $C_{10}H_{10}O$ (M+): 146.0732; found: 146.0732; $[\alpha]^{20}_D$ = -6.7 (c = 0.4, $CHCl_3$), $[\alpha]^{20}_D$ = -8.8 (c = 0.5, $CHCl_3$), $[\alpha]^{20}_D$ = -10.5 (c = 0.5, $CHCl_3$) for intermediate **149a**, **149b** and **149c** respectively. The enantioselectivity was determined by HPLC analysis on a chiral column (OD-H, hexane/iprOH 95:5, flow rate 1.0 $mLmin^{-1}$) to be 84:16 er, 68% ee: t_{minor} = 9.33 min , t_{major} = 10.40 min , 87.5:12.5 er, 75% ee: t_{minor} = 9.29

min, t_{major} = 10.49 min, 90:10 er, 80% ee: t_{minor} = 9.36 min, t_{major} = 10.43 min for intermediate **149a**, **149b** and **149c** respectively.

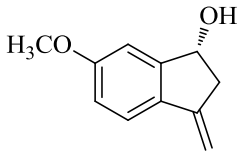

(*R*)-6-methoxy-3-methylene-2,3-dihydro-1H-inden-1-ol, (150e). (in Table 4, entry 5). ^{1}H NMR: (300 MHz, $CDCl_3$): δ = 7.45 (d, *J* = 8.1, 1H), 7.00 (d, *J* = 2.0, 1H), 6.93 (dd, *J* = 8.5 Hz, 2.3 Hz, 1H), 5.37 (t, *J* = 2.3 Hz, 1H), 5.22-5.28 (m, 1H), 4.98 (t, *J* = 1.8 Hz, 1H), 3.83 (s, 3H), 3.19-3.27 (m, 1H), 2.65-2.72 (m, 1H), 1.79 (d, *J* = 7.9, 1H); ^{13}C NMR (75.5 MHz, $CDCl_3$): δ = 160.6, 148.6, 145.7, 133.0, 121.7, 116.3, 108.6, 101.9, 73.3, 55.5, 43.0. IR: 3300, 3075, 2920, 1640. MS (EI) m/z 176 (M+); HRMS (EI): m/z calcd for $C_{11}H_{12}O_2$ (M+): 176.0837; found: 176.0837; $[\alpha]^{20}_D$ = -42.7 (c = 0.9, $CHCl_3$); The enantioselectivity was determined by HPLC analysis on a chiral column (OD-H, hexane/*i*prOH 95:5, flow rate 1.0 mLmin^{-1}) to be 87:13 er, 74% ee: t_{minor} = 11.81 min, t_{major} = 13.56 min.

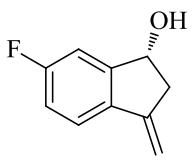

(*R*)-6-fluoro-3-methylene-2,3-dihydro-1H-inden-1-ol, (150f). (Table 4, entry 6). ^{1}H NMR: (300 MHz, $CDCl_3$): δ = 7.45 (dd, *J* = 8.3 Hz, 4.9 Hz, 1H), 7.02-7.13 (m, 2H), 5.43 (br ,1H), 5.19 (br, 1H), 5.05 (br, 1H), 3.14-3.22 (m, 1H), 2.62-2.68 (m, 2H); ^{13}C NMR (75.5 MHz, $CDCl_3$): δ = 161.9, 149.1, 145.3, 136.3, 122.2, 116.3, 111.7, 103.9, 73.0, 42.9. IR: 3347, 2922, 1609. MS (EI) m/z 164 (M+); HRMS (EI): m/z calcd for $C_{10}H_9FO$ (M+): 164.0637; found: 164.0637; $[\alpha]^{20}_D$ = 2.9 (c = 1, $CHCl_3$); The enantioselectivity was determined by HPLC analysis on a chiral column (OD-H, hexane/*i*prOH 95:5, flow rate 1.0 mLmin^{-1}) to be 79:21 er, 58% ee: t_{minor} = 7.55 min, t_{major} = 8.22 min.

4.3. Enantioselective Indium-mediated Synthetic Approach to $C_{(3)}$-Chiral Substituted Phthalides.

4.3.1. Representative Procedure A: Synthesis of Alkyl 2-Formylbenzoate.

Iodomethane (0.6 mL, 9.5mmol) was added to a stirred solution of 2-formylbenzoic acid (0.765 g, 5.1 mmol) and potassium carbonate (0.387 g, 2.8 mmol) in DMF (4 mL). The reaction mixture was refluxed for 4 h, diluted with water (8 mL) and extracted with DCM. The combined organic phases were washed with 1N HCl (4 mL), saturated aqueous $NaHCO_3$ (4 mL) and dried over Na_2SO_4. After filtration and evaporation of the solvents in vacuum, the crude product was purified by column chromatography on silica gel (*n*-hexane/EtOAc: 6/1) to yield **151a** as a colorless oil (0.673 g, 80.4%).

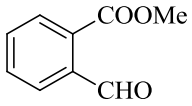

Methyl 2-formylbenzoate (151a). ^{1}H NMR (300 MHz, $CDCl_3$): δ = 10.59 (s, 1H), 7.97-7.90 (m, 2H), 7.65-7.62 (m, 2H), 3.96 (s, 3H). ^{13}C NMR (75 MHz, $CDCl_3$): δ = 192.3, 166.9, 137.1, 134.5, 133.1, 132.5, 130.5, 128.5, 52.9. HRMS (EI): m/z calcd for $C_9H_8O_3$ (M+): 164.0473; found: 164.0468.

4.3.2. Representative procedure B: Synthesis of 5-Substituted 2-Formylbenzoic Acid.

1,2-Dichloroethane (25 mL) was added to a mixture of 6-methoxyphthalide (670 mg, 4.5 mmol), N-bromosuccinimide (890 mg, 5 mmol), azobisisobutyronitrile (41 mg, 0.2 mmol) and refluxed for 1 h. The reaction mixture was kept in an ice bath for 2 hours then filtered. The solvent was removed under reduced pressure. Water (10 mL) was then added and the resulting mixture refluxed for 1 h. The reaction mixture was then cooled to room temperature and extracted with EtOAc. The combined organic phases were dried and concentrated under reduced pressure.

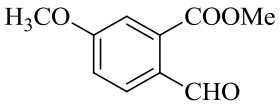

Methyl 2-formyl-5-methoxybenzoate (151b). Starting 6-methoxyphthalide was prepared by the reported procedure of Napoletano *et al.*[131] The representative procedures B and A outlined above were then followed, respectively. ^{1}H NMR (300 MHz, $CDCl_3$): δ = 10.39 (s, 1H), 7.89 (d, *J* = 8.7 Hz, 1H), 7.32 (d, *J* = 2.4 Hz, 1H), 7.04 (dd, *J* = 8.4, 2.1 Hz, 1H), 3.91 (s, 3H), 3.84 (s, 3H). ^{13}C NMR (75 MHz, $CDCl_3$): δ = 190.5, 166.6, 163.2, 134.4, 130.8, 129.4, 117.4, 115.3, 55.7, 52.7. HRMS (EI): m/z calcd for $C_{10}H_{10}O_4$ (M^+): 194.0579; found: 194.0573.

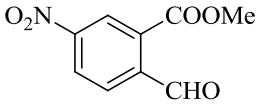

Methyl 2-formyl-5-nitrobenzoate (151c). The starting 6-nitrophthalide was prepared by the reported procedure of Wang, J. *et al.*[132] Thereafter, the representative procedures B and A outlined above were followed, respectively. m.p. = 62-64 °C. ^{1}H NMR (300 MHz, $CDCl_3$): δ = 10.67 (s, 1H), 8.80 (d, *J* = 2.1 Hz, 1H), 8.47-8.43 (m, 1H), 8.08 (d, *J* = 8.4, 1H), 4.03 (s, 3H). ^{13}C NMR (75 MHz, $CDCl_3$): δ = 190.5, 164.7, 150.0, 141.5, 133.0, 130.1, 127.2, 125.8, 53.6. HRMS (EI): m/z calcd for $C_9H_7NO_5$ (M^+): 209.0324; found: 209.0326.

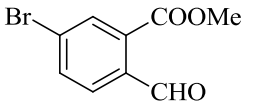

Methyl 5-bromo-2-formylbenzoate (151d). 6-Bromophthalide **155d** was prepared by portionwise addition of N-bromo succinimide (NBS) to phthalide (**157**) (1g, 7.45 mmol) in a mixture of triflouroacetic acid (TFA) (3.7 mL) and sulphuric acid (1.7 mL) at room temperature for 9h. The reaction mixture was stirred at r.t. for 60 h, then poured onto ice and extracted with ethyl acetate. The combined organic phases were subsequently washed with a saturated solution of sodium bicarbonate and brine. After evaporation of the solvents in vacuum, the crude product was purified by column chromatography on silica gel (*n*-hexane/EtOAc: 9/1) to yield the desired product. ^{1}H NMR (300 MHz, $CDCl_3$): δ = 8.01 (d, *J* = 1.8 Hz, 1H), 7.80 (dd, *J* = 8.4, 1.8 Hz, 1H), 7.41 (d, *J* =

7.8 Hz, 1H), 5.29 (s, 2H). ^{13}C NMR (75 MHz, $CDCl_3$): δ = 169.5, 145.2, 137.2, 128.7, 127.9, 123.9, 123.1, 69.6. The representative procedures B and A outlined above were followed to prepare **151d** which was isolate as a light yellow solid. m.p. = 114-116 °C. ^{1}H NMR (300 MHz, $CDCl_3$): δ = 10.57 (s, 1H), 8.11 (d, *J* = 1.8 Hz, 1H), 7.80 (s, 1H), 7.79 (d, *J* = 1.8 Hz, 1H), 3.99 (s, 3H). ^{13}C NMR (75 MHz, $CDCl_3$): δ = 191.0, 165.4, 135.7, 133.5, 133.4, 130.0, 128.1, 53.2. HRMS (EI): m/z calcd for $C_9H_7BrO_3$ (M^+): 241.9579; found: 241.9577.

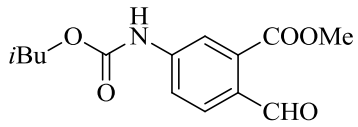

Methyl 2-formyl-5-((isobutoxycarbonyl)amino)benzoate (151e). 6-Aminophthalide was prepared by the reported procedure of Pokhodylo, N. T. and coworkers.[133] 4-Dimethylaminopyridine (DMAP) (0.12 g, 1 mmol) and isobutyl chloroformate (1.5 g, 11 mmol) were added to a mixture of 6-aminophthalide (1.49 g, 10 mmol) in acetonitrile (30 mL). The reaction mixture was stirred at room temperature overnight. After evaporation of the solvents in vacuum, the crude product was purified by column chromatography on silica gel (*n*-hexane/EtOAc: 1/1) to yield carbamate **155e.** ^{1}H NMR (300MHz, $CDCl_3$): δ = 7.93 (s, 1H), 7.85 (d, *J* = 8.4 Hz, 1H), 7.60 (s, 1H), 7.40 (d, *J* = 8.4 Hz, 1H), 5.26 (s, 2H), 3.94 (d, *J* = 6.6 Hz, 2H), 1.98-1.89 (m, 1H), 0.92 (d, 6.9 Hz, 6H). ^{13}C NMR (75 MHz, $CDCl_3$): δ = 171.2, 153.9, 140.9, 139.6, 126.4, 125.1, 122.7, 114.9, 71.6, 69.7, 27.94, 19.02. HRMS (EI): m/z calcd for $C_{13}H_{15}NO_4$ (M^+): 249.1001; found: 249.1006. The representative procedure B and A was followed recpectively to yield **151e** as a light yellow solid. m.p. = 104-106 °C. ^{1}H NMR (300MHz, $CDCl_3$): δ = 10.50 (s, 1H), 8.04 (d, *J* = 2.1 Hz, 1H), 7.95 (d, *J* = 8.4 Hz, 1H), 7.70 (dd, *J* = 8.4, 1.9 Hz, 1H), 7.45 (s, 1H), 4.00 (d, *J* = 6.6 Hz, 2H), 3.95 (s, 3H), 2.04-1.89 (m, 1H), 0.95 (d, *J* = 6.6 Hz, 6H). ^{13}C NMR (75 MHz, $CDCl_3$): δ = 190.9, 166.6, 153.2, 142.9, 133.7,

131.1, 130.2, 120.8, 119.2, 71.9, 52.8, 27.9, 19.0. HRMS (EI): m/z calcd for $C_{14}H_{17}NO_5$ (M^+): 279.1107; found: 279.1110.

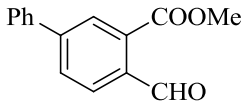

Methyl 4-formyl-[1,1'-biphenyl]-3-carboxylate (151f). For preparation of the intermediate **151f**, toluene (2.3 mL) was added to a mixture of 6-bromophthalide (280 mg, 1.3 mmol), phenylboronic acid (319.4 mg, 2.6 mmol), tetrakis(triphenylphosphine)palladium ($Pd(PPh_3)_4$) (75.7 mg, 0.065 mmol) and sodium carbonate solution (1.9 mL, 2M). The reaction mixture was refluxed for 5 h followed by addition of water (2 mL) and extraction with ethylacetate (10 mL, 3 times). The combined organic phase was dried and concentrated under the reduced pressure. The crude product was purified by column chromatography on silica gel (*n*-hexane/EtOAc: 1/1) to yield the desired product. ^{1}H NMR (300 MHz, $CDCl_3$): δ = 8.14 (s, 1H), 7.93 (dd, *J* = 8.1, 1.8 Hz, 1H), 7.65-7.60 (m, 3H), 7.50-7.43 (m, 3H), 5.38(s, 2H). ^{13}C NMR (75 MHz, $CDCl_3$): δ = 171.2, 145.4, 142.8, 139.5, 133.3, 129.2, 128.3, 127.3, 124.1, 122.6, 69.7. HRMS (EI): m/z calcd for $C_{14}H_{10}O_2$ (M^+): 210.0681; found: 210.0684. The representative procedures B and A outlined above were then followed, respectively, to yield **151f** as a white solid. m.p. = 77-79 °C. ^{1}H NMR (300 MHz, $CDCl_3$): δ = 10.62 (s, 1H), 8.15 (s, 1H), 7.97 (d, *J* = 8.1 Hz, 1H), 7.79 (dd, *J* = 8.1, 1.5 Hz, 1H), 7.60 (dd, *J* = 8.4, 1.8 Hz, 2H), 7.48-7.40 (m, 3H), 3.40 (s, 3H). ^{13}C NMR (75 MHz, $CDCl_3$): δ = 191.6, 166.7, 145.7, 138.6, 130.5, 129.1, 128.9, 128.8, 127.2, 52.8. HRMS (EI): m/z calcd for $C_{15}H_{12}O_3$ (M^+): 240.0786; found: 240.0783.

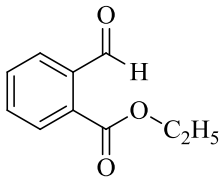

Ethyl 2-formylbenzoate (151g): ^{1}H NMR (300 MHz, $CDCl_3$): δ = 10.90 (s, 1H), 7.96-7.88 (m, 2H), 7.63-7.60 (m, 2H), 4.41 (q, *J* = 7.2 Hz, 2H), 1.40 (t, *J* = 7.2, 3H). ^{13}C NMR (75 MHz, $CDCl_3$): δ = 192.1, 166.3,

137.0, 132.9, 132.5, 132.3, 130.3, 128.3, 61.9, 14.3. HRMS (EI): m/z calcd for $C_{10}H_{10}O_3$ (M^+): 178.0630; found: 178.0627.

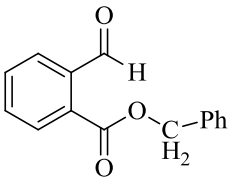

Benzyl 2-formylbenzoate (151h): ^{1}H NMR (300 MHz, $CDCl_3$): δ = 10.62 (s, 1H), 7.97-7.87 (m, 2H), 7.58-7.55 (m, 2H), 7.46-7.33 (m, 5), 5.39 (s, 2H). ^{13}C NMR (75 MHz, $CDCl_3$): δ = 191.7, 165.8, 136.9, 135.2, 132.7, 132.2, 131.7.3, 130.2, 128.5, 128.3, 128.2, 128.2, 67.3, HRMS (EI): m/z calcd for $C_{15}H_{12}O_3$ (M^+): 240.0786; found: 240.0783.

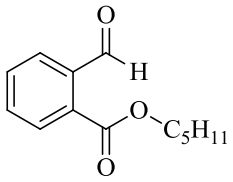

Pentyl 2-formylbenzoate (151i): ^{1}H NMR (300 MHz, $CDCl_3$): δ = 10.59 (s, 1H), 7.93-7.86 (m, 2H), 7.61-7.58 (m, 2H), 4.33 (t, *J* = 6.6 Hz, 2H), 1.75-1.73 (m, 2H), 1.37-1.36 (m, 6H), 0.89 (t, *J* = 6.6, 3H). ^{13}C NMR (75 MHz, $CDCl_3$): δ = 192.0, 166.3, 137.0, 132.9, 132.4, 132.2, 130.3, 128.3, 66.0, 28.3, 28.1, 22.3, 13.9. HRMS (EI): m/z calcd for $C_{13}H_{16}O_3$ (M^+): 220.1099; found: 220.1096.

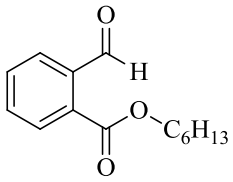

Hexyl 2-formylbenzoate (151j): ^{1}H NMR (300 MHz, $CDCl_3$): δ = 10.59 (s, 1H), 7.95-7.87 (m, 2H), 7.63-7.57 (m, 2H), 4.34 (t, *J* = 3.6 Hz, 2H), 1.80-1.70 (m, 2H), 1.43-1.25 (m, 6H), 0.87 (t, *J* = 6.9 Hz, 3H). ^{13}C NMR (75 MHz, $CDCl_3$): δ = 192.0, 166.2, 137.0, 132.8, 132.2, 130.3, 128.3, 66.0, 31.3, 28.5, 25.6, 22.5, 13.9. HRMS (EI): m/z calcd for $C_{14}H_{18}O_3$ (M^+): 234.1256; found: 234.1250.

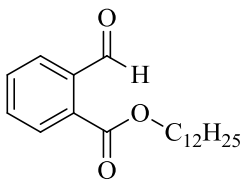

Dodecyl 2-formylbenzoate (1k): ^{1}H NMR (300 MHz, $CDCl_3$): δ = 10.62 (s, 1H), 7.98-7.91 (m, 2H), 7.65-7.62 (m, 2H), 4.37 (t, *J* = 6.6 Hz, 2H), 1.81-1.76 (m, 2H), 1.43-1.26 (m, 18H), 0.87 (t, *J* = 6.3 Hz, 3H). ^{13}C NMR (75 MHz, $CDCl_3$): δ = 192.0, 166.3, 137.1, 132.9, 132.4, 132.2, 130.3, 128.3, 66.0, 31.9, 29.6, 29.5, 29.5, 29.3, 29.2, 28.6, 26.0, 24.7, 22.7, 14.1. HRMS (EI): m/z calcd for $C_{20}H_{30}O_3$ (M^+): 318.2195; found: 318.22047.

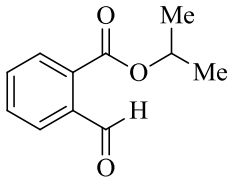

Isopropyl 2-formylbenzoate (151l): m.p. = 77-79 °C. ^{1}H NMR (300 MHz, $CDCl_3$): δ = 10.45 (s, 1H), 7.81-7.67 (m, 2H), 7.51-7.41 (m, 2H), 5.20-5.05 (m, 1H), 1.24 (d, *J* = 6, 6H). ^{13}C NMR (75 MHz, $CDCl_3$): δ = 192.0, 165.7, 136.9, 132.8, 132.0, 130.2, 128.2, 69.7, 21.8. HRMS (EI): m/z calcd for $C_{11}H_{12}O_3$ (M^+): 192.0786; found: 192.0781.

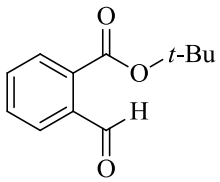

***tert*-Butyl 2-formylbenzoate (151m):** To a vigorously stirred suspension of anhydrous magnesium sulphate (3.2 g, 27 mmol) in DCM (27 mL), sulphuric acid (0.4 mL, 6.7 mmol) was added. The reaction mixture was stirred for 15 minutes; 2-carboxybenzaldehyde (1 g, 6.7 mmol) and *tert*-butanol (3.2 mL) were added and stirred for 18 h at room temperature followed by quenching with saturated sodium bicarbonate (75 mL). The organic phase was separated, washed with brine and dried. The crude product was purified by column chromatography on silica gel (*n*-hexane/EtOAc: 6/1) to yield **1m** as a white solid (1.1 g, 80.0%). m.p. = 80-81 °C. ^{1}H NMR (300 MHz, $CDCl_3$): δ = 10.58 (s, 1H), 7.85 (d, *J* = 7.8 Hz, 1H), 7.70-7.65 (m, 1H), 7.57-7.47 (m, 2H), 6.54 (s, 1H), 1.44 (s, 9H). ^{13}C NMR (75 MHz, $CDCl_3$): δ = 196.2, 146.5, 134.3, 130.5, 127.2, 125.2, 123.3, 98.0, 77.8, 28.7. HRMS (EI): m/z calcd for $C_{12}H_{14}O_3$ (M^+): 206.0943; found: 206.0937.

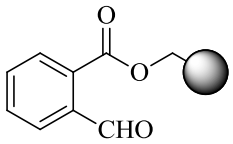

2-Formylphenylcarboxymethyl polystyrene (151n): 151n was synthesized by following the procedure reported by Knepper K. and coworkers.[133] Spectroscopic data was in full agreement with spectral data of an authentic sample.

4.3.3. Representative Procedure C: Synthesis of Substituted (*R*)-3-Allylisobenzofuran-1(3H)-one.

THF (6 mL) was added to a mixture of (1*R*, 2*S*)-2-amino-1,2-diphenylethanol (213.2 mg, 1 mmol) and indium powder (114.8 mg, 1 mmol) followed by addition of anhydrous pyridine (0.16 mL, 2 mmol), allyl bromide (0.17 mL, 2 mmol) and *n*-hexane (1 mL). The reaction mixture was stirred for 30 min at room temperature then cooled to -78°C and substrate **151a** (82.05 mg, 0.5 mmol) in THF (1 mL) added dropwise. The reaction mixture was stirred for 1 h then saturated ammonium chloride was added (1 mL) and extracted with ethyl acetate. After drying with anhydrous sodium sulfate and evaporation of the solvents in vacuum, the crude product was purified by column chromatography on silica gel (*n*-hexane/EtOAc: 1/1) to yield **152a** as a colorless oil (67.4 mg, 77%).

4.3.4. Determination of the Absolute Stereochemistry.

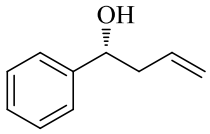

(*R*)-1-phenylbut-3-en-1-ol (160): Representative Procedure C was followed. ^{1}H NMR (300 MHz, $CDCl_3$): δ = 7.30-7.39 (m, 5H), 5.77-5.91 (m, 1H), 5.15-5.22 (m, 1H), 4.75 (t, *J* = 7 Hz, 1H), 2.50-2.59 (m, 2H), 2.22 (s, 1H, OH). ^{13}C NMR (75 MHz, $CDCl_3$): δ = 144.0, 134.5, 128.5, 127.7, 125.9, 118.5, 73.4, 43.96. The absolute stereochemistry was determined by comparison of the sign of optical rotation with reported literature values ($[\alpha]^{20}_{D}$= +37 (c = 1, $CHCl_3$)).[134]

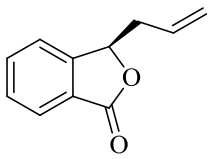

(*R*)-3-allylisobenzofuran-1(3H)-one (152a): Representative Procedure C was followed to prepare **152a** from substrates **151a**, **151g-l**, and **151n**. The crude product was purified by column chromatography on silica gel (*n*-hexane/EtOAc: 1/1) to yield **152a** from substrate (**151g** (54.1 mg, 62%), **151h** (50.6 mg, 58%), **151i** (52.3 mg, 60%), **151j** (48.1 mg, 55%), **151k** (49.8 mg, 57%), **151l** (68.1 mg,

78%), **151n** (45.3 mg, 52%)). ^{1}H NMR (300 MHz, $CDCl_3$): δ = 7.91 (d, *J* = 7.8 Hz, 1H), 7.69 (t, *J* = 7.6 Hz, 1H), 7.57-7.47 (m, 2H), 5.85-5.71 (m, 1H), 5.53 (t, *J* = 6 Hz, 1H), 5.23-5.15 (m, 2H), 2.81-2.62 (m, 2H). ^{13}C NMR (75 MHz, $CDCl_3$): δ = 170.5, 149.4, 134.0, 131.3, 129.3, 126.3, 125.7, 122.1, 119.8, 80.3, 38.7. IR: 3081, 2921, 2850, 1760, 1614. HRMS (EI): m/z calcd for $C_{11}H_{10}O_2$ (M^+): 174.0681; found: 174.0677. For **152a** prepared from **151a** $[\alpha]^{20}_D$= +62.60 (c = 1.98, $CHCl_3$). For **152a** prepared from **151g** $[\alpha]^{20}_D$= +61.50 (c = 1.90, $CHCl_3$). For **152a** prepared from **151h** $[\alpha]^{20}_D$= +61.4 (c = 1.95, $CHCl_3$). For **152a** prepared from **151i** $[\alpha]^{20}_D$= +60.4 (c = 1.5, $CHCl_3$). For **152a** prepared from **151j** $[\alpha]^{20}_D$= +59.2 (c = 1.5, $CHCl_3$). For **152a** prepared from **151k** $[\alpha]^{20}_D$= +57.0 (c = 1.50, $CHCl_3$). For **152a** prepared from **151l** $[\alpha]^{20}_D$= +58.0 (c = 1.6, $CHCl_3$). For **152a** prepared from **151n** $[\alpha]^{20}_D$= +4.2 (c = 0.6, $CHCl_3$). The enantioselectivity was determined by HPLC analysis on a chiral column (OD-H, hexane/*i*prOH 95:5, flow rate 0.5 mLmin^{-1}, wavelength = 245 nm). For **152a** prepared from **151a** 90:10 er, 80% ee: t_{minor} = 20.07 min, t_{major} = 18.82 min. For **152a** prepared from **151g** 89.5:10.5 er, 79% ee: t_{minor} = 19.52 min, t_{major} = 18.56 min. For **152a** prepared from **151h** 88:12 er, 76% ee: t_{minor} = 20.06 min, t_{major} = 18.75 min, For **152a** prepared from **151i** 85.5:14.5 er, 71% ee: t_{minor} = 19.39 min, t_{major} = 18.37 min. For **152a** prepared from **151j** 82.5:17.5 er, 65% ee: t_{minor} = 19.40 min, t_{major} = 18.39 min. For **152a** prepared from **151k** 75:25 er, 50%: t_{minor} = 19.79 min, t_{major} = 18.54 min. For **152a** prepared from **151l** 82:18 er, 64% ee: t_{minor} = 18.87 min, t_{major} = 17.96 min. For **152a** prepared from **151n** 50.6:49.9 er, 0.12% ee (racemic): t_{minor} = 20.07 min, t_{major} = 18.645 min. Absolute configuration assigned as (*R*) by comparison of optical rotation with a literature value.[135]

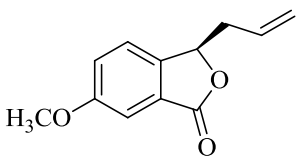

(*R*)-3-allyl-6-methoxyisobenzofuran-1(3H)-one (152b): Representative Procedure C was followed. The crude product was

purified by column chromatography on silica gel (*n*-hexane/EtOAc: 1/1) to yield **152b** (68.4 mg, 67%). ^{1}H NMR (300 MHz, $CDCl_3$): δ = 7.35 (s, 1H), 7.33 (d, *J* = 2.1 Hz, 1H), 7.20-7.24 (m, 1H), 5.80-5.69 (m, 1H), 5.47 (t, *J* = 5.9 Hz, 1H), 5.21-5.14 (m, 2H), 3.87 (s, 3H), 2.71-2.60 (m, 2H). ^{13}C NMR (75 MHz, $CDCl_3$): δ = 170.5, 160.7, 141.8, 131.3, 127.6, 122.9, 122.8, 119.7, 107.5, 80.12, 55.8, 38.8. IR: 2980, 1760, 1633, 1281, 1063. HRMS (EI): m/z calcd for $C_{12}H_{12}O_3$ (M^+): 204.0786; found: 204.0782. $[\alpha]^{20}_D$= +15.3 (c = 0.32, $CHCl_3$). The enantioselectivity was determined by HPLC analysis on a chiral column (OD-H, hexane/*i*prOH 99:1, flow rate 0.5 mLmin^{-1}, wavelength = 245 nm) to be 88.5:11.5 er, 77% ee: t_{minor} = 31.92 min, t_{major} = 33.11 min.

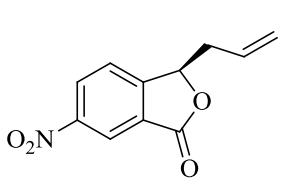

(*R*)-3-allyl-6-nitroisobenzofuran-1(3H)-one (152c): Representative Procedure C was followed. The crude product was purified by column chromatography on silica gel (*n*-hexane/EtOAc: 1/1) to yield **152c** (74.5 mg, 68%). ^{1}H NMR (300 MHz, $CDCl_3$): δ = 8.74 (s, 1H), 8.56 (dd, *J* = 8.1, 2.1 Hz, 1H), 7.69 (t, *J* = 8.4 Hz, 1H), 5.81-5.65 (m, 2H), 5.25-5.19 (m, 2H), 2.88-2.71 (m, 2H). ^{13}C NMR (75 MHz, $CDCl_3$): δ = 167.8, 154.5, 149.1, 130.1, 128.8, 128.1, 123.5, 121.4, 120.8, 80.2, 38.2. IR: 3150, 2921, 1766, 1615, 1537, 1434, 1346. HRMS (EI): m/z calcd for $C_{11}H_9NO_4$ (M^+): 219.0532; found: 219.0536. $[\alpha]^{20}_D$= +11.05 (c = 0.57, $CHCl_3$). The enantioselectivity was determined by HPLC analysis on a chiral column (AS-H, hexane/*i*prOH 80:20, flow rate 1 mLmin^{-1}, wavelength = 245 nm) to be 72.5:27.5 er, 45% ee: t_{minor} = 12.64 min, t_{major} = 16.23 min.

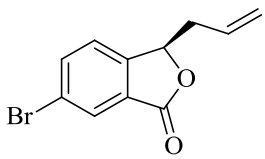

(*R*)-3-allyl-6-bromoisobenzofuran-1(3H)-one (152d): Representative Procedure C was followed. The crude product was purified by column chromatography on silica gel (*n*-hexane/EtOAc:

1/1) to yield **152d** (87.3 mg, 69%). ^{1}H NMR (300 MHz, $CDCl_3$): δ = 8.01 (d, *J* = 1.6 Hz, 1H), 7.77 (dd, *J* = 8.1, 1.7 Hz, 1H), 7.35 (d, *J* = 6 Hz, 1H), 5.80-5.66 (m, 1H), 5.48 (t, *J* = 6 Hz, 1H), 5.21-5.15 (m, 2H), 2.72-2.65 (m, 2H). ^{13}C NMR (75 MHz, $CDCl_3$): δ = 168.8, 148.0, 137.1, 130.9, 128.9, 123.7, 120.3, 80.2, 38.6. IR: 2922, 2851, 1769, 1203, 1073. HRMS (EI): m/z calcd for $C_{11}H_9O_2$ (M^+): 215.9786; found: 215.9789. $[\alpha]^{20}_D$= +0.28 (c = 11.8, $CHCl_3$), The enantioselectivity was determined by HPLC analysis on a chiral column (AS-H, hexane/*i*prOH 90:10, flow rate 1 $mLmin^{-1}$, wavelength = 245 nm) to be 84.5:15.5 er, 69% ee: t_{minor} = 14.78 min, t_{major} = 16.50 min.

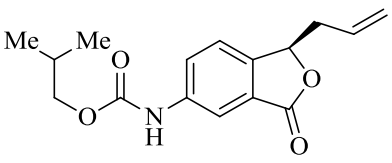

(R)-isobutyl (1-allyl-3-oxo-1,3-dihydroisobenzofuran-5-yl)carbamate (152e): Representative Procedure C was followed. The crude product was purified by column chromatography on silica gel (*n*-hexane/EtOAc: 1/1) to yield **152e** (94.2 mg, 65%). m.p. = 130-133 °C. ^{1}H NMR (300 MHz, $CDCl_3$): δ = 7.85 (s, 1H), 7.82 (s, 1H), 7.39 (d, *J* = 8.4, Hz, 1H), 6.70 (s, 1H), 5.81-5.67 (m, 1H), 5.47 (t, *J* = 6 Hz, 1H), 5.20-5.13 (m, 2H), 3.97 (d, *J* = 6.6 Hz, 2H), 2.76-2.58 (m, 2H), 2.05-1.91 (m, 1H), 0.96 (d, *J* = 6.6 Hz, 6H). ^{13}C NMR (75 MHz, $CDCl_3$): δ = 170.2, 153.7, 144.0, 139.6, 131.3, 127.3, 124.9, 122.8, 119.9, 114.9, 80.3, 71.9, 38.9, 28.1, 19.1. IR: 3353, 1754, 1713, 1562. HRMS (EI): m/z calcd for $C_{16}H_{19}NO_4$ (M^+): 289.1314; found: 289.1319. $[\alpha]^{20}_D$= +40.8 (c = 0.13, $CHCl_3$). The enantioselectivity was determined by HPLC analysis on a chiral column (AS-H, hexane/*i*prOH 90:10, flow rate 1 $mLmin^{-1}$, wavelength = 245 nm) to be 84.5:15.5 er, 69% ee: t_{major} = 27.32 min, t_{minor} = 32.38 min.

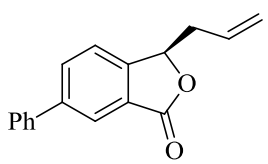

(*R*)-3-allyl-6-phenylisobenzofuran-1(3H)-one (152f): Representative Procedure C was followed. The crude product was

purified by column chromatography on silica gel (*n*-hexane/EtOAc: 1/1) to yield **152f** (84.1 mg, 67%). m.p. = 80-82 °C. ^{1}H NMR (300 MHz, $CDCl_3$): δ = 8.12 (s, 1H), 7.91 (dd, *J* = 6.6, 1.6 Hz, 1H), 7.65-7.62 (m, 2H), 7.67-7.43 (m, 4H), 5.87-5.76 (m, 1H), 5.59 (t, *J* = 6 Hz, 1H), 5.27-5.19 (m, 2H), 2.80-2.96 (m, 2H). ^{13}C NMR (75 MHz, $CDCl_3$): δ = 170.5, 148.2, 142.9, 139.5, 133.2, 131.3, 129.2, 128.3, 127.4, 127.2, 124.1, 122.5, 119.9, 80.3, 38.9. IR: 2922, 1755, 1462, 793, 690. HRMS (EI): m/z calcd for $C_{17}H_{14}O_2$ (M^+): 250.0994; found: 250.0992. $[\alpha]^{20}_D$= +35.1 (c = 0.71, $CHCl_3$). The enantioselectivity was determined by HPLC analysis on a chiral column (AS-H, hexane/*i*prOH 90:10, flow rate 1 mLmin^{-1}, wavelength = 245 nm) to be 84:16 er, 68% ee: t_{minor} = 14.89 min, t_{major} = 20.20 min.

4.3.5. Transesterification Under Different Reaction Conditions.

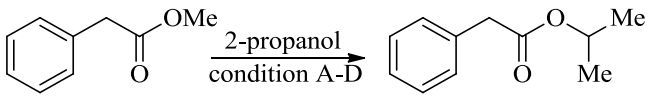

Isopropyl 2-phenylacetate: Isopropyl 2-phenylacetate was prepared by using the protocol previously reported by Ranu[136] and applying the following conditions:

Condition A: In a 25 mL round bottom flask**,** 2-propanol (6 mL) was mixed with methyl phenylacetate (150 mg, 1 mmol) and it was refluxed for 6 hours.

Condition B: Indium (173 mg, 1.5 mmol) and bromine (360 mg, 2.25 mmol) were added to the mixture described in condition A.

Condition C: Pyridinium salt was prepared by the addition of toluene (3 mL) to a mixture of pyridine (1 mL) and HBr 48% (2 mL) and then the solvent was removed under reduced pressure. Pyridinium salt (240 mg, 1.5 mmol) was used instead of indium and bromine in condition B.

Condition D: Indium (173 mg, 1.5 mmol), bromine (360 mg, 2.25 mmol) and pyridinium salt (240 mg, 1.5 mmol) were used as a catalyst.

The product's spectra obtained from conditions B and C were in full agreement with spectral data of an authentic sample.

4.3.6. DFT Calculations of TS1- TS6.

Transition states (*R*)-**TS1** and (*S*)-**TS2** correspond to the enantiodetermining first-order saddle points for (*R*)- vs (S)-allylation, while (*R*)-**TS3** and (*S*)-**TS4** correspond to the subsequent transesterification transitions generated from (*R*)-**TS1** and (*S*)-**TS2** in the presence of pyridinium salt (pyr-H^+). Moreover, (*R*)-**TS5** and (S)-**TS6** refer to the transesterification transition states formed in the absence of pyr-H^+ and a ligand **153** bound indium complex. The respective local minima referred to below corresponding to the direct products and precomplexes of the transition states discussed herein which were located using the **I**ntrinsic **R**eaction **C**oordinate (IRC) method. All of the reported calculations were carried using the Gaussian 09revB.01 and Gaussview 5.0.8 suite of programs.[137]

(*R*)-TS1

(*R*)-TS1 had one and only one imaginary frequency (imaginary frequency = -137.55).

---

opt=(calcfc,ts,noeigen) freq=noraman b3lyp/lanl2dz scrf=(iefpcm,solvent=thf,smd)

- Thermochemistry-

Zero-point correction=	0.469160 (Hartree/Particle)
Thermal correction to Energy=	0.507381
Thermal correction to Enthalpy=	0.508326
Thermal correction to Gibbs Free Energy=	0.391689
Sum of electronic and zero-point Energies=	-1404.994358

Sum of electronic and thermal Energies= -1404.956137
Sum of electronic and thermal Enthalpies= -1404.955193
Sum of electronic and thermal Free Energies= -1405.071830

C	-1.48769900	-1.14228400	1.38781500	C	-3.39226000	-1.17279600	3.07916000
C	-2.20858200	-0.25216500	0.29993800	C	-4.28590800	-1.85046900	3.92976200
N	-1.12767600	0.30371400	-0.64065800	C	-3.33985300	-3.97980100	3.22224700
In	-0.27007400	2.22490000	-0.29240200	H	-1.72240200	-3.84186400	1.77110700
C	1.28483900	2.94948700	-1.70923100	H	-3.41158300	-0.08504300	3.04058300
H	0.83492900	3.90018100	-2.01451300	H	-4.99061300	-1.28412400	4.53471900
H	1.25667400	2.21597100	-2.52286000	H	-3.31166600	-5.06606100	3.27811700
C	2.59504500	3.11370000	-1.08660300	H	-4.95198400	-3.78298100	4.66450000
C	3.61961600	2.18758300	-1.08403900	C	3.91455100	0.14123200	1.08792800
H	3.57912000	1.29758800	-1.70926400	C	4.77655800	0.91615500	1.91047000
H	4.57689200	2.42979100	-0.63108900	C	4.35822000	-1.17660800	0.72034800
O	-0.52515400	-2.04427200	0.78078200	C	6.02230100	0.44932300	2.35069600
In	0.49828700	-1.13049800	-0.62534400	H	4.45916400	1.91380500	2.20135400
O	1.55352200	0.48456800	0.23321400	C	5.62611600	-1.62636700	1.16278700
C	2.66734600	0.88497400	0.77530600	C	6.45646400	-0.83054100	1.96554900
H	-1.54585400	0.37730600	-1.57685300	H	6.64307400	1.07823600	2.98168900
H	-2.67480300	0.58368800	0.83387900	H	5.95273600	-2.62093600	0.88457300
C	-3.30472200	-0.94326000	-0.51179500	H	7.42020700	-1.21049700	2.29060800
C	-5.36602300	-2.10714500	-2.08463900	H	2.58311500	1.80800700	1.34788500
C	-4.50279200	-0.23965600	-0.77221200	Br	-0.01688800	2.84579000	2.25460700
C	-3.15569800	-2.24429600	-1.04876600	Br	-2.34882800	3.76133200	-0.99800400
C	-4.17724300	-2.81999700	-1.82688700	Br	0.70039100	-1.65942400	-3.17475300
C	-5.52644300	-0.81297900	-1.55159300	C	3.56040300	-2.15810500	-0.05211300
H	-4.63526800	0.76050100	-0.36462000	O	2.32317000	-2.07789800	-0.29691100
H	-2.25239300	-2.81131500	-0.84528800	O	4.25477600	-3.22920800	-0.47436100
H	-4.04773000	-3.82279800	-2.22786900	C	3.54339400	-4.31971000	-1.20148900
H	-6.44053500	-0.25442800	-1.73960400	H	3.07576100	-3.91651300	-2.10288200
H	-6.15361500	-2.55373700	-2.68716700	H	4.32720700	-5.03483700	-1.44967900
H	-0.94534400	-0.42612600	2.03115100	H	2.79469700	-4.76809200	-0.54263500
C	-2.46998400	-1.89255000	2.28435100	H	2.75072600	4.03576500	-0.52139100
C	-4.26423700	-3.25910700	4.00443600				
C	-2.44730500	-3.29930200	2.36910300				

Minima: Precomplex of (*R*)-TS1

---

opt=calcfc freq=noraman b3lyp/lanl2dz scrf=(iefpcm,solvent=thf,smd)

- Thermochemistry-

Zero-point correction= 0.468738 (Hartree/Particle)
Thermal correction to Energy= 0.508336
Thermal correction to Enthalpy= 0.509280
Thermal correction to Gibbs Free Energy= 0.387495
Sum of electronic and zero-point Energies= -1404.997165
Sum of electronic and thermal Energies= -1404.957567
Sum of electronic and thermal Enthalpies= -1404.956622
Sum of electronic and thermal Free Energies= -1405.078408

C	-1.57568100	-1.10568500	1.28507500	C	-3.69550700	-1.29164900	2.68683100
C	-2.21055400	-0.32656200	0.07352300	C	-4.62866000	-2.03572800	3.43336600
N	-1.05444900	0.33025600	-0.70211600	C	-3.36845300	-4.06838600	2.97703300
In	-0.56815200	2.37725800	-0.25031400	H	-1.57804500	-3.80059000	1.76824600
C	0.66831600	3.36384400	-1.73373400	H	-3.82466900	-0.21496800	2.59206300
H	-0.05248200	3.99131700	-2.27789900	H	-5.47084600	-1.53125300	3.90187500
H	1.03528300	2.58200000	-2.41256200	H	-3.23362900	-5.14208500	3.09120800
C	1.78240500	4.19272600	-1.17548000	H	-5.18923900	-4.00480200	4.15966400
C	3.11036000	3.92911300	-1.28072200	C	4.23771900	0.22585900	0.72280800
H	3.48192500	3.06091500	-1.82560700	C	5.28538800	1.12948500	1.04592700
H	3.85516300	4.58613600	-0.83379200	C	4.54748600	-1.18138200	0.65683300
O	-0.45229600	-1.91582100	0.85441900	C	6.60486200	0.69848800	1.25967000
In	0.61621500	-1.05472100	-0.54859000	H	5.05920400	2.18966800	1.11766800
O	1.87340400	0.52952200	0.02026900	C	5.87537900	-1.59269900	0.88421800
C	2.97643600	0.94062900	0.49451500	C	6.90026300	-0.66881100	1.17088100
H	-1.34141300	0.39088300	-1.69005600	H	7.38096000	1.42031600	1.49314400
H	-2.83564900	0.46792800	0.49625400	H	6.11355400	-2.64828400	0.84139200
C	-3.09126200	-1.13713800	-0.87941600	H	7.91298200	-1.02587500	1.33175700
C	-4.75239000	-2.51062100	-2.73200700	H	3.01099100	2.00238500	0.75333300
C	-4.22016600	-0.50385800	-1.44980400	Br	0.14714600	2.53966200	2.29119600
C	-2.80892100	-2.47346400	-1.24881100	Br	-2.97703700	3.51256400	-0.22509600
C	-3.63293100	-3.15312500	-2.16560700	Br	1.09069300	-1.67743100	-3.02445000
C	-5.04496600	-1.18093800	-2.36865000	C	3.55311800	-2.26218800	0.40484100
H	-4.45517400	0.52192500	-1.17174500	O	2.34508500	-2.10137100	0.08429600
H	-1.95685600	-2.98574800	-0.81318200	O	4.04781700	-3.50357300	0.55520200
H	-3.40287800	-4.18137800	-2.43551000	C	3.15443900	-4.67347000	0.31379900
H	-5.90917200	-0.67640000	-2.79453400	H	2.77694500	-4.64106700	-0.71138000
H	-5.38691400	-3.03765400	-3.44083500	H	3.79589900	-5.53994900	0.47185500
H	-1.19955000	-0.32083200	1.96463100	H	2.33125800	-4.65476600	1.03285500
C	-2.59530600	-1.93012300	2.06830200	H	1.47915500	5.09115600	-0.63069800
C	-4.47007300	-3.42982700	3.58060800				
C	-2.43644500	-3.32165000	2.22795400				

Minima: Direct product of (*R*)-TS1

---

opt=calcfc freq=noraman b3lyp/lanl2dz scrf=(iefpcm,solvent=thf,smd)

- Thermochemistry-

Zero-point correction= 0.471966 (Hartree/Particle)
Thermal correction to Energy= 0.510246
Thermal correction to Enthalpy= 0.511191
Thermal correction to Gibbs Free Energy= 0.393785
Sum of electronic and zero-point Energies= -1405.051103
Sum of electronic and thermal Energies= -1405.012822
Sum of electronic and thermal Enthalpies= -1405.011878
Sum of electronic and thermal Free Energies= -1405.129284

C	1.96490900	0.47265900	1.11722400	C	-3.63603700	-0.39425300	-3.48167300
C	2.19575900	-0.87154400	0.32252500	H	-3.87144000	-1.25237700	-4.10925200
N	0.92628500	-1.14029600	-0.49115200	H	-3.14165700	0.44718000	-3.96448400
In	-0.78524500	-1.93504300	0.39903800	C	-3.93587700	-0.38431400	-2.16622500

C	-3.68955200	0.77620500	-1.22512100	H	3.29978800	2.83812700	0.78633800
H	-3.13857400	1.57048200	-1.73747500	H	3.39874600	-0.80793300	3.08230600
H	-4.66109800	1.19912400	-0.92512000	H	5.43391800	-0.02217600	4.26867000
O	1.39906700	1.49759000	0.27106100	H	5.35489300	3.64510000	1.97815500
In	0.04132400	0.84706800	-1.00182300	H	6.42777800	2.20902800	3.72324500
O	-1.60825100	-0.14771000	-0.15820700	C	-3.03920900	1.38054400	1.21389700
C	-2.98844500	0.34001600	0.08630000	C	-3.70443300	0.97839800	2.39127400
H	1.18560700	-1.69642300	-1.31493400	C	-2.56530000	2.72867800	1.15470400
H	2.31428600	-1.66660500	1.06813600	C	-3.89950300	1.85002400	3.47840600
C	3.41817800	-0.92713400	-0.59327000	H	-4.08391000	-0.03751800	2.45816500
C	5.65750700	-1.17492000	-2.32328000	C	-2.77775200	3.60761700	2.24712000
C	4.14481000	-2.13784500	-0.66950600	C	-3.43555700	3.17543400	3.40637000
C	3.83290100	0.16209400	-1.39514700	H	-4.41123600	1.49467200	4.36872600
C	4.94352300	0.03849600	-2.25065600	H	-2.40949000	4.62573900	2.18385000
C	5.25475800	-2.26519100	-1.52688100	H	-3.57952700	3.85913300	4.23768800
H	3.84242400	-2.98268900	-0.05285400	H	-3.54603200	-0.52870600	0.45436000
H	3.29799900	1.10495700	-1.34390100	Br	-0.81060700	-2.24297800	2.95357200
H	5.25133900	0.88649700	-2.85809100	Br	-1.87141300	-3.97772000	-0.70977700
H	5.80110400	-3.20448200	-1.57071500	Br	0.27501500	1.09607200	-3.56591800
H	6.51433200	-1.26788500	-2.98653200	C	-1.81387800	3.27832900	0.00607200
H	1.23078700	0.21789500	1.90539800	O	-1.10921200	2.60509500	-0.80861500
C	3.22499000	0.96047600	1.83082100	O	-1.90204400	4.61182600	-0.13517100
C	5.53971200	1.86304900	3.19913300	C	-1.10201000	5.28526500	-1.19799300
C	3.78249000	2.22132900	1.53745500	H	-1.42528100	4.93033700	-2.17972000
C	3.82764000	0.15988400	2.82849300	H	-1.32103900	6.34520100	-1.07016900
C	4.97941000	0.60492200	3.50480000	H	-0.03967300	5.07871900	-1.04285000
C	4.93422900	2.67006600	2.21521100	H	-4.42682000	-1.25478900	-1.7229650

***(S)*-TS2**

(*S*)-TS2 had one and only one imaginary frequency (imaginary frequency = -129.17).

---

opt=(calcfc,ts,noeigen) freq=noraman b3lyp/lanl2dz scrf=(iefpcm,solvent=thf,smd)

- Thermochemistry-

Zero-point correction=	0.468830 (Hartree/Particle)
Thermal correction to Energy=	0.507102
Thermal correction to Enthalpy=	0.508046
Thermal correction to Gibbs Free Energy=	0.390969
Sum of electronic and zero-point Energies=	-1404.989652
Sum of electronic and thermal Energies=	-1404.951380
Sum of electronic and thermal Enthalpies=	-1404.950436
Sum of electronic and thermal Free Energies=	-1405.067513

C	-2.16066600	-0.63498800	1.11275000	H	2.74540300	2.72310000	-3.01653600
C	-2.32726300	0.16269600	-0.24318300	C	3.94537800	2.37040100	-1.30834600
N	-0.92735200	0.37234200	-0.82292600	H	4.78939200	2.01565500	-1.89119000
In	0.18217700	2.14224500	-0.37834800	H	4.10098300	2.50573100	-0.23954300
C	1.68456200	3.49715700	-1.27930700	O	-1.22741000	-1.73317400	0.96784800
H	1.95002300	4.06942700	-0.38211300	In	0.29878300	-1.28821100	-0.19802100
H	1.06971000	4.09441000	-1.95881500	O	1.77905700	0.19647600	-0.82619600
C	2.82156100	2.86496600	-1.93587100	C	2.99088700	0.06933100	-1.29797700

H	3.12318100	0.18126600	-2.37415900	H	-5.22704400	-3.94502400	2.51404600
H	-1.00404000	0.37823200	-1.84991800	H	-6.92926300	-2.24718000	3.20381600
H	-2.74639300	1.14072100	0.01581700	C	4.12267800	-0.57447500	-0.59599600
C	-3.24292900	-0.46498600	-1.29402400	C	6.52659400	-1.65078900	0.48457400
C	-4.92839600	-1.51884200	-3.32654900	C	4.15073100	-1.07916100	0.74621200
C	-4.15274500	0.36729600	-1.98612700	C	5.30581300	-0.67541500	-1.37147900
C	-3.19417700	-1.83838200	-1.63319300	C	6.49166800	-1.21203600	-0.85113700
C	-4.02867400	-2.35931700	-2.63944900	C	5.36252200	-1.58620300	1.26868700
C	-4.98952200	-0.15122000	-2.99385400	H	5.29164300	-0.30961700	-2.39464700
H	-4.20901100	1.42444400	-1.73409700	H	7.37754700	-1.27738600	-1.47562800
H	-2.52008000	-2.50267500	-1.10133500	H	5.38252200	-1.96152700	2.28550400
H	-3.98051800	-3.41817600	-2.88337300	H	7.44053700	-2.05472100	0.90970000
H	-5.68367500	0.50616400	-3.51243100	Br	0.92382900	-3.15358500	-1.87613300
H	-5.57252100	-1.92381300	-4.10368200	Br	-1.83430600	3.91686500	-0.33842900
H	-1.73779100	0.09564400	1.82401400	Br	0.80023400	1.90724000	2.20371100
C	-3.49694900	-1.10140800	1.68462700	C	2.96161000	-1.24100600	1.62615400
C	-5.97769100	-1.92918200	2.78359400	O	1.78920800	-1.53046500	1.24151300
C	-3.78389200	-2.47159700	1.84986900	O	3.23871700	-1.16589000	2.93393500
C	-4.45804800	-0.14653400	2.09007100	C	2.15403800	-1.42570000	3.92657100
C	-5.69140000	-0.55608200	2.63142200	H	1.32669300	-0.73584700	3.74776900
C	-5.01754000	-2.88411300	2.39334100	H	1.82295700	-2.46373900	3.83505900
H	-3.03124100	-3.19739100	1.55914200	H	2.62386300	-1.24370600	4.89282300
H	-4.24386400	0.91608300	1.98861500				
H	-6.42155400	0.18959300	2.93844000				

Minima: Precomplex of (*S*)-TS2

---

opt=calcfc freq=noraman b3lyp/lanl2dz scrf=(iefpcm,solvent=thf,smd)

- Thermochemistry-

Zero-point correction=	0.468697 (Hartree/Particle)
Thermal correction to Energy=	0.508292
Thermal correction to Enthalpy=	0.509236
Thermal correction to Gibbs Free Energy=	0.388624
Sum of electronic and zero-point Energies=	-1404.997449
Sum of electronic and thermal Energies=	-1404.957854
Sum of electronic and thermal Enthalpies=	-1404.956910
Sum of electronic and thermal Free Energies=	-1405.077521

C	-2.08597400	-0.61980500	1.08916900	O	-1.08309600	-1.65094200	0.96038600
C	-2.29824200	0.13603900	-0.27510800	In	0.35852500	-1.21985600	-0.31340500
N	-0.89725100	0.48360300	-0.81859900	O	2.01157800	-0.10573100	-1.11734600
In	-0.12959300	2.42749700	-0.29755200	C	3.26585500	0.00662500	-1.24276900
C	0.73710600	3.73311900	-1.78591200	H	3.61292100	0.60960600	-2.08837600
H	1.04890400	4.63313400	-1.23959900	H	-0.96797700	0.54563400	-1.84577600
H	-0.12593800	3.98919700	-2.41828800	H	-2.81634200	1.07253000	-0.04297700
C	1.85121300	3.15692500	-2.60239700	C	-3.12077700	-0.57711700	-1.34935200
H	1.55817500	2.41195200	-3.34753600	C	-4.64834400	-1.76594700	-3.43069200
C	3.16678800	3.47718700	-2.50238400	C	-3.90351500	0.21686900	-2.22138100
H	3.91413900	3.01198900	-3.14343200	C	-3.11734300	-1.97911000	-1.53544100
H	3.52514100	4.21731000	-1.78696300	C	-3.87617300	-2.56665800	-2.56565400

C	-4.65989600	-0.36758500	-3.25470600	C	6.80856800	-0.76344400	-0.37894600
H	-3.92640300	1.29696000	-2.08543100	C	5.47768800	-1.67032300	1.44700000
H	-2.53040400	-2.61089800	-0.87766600	H	5.69066800	0.22474200	-1.93210500
H	-3.86449400	-3.64686500	-2.69176900	H	7.76874000	-0.57453500	-0.84873200
H	-5.25714300	0.26063800	-3.91160400	H	5.43203500	-2.18745000	2.39808700
H	-5.23332000	-2.22341300	-4.22527500	H	7.63367900	-1.78753600	1.34227500
H	-1.71231000	0.15019800	1.78853100	Br	0.69184100	-3.12641200	-2.04443800
C	-3.38405600	-1.16894200	1.68434700	Br	-2.14893100	3.76130100	0.77596000
C	-5.76993300	-2.16665100	2.85399400	Br	1.46050900	1.87358300	1.76085500
C	-3.50974700	-2.53730800	1.99960400	C	3.02107800	-1.58247800	1.55621900
C	-4.46099600	-0.29949800	1.97475600	O	1.87687500	-1.70673300	1.03895000
C	-5.64666300	-0.79459200	2.55027100	O	3.19146800	-1.79915200	2.86850700
C	-4.69472800	-3.03487900	2.57864700	C	2.01356000	-2.19627800	3.69536200
H	-2.67154900	-3.19417300	1.79092600	H	1.25049500	-1.41665100	3.63930700
H	-4.37906900	0.76379500	1.75835200	H	1.62080000	-3.14983200	3.33291400
H	-6.46714900	-0.11362600	2.76578500	H	2.41337600	-2.28899700	4.70472000
H	-4.77666200	-4.09356200	2.81623000				
H	-6.68460700	-2.54910800	3.30145800				
C	4.34795300	-0.55905300	-0.42557300				
C	6.73188600	-1.44093000	0.84667000				
C	4.28069800	-1.25238300	0.83364300				
C	5.62618200	-0.31823500	-0.99322600				

Minima: Direct product of (*S*)-TS2

---

opt=calcfc freq=noraman b3lyp/lanl2dz scrf=(iefpcm,solvent=thf,smd)

- Thermochemistry-

Zero-point correction= 0.472157 (Hartree/Particle)
Thermal correction to Energy= 0.510414
Thermal correction to Enthalpy= 0.511358
Thermal correction to Gibbs Free Energy= 0.394624
Sum of electronic and zero-point Energies= -1405.050707
Sum of electronic and thermal Energies= -1405.012450
Sum of electronic and thermal Enthalpies= -1405.011505
Sum of electronic and thermal Free Energies= -1405.128240

C	-2.31178800	-0.43877000	0.97558000	C	2.55822600	0.38208200	1.40492400
C	-2.41058800	0.44352000	-0.33285300	H	2.88615200	1.42232000	1.50531600
N	-0.99212300	0.62150800	-0.88549100	H	-1.05935200	0.69460000	-1.90733600
In	0.32922600	2.06258000	-0.15485700	H	-2.79820700	1.42103700	-0.02434200
C	0.09823600	0.33875700	4.15260100	C	-3.32802500	-0.08147200	-1.43562300
H	-0.18264500	-0.71418000	4.15364000	C	-5.00959500	-0.94017600	-3.55771100
H	-0.56802000	1.02629000	4.67046900	C	-4.17097900	0.83320900	-2.10704500
C	1.22006100	0.77467900	3.54169400	C	-3.34100300	-1.43700200	-1.84148200
H	1.46425500	1.83922500	3.56854900	C	-4.17521500	-1.86147900	-2.89214700
C	2.21933200	-0.11453700	2.83477200	C	-5.00600700	0.41133600	-3.16011200
H	3.16861300	-0.10347800	3.39283300	H	-4.17488500	1.87869900	-1.80350800
H	1.85662000	-1.14607300	2.83426600	H	-2.71219200	-2.15951700	-1.33077700
O	-1.44417600	-1.58196000	0.78624700	H	-4.17606300	-2.90775800	-3.18908100
In	0.18774300	-1.14811700	-0.21505100	H	-5.64830200	1.13011600	-3.66367200
O	1.35502800	0.42813800	0.53766900	H	-5.65258800	-1.27065800	-4.37015900

H	-1.86035100	0.22456300	1.73705600
C	-3.68229400	-0.85600200	1.50377200
C	-6.21960800	-1.60236400	2.52725300
C	-4.03683000	-2.21577100	1.61252900
C	-4.60440400	0.12919200	1.92629300
C	-5.86594100	-0.24011800	2.43029600
H	-5.56033000	-3.64105600	2.19674400
H	-7.19305800	-1.88901200	2.91877900
C	3.71718700	-0.36767500	0.73654700
C	6.08589200	-1.55187500	-0.34110400
C	3.83089300	-1.78580800	0.59245100
C	4.81101600	0.41735200	0.31757600
C	5.97777100	-0.15471700	-0.22314200
C	5.01703600	-2.35949900	0.07139800
H	4.75490200	1.49721000	0.42517300
H	6.79479600	0.48714000	-0.54141300
H	5.08411700	-3.43774100	-0.02721500
H	6.98317600	-2.00492500	-0.75214100
Br	0.89399500	-2.15868900	-2.51171600
Br	1.76813000	3.20538400	-1.95958800
Br	-0.45617600	3.85120700	1.51460800
C	2.73150400	-2.72264600	0.90891000
O	1.49063500	-2.46179700	0.79272000
O	3.12218100	-3.94015000	1.31188400
C	2.09374100	-4.99628600	1.54515100
H	1.44571200	-4.69680900	2.37266800
H	1.51143200	-5.14833000	0.63274100
H	2.67214000	-5.88435000	1.79901300
C	-5.29872100	-2.58781500	2.11892400
H	-3.31400700	-2.96535500	1.30724000
H	-4.33944100	1.18342500	1.86757000
H	-6.56605400	0.52822300	2.75097300

(*R*)-TS3

(*R*)-TS3 had one and only one imaginary frequency (imaginary frequency = -46.12).

---

opt=(calcfc,ts,noeigen) freq=noraman b3lyp/lanl2dz scrf=(iefpcm,solvent=thf,smd)

- Thermochemistry-

Zero-point correction= 0.575962 (Hartree/Particle)
Thermal correction to Energy= 0.619265
Thermal correction to Enthalpy= 0.620210
Thermal correction to Gibbs Free Energy= 0.491881
Sum of electronic and zero-point Energies= -1653.616735
Sum of electronic and thermal Energies= -1653.573432
Sum of electronic and thermal Enthalpies= -1653.572488
Sum of electronic and thermal Free Energies= -1653.700816

C	-2.43280400	-0.08027600	-0.57430500	H	-4.70302700	1.06414200	0.48425400
C	-1.88074100	-1.43058100	0.03020200	H	-3.36256500	-1.49347100	-2.72214700
N	-0.47514600	-1.16584400	0.63785900	H	-5.70277800	-1.73923600	-3.51825500
In	1.25709400	-1.70295100	-0.49154700	H	-7.06235400	0.82720900	-0.31454200
C	4.29412500	-2.39859600	-2.35124300	H	-7.56786700	-0.57970100	-2.31888400
H	3.95723500	-1.52827900	-2.90941200	C	4.17933300	1.36947200	0.14042200
H	4.33156300	-3.33425800	-2.90469100	C	4.15532600	3.82756500	1.50116500
C	4.66444300	-2.35584600	-1.05226200	C	3.03284300	2.17957000	0.14089400
H	4.99749200	-3.27780800	-0.57601100	C	5.33393600	1.78777900	0.81726100
C	4.69817700	-1.14130400	-0.14257600	C	5.31394800	3.02379500	1.49859600
H	4.32678600	-1.40498400	0.85661900	C	2.99838500	3.40785600	0.81331700
H	5.75156700	-0.85947300	0.00523900	H	6.23220700	1.17749300	0.82626100
O	-2.26938600	1.02754000	0.36062100	H	6.20041700	3.35622300	2.03240100
In	-0.52354200	0.87192200	1.24889000	H	2.10594200	4.02741800	0.80822700
O	2.46524700	-0.04216500	-0.65637000	H	4.15348900	4.77370700	2.03523300
C	3.97663000	0.09750500	-0.66453500	Br	-0.16041700	2.11488700	3.44002500
H	4.24305400	0.27557600	-1.71306400	Br	2.08292700	-3.59694800	1.06126800
H	-0.39923000	-1.76735900	1.47074500	Br	0.51489600	-2.50638500	-2.82012700
H	-1.75865200	-2.11647400	-0.81383300	C	1.90791100	1.61474700	-0.68738600
C	-2.75386500	-2.12775600	1.07059900	O	0.64664300	1.60701000	-0.23058500
C	-4.27490300	-3.54566100	3.00339200	O	2.05188700	2.00896100	-2.01022400
C	-2.93398300	-3.52591000	0.96572000	H	-0.32131600	3.11296800	-0.96553800
C	-3.35156300	-1.44615000	2.15793700	C	-0.33915500	4.99076700	-1.83645700
C	-4.10482300	-2.15062300	3.11529800	C	-2.25873200	3.81410700	-1.01166800
C	-3.68862100	-4.23205300	1.92202500	C	-1.13576200	6.07155000	-2.21773100
H	-2.48503600	-4.06309200	0.13240900	H	0.73386900	4.96357800	-1.97930800
H	-3.24954500	-0.36889400	2.24896200	C	-3.08981600	4.87560800	-1.37893500
H	-4.56104400	-1.61289600	3.94296500	H	-2.59870100	2.89667500	-0.53309900
H	-3.81763900	-5.30709600	1.82317300	C	-2.52623300	6.01518600	-1.98678800
H	-4.85697300	-4.08746600	3.74493500	H	-0.67453200	6.93486000	-2.68256200
H	-1.80911200	0.11930900	-1.46351400	H	-4.15434700	4.80620700	-1.18848700
C	-3.87755000	-0.20975200	-1.04647500	H	-3.15941500	6.84821700	-2.27612200
C	-6.54418200	-0.47718500	-1.96653600	N	-0.91913300	3.90546700	-1.25175600
C	-4.93102900	0.44816200	-0.37977300	C	1.12201100	1.49547400	-3.04590400
C	-4.16762000	-0.99442800	-2.18579200	H	0.12669700	1.30569200	-2.63481600
C	-5.49260200	-1.13183100	-2.64094100	H	1.07525000	2.27707100	-3.80668800
C	-6.25733500	0.31528700	-0.83711000	H	1.54560200	0.58317300	-3.47379000

Minima: Precomplex of (*R*)-TS3

---

opt=calcfc freq=noraman b3lyp/lanl2dz scrf=(iefpcm,solvent=thf,smd)

- Thermochemistry-

Zero-point correction= 0.576293 (Hartree/Particle)
Thermal correction to Energy= 0.620986
Thermal correction to Enthalpy= 0.621930
Thermal correction to Gibbs Free Energy= 0.487477
Sum of electronic and zero-point Energies= -1653.621254
Sum of electronic and thermal Energies= -1653.576561
Sum of electronic and thermal Enthalpies= -1653.575617
Sum of electronic and thermal Free Energies= -1653.710070

C	-2.06855600	-1.02780100	-0.60303100	H	-4.58584900	-0.64223400	0.47266900
C	-1.07992900	-1.95755600	0.20248400	H	-2.46461500	-2.97245200	-2.47805400
N	0.14389000	-1.10615400	0.63892300	H	-4.56232000	-4.17459300	-3.04829200
In	1.95346400	-1.24896400	-0.54117700	H	-6.69976600	-1.83870400	-0.10318200
C	4.76711800	-0.75329800	-2.48783100	H	-6.69410700	-3.61645300	-1.86245200
H	4.09022900	-0.06594200	-2.98971500	C	3.42619100	2.66656100	0.15807300
H	5.08006300	-1.62275900	-3.06190000	C	2.76955200	4.93202600	1.74950900
C	5.22396700	-0.55642300	-1.23004800	C	2.13426300	3.24820000	0.11581700
H	5.90942500	-1.29242400	-0.80803300	C	4.38253300	3.24784900	1.01000300
C	4.90922000	0.60975100	-0.30991000	C	4.06089500	4.37650400	1.79219500
H	4.81038300	0.24358300	0.72194900	C	1.79536200	4.35940000	0.91161100
H	5.78275800	1.27835600	-0.31406100	H	5.37946700	2.82714600	1.08399000
O	-2.30181600	0.22909500	0.10176100	H	4.81615900	4.81010900	2.44246900
In	-0.64875400	0.83266100	0.97703500	H	0.79614600	4.78410600	0.86804400
O	2.42479000	0.63744200	-0.60465200	H	2.52054600	5.79489200	2.36038000
C	3.66009900	1.41665400	-0.69659800	Br	-0.92278000	2.14194600	3.15540800
H	3.76735600	1.73831100	-1.74366500	Br	3.29016400	-2.89732200	0.95748500
H	0.45168700	-1.47762900	1.55076400	Br	1.31636300	-2.36565900	-2.79248400
H	-0.72304400	-2.70813100	-0.50965000	C	1.10719800	2.69490800	-0.80741300
C	-1.65061500	-2.70611100	1.40581900	O	-0.02716200	2.21194200	-0.42171300
C	-2.56721400	-4.18381100	3.65227700	O	1.34344900	2.90010500	-2.09746200
C	-1.28384900	-4.06035000	1.58146100	H	-2.06553900	2.88757100	-1.34001300
C	-2.49044500	-2.10291800	2.37264000	C	-3.20975000	4.44999200	-2.03819200
C	-2.94285500	-2.83546000	3.48560600	C	-4.04450800	2.45483800	-0.99418500
C	-1.73686300	-4.79606900	2.69314200	C	-4.50727200	4.93828800	-2.19648900
H	-0.64434800	-4.54174900	0.84415700	H	-2.32509800	4.98556300	-2.35932300
H	-2.80800600	-1.07131100	2.25394700	C	-5.35755600	2.91140100	-1.13508900
H	-3.58911500	-2.35703400	4.21764900	H	-3.75084800	1.50717800	-0.54476200
H	-1.44480400	-5.83700400	2.80833300	C	-5.59355300	4.16169500	-1.74054000
H	-2.91823400	-4.74775900	4.51310600	H	-4.65957900	5.90291000	-2.66611400
H	-1.54955200	-0.80415500	-1.55006200	H	-6.17409900	2.29546000	-0.77722100
C	-3.37741600	-1.73264800	-0.94618100	H	-6.60908500	4.52744900	-1.85655000
C	-5.77479000	-3.09322900	-1.61003700	N	-3.02289400	3.23576600	-1.44820600
C	-4.58474100	-1.41476700	-0.29009500	C	0.42394800	2.36733700	-3.14574500
C	-3.38396900	-2.72880400	-1.94886300	H	0.17150200	1.32792500	-2.92638200
C	-4.57264400	-3.40880400	-2.27608700	H	-0.47126000	2.99317900	-3.18706200
C	-5.77603500	-2.09096500	-0.61925400	H	0.99381000	2.44733900	-4.07109000

Minima: Direct product of (*R*)-TS3

---

opt=calcfc freq=noraman b3lyp/lanl2dz scrf=(iefpcm,solvent=thf,smd)

- Thermochemistry-

Zero-point correction= 0.576293 (Hartree/Particle)
Thermal correction to Energy= 0.620253
Thermal correction to Enthalpy= 0.621197
Thermal correction to Gibbs Free Energy= 0.491121
Sum of electronic and zero-point Energies= -1653.616516
Sum of electronic and thermal Energies= -1653.572556
Sum of electronic and thermal Enthalpies= -1653.571611
Sum of electronic and thermal Free Energies= -1653.701688

C	-2.46049400	0.00363400	-0.55651300	C	-6.27202200	0.52813400	-0.78202200
C	-1.93667200	-1.37383000	0.01366600	H	-4.68339900	1.20818800	0.53555100
N	-0.52496600	-1.15745700	0.62829300	H	-3.45526400	-1.35727100	-2.70943300
In	1.19493800	-1.71239000	-0.50415100	H	-5.80804500	-1.51299200	-3.49045800
C	4.23613100	-2.45904200	-2.40121100	H	-7.05501100	1.06156700	-0.24759100
H	3.92550200	-1.56995600	-2.94477500	H	-7.62337100	-0.30363400	-2.26402100
H	4.25102700	-3.38534600	-2.97124600	C	4.20249300	1.26244300	0.17166100
C	4.60024900	-2.44997600	-1.10005000	C	4.20206100	3.69044000	1.58071000
H	4.90544900	-3.38898800	-0.63872300	C	3.06856300	2.08956700	0.17645900
C	4.66196300	-1.25432300	-0.16732900	C	5.35616100	1.64529800	0.86991400
H	4.27964600	-1.52721800	0.82482800	C	5.34708200	2.86720400	1.57675700
H	5.72162000	-1.00266300	-0.00884000	C	3.04618700	3.30504100	0.87072100
O	-2.25902900	1.08825600	0.39804400	H	6.24426100	1.02020400	0.87561400
In	-0.50711500	0.87363400	1.25891400	H	6.23170600	3.17366100	2.12884100
O	2.45993400	-0.07893100	-0.68115100	H	2.16460300	3.93993800	0.86811800
C	3.98333300	0.01609400	-0.66711500	H	4.20984900	4.62560300	2.13375100
H	4.26136000	0.21112900	-1.70925300	Br	-0.07133300	2.05145400	3.46924800
H	-0.46875100	-1.77294200	1.45235400	Br	2.01327900	-3.60851900	1.04864700
H	-1.83051800	-2.04073800	-0.84758900	Br	0.44939600	-2.49253400	-2.83618100
C	-2.82500300	-2.07731300	1.03638100	C	1.95133000	1.54138100	-0.67646400
C	-4.38314200	-3.50600000	2.93057100	O	0.67553800	1.55697000	-0.23784400
C	-3.04152000	-3.46689700	0.89372900	O	2.11241000	1.98806900	-1.98992200
C	-3.40335400	-1.40980100	2.14258500	H	-0.21988400	3.06200900	-0.98091300
C	-4.17537000	-2.11964700	3.08080800	C	-0.15402800	4.92356100	-1.88646300
C	-3.81499800	-4.17832800	1.83082300	C	-2.11636500	3.87206000	-0.99765400
H	-2.60626100	-3.99286800	0.04610100	C	-0.89626000	6.04292200	-2.26631900
H	-3.27069100	-0.33864600	2.26292800	H	0.91200500	4.83190300	-2.05330600
H	-4.61698900	-1.59288300	3.92330000	C	-2.89458000	4.97362500	-1.36301300
H	-3.97280000	-5.24644900	1.70292000	H	-2.49815100	2.98308500	-0.49755500
H	-4.98016200	-4.05195600	3.65702900	C	-2.28165200	6.07003600	-2.00174400
H	-1.84224300	0.20584100	-1.44863700	H	-0.39808600	6.87140100	-2.75573200
C	-3.91325500	-0.07590400	-1.01563300	H	-3.95653500	4.96789800	-1.14734000
C	-6.59429900	-0.24069500	-1.91818300	H	-2.87300400	6.93402500	-2.28896300
C	-4.93860900	0.60992000	-0.33329600	N	-0.78001500	3.88278900	-1.26961000
C	-4.23865900	-0.83686900	-2.16140200	C	1.22264000	1.46857900	-3.05616600
C	-5.57083300	-0.92326900	-2.60797700	H	0.21033700	1.28879400	-2.68366300

H	1.20930200	2.24371500	-3.82481600	H	1.65375300	0.55015500	-3.4630390

(S)-TS4

(S)-TS4 had one and only one imaginary frequency (imaginary frequency = -62.53).

# opt=(calcfc,ts,noeigen) freq=noraman b3lyp/lanl2dz scrf=(iefpcm,solv
ent=thf,smd)

- Thermochemistry-

Zero-point correction= 0.575134 (Hartree/Particle)
Thermal correction to Energy= 0.619095
Thermal correction to Enthalpy= 0.620040
Thermal correction to Gibbs Free Energy= 0.488622
Sum of electronic and zero-point Energies= -1653.625801
Sum of electronic and thermal Energies= -1653.581840
Sum of electronic and thermal Enthalpies= -1653.580896
Sum of electronic and thermal Free Energies= -1653.712314

C	-2.49077000	-0.42561000	-0.63975100	C	-4.99030500	0.13154400	-0.60706000
C	-1.87944000	-1.65476500	0.13260600	C	-4.20965300	-1.69258200	-2.01681500
N	-0.46738700	-1.24720900	0.64505400	C	-5.52813000	-1.92518200	-2.45075900
In	1.22419400	-1.71182200	-0.55347000	C	-6.31044300	-0.09768000	-1.04425500
C	7.01665100	-1.27878800	-1.06684900	H	-4.77353600	0.92514800	0.10082200
H	6.64661400	-2.20578600	-1.50448300	H	-3.40149200	-2.30685000	-2.40927500
H	8.07473500	-1.24440800	-0.81258700	H	-5.72899300	-2.71860700	-3.16684700
C	6.20630200	-0.22033500	-0.85113200	H	-7.11924300	0.52460500	-0.66761700
H	6.62528800	0.68934800	-0.41800700	H	-7.60401100	-1.30537600	-2.30195400
C	4.73310000	-0.18735900	-1.20339300	C	3.89664600	1.30866900	0.74646300
H	4.52799800	0.64251700	-1.89325200	C	3.81605100	3.84555500	1.96963300
H	4.46316200	-1.12107400	-1.71270600	C	2.86376000	2.21533200	0.45183200
O	-2.36714900	0.80121400	0.14137700	C	4.89023000	1.66509900	1.67331800
In	-0.66124600	0.82554500	1.11608100	C	4.84926500	2.93677900	2.27928900
O	2.38655200	-0.06902700	-0.42952500	C	2.81096400	3.48516100	1.05249300
C	3.79755000	-0.02550500	0.02684500	H	5.67686800	0.96210900	1.93161200
H	3.96906200	-0.85084000	0.72770400	H	5.61481300	3.21504600	2.99878900
H	-0.30744200	-1.77042000	1.51943800	H	2.00881300	4.17936000	0.81612000
H	-1.75062800	-2.45623200	-0.60179900	H	3.78916000	4.82169500	2.44582800
C	-2.68890300	-2.21947100	1.29892700	Br	-0.58600900	2.06305600	3.33744100
C	-4.05768600	-3.37935100	3.49808500	Br	2.49224700	-3.68607600	0.50641500
C	-2.63647900	-3.61380700	1.52973300	Br	0.69615200	-2.24570000	-3.01454200
C	-3.44134300	-1.41202800	2.18460800	C	1.84268400	1.76567700	-0.55374800
C	-4.11989600	-1.98941000	3.27419800	O	0.54479300	1.70981100	-0.26383600
C	-3.31448200	-4.19222100	2.61921100	O	2.18424500	2.11335800	-1.82027100
H	-2.06790600	-4.24886400	0.85252800	H	-0.59706700	3.13980100	-1.06470700
H	-3.51136300	-0.34151000	2.02031200	C	-0.81799000	5.01000200	-1.90658300
H	-4.69690200	-1.35660500	3.94427100	C	-2.60831200	3.54581800	-1.26811000
H	-3.26565700	-5.26647000	2.77927300	C	-1.72848100	5.96999100	-2.35043700
H	-4.58262900	-3.82230000	4.34095500	H	0.25633700	5.13869800	-1.95187600
H	-1.87661400	-0.31782900	-1.55086900	C	-3.55068600	4.48115000	-1.70342400
C	-3.93158200	-0.66788500	-1.08328500	H	-2.84947400	2.57852800	-0.82903100
C	-6.58540400	-1.12786700	-1.96510400	C	-3.11016200	5.70356700	-2.24903600

H	-1.36093600	6.90114400	-2.76511200	C	1.34043600	1.74121600	-2.98618300
H	-4.60591300	4.25121700	-1.61418900	H	0.32266700	1.48895300	-2.68218800
H	-3.83158500	6.43905700	-2.59121300	H	1.34152800	2.61150400	-3.64475300
N	-1.28177200	3.83963900	-1.38522300	H	1.82186000	0.89307200	-3.47780100

Minima: precomplex of (S)-TS4

---

opt=calcfc freq=noraman b3lyp/lanl2dz scrf=(iefpcm,solvent=thf,smd)

- Thermochemistry-

Zero-point correction= 0.575506 (Hartree/Particle)
Thermal correction to Energy= 0.620574
Thermal correction to Enthalpy= 0.621518
Thermal correction to Gibbs Free Energy= 0.485144
Sum of electronic and zero-point Energies= -1653.629049
Sum of electronic and thermal Energies= -1653.583981
Sum of electronic and thermal Enthalpies= -1653.583037
Sum of electronic and thermal Free Energies= -1653.719411

C	-2.17939600	-0.93629700	-0.60901900	C	-4.73385900	-1.07865600	-0.41880100
C	-1.30022900	-1.92389000	0.25205400	C	-3.57412100	-2.58966300	-1.93267500
N	-0.02252100	-1.16476700	0.70320900	C	-4.80215300	-3.17380700	-2.29640300
In	1.76863500	-1.49709800	-0.41972900	C	-5.96434200	-1.65980300	-0.78446800
C	7.28969000	0.33376400	-1.56558200	H	-4.70256000	-0.27072700	0.30530600
H	7.17300200	-0.70637900	-1.86953700	H	-2.65456600	-2.94717700	-2.39212000
H	8.30871300	0.69589500	-1.43829100	H	-4.82203500	-3.97974900	-3.02634800
C	6.22511900	1.13930600	-1.35871200	H	-6.88693500	-1.29578100	-0.33759300
H	6.39707700	2.17578600	-1.06203500	H	-6.95374900	-3.15910600	-2.00445300
C	4.78170800	0.71790600	-1.53318100	C	3.78191500	2.11591500	0.40577200
H	4.28167400	1.37629200	-2.25693500	C	3.37937400	4.66110600	1.58596000
H	4.74381500	-0.30544500	-1.92880600	C	2.61437000	2.86316600	0.13323900
O	-2.32774400	0.35324700	0.05957400	C	4.73744100	2.65381200	1.28864100
In	-0.63910500	0.86732900	0.92444400	C	4.54363500	3.92074500	1.87077200
O	2.59534900	0.26666500	-0.51094600	C	2.40811200	4.12922600	0.71923600
C	3.94058100	0.73460300	-0.21999300	H	5.62560800	2.07647100	1.53144900
H	4.42906100	0.07343100	0.50950400	H	5.28949000	4.32222000	2.55180300
H	0.21499100	-1.51284500	1.64493100	H	1.50618700	4.69582700	0.50212000
H	-0.99152100	-2.72701800	-0.42460300	H	3.22359700	5.63565200	2.04021100
C	-1.96316900	-2.57501200	1.46341500	Br	-0.83898400	2.34664700	2.99398400
C	-3.05007100	-3.86966200	3.74428400	Br	3.27275600	-3.20446900	0.79681100
C	-1.69779200	-3.94064200	1.71522800	Br	1.16206800	-2.36378900	-2.78119300
C	-2.78574900	-1.86545000	2.37039800	C	1.57428200	2.32668300	-0.79742600
C	-3.32351400	-2.50838800	3.50082100	O	0.39890600	1.94771700	-0.43367100
C	-2.23612200	-4.58603600	2.84487000	O	1.82927100	2.53655200	-2.08944800
H	-1.07145500	-4.50087000	1.02344900	H	-2.50884600	3.86692400	-0.98935900
H	-3.02282000	-0.82153200	2.19014500	C	-4.10503900	4.95889000	-1.68136900
H	-3.95617800	-1.95038600	4.18699100	C	-4.16394200	2.65104900	-1.01301800
H	-2.02246700	-5.63751900	3.02037000	C	-5.46655200	4.93206400	-1.98503900
H	-3.46711400	-4.36387600	4.61836500	H	-3.48183300	5.83677400	-1.79772100
H	-1.61433900	-0.77890300	-1.54312600	C	-5.52969900	2.58851100	-1.30657300
C	-3.52854300	-1.54195900	-0.98443600	H	-3.58021400	1.80775100	-0.63798700
C	-6.00413700	-2.71049800	-1.72249400	C	-6.18766300	3.73454200	-1.79477900

H	-5.94635200	5.82798300	-2.36085800	C	0.87230000	2.07052800	-3.13293700
H	-6.06091000	1.65663300	-1.15575000	H	0.81426400	0.97928100	-3.10381000
H	-7.24766300	3.69685400	-2.02624600	H	-0.10889600	2.52142700	-2.96593400
N	-3.50566600	3.82916100	-1.21021100	H	1.30805600	2.41058600	-4.07203500

Minima: Direct product of (S)-TS4

---

opt=calcfc freq=noraman b3lyp/lanl2dz scrf=(iefpcm,solvent=thf,smd)

- Thermochemistry-

Zero-point correction= 0.575677 (Hartree/Particle)
Thermal correction to Energy= 0.619929
Thermal correction to Enthalpy= 0.620873
Thermal correction to Gibbs Free Energy= 0.488649
Sum of electronic and zero-point Energies= -1653.625855
Sum of electronic and thermal Energies= -1653.581603
Sum of electronic and thermal Enthalpies= -1653.580659
Sum of electronic and thermal Free Energies= -1653.712883

C	-2.57890300	-0.20765800	-0.63795200	C	-6.72434500	-0.53586700	-1.95014400
C	-2.06394800	-1.50951400	0.08723300	C	-5.03024000	0.52614100	-0.54401100
N	-0.62824200	-1.23024700	0.62120600	C	-4.39705100	-1.26883800	-2.06161200
In	1.01553200	-1.71342800	-0.60810900	C	-5.73258200	-1.37993000	-2.49196700
C	6.80333800	-1.92807300	-0.99274600	C	-6.36704500	0.41856800	-0.97736700
H	6.31679800	-2.74790200	-1.52049500	H	-4.74828400	1.26419000	0.19999500
H	7.83743200	-2.08422600	-0.69037500				
C	6.16126300	-0.77061800	-0.72786500	H	-3.63851500	-1.91721300	-2.49652400
H	6.69099600	0.02651700	-0.20450200	H	-5.99728800	-2.11448500	-3.24895100
C	4.73231300	-0.47624500	-1.14254200	H	-7.12467800	1.07696200	-0.55817300
H	4.69546200	0.43850900	-1.74861400	H	-7.75579600	-0.61866000	-2.28457100
H	4.35594400	-1.30365000	-1.75596500	C	3.97087900	0.96719100	0.88480500
O	-2.35654400	0.97651700	0.18231400	C	3.97717600	3.44210500	2.20707300
In	-0.65229500	0.84398000	1.15135700	C	2.98521000	1.92713300	0.61116000
O	2.36295500	-0.13283300	-0.44039000	C	4.96588400	1.22762800	1.83900300
C	3.78591300	-0.29631700	0.06949000	C	4.96389900	2.47532100	2.49636700
H	3.79524000	-1.19176000	0.69783600	C	2.97298300	3.17136500	1.25644900
H	-0.50736900	-1.80484300	1.46830400	H	5.71839200	0.48231700	2.07849500
H	-1.99302100	-2.28956900	-0.67776800	H	5.72596600	2.69080100	3.24066000
C	-2.91780600	-2.05942700	1.22760000	H	2.20553200	3.90917100	1.03923000
C	-4.39279800	-3.20663200	3.36370200	H	3.98667700	4.39639100	2.72635400
C	-3.01665000	-3.46317600	1.36641000	Br	-0.50792200	1.97973400	3.42022800
C	-3.57367700	-1.23542000	2.17280200	Br	2.25391400	-3.72614200	0.40191700
C	-4.30456900	-1.80628800	3.23127700	Br	0.51644300	-2.13435400	-3.08506600
C	-3.74763500	-4.03548700	2.42456100	C	2.00358800	1.47624600	-0.44390300
H	-2.52566400	-4.10993300	0.64135000	O	0.66111800	1.56294700	-0.20228000
H	-3.53185300	-0.15477700	2.07692700	O	2.38423000	1.99564200	-1.68317500
H	-4.80613800	-1.16024700	3.94775700	H	-0.10604500	3.06495900	-1.00169700
H	-3.81519400	-5.11695500	2.51325300	C	-0.03182900	4.91230400	-1.94068700
H	-4.95840900	-3.64450000	4.18255800	C	-2.03002300	3.73020300	-1.34722300
H	-1.96636300	-0.11838300	-1.55277700	C	-0.78126400	5.95962400	-2.47906000
C	-4.03723200	-0.32025200	-1.07707600	H	1.05094900	4.90169300	-1.92778200

C	-2.81646500	4.75823900	-1.87407100	N	-0.67160700	3.83989100	-1.39643900
H	-2.42882400	2.82758200	-0.88609100	C	1.67767000	1.56386800	-2.91150500
C	-2.18923100	5.88326900	-2.44578200	H	0.59671500	1.50234400	-2.75722800
H	-0.27153500	6.81225100	-2.91187900	H	1.90766800	2.32884400	-3.65514700
H	-3.89608900	4.67363100	-1.83502200	H	2.07467600	0.59867300	-3.23633500
H	-2.78728900	6.68939800	-2.85939000				

Pyridinium salt

---

opt=calcfc freq=noraman b3lyp/lanl2dz scrf=(iefpcm,solvent=thf,smd)

- Thermochemistry-

Zero-point correction= 0.103690 (Hartree/Particle)
Thermal correction to Energy= 0.108015
Thermal correction to Enthalpy= 0.108959
Thermal correction to Gibbs Free Energy= 0.076192
Sum of electronic and zero-point Energies= -248.602384
Sum of electronic and thermal Energies= -248.598060
Sum of electronic and thermal Enthalpies= -248.597116
Sum of electronic and thermal Free Energies= -248.629883

C	0.67324900	1.19869600	-0.00002500	H	1.28712700	-2.09071800	-0.00001900
C	-0.72270900	1.22038700	-0.00001200	N	1.32092700	-0.00003300	0.00001600
C	-1.42923500	0.00003200	0.00002600	H	2.34267700	-0.00002800	0.00017100
C	-0.72276400	-1.22035400	-0.00000800				
C	0.67319500	-1.19872700	-0.00003100				
H	1.28722300	2.09065700	-0.00001200				
H	-1.23954000	2.17258300	-0.00001900				
H	-2.51474400	0.00005700	0.00007500				
H	-1.23963800	-2.17252700	-0.00000600				

(*R*)-TS5

(*R*)-TS5 had one and only one imaginary frequency (imaginary frequency = -1369.52).

# opt=(calcfc,ts,noeigen) freq=noraman b3lyp/lanl2dz scrf=(iefpcm,solv
ent=thf,smd)

- Thermochemistry-

Zero-point correction= 0.232783 (Hartree/Particle)
Thermal correction to Energy= 0.246971
Thermal correction to Enthalpy= 0.247915
Thermal correction to Gibbs Free Energy= 0.190784

Sum of electronic and zero-point Energies= -690.987298
Sum of electronic and thermal Energies= -690.973111
Sum of electronic and thermal Enthalpies= -690.972166
Sum of electronic and thermal Free Energies= -691.029297

C	1.24651300	-1.06082700	0.23313100
O	1.30863600	-1.65625400	1.45339300
O	1.75195600	-1.71531700	-0.82797500
C	2.01543800	-3.17589800	-0.72076700
H	2.81282100	-3.35642700	0.00379300
H	2.32229400	-3.47053800	-1.72528700
H	1.10047900	-3.69502300	-0.42343800
C	-1.23474300	0.14660800	0.53184900
O	-0.70552900	-1.20589800	0.57199200
H	0.15888600	-1.55269500	1.53882100
C	-0.04280300	1.06965400	0.27944000
C	-0.11469400	2.47343500	0.21140600
C	1.04061600	3.22265900	-0.08234400
H	-1.06300300	2.97888900	0.37710200
C	2.35067900	1.17050400	-0.24658900
C	2.27129400	2.57308400	-0.31753600
H	0.98312200	4.30712300	-0.13505600
H	3.29774500	0.66578500	-0.41760100
H	3.15924900	3.15500300	-0.55022800
H	-1.68732700	0.38607900	1.50677700
C	-2.32180800	0.26378900	-0.56797900
H	-2.64178100	1.31015500	-0.65728100
H	-1.85545100	-0.02515700	-1.52223500
C	-3.51437600	-0.62385800	-0.28980200
H	-3.28221500	-1.67442300	-0.10513300
C	-4.80014800	-0.20960600	-0.26064000
H	-5.07262100	0.83107500	-0.43730900
H	-5.61617500	-0.90242300	-0.05976900
C	1.19460900	0.42751300	0.06775800

Minima: Precomplex of (*R*)-TS5

---

opt=(calcfc,noeigen) freq=noraman b3lyp/lanl2dz scrf=(iefpcm,solvent =thf,smd)

- Thermochemistry-

Zero-point correction= 0.237988 (Hartree/Particle)
Thermal correction to Energy= 0.252661
Thermal correction to Enthalpy= 0.253606
Thermal correction to Gibbs Free Energy= 0.195142
Sum of electronic and zero-point Energies= -691.036525
Sum of electronic and thermal Energies= -691.021852
Sum of electronic and thermal Enthalpies= -691.020908
Sum of electronic and thermal Free Energies= -691.079371

C	1.77949700	-0.79675700	0.21670700
O	1.56537500	-1.63862600	1.12539600

O	2.76275300	-0.98464900	-0.71399900
C	3.58538000	-2.21379800	-0.61310500
H	4.10425400	-2.24180400	0.34965900
H	4.29758400	-2.14108700	-1.43607100
H	2.95145500	-3.09832600	-0.72396300
C	-1.40671300	-0.27534700	0.54374700
O	-1.00030100	-1.66993500	0.57814700
H	-0.20028600	-1.79779000	1.14343400
C	-0.28351500	0.76494100	0.34387900
C	-0.71750100	2.11385700	0.37183300
C	0.14471300	3.18717700	0.10503400
H	-1.75830100	2.32410700	0.60546600
C	1.95595600	1.61694400	-0.23175100
C	1.49225800	2.93783200	-0.22043600
H	-0.23206000	4.20604900	0.14307200
H	2.99894900	1.41406800	-0.45165900
H	2.17018400	3.75672600	-0.44445300
H	-1.91817600	-0.01860500	1.48583100
C	-2.44412000	-0.19329600	-0.61365200
H	-2.79625500	0.83677600	-0.73002400
H	-1.91650100	-0.47510100	-1.53756700
C	-3.62197500	-1.11725700	-0.39414500
H	-3.37187100	-2.15800000	-0.18704500
C	-4.91714100	-0.73610400	-0.44780200
H	-5.20485700	0.29619200	-0.64827000
H	-5.72605900	-1.44888500	-0.29301400
C	1.09638100	0.52703600	0.07440000

Minima: Direct product of (*R*)-TS5

---

opt=(calcfc,noeigen) freq=noraman b3lyp/lanl2dz scrf=(iefpcm,solvent =thf,smd)

- Thermochemistry-

Zero-point correction=	0.237425 (Hartree/Particle)
Thermal correction to Energy=	0.251743
Thermal correction to Enthalpy=	0.252687
Thermal correction to Gibbs Free Energy=	0.196014
Sum of electronic and zero-point Energies=	-691.029413
Sum of electronic and thermal Energies=	-691.015096
Sum of electronic and thermal Enthalpies=	-691.014152
Sum of electronic and thermal Free Energies=	-691.070825

C	-0.46793600	1.30827900	0.29521600
O	-0.95390600	2.23048100	1.29309800
O	-0.35349100	2.02516300	-0.92387200
C	0.50549900	3.22171300	-0.89350400
H	0.11155500	3.96450900	-0.19321300
H	0.48559600	3.61439800	-1.91328400
H	1.53114500	2.95062200	-0.61770500
C	0.89039100	-0.70018500	0.61124800
O	0.82283900	0.78587700	0.77588200

H	-0.78409500	1.86013600	2.18761600
C	-0.53470200	-1.08178500	0.26313500
C	-1.10027400	-2.35727300	0.11254000
C	-2.46615600	-2.44996700	-0.22852500
H	-0.50612400	-3.25590500	0.25722800
C	-2.66896400	-0.00737300	-0.26724100
C	-3.24533900	-1.28558500	-0.41729900
H	-2.92721100	-3.42777200	-0.34574700
H	-3.26250900	0.89104000	-0.41175300
H	-4.29615600	-1.37830900	-0.67999100
H	1.20632800	-1.10086400	1.58147600
C	1.92587300	-1.07347700	-0.47299200
H	1.89703000	-2.16183700	-0.61772500
H	1.61035900	-0.60542500	-1.41698700
C	3.32963500	-0.63285000	-0.11848500
H	3.44258400	0.42267900	0.13691900
C	4.41457400	-1.43721500	-0.11278100
H	4.34709600	-2.49644100	-0.36132400
H	5.40234200	-1.05543900	0.14107200
C	-1.31284600	0.07012400	0.07744900

(*S*)-TS6

(*S*)-TS6 had one and only one imaginary frequency (imaginary frequency = -1391.29).

# opt=(calcfc,ts,noeigen) freq=noraman b3lyp/lanl2dz scrf=(iefpcm,solv
ent=thf,smd)

- Thermochemistry-

Zero-point correction=	0.232763 (Hartree/Particle)
Thermal correction to Energy=	0.246896
Thermal correction to Enthalpy=	0.247840
Thermal correction to Gibbs Free Energy=	0.190903
Sum of electronic and zero-point Energies=	-690.986331
Sum of electronic and thermal Energies=	-690.972198
Sum of electronic and thermal Enthalpies=	-690.971254
Sum of electronic and thermal Free Energies=	-691.028191

C	-0.93901100	1.21383600	0.18083700
O	-0.29545200	1.77708500	1.23787400
O	-1.78497600	1.97725200	-0.53547700
C	-1.70844200	3.45714300	-0.40624000
H	-1.97280400	3.75534600	0.61069900
H	-2.43598500	3.83068400	-1.12817200
H	-0.70023900	3.79690600	-0.65804200
C	1.13961700	-0.40987000	-0.66902900
O	0.91124300	1.01468400	-0.49465600
H	0.71374900	1.48343500	0.74829200
C	-0.16822200	-1.10622200	-0.28732200
C	-0.38559400	-2.49533300	-0.34496000
C	-1.65121200	-3.02281400	-0.02420200
H	0.41837800	-3.16022700	-0.65129900

C	-2.49832500	-0.77481100	0.40325400
C	-2.70782300	-2.16479800	0.34814300
H	-1.81840800	-4.09596700	-0.07345300
H	-3.30873100	-0.10921200	0.68813400
H	-3.68497800	-2.57548800	0.58830100
H	1.35623500	-0.59933700	-1.73093700
C	2.34890300	-0.89971400	0.17343100
H	2.17035500	-0.68009900	1.23454600
H	2.40066600	-1.99437000	0.06773900
C	3.66004400	-0.29825600	-0.28088900
H	3.88835100	-0.40823500	-1.34475500
C	4.54816600	0.32634100	0.52189800
H	4.35987200	0.46359900	1.58662500
H	5.48689300	0.71945500	0.13450800
C	-1.22474500	-0.25527900	0.09606000

Minima: Precomplex of (*S*)-TS6

---

opt=(calcfc,noeigen) freq=noraman b3lyp/lanl2dz scrf=(iefpcm,solvent =thf,smd)

- Thermochemistry-

Zero-point correction=	0.238346 (Hartree/Particle)
Thermal correction to Energy=	0.252995
Thermal correction to Enthalpy=	0.253939
Thermal correction to Gibbs Free Energy=	0.195595
Sum of electronic and zero-point Energies=	-691.045186
Sum of electronic and thermal Energies=	-691.030537
Sum of electronic and thermal Enthalpies=	-691.029592
Sum of electronic and thermal Free Energies=	-691.087937

C	0.75915800	1.35239700	0.22210400
O	-0.23783800	1.75092300	0.87727200
O	1.59321500	2.24234000	-0.39686900
C	1.30439900	3.68716800	-0.24271800
H	0.32931100	3.92323500	-0.67876100
H	2.10476000	4.18905800	-0.78819600
H	1.31936600	3.96498600	0.81532500
C	-1.20949800	-1.09262800	0.46583400
O	-1.53666000	-0.41873000	1.72075700
H	-1.22568300	0.51975400	1.64046600
C	0.30257100	-1.17801500	0.20406700
C	0.84372900	-2.47358800	0.05226000
C	2.20198100	-2.68910700	-0.24219100
H	0.18393300	-3.33029000	0.16544300
C	2.55536700	-0.29134800	-0.25911600
C	3.06561400	-1.58972300	-0.40024300
H	2.57898700	-3.70335500	-0.34657000
H	3.21350500	0.56240100	-0.37610400
H	4.11764000	-1.74002100	-0.62621100
H	-1.56682300	-2.11582600	0.61854700
C	-1.98297000	-0.50342600	-0.74966900
H	-1.69594300	0.53981400	-0.92677000

H	-1.67762100	-1.08191000	-1.63587500
C	-3.48304100	-0.61306600	-0.58695200
H	-3.85928000	-1.60752600	-0.33071300
C	-4.36299700	0.39698000	-0.75641700
H	-4.03753800	1.40663800	-1.00646100
H	-5.43517900	0.24004600	-0.64751100
C	1.18915800	-0.06618700	0.04539100

Minima: Direct product of (*S*)-TS6

---

opt=(calcfc,noeigen) freq=noraman b3lyp/lanl2dz scrf=(iefpcm,solvent =thf,smd)

- Thermochemistry-

Zero-point correction=	0.237159 (Hartree/Particle)
Thermal correction to Energy=	0.251598
Thermal correction to Enthalpy=	0.252542
Thermal correction to Gibbs Free Energy=	0.195278
Sum of electronic and zero-point Energies=	-691.029327
Sum of electronic and thermal Energies=	-691.014888
Sum of electronic and thermal Enthalpies=	-691.013944
Sum of electronic and thermal Free Energies=	-691.071209

C	-0.39790100	1.27761300	0.22837500
O	-0.34950700	1.94186400	1.50724200
O	-0.85506900	2.22306800	-0.72727400
C	-0.06038500	3.45868800	-0.84363000
H	-0.12175000	4.04586700	0.07780400
H	-0.50857500	4.01012200	-1.67408600
H	0.98555500	3.22346000	-1.07166000
C	0.91369000	-0.60569100	-0.60315800
O	0.95900800	0.78694200	-0.06143400
H	0.21444900	1.42115200	2.12124500
C	-0.51356600	-1.04357400	-0.32916100
C	-1.10851100	-2.30239900	-0.50574700
C	-2.47258500	-2.45242300	-0.17767500
H	-0.53763900	-3.14566200	-0.88572000
C	-2.61986300	-0.09689700	0.48361800
C	-3.22312300	-1.36038000	0.31444600
H	-2.95372800	-3.41936100	-0.30403000
H	-3.19211400	0.74699400	0.85869700
H	-4.27275700	-1.49705200	0.56218400
H	1.10877500	-0.54493800	-1.68273500
C	1.99975300	-1.46034300	0.07461800
H	1.85269700	-1.44746100	1.16167100
H	1.84298400	-2.49592300	-0.26766000
C	3.40665000	-1.03309000	-0.28250200
H	3.61878200	-0.94594300	-1.35179200
C	4.39167300	-0.78618300	0.60705800
H	4.22436100	-0.85576200	1.68172200
H	5.39212900	-0.50356800	0.28315100
C	-1.26393600	0.03685900	0.15758100

4.4. Synthesis of Chiral $C_{(3)}$-Functionalized Phthalides via a Ag(I)-Catalyzed Allylation /Transesterification Sequence.

Preparation of the starting material 151a-m: The procedure for preparation of starting material **151a-m** was described in section 4.3.1 and 4.3.2.[138]

4.4.1. Representative Procedure D for Synthesis of Substituted (*R*)-3-Allylisobenzofuran-1(3H)-one.

A round-bottomed flask wrapped in an aluminium foil was charged with AgF (7.75 mg, 0.061mmol), (*R*)-BINAP (22.8 g, 0.035 mmol) and anhydrous MeOH (0.2 mL) and stirred for 10 min at room temperature. The mixture was cooled to -20 °C (dry ice/xylene bath) followed by dropwise addition of methyl 2-formylbenzoate **151a** (100 mg, 0.61 mmol) and allyltrimethoxysilane (154 μL, 0.91mmol). After 4 hours, the reaction mixture was quenched with a mixture of 1N HCl (3 mL) and KF (ca. 0.3 g) and stirred for 30 min. The resulting precipitate was filtered and the filtrate was dried over $MgSO_4$. After evaporation of the solvents in vacuum, the crude product was purified by column chromatography on silica gel (*n*-hexane/EtOAc: 1/1) to yield **152a** as a colorless oil (72.1 mg, 68% yield).

(*R*)-3-allylisobenzofuran-1(3H)-one (152a). Representative procedure D was followed to prepare **152a** from substrates **151a**, **151g-j**, and **151m** and the spectroscopic data was in full agreement with spectral data of an authentic sample.[138] ^{1}H NMR (300 MHz, $CDCl_3$): δ = 7.88 (d, *J* = 7.8 Hz, 1H), 7.67 (t, *J* = 7.6 Hz, 1H), 7.53-7.47 (m, 2H), 5.77-5.50 (m, 1H), 5.521 (t, *J* = 6 Hz, 1H), 5.16-5.13 (m, 2H), 2.75-2.62 (m, 2H). ^{13}C NMR (75 MHz, $CDCl_3$): δ = 170.5, 149.4, 134.0, 131.3, 129.3, 126.3, 125.8, 122.1, 119.8, 80.3, 38.7. The product **152a** was obtained from substrate **151g** (61.5 mg, 58%), **151h** (77.4 mg, 73%), **151i** (74.3 mg, 70%), **151j** (57.3 mg, 54%), **151m** (72.1 mg, 68%). For **152a** prepared from **151a** $[\alpha]^{20}_D$ =

+50.5 (c = 1.74, $CHCl_3$). For **152a** prepared from **151g** $[\alpha]^{20}_D$ = +63.0 (c = 2.0, $CHCl_3$). For **152a** prepared from **151h** $[\alpha]^{20}_D$ = +70.1 (c = 2.05, $CHCl_3$). For **152a** prepared from **151i** $[\alpha]^{20}_D$ = +65.7 (c = 1.5, $CHCl_3$). For **152a** prepared from **151j** $[\alpha]^{20}_D$ = +62.3 (c = 1.5, $CHCl_3$). For **152a** prepared from **151m** $[\alpha]^{20}_D$ = +61.4 (c = 1.95, $CHCl_3$). The enantioselectivity was determined by HPLC analysis on a chiral column (OD-H, hexane/*i*prOH 95:5, flow rate 0.5 $mLmin^{-1}$, wavelength = 245 nm). For **151a** prepared from **151a** 85.5:14.5 er, 71% ee: t_{minor} = 20.41 min, t_{major} = 19.00 min. For **152a** prepared from **151g** 81.5:18.5 er, 63% ee: t_{minor} = 18.97 min, t_{major} = 20.47 min. For **152a** prepared from **151h** 93:7 er, 86% ee: t_{minor} = 18.58 min, t_{major} = 19.516 min. For **152a** prepared from **151i** 93:7 er, 86% ee: t_{minor} = 18.72 min, t_{major} = 19.85 min. For **152a** prepared from **151j** 81.5:18.5 er, 63% ee: t_{minor} = 18.97 min, t_{major} = 20.47 min. For **152a** prepared from **151m** 88:12 er, 76% ee, t_{minor} = 19.37 min, t_{major} = 20.68 min. Absolute configuration assigned as (*R*) by comparison of optical rotation with a literature value.[139]

(*R*)-3-allyl-6-bromoisobenzofuran-1(3H)-one (152b): Representative procedure D was followed. The crude product was purified by column chromatography on silica gel (*n*-hexane/EtOAc: 1/1) to yield **152b** (87.9 mg, 57%). The spectroscopic data was in full agreement with spectral data of an authentic sample.[138] ^{1}H NMR (300 MHz, $CDCl_3$): δ = 8.05 (d, *J* = 1.6 Hz, 1H), 7.79 (dd, *J* = 8.1, 1.7 Hz, 1H), 7.37 (d, *J* = 6 Hz, 1H), 5.82-5.69 (m, 1H), 5.51 (t, *J* = 6 Hz, 1H), 5.23-5.17 (m, 2H), 2.75-2.67 (m, 2H). ^{13}C NMR (75 MHz, $CDCl_3$): δ = 170.5, 160.7, 141.8, 131.3, 127.6, 122.9, 122.8, 119.7, 107.5,80.1, 56.8, 38.8. $[\alpha]^{20}_D$ = +0.14 (c = 10, $CHCl_3$). The enantioselectivity was determined by HPLC analysis on a chiral column (AS-H, hexane/*i*prOH 90:10, flow rate 1 $mLmin^{-1}$, wavelength = 245 nm) to be 69.5:30.5 er, 39% ee: t_{minor} = 7.51 min, t_{major} = 8.02 min.

(*R*)-3-allyl-6-nitroisobenzofuran-1(3H)-one (152c): Representative procedure D was followed. The crude product was purified by column chromatography on silica gel (*n*-hexane/EtOAc: 1/1) to yield **152c** (69.5 mg, 52%). The spectroscopic data was in full agreement with spectral data of an authentic sample.[138] ^{1}H NMR (300 MHz, $CDCl_3$): δ = 8.72 (s, 1H), 8.54 (dd, *J* = 8.1, 2.1 Hz, 1H), 7.67 (t, *J* = 8.4 Hz, 1H), 5.67-5.63 (m, 2H), 5.23-5.17 (m, 2H), 2.78-2.76 (m, 2H). ^{13}C NMR (75 MHz, $CDCl_3$): δ = 167.8, 154.5, 149.1, 130.0, 128.8, 128.1, 123.5, 121.4, 121.4, 80.2, 38.2. $[\alpha]^{20}_{D}$ = +10.1 (c = 0.62, $CHCl_3$). The enantioselectivity was determined by HPLC analysis on a chiral column (AS-H, hexane/*i*prOH 80:20, flow rate 1 mLmin^{-1}, wavelength = 245 nm) to be 66.5:33.5 er, 33% ee: t_{minor} = 13.20 min, t_{major} = 17.65 min (*R*).

(*R*)-isobutyl(3-allyl-1-oxo-1,3-dihydroisobenzofuran-5-yl)carbamate(152d):

Representative procedure D was followed. The crude product was purified by column chromatography on silica gel (*n*-hexane/EtOAc: 1/1) to yield **152d** (114.7 mg, 65%). The spectroscopic data was in full agreement with spectral data of an authentic sample.[138] ^{1}H NMR (300 MHz, $CDCl_3$): δ = 7.87 (s, 1H), 7.86 (s, 1H), 7.41 (d, *J* = 8.4, Hz, 1H), 7.22 (s, 1H), 5.82-5.68 (m, 1H), 5.49 (t, *J* = 6 Hz, 1H), 5.21-5.13 (m, 2H), 3.98 (d, *J* = 6.6 Hz, 2H), 2.77-2.58 (m, 2H), 2.05-1.94 (m, 1H), 0.98 (d, *J* = 6.6 Hz, 6H). ^{13}C NMR (75 MHz, $CDCl_3$): δ = 168.8, 148.0, 137.1, 130.9, 128.9, 128.7, 123.7, 123.6, 120.3, 80.2, 38.6. $[\alpha]^{20}_{D}$ = +30.3 (c = 0.23, $CHCl_3$). The enantioselectivity was determined by HPLC analysis on a chiral column (AS-H, hexane/*i*prOH 90:10, flow rate 1 mLmin^{-1}, wavelength = 245 nm) to be 71.5:28.5 er, 43% ee: t_{major} = 31.31 min, t_{minor} = 28.28 min.

(*R*)-3-allyl-6-phenylisobenzofuran-1(3H)-one (152e): Representative procedure D was followed. The crude product was purified by column chromatography on silica gel (*n*-

hexane/EtOAc: 1/1) to yield **152e** (102.3 mg, 67%). The spectroscopic data was in full agreement with spectral data of an authentic sample.[138] ^{1}H NMR (300 MHz, $CDCl_3$): δ = 8.13 (s, 1H), 7.92 (dd, *J* = 6.6, 1.6 Hz, 1H), 7.65-7.63 (m, 2H), 7.67-7.43 (m, 4H), 5.90-5.76 (m, 1H), 5.59 (t, *J* = 6 Hz, 1H), 5.27-5.19 (m, 2H), 2.83-2.72 (m, 2H). ^{13}C NMR (75 MHz, $CDCl_3$): δ = 170.2, 153.7, 144.0, 139.6, 131.3, 127.3, 124.8, 122.8, 119.9, 114.9, 80.3, 71.9, 38.9, 28.1, 19.15. $[\alpha]^{20}_{D}$ = +30.1 (c = 0.71, $CHCl_3$). The enantioselectivity was determined by HPLC analysis on a chiral column (AS-H, hexane/*i*prOH 90:10, flow rate 1 mLmin^{-1}, wavelength = 245 nm) to be 80.5:19.5 er, 61% ee: t_{minor} = 20.14 min, t_{major} = 14.88 min (*R*).

(*R*)-3-allyl-6-methoxyisobenzofuran-1(3H)-one (152f): Representative procedure D was followed. The crude product was purified by column chromatography on silica gel (*n*-hexane/EtOAc: 1/1) to yield **152f** (68.5 mg, 55%). The spectroscopic data was in full agreement with spectral data of an authentic sample.[138] ^{1}H NMR (300 MHz, $CDCl_3$): δ = 7.36 (s, 1H), 7.33 (d, *J* = 2.1 Hz, 1H), 7.20-7.24 (m, 1H), 5.80-5.69 (m, 1H), 5.47 (t, *J* = 5.9 Hz, 1H), 5.21-5.14 (m, 2H), 3.87 (s, 3H), 2.71-2.57 (m, 2H). ^{13}C NMR (75 MHz, $CDCl_3$): δ = 170.5, 160.7, 141.8, 131.3, 127.6, 122.9, 122.9, 119.7, 107.5, 80.1, 55.8, 38.8. $[\alpha]^{20}_{D}$ = +19.3 (c = 0.4, $CHCl_3$). The enantioselectivity was determined by HPLC analysis on a chiral column (OD-H, hexane/*i*PrOH 99:1, flow rate 0.5 mLmin^{-1}, wavelength = 245 nm) to be 93:7 er, 86% ee: t_{minor} = 36.09 min, t_{major} = 37.59 min.

Preparation of the (*R*)-1-phenylbut-3-en-1-ol (160): Representative procedure D was followed. The crude product was purified by column chromatography on silica gel (*n*-hexane/EtOAc: 6/1) to yield **160** (79.5 mg, 88%). The spectroscopic data was in full agreement with spectral data of an authentic sample.[138] ^{1}H NMR (300 MHz, $CDCl_3$): δ = 7.30-7.39 (m, 5H), 5.77-5.91 (m, 1H), 5.15-5.22 (m, 2H), 4.75 (t, *J* = 7 Hz, 1H), 2.51-2.57

(m, 2H), 2.22 (s, 1H, OH). ^{13}C NMR (75 MHz, $CDCl_3$): δ = 144.0, 134.5, 128.5, 127.7, 125.9, 118.5, 73.4, 43.9. $[\alpha]^{20}_D$ = +43.1 (c = 0.8, $CHCl_3$). The enantioselectivity was determined by HPLC analysis on a chiral column (OD-H, hexane/*i*prOH 97:3, flow rate 0.5 $mLmin^{-1}$, wavelength = 245 nm) to be 93.5:6.5 er, 87% ee: t_{minor} = 12.03 min, t_{major} = 10.52 min.

4.5. Synthesis of A Class of Phase-Transfer Catalyst with Interionic Strain.

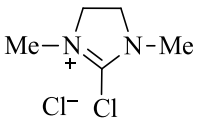

2-Chloro-1,3-dimethylimidazolinium chloride (DMC) (162): DMC was synthesized from commercially available 1,3-dimethyl-2-imidazolidinone by following the procedure reported by Isobe *et al*. with slightly changes. Spectroscopic data was in full agreement with spectral data of an authentic sample.[140]

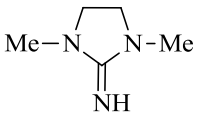

1,3-dimethylimidazolidin-2-imine (163): 163 was synthesized from DMC by following the procedure reported by Ma *et al*.[141] ^{1}H NMR (300 MHz, $CDCl_3$): δ = 9.00 (s, 2H), δ = 3.55 (s, 4H), 3.23 (s, 6H).^{13}C NMR (75 MHz, $CDCl_3$): δ = 158.9, 48.4, 34.0.

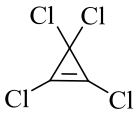

Tetrachlorocyclopropene (167): 167 was synthesized from commercially available trichloroethylene and sodium trichloroacetate, following the procedure reported by Tobey and West.[142]

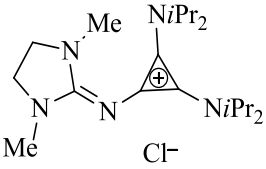

168•Cl⁻ : Tetrachlorocyclopropene (**167**) (450 mg, 2.5 mmol) was mixed with DCM (10 mL) and diisopropylamine (2.1 ml, 15 mmol) added dropwise at 0 °C. After stirring for an hour, imine **163** (300 mg, 2.5 mmol) was added and stirred overnight. Solvent was removed by rotary evaporation and the crude product purified by column chromatography on silica gel (DCM:MeOH, 97:3) to yield **168•**Cl^- as a white solid (775 mg, 80.4%). ^{1}H NMR (300 MHz, $CDCl_3$): δ = 3.69-

3.77 (m, 4H), 3.64 (s, 4H), 2.81 (s, 6H), 1.27 (d, J = 6.9, 24H). ^{13}C NMR (75 MHz, $CDCl_3$): δ = 161.1, 121.3, 118.0, 51.04, 48.1, 33.9, 22.32. ^{15}N NMR (60 MHz, $CDCl_3$): δ = 128.58, 105.50, 81.28. IR: 3415, 3361, 2963. HRMS (EI): m/z calcd for $C_{20}H_{38}N_5^+$ (M^+): 348.3122; found: 348.3119.

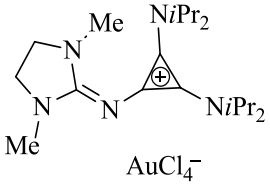

168•$AuCl_4^-$: Compound **168•Cl^-** (116 mg, 0.3 mmol) was dissolved in THF (3 mL), AuCl (139.4 mg, 0.6 mmol) added and stirred for 2 hours. The solvent was removed and the resulting solid recrystallized from ethanol to yield **168**•$AuCl_4^-$ as an orange solid (78.8 mg, 45%). ^{1}H NMR (300 MHz, $CDCl_3$): δ = 3.59-3.84 (m, 4H), 2.87 (s, 6H), 1.33 (d, J = 6.9, 24H). IR: 3256, 2961. ^{13}C NMR (75 MHz, $CDCl_3$): δ = 161.2, 121.4, 118.0, 51.1, 48.2, 34.0, 22.4.

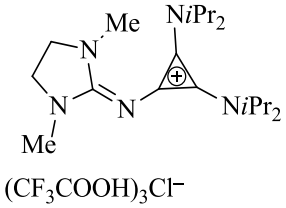

168•$(TFA)_3Cl^-$: Compound **168**•Cl^- (116 mg, 0.3 mmol) was dissolved in DCM (3 mL) and trifluoroacetic acid (TFA) (0.4 mL, 6 mmol) added followed by stirring for 1 hour. The volatiles were removed under reduced pressure and the resulting solid recrystallized from DCM and hexanes to yield **168**•$(TFA)_3Cl^-$ as a white solid (150 mg, 65%). ^{1}H NMR (300 MHz, $CDCl_3$): δ = 14.47 (s, 3H), 3.69-3.78 (m, 4H), 3.54 (s, 4H), 2.80 (s, 6H), 1.24 (d, J = 6.9, 24H). ^{13}C NMR (75 MHz, $CDCl_3$): δ = 160.6, 160.4, 160.0, 159.5, 122.3,121.2, 117.4, 115.32, 113.6,109.8, 51.3, 47.9, 33.6, 21.8. ^{15}N NMR (60 MHz, $CDCl_3$): δ = 120.96, 108.11, 82.68.

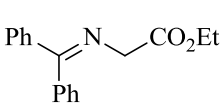

Ethyl N-(diphenylmethylene)glycinate (169): **169** was synthesized from commercially available glycine ethyl ester hydrochloride by following the procedure reported by O'Donnell *et al*. Spectroscopic data was in full agreement with spectral data of an authentic sample.[143]

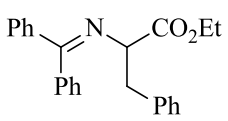

Ethyl 2-((diphenylmethylene)amino)-3-phenylpropanoate (170): In a 25 mL flask, ethyl N-(diphenylmethylene)glycinate (**169**) **(**310 mg, 1.1 mmol**)** and catalyst **5•Cl**$^{-}$ (8.5 mg, 2 mol%) were dissolved in 10 mL of DCM. To the resulting solution, aqueous KOH solution (50%, 3.2 mL) was added followed by the addition of benzyl bromide (0.2 mL, 7.5 mmol). After stirring for four hours at room temperature, water was added (10 mL) and the solution was neutralized with HCl (1N). The reaction mixture was extracted with DCM (3 x 10 mL) and the combined organic phases dried over $MgSO_4$. The solvent was removed under reduced pressure and the crude product purified by column chromatography on silica gel (n-hexane/EtOAc: 12/1) to yield **170** as an oil. ^{1}H NMR (300 MHz, $CDCl_3$): δ = 7.60 (d, *J* = 7.8 Hz, 2H), 7.36-7.19 (m, 9H), 7.07-7.05 (m, 2H), 6.63-6.61 (m, 2H), 4.27-4.13 (m, 3H), 3.33-3.21 (m, 2H), 1.30-1.25 (m, 3H). ^{13}C NMR (75 MHz, $CDCl_3$): δ = 171.7, 138, 139.9, 128.8, 128.3, 128.2, 128.0, 127.7, 126.3, 67.3, 61.0, 39.7, 14.2. Spectroscopic data was in full agreement with spectral data of an authentic sample.[143]

4.5.1. DFT Calculated Geometries and Thermochemical Data of 168•$AuCl_4^-$, and 168•$(TFA)_3Cl^-$.

168•$AuCl_4^-$

---

opt=calcfc freq=noraman b3lyp/sdd

- Thermochemistry -

Zero-point correction= 0.575184 (Hartree/Particle)

Thermal correction to Energy= 0.616514

Thermal correction to Enthalpy= 0.617458

Thermal correction to Gibbs Free Energy= 0.495456

Sum of electronic and zero-point Energies= -3034.576599

Sum of electronic and thermal Energies= -3034.535269

Sum of electronic and thermal Enthalpies= -3034.534325

Sum of electronic and thermal Free Energies= -3034.656327

0 1

N	-1.05383900	3.81471300	0.83546700
N	-2.98068500	3.34831300	-0.24429400
N	-1.70625900	1.55437100	0.81225200
N	-1.67818200	-0.79234500	-2.14186800
N	-2.37420300	-1.95552900	1.39560200
C	-1.95666000	0.37632400	0.24342900
C	-1.89516700	-0.53939500	-0.84071000
C	-2.14214100	-0.99699200	0.48835900
C	-4.28982800	2.69708700	-0.33192100
H	-4.17451100	1.61155500	-0.36590400
H	-4.80020300	3.01382600	-1.24841700
H	-4.92705300	2.95346500	0.53063800
C	-2.92542300	4.83021100	-0.19645200
H	-3.66987300	5.21260700	0.51948600
H	-3.13368300	5.26520000	-1.17916300
C	-1.47663400	5.11432800	0.28273700
H	-0.82060200	5.40568500	-0.55024900
H	-1.43512800	5.90117000	1.04389500
C	-1.68052200	-2.20151400	-2.65851900
H	-1.94537100	-2.82645500	-1.79959300
C	-0.28044700	-2.63726700	-3.14258900
H	0.03437100	-2.08435000	-4.03634200
H	-0.30085800	-3.70306300	-3.40552700
H	0.47373500	-2.48741600	-2.36436000
C	-2.76733600	-2.40519700	-3.73745700
H	-3.75986700	-2.12899200	-3.36042600
H	-2.79366200	-3.46005600	-4.03807500
H	-2.56150100	-1.81327700	-4.63778900
C	-2.56865300	-1.55400200	2.83177800
H	-2.78318500	-2.48746500	3.36353200
C	-3.79251300	-0.62489500	2.99266800
H	-3.61703600	0.34363300	2.51006700
H	-3.97305300	-0.43578000	4.05835000
H	-4.69574000	-1.07804600	2.56460700
C	-1.28566300	-0.93233900	3.42121400
H	-0.42478300	-1.59639900	3.29690700
H	-1.42549600	-0.73668900	4.49260100
H	-1.04188800	0.01549000	2.92981600
C	-2.40587500	-3.40554100	1.02648000
H	-2.08369100	-3.45194600	-0.01860700
C	-1.39699700	-4.23577400	1.84923500
H	-0.39411000	-3.80302800	1.78290500
H	-1.35990700	-5.25836700	1.45275600
H	-1.68363600	-4.30325300	2.90607100
C	-3.84152000	-3.97058500	1.12045200
H	-4.21654800	-3.93644300	2.15132800
H	-3.85452300	-5.01934200	0.79767500
H	-4.53324700	-3.40409300	0.48462200
C	-1.34948900	0.32188600	-3.09382700
H	-1.08724100	-0.17851900	-4.03194600
C	-0.12250200	1.13743700	-2.63967000
H	-0.30500600	1.64578800	-1.68590100
H	0.10526800	1.90573300	-3.38989600
H	0.76125200	0.50318200	-2.52652900
C	-2.57743300	1.22050800	-3.36295700
H	-3.45194100	0.62543700	-3.65236300
H	-2.35042600	1.91829400	-4.17945000
H	-2.82913600	1.81749700	-2.47986600
C	0.28476100	3.60357300	1.39857000
H	0.36037000	2.58224800	1.77689600
H	0.45340400	4.30474900	2.22451200
H	1.06955100	3.74264400	0.64253400
C	-1.90225300	2.80481400	0.46141200
Au	2.64912400	-0.19266900	0.19591700
Cl	3.18090100	-0.79747500	-2.07567000
Cl	3.64527700	1.96632900	-0.14056400
Cl	2.14697400	0.40126100	2.47717800
Cl	1.53744300	-2.32052900	0.48436200

168•$(TFA)_3Cl^-$

---

opt=calcfc freq=noraman b3lyp/6-311g(d)

- Thermochemistry -

Zero-point correction= 0.686861 (Hartree/Particle)

Thermal correction to Energy= 0.744062

Thermal correction to Enthalpy= 0.745006

Thermal correction to Gibbs Free Energy= 0.580021

Sum of electronic and zero-point Energies= -3099.384665

Sum of electronic and thermal Energies= -3099.327464

Sum of electronic and thermal Enthalpies= -3099.326520

Sum of electronic and thermal Free Energies= -3099.491505

0 1

N	2.86582200	-1.91971600	0.28057800
N	1.17674300	-1.82627200	-1.44882300
N	0.67862900	-2.70655300	0.53060800
N	3.62073800	1.69937700	-0.43848200
N	6.28103400	-0.86900200	0.05034400
C	8.11781500	0.13717500	1.41474700
H	8.67532400	-0.79025300	1.56719600
H	7.43397700	0.26575800	2.25644200
H	8.84028600	0.95703500	1.43762100
C	5.04797600	3.57667400	0.40135700
H	5.85753900	4.25735200	0.12429400
H	5.39256100	2.96206500	1.23678400
H	4.21569800	4.18847000	0.75738100
C	2.02940100	-1.68864000	-2.61509900
H	2.92022200	-1.10885300	-2.38547600
H	1.47238900	-1.15961500	-3.38913000
H	2.33499900	-2.66750400	-3.00894600
C	1.63873600	-2.10707100	-0.19118000
C	-0.13046000	-2.47962500	-1.64198900
H	-0.80301300	-1.83532900	-2.20341000
H	0.01465200	-3.42017000	-2.19190500
C	-0.59375000	-2.72630400	-0.20567400
H	-1.10661500	-3.67855900	-0.06923800
H	-1.24570100	-1.93410800	0.16632200
C	3.98863100	0.43130200	-0.24126100
C	3.66852900	-0.91615000	-0.01743500
C	4.99793300	-0.51316600	-0.04827400
C	2.24045100	2.14913700	-0.07532100
H	2.30785000	3.23848100	-0.05229300
C	4.64301300	2.71187900	-0.79870100
H	5.51399000	2.13534300	-1.11843400
C	4.20599700	3.55543100	-2.00117800
H	3.34883400	4.19257800	-1.77237700
H	3.94267800	2.92207100	-2.85045800
H	5.02494800	4.21132000	-2.30730700
C	1.20248900	1.76207900	-1.12844500
H	1.09350000	0.67992800	-1.20988800
H	1.46815200	2.15657100	-2.11167000
H	0.22303000	2.15820000	-0.85664500
C	7.36118600	0.14437800	0.08093900
H	6.85179000	1.10576100	0.00318600
C	0.71632900	-2.90255000	1.97029700
H	0.43599700	-3.93066100	2.20815800
H	0.00333700	-2.23836400	2.46452500
H	1.72646800	-2.71026200	2.32506800
C	8.30133300	0.00974700	-1.12236000
H	7.74793200	0.05755900	-2.06306100
H	8.85664300	-0.93161100	-1.10384800
H	9.03586200	0.81919100	-1.11953900
C	6.60974700	-2.31216400	0.21257100
H	7.70000100	-2.35004400	0.25152800
C	6.06115000	-2.87714900	1.52760400
H	4.96895600	-2.88508400	1.52830200
H	6.40579300	-2.29364500	2.38424800
H	6.40224400	-3.90704700	1.66338900
C	6.15173400	-3.12929100	-0.99958000
H	6.50062800	-4.16119600	-0.90946700
H	6.55075300	-2.71700100	-1.92936600
H	5.06192400	-3.15678400	-1.06791000
C	1.86001400	1.68727200	1.33375200
H	0.92846300	2.16434000	1.63647100
H	2.62952300	1.95768200	2.06140000
H	1.70415700	0.60740100	1.38194100
F	-7.18454700	0.35825000	-0.34168300
F	-8.14655800	-1.48720900	-0.96522200
F	-6.25007900	-0.90133700	-1.85002300
O	-4.93239100	-1.37477900	0.40641500
H	-4.40108000	-1.78251000	1.17830200
O	-6.80188600	-2.39506100	1.18659000
C	-6.22699300	-1.67734000	0.42487100
C	-6.96930900	-0.91882700	-0.70519500
F	-1.20025300	3.00911800	3.19759300
F	-1.47544600	3.40010600	1.08054800
F	-3.20046200	3.32370600	2.39729600
O	-1.73245700	0.76046400	0.84419000
O	-2.65512700	0.65629500	2.91190400
H	-2.76265300	-0.34765800	2.77550400
C	-2.12237800	1.24640800	1.88024700
C	-2.00822100	2.77178800	2.14121100
F	-4.34739800	1.81476100	-2.78491600
F	-2.75829400	2.65439700	-1.56693600

F	-4.30050900	1.42795900	-0.64611300	C	-2.67348100	0.32171000	-2.04194800
O	-3.11415200	-0.82528700	-1.55702500	C	-3.53043800	1.58071200	-1.74173900
H	-3.85268100	-0.77849100	-0.90979600	Cl	-3.05936600	-2.24761000	2.49769400
O	-1.70443600	0.41460900	-2.74413200				

4.6. Fluorination of Benzyl Bromide, and its Derivatives.

4.6.1. Representative Procedure for Fluorination at Benzylic Position.

Synthesis of Benzyl fluoride (172). Benzyl bromide (102.62 mg, 0.6 mmol), cesium fluoride (328.14 mg, 1.8 mmol), and synthesized catalyst **168•**Cl^- (11.03 mg, 0.03 mmol) was dissolved in acetonitrile and heated under reflux for 9 hours. Solvent was removed and the product extracted with hexane to give product **172** as a colorless oil in 100% conversion and 94% isolated yield. Additionally, undissolved residual solid from hexane extraction was then dissolved in acetonitrile, solution was decanted, and after removing acetonitrile the catalyst was recovered. ^{1}H NMR (300 MHz, $CDCl_3$): δ = 5.46 (d, *J* = 48 Hz, 2H), 7.14 (m, 5H); ^{19}F NMR (292 MHz, $CDCl_3$): δ = -206.7.

Table 7. Fluorination reaction conditions for products **172**-**175** from corresponding bromide substrates in presence and absence of catalyst **168•**Cl^-.

product	T (°C)	t (h)	yield in the absence of catalyst[a]	yield in the presence of catalyst **5•**Cl^-
172	80	9	5%	94%
173	60	10	13%	93%
174	25	13	7%	90%
175	45	14	10%	95%

[a] Yields in the absence of catalyst were calculated based on ^{1}H NMR spectral data.

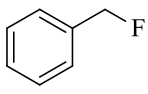

(Fluoromethyl)benzene (**172**). ^{1}H NMR (300 MHz, $CDCl_3$): δ = 7.14 (m, 5H), 5.33 (d, *J* = 48 Hz, 2H), ^{19}F NMR (292 MHz, $CDCl_3$): δ = -208.7.

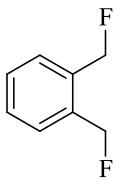

1,2-Bis(fluoromethyl)benzene (**173**). ^{1}H NMR (300 MHz, $CDCl_3$): 7.45-7.46 (m, 5H), 5.61 (s, 2H), δ = 5.45 (s, 2H); ^{13}C NMR (75.5 MHz, $CDCl_3$): δ = 134.6 (d, *J* = 1.9 Hz), 134.3 (d, *J* = 2 Hz), 128.7-129.2 (m), 82.3 (d, *J* = 165.7 Hz); ^{19}F NMR (292 MHz, $CDCl_3$): δ = -206.7.

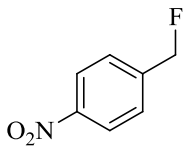

1-(Fluoromethyl)-4-nitrobenzene (**175**). ^{1}H NMR (300 MHz, $CDCl_3$): δ = 8.26-8.29 (d, *J* = 8.1 Hz, 2H), 7.54-7.56 (d, *J* = 8.1 Hz, 2H), 5.61 (s, 1H), 5.45 (s, 1H); ^{13}C NMR (75.5 MHz, $CDCl_3$): δ = 147.9, 143.4 (d, *J* = 17 Hz), 127.0 (d, *J* = 7.3 Hz), 123.8, 82.9 (d, *J* = 170 Hz); ^{19}F NMR(292 MHz, $CDCl_3$): δ = -215.7.

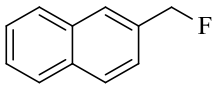

2-(fluoromethyl)naphthalene (177). ^{1}H NMR (300 MHz, $CDCl_3$): δ = 7.89-7.94 (m, 4H), 7.55-7.59 (m, 3H), 5.67 (s, 1H), 5.51 (s, 1H); ^{13}C NMR (75.5 MHz, $CDCl_3$): 133.8, 133.6, 133.4 (d, *J* = 1.9 Hz), 133.2, 128.1, 127.8, 126.8 (d, *J* = 7.5 Hz), 126.5 (d, *J* = 5.7 Hz), 125.0 (d, *J* = 4.5 Hz), δ =84.8 (d, *J* = 199 Hz); ^{19}F NMR(292 MHz, CDCl3): δ = -206.6.

5. References.

[1] Kurti, L.; Czako, B. *Strategic Applications of Named Reactions in Organic Synthesis*; Elsevier academic press: London, 2005.

[2] Yus, M.; González-Gómez, J. C.; Foubelo, F. *Chem. Rev*. **2011**, *111*, 7774.

[3] Denmark, S. E.; Fu, J. *Chem. Rev*. **2003**, *103*, 2763.

[4] Kobayashi, S.; Nishio, K. *J. Org. Chem.***1994**, *59*, 6620.

[5] Zimmerman, H. E.; Traxler, M. D. *J. Am. Chem. Soc*, **1957**, *79*, 1920.

[6] Denmark, S. E.; Coe, D. M.; Pratt, N.E.; Griedel, B. D. *J. Org. Chem*. **1994**, *59*, 6161.

[7] Rowlands, G. J.; Barnes, W. K. *Chem. Commun*., **2003**, 2712.

[8] Takeuchi, K.; Takeda, T.; Fujimoto, T.; Yamamoto, I. *Tetrahedron*, 2007, 63, 5319.

[9] A. Hosomi, H. Sakurai, *Tetrahedron Lett*. **1976**, *17*, 1295.

[10] A. Hosomi, H. Sakurai, *J. Am. Chem. Soc.***1977**, *99*, 1673.

[11] A. Hosomi, A. Shirahata, H. Sakurai, *Tetrahedron Lett.***1978**, *19*, 3043.

[12] Fleming, I.; Langley, J. A. *J. Chem. Soc., Perkin Trans. 1* **1981**,1421.

[13] Corey, E. J.; Rohde, J. J.; Fischer, A.; Azimioara, M. D. *Tetrahedron Lett*. **1997**, *38*, 33.

[14] Bottoni, A.; Costa, A. L.; Di Tommaso, D.; Rossi, I.; Tagliavini, E. *J. Am. Chem. Soc.***1997**, *119*, 12131.

[15] Rendler, S.; Oestreich, M. *Synthesis*, **2005**, *11*, 1727.

[16] W. B. Jensen, *Chem. Rev*. **1978**, *78*, 1 .

[17] V. Gutmann, Coord. *Chem. Rev*. **1975**, *15*, 207.

[18] Denmark, S. E.; Beutner, G. L. *Angew. Chem., Int. Ed.* **2008**, *47*, 1560.

[19] Furuta, K.; Mouri, M.; Yamamoto, H. *Synlett* **1991**, 561.

[20] Yanagisawa, A.; Kageyama, H.; Nakatsuka, Y.; Asakawa, K.; Matsumoto, Y.; Yamamoto, H. *Angew. Chem. Int. Ed.* **1999**, *38*, 3701.

[21] Jiménez-González, L.; García-Muñoz, S; Álvarez-Corral, M.; Muñoz-Dorado, M.; Rodríguez- García, I. *Chem. Eur. J.* **2006**, *12*, 8762.

[22] Maki, K; Motodi, R.; Fujii, K.; Kanai, M.; Kobayashi, T.; Tamura, S.; Shibasaki, M. *J. Am. Chem. Soc.* **2005**, *127*, 17111.

[23] Hrdina, R.; Valterova, I; Hodacova, J.; Cisarova, I.; Kotora, M. *Adv. Synth. Catal*. **2007**, *349*, 822.

[24] Haddad, T. D.; Hirayama, L. C.; Singaram, B. *J. Org. Chem.* **2010**, *75*, 642.

[25] Shen, Z. –L.; Wang, S. –Y; Chok, Y. –K; Xu, Y. –K; Loh, T. –P. *Chem. Rev.* **2013**, *113*, 271.

[26] Araki, S.; Ito, H.; Butsugan, Y. J. *Org. Chem*. **1988**, *53*, 1831.

[27] Loh, T.-P.; Zhou, J.-R.; Yin, Z. *Org. Lett*. **1999**, *1*, 1855.

[28] Hirayama, L.C.;Gamsey, S.;Knueppel,D.;DeLaTorre,K.; Steiner, D.; Singaram, B. *Tetrahedron Lett.* **2005**, *46*, 2315.

[29] Blaser, M. J. *Clin. Infect. Dis*. **1992**, *15*, 386.

[30] Bava, A.; Clericuzio, M.; Giannini, G.; Malpezzi, L.; Meille, S. V.; Nasini, G. *Eur. J. Org. Chem.* **2005**, *11*, 2292.

[31] Radcliff, F. J.; Fraser, J. D.; Wilson, Z. E.; Heapy, A. M.; Robinson, J. E.; Bryant, C. J.; Flowers, C. L.; Brimble, M. A. *Bioorg. Med. Chem.* **2008**, *16*, 6179.

[32] Tianpanich, K.; Prachya, S.; Wiyakrutta, S.; Mahidol, C.; Ruchirawat, S.; Kittakoop, P. *J. Nat. Prod.* **2011**, *74*, 79.

[33] Robinson, J. E.; Brimble, M. A. *Chem. Commun.***2005**, 1560.

[34] Nannei, R.; Dallavalle, S.; Merlini, L.; Bava, A.; Nasini, G. *J. Org. Chem.* **2006**, *71*, 6277.

[35] Arnone, A.; Assante, G.; Nasini, G.; Depava, O. V. *Phytochemistry* **1990**, *29*, 613.

[36] Xiong, N.; Huang, J.; Chen, C.; Zhao, Y.; Zhang, Z.; Jia, M.; Zhang, Z.; Hou, L.; Yang, H.; Cao, X.; Liang, Z.; Zhang, Y.; Sun, S.; Lin, Z.; Wang, T. *Neurobiol Aging* **2012**, *33*, 1777.

[37] Ohkuma, T.; Kitamura, M.; Noyori, R. *Tetrahedron Lett.***1990**, *31*, 5509.

[38] Soai, K.; Hori, H.; Kawahara, M. *Tetrahedron: Asymmetry*, **1991**, *2*, 253.

[39] Ramachandran, P. V.; Chen, G.-M.; Brown, H. C. *Tetrahedron lett*. **1996**, *37*, 2205.

[40] Phan, D. H. T.; Kim, B.; Dong, V. M., *J. Am. Chem. Soc*. **2009**, *131*, 15608.

[41] Loh, T.-P.; Hu, Q.-Y. *Org. Lett*. **2001**, *3*, 279.

[42] Smith, A. B., III; Charnley, A. K.; Harada, H.; Beiger, J. J.; Cantin, L.-D.; Kenesky, S.;Hirschmann, R.; Munshi, S.; Olsen, D. B.; Stahlhut, M. W.; Schleifb, W. A.; Kuo,L. C. *Bioorg. Med. Chem. Lett*. **2006**, 16, 859.

[43] Kesavan, S.; Panek, J. S.; Porco, J. A., Jr. *Org. Lett*. **2007**, *9*, 5203.

[44] Mark Froimowitz, M.;Wu, K.-M.; Moussa, A.; Haidar, R. M.; Jurayj, J.; George, C.;Gardner, E. *J. Med. Chem*. **2000**, *43*,4981.

[45] Gai, X.; Grigg, R.; Collard, S.; Muir, J. E.*Chem. Commun*., **2000**, 1765.

[46] CvengroŠ, J.; Schütte, J.; Schlörer, N.; Neudörfl, J.; Schmalz, H.-G.*Angew. Chem*. **2009**, *121*, 6264.

[47] Schütte, J.; Ye, S.; Schmalz, H.-G. *Synlett* **2011**,*18*, 2725.

[48] Glorius, F; *N-Heterocyclic Carbenes in Transition Metal Catalysis*; Springer-Verlag Berlin Heidelberg, 2007.

[49] Bourissou, D.; Guerret, O.; Gabbai, F. P.; Bertrand, G. *Chem. Rev*. **2000**, *100*, 39.

[50] Doering, W. v. E.; Hoffmann, A. K. *J. Am. Chem. Soc*. **1954**, *76*,6162.

[51] Fischer, E. O.; Maasbòl, A. *Angew. Chem., Int. Ed. Engl*. **1964**, *3*, 580.

[52] Schrock, R. R. *J. Am. Chem. Soc*. **1975**, *97*, 6577.

[53] Tomioka, H. *Acc. Chem. Res*. **1997**, *30*, 315.

[54] Arduengo, A. J.; Harlow, R. L. ; Kline, M.*J. Am. Chem. Soc.* **1991**,*113.*

[55] A. Baceiredo, G. Bertrand, G. Sicard, *J. Am. Chem. Soc.* **1985**,*107*, 4781.

[56] Schmidbaur, H.; Costa, T.; Milewski-Mahrla, B.; Schubert,U.*Angew. Chem. Int. Ed. Engl*. **1980**, *19*, 555.

[57] Marrot, S.; Kato, T.; Gornitzka, H.; Baceiredo, A.*Angew. Chem.* **2006**, *118*, 2660.

[58] Walker, J. D.; Poli, R. *Polyhedron* **1989**, *8*, 1293.

[59] Tonner, R.; Oxler, F.; Neumuller, B.; Petz, W.; Frenking, G. *Angew. Chem. Int. Ed.* **2006**, *45*, 8038.

[60] Breslow, R. *J. Am. Chem. Soc*. **1957**, *79*, 5318.

[61] Yoshida, Z.; Tawara, Y. J. *Am. Chem. Soc*. **1971**, *93*, 2573.

[62] Weiss, R. *Tetrahedron Lett*. **1979**, *35*, 3295.

[63] Weiss, R.; Schloter, K. *Tetrahedron Lett.* **1975**,*16*, 3491.

[64] Weiss. R.; Brenner, T.; Hampel, F.; Wolski, A. *Angew. Chem. Int. Ed. Engel*. **1995**, *34*, 439.

[65] Lavallo, V.; Canac, Y,; Donnadieu, B,; Schoeller, W. W. ; Bertrand, G. *Science* **2006,** *312*, 722.

[66] Fùrstner, A.; Alcarazo, M.; Krause, H. *Org. Synth*. **2009**, *86*, 298.

[67] Bruns, H.; Patil, M.; Carreras, J.; Vázquez, A.; Thiel, W.; Goddard, R.; Alcarazo, M. *Angew. Chem. Int. Ed.* **2010**, *49*, 3680.

[68] Kozma, Á.; Gopakumar, G.; Farès, C.; Thiel, W.; Alcarazo, M. *Chem. Eur. J.* **2013**, *19*, 3542.

[69] Ooi, T.; Maruoka, K. *Angew. Chem. Int. Ed.* **2007**, *46*, 4222.

[70] Schwesinger, R.; Link, R.; Thiele, G.; Rotter, H.; Honert, D.; Limbach, H.-H.; Mannle,F.*Angew. Chem. Int. Ed. Engl*. **1991**, *30*, 1372.

[71] Kunetskiy, R. A.; Cisarova, I.; Saman, D.; Lyapkalo, I. M. *Chem. Eur. J.* **2009**, *15*, 9477.

[72] Ma, T.; Fu, X.; Kee, C. W.; Zong, L.; Pan, Y.; Huang, K-W.; Tan, C-H. *J. Am. Chem. Soc*. **2011**, *133*, 2828.

[73] Etesin, U.; Ogbonna, I; Harry, T. *Journal of Biology, Agriculture and Healthcare*, **2013**, *3*, 47.

[74] Shimizu, M.; Hiyama, T. *Angew. Chem., Int. Ed.* **2005**, *44*, 214.

[75] Kirk, K. L. *Org. Proc. Res. Dev*. **2008**, *12*, 305.

[76] O'Hagan, D. *Chem. Soc. Rev*. **2008**, *37*, 308.

[77] Purser, S.; Moore, P. R.; Swallow, S.; Gouverneur, V. *Chem. Soc. Rev*. **2008**, *37*, 320.

[78] Littich, R.; Scott, P. J. H. *Angew. Chem., Int. Ed.* **2012**, *51*, 1106.

[79] Sun, H.; DiMagno, S. G. *Angew. Chem., Int. Ed*. **2006**, *45*, 2720.

[80] Liu, Y.; Chen, C.; Li, H.; Huang, K-W; Tan, J; Weng Z. *Organometallics* **2013**, *32*, 6587.

[81] Kim, K.-Y.; Kim, B. C.; Lee, H. B.; Shin, H. *J. Org. Chem*. **2008**, *73*, 8106.

[82] Landini, D.; Montanari, F.; Rolla, F. *Synthesis*, **1974**, 428.

[83] Cox, D. P.; Terpinski, J.; Lawrynowicz,W. *J. Org. Chem.*, **1984**, *49*, 3216.

[84] Leroy, J.; Herbert, E.; Wakselman, C. *J. Org. Chem*. **1979**, 3406.

[85] Kim, K.-Y.; Kim, B. C.; Lee, H. B.; Shin, H. *J. Org. Chem.* **2008**, 73, 8106.

[86] Makosza, M.; Bujok, K. *Tetrahedron Lett*. **2002**, *43*, 2761.

[87] Landini, D.; Maia, A.; Rampoldi, A. *J. Org. Chem.* **1989**, *54*, 328.

[88] Albanese, D.; Landini, D.; Penso, M. *J. Org. Chem.* **1998**, *63*, 9587.

[89] Pliego, J. R.; Pilo -Veloso, J.; Pilo –Veloso, D. *J. Phys. Chem. B* **2007**, *111*, 1682.

[90] Dong Wook Kim, D. W; Ahn, D-S.; Oh, Y-H.; Lee, S.; Kil, H. S.; Oh, S. J.; Lee, S. J.; Jae Seung Kim, J. S.; Ryu, J. S.; Moon, D. H.; Chi, D. Y. *J. Am. Chem. Soc*. **2006**, *128*, 16394.

[91] Barnett, D. S.; Moquist, P. N.; Schaus, S. E. *Angew. Chem., Int. Ed*. **2009**, *48*, 8679.

[92] Keck, G. E.; Tarbet, K. H.; Geraci, L. S. *J. Am. Chem. Soc*. **1993**, *115*, 8467.

[93] Dounay, A. B.; Overman, L. E. *Chem. Rev*. **2003**, *103*, 2945.

[94] Hirayama, L. C.; Gamsey, S.; Knueppel, D.; Steiner, D.; DeLaTorre, K.; Singaram, B. *Tetrahedron Lett.* **2005**, *46*, 2315.

[95] Yus, M.; Gonzalez-Gomez, J. C.; Foubelo, F. *Chem. Rev.* **2011**, *111*, 7774.

[96] Kargbo, R. B.; Cook, G. R. *Curr. Org. Chem*. **2007**, *11*, 1287.

[97] (a) Asami, M.; Mukaiyama, T. *Chem. Lett.* **1980**, 17. (b) Meyers, A. I.; Hanagan, M. A.; Trefonas, L. M.; Baker, R. J. *Tetrahedron* **1983**, *39*, 1991. (c) Ohkuma, T.; Kitamura, M.; Noyori, R. *Tetrahedron Lett.* **1990**, *31*, 5509. (d) Watanabe, M.; Hashimoto, N.; Araki, S.; Butsugan, Y. *J. Org. Chem.* **1992**, *57*, 742. (e) Zhang, H.; Zhang, S.; Liu, L.; Luo, G.; Duan, W.; Wang, W. *J. Org. Chem.* **2010**, *75*, 368. (f) Phan, D. H. T.; Kim, B.; Dong, V. M. *J. Am. Chem. Soc.* **2009**, *131*, 15608. (g) Huang, X.; Pan, X.; Lee, G.; Chen, C. *Adv. Synth. Catal.* **2011**, *353*, 1949.

[98] Mirabdolbaghi, R.; Dudding, T. *Tetrahedron* **2012**, *68*, 1988.

[99] Rauniyar, V.; Zhai, H.; Hall, D. G. *J. Am. Chem. Soc.* **2008**, *130*, 8481.

[100] Loh, T.; Zhou, J.; Li, X. *Tetrahedron Lett.* **1999**, *40*, 9333.

[101] Jung, G. Combinatorial Chemistry. *Combinatorial Chemistry, Synthesis, Analysis, Screening*; Wiley VCH: Weinheim, Germany, 1999; pp. 1- 34.

[102] Mirabdolbaghi, R.; Dudding, T. *Tetrahedron* **2013**, *69*, 3287.

[103] Tonner, R.; Frenking, G. *Angew. Chem. Int. Ed.* **2007**, *46*, 8695.

[104] Tonner, R.; Frenking, G. *Chem. Eur. J.* **2008**, *14*, 3260.

[105] Tonner, R.; Frenking, G. *Chem. Eur. J.* **2008**, *14*, 3273.

[106] Tonner, R.; Frenking, G. *Pure Appl. Chem.* **2009**, *81*, 597.

[107] Takagi, N.; Shimizu, T.; Frenking, G. *Chem. Eur. J.* **2009**, *15*, 3448.

[108] Takagi, N.; Tonner, R.; Frenking, G. *Chem. Eur. J.* **2012**, *18*, 1772.

[109] Mondal, K. C.; Roesky, H. W.; Schwarzer, M. C.; Frenking, G.; Niepötter, B.; Wolf, H.; Herbst-Irmer, R.; Stalke, D.; *Angew. Chem. Int. Ed.* **2013**, *52*, 2963.

[110] Himmel, D.; Krossing, I.; Schnepf, A. *Angew. Chem. Int. Ed.* **2013**, *52*, 2.

[111] Kozma, Á.; Gopakumar, G.; Farès, C.; Thiel, W.; Alcarazo, M. *Chem. Eur. J.* **2013**, *19*, 3542.

[112] Bruns, H.; Patil, M.; Carreras, J.; Vázquez, A.; Thiel, W.; Goddard, R.; Alcarazo, M. *Angew. Chem., Int. Ed.* **2010**, *49*, 3680.

[113] Celik, A.; Sure, M. R.; Klein, S.; Rei Kinjo, R.; Bertrand, G.; Frenking, G. *Chem. Eur. J.* **2012**, *18*, 5676.

[114] Bhatia, S.; Malkhede, Y. J.; Bharatam, P. V. *J. Comput. Chem.* **2013**, *34*, 1577.

[115] Bhatia, S.; Bagul, C.; Kasetti, Y.; Patel, D. S.; Bharatam, P. V. *J. Phys. Chem. A* **2012**, *116*, 9071.

[116] Patel, D. S.; Bharatam, P. V. *Chem. Commun.* **2009**, 1064.

[117] Patel, D. S.; Bharatam, P. V. *J. Phys. Chem. A* **2011**, *115*, 7645.

[118] Mirabdolbaghi, R.; Dudding, T.; Stamatatos, T. *Org. lett*. **2014**, *16*, 2790.

[119] Celik, M. A.; Sure, R.; Klein,S.; Kinjo, R.; Bertrand, G. *Chem. Eur. J.* **2012**, *18*, 5676.

[120] The tetrahedrality for a four-coordinate complex can be determined from the angle subtended by two planes, each encompassing the metal and two adjacent atoms; for strictly square planar complexes with D4h symmetry, the tetrahedrality is 0°; for tetrahedral complexes with D2d symmetry, the tetrahedrality equals 90°.

[121] Becke, A. *The quantum theory of atoms in molecules: from solid state to DNA and drug design.* (Eds.: Matta, C. F.; Boyd, R. J.), Wiley, New York, 2007, pp. 10-15.

[122] Saigo, K.; Kobayashi, Y. *Chem. Rec.* **2007**, *7*, 47.

[123] (a) Muktha, B.; Srinivas, O.; Amresh, M. R.; Row, T. N. G.; Jayaraman, N.; Sekar, K. *Carbohydorate Res.* **2003**, *338*, 2005; (b) Spiwok, V.; Lipovova, P.; Skalova, T.; Buchtelova, E.; Hasek, J.; Kralova, B. *Carbohydrate Res.* **2004**, *339*, 2275; (c) Plevin, M. J.; Bryce, D. L. *J. Boisbouvier, Nat. Chem.* **2010**, *2*, 466.

[124] (a) Kobayashi, K.; Asakawa, Y.; Kato, Y.; Aoyama, Y. *J. Am. Chem. Soc.* **1992**, *114*, 10307; (b) Amabilino, D. B. *et al*., *J. Am. Chem. Soc.* **1995**, *117*, 1271; (c) Lakshminarayanan, P. S.; Kumar D. K.; Ghosh, P. *J. Am. Chem. Soc.* **2006**, *128*, 9600; (d) Yamamoto, Y.; Yamamoto, A.; Furuta, S.; Horie, M.; Kodama, M.; Sato, W.; Akiba, K. Y.; Tsuzuki, S.; Uchimaru, T.; Hashizume D.; Iwasaki, F. *J. Am. Chem. Soc.* **2005**, *127*, 14540.

[125] Anderson, C. D.; Dudding, T.; Gordillo, R.; Houk, K. N. *Org. Lett.* **2008**, *10*, 2749.

[126] Belding, L.; Dudding, T. *Chem. Eur. J.* **2014**, *20*, 1032.

[127] O'Donnel, M. J.; Polt, R. L. *J. Org. Chem.* **1982**, *47*, 2663.

[128] (a) Ooi, T.; Maruoka, K. *Angew. Chem. Int. Ed.* **2007**, *46*, 4222; b) Denmark, S. E.; Gould, N. D.; Wolf, L. M. *J. Org. Chem.* **2011**, *76*, 4260; (c) Denmark, S. E.; Gould, N. D.; Wolf, L. M. *J. Org. Chem.* **2011**, *76*, 4337; (d) Denmark, S. E.; Weintraub, R. C.; Gould, N. D. *J. Am. Chem. Soc.* **2012**, *134*, 13415.

[129] Ge, S.; Chaladaj, W.; Hartwig, J. F. *J. Am. Chem. Soc.* **2014**, *136*, 4149.

[130] Bhadury, P. S.; Pandey, M.; Jaiswal, D. K. J. *Fluorine Chem.* **1995**, *73*, 185.

[131] Napoletano, M.; Norcini, G.; Pellacini, F.; Marchini, F.; Morazzoni, G.; Ferlenga, P.; Pradella, L. *Bioorg. Med. Chem. Lett*. **2001**, *11*, 33.

[132] Wang, J.; Johnson, D. M. *Polym. Int.* **2009**, *58*, 1234.

[133] Knepper, K.; Ziegert, R. E.; Brase, S. *Tetrahedron*, **2004**, *60*, 8591.

[134] Rauniyar, V.; Zhai, H.; Hall, D. G. *J. Am. Chem. Soc.* **2008**, *130*, 8481-8490.

[135] Pedrosa, R.; Sayalero, S.; Vicente, M. *Tetrahedron*, **2006**, *62*, 10400-10407.

[136] Ranu, B.; Dutta, P.; Sarkar, A. *J. Org. Chem.* **1998**, *63*, 6027.

[137] Frisch, M. J.; *et al*. *Gaussian 09*, revision B.01; Gaussian, Inc.: Wallingford, CT, **2009**.

[138] Mirabdolbaghi, R.; Dudding, T. *Org. Lett.* **2012**, *14*, 3748-3751.

[139] Pedrosa, R.; Sayalero, S.; Vicente, M. *Tetrahedron* **2006**, *62*, 10400.

[140] Isobe, T. *J. Org. Chem*. **1999**, *64*, 6984.

[141] Ma, T.; Fu, X.; Kee, C. W.; Zong, L.; Pan, Y.; Huang, K-W.; Tan, C-H. *J. Am. Chem. Soc.* **2011**, *133*, 2828.

[142] Tobey, S. W.; West, R. *J. Am. Chem. Soc.* **1966**, *88*, 2481.

[143] O'Donnel, M. J.; Polt, R. L. *J. Org. Chem.* **1982**, *47*, 2663.

6. Selected Spectra.

^{1}H NMR 149a

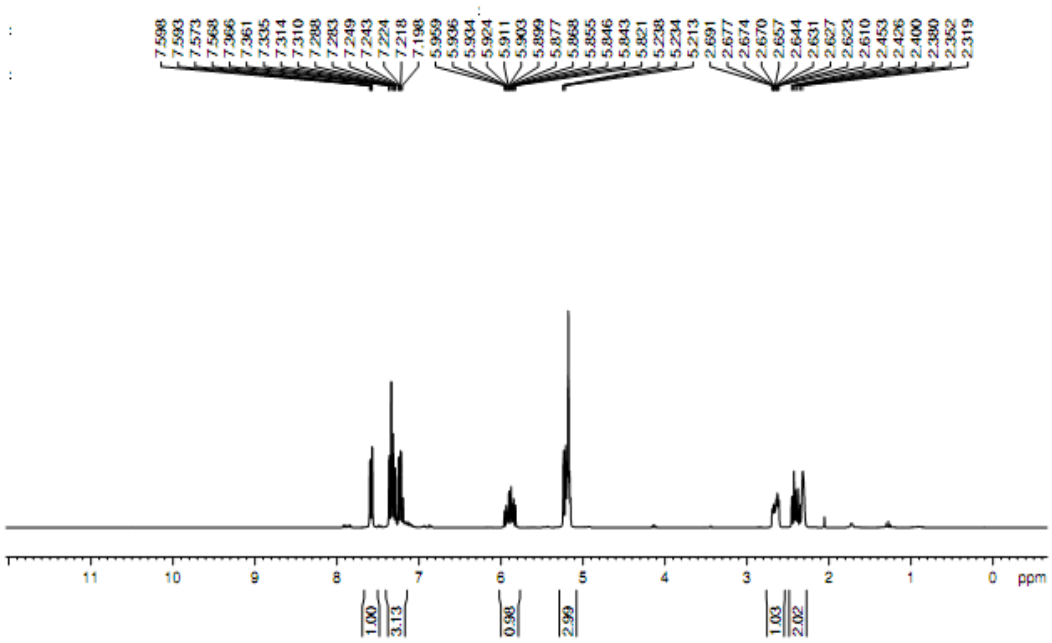

^{13}C NMR 149a

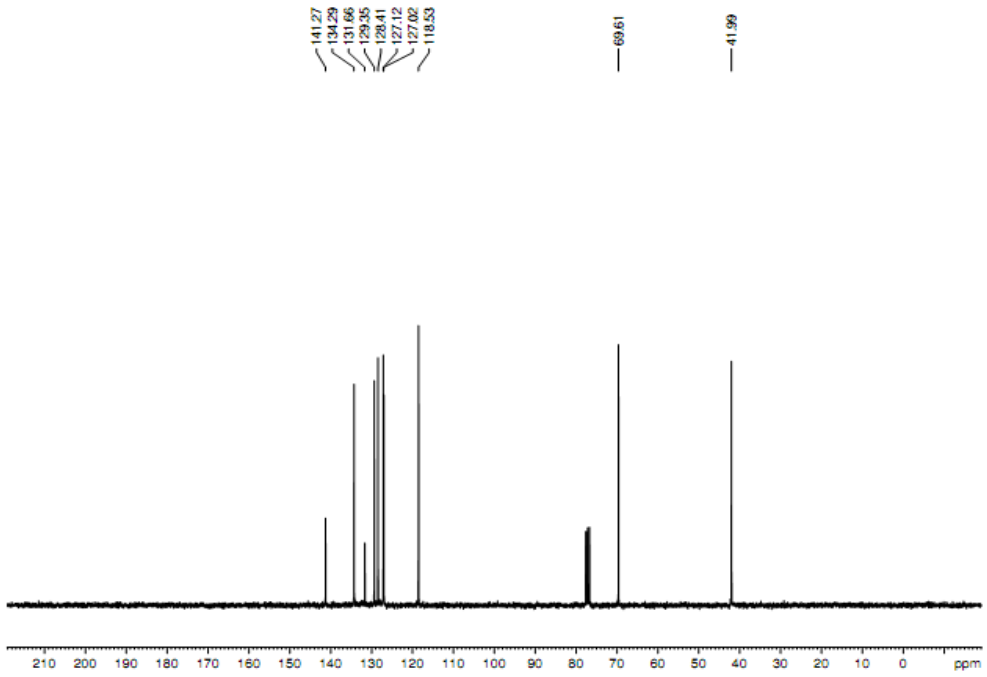

IR 149a

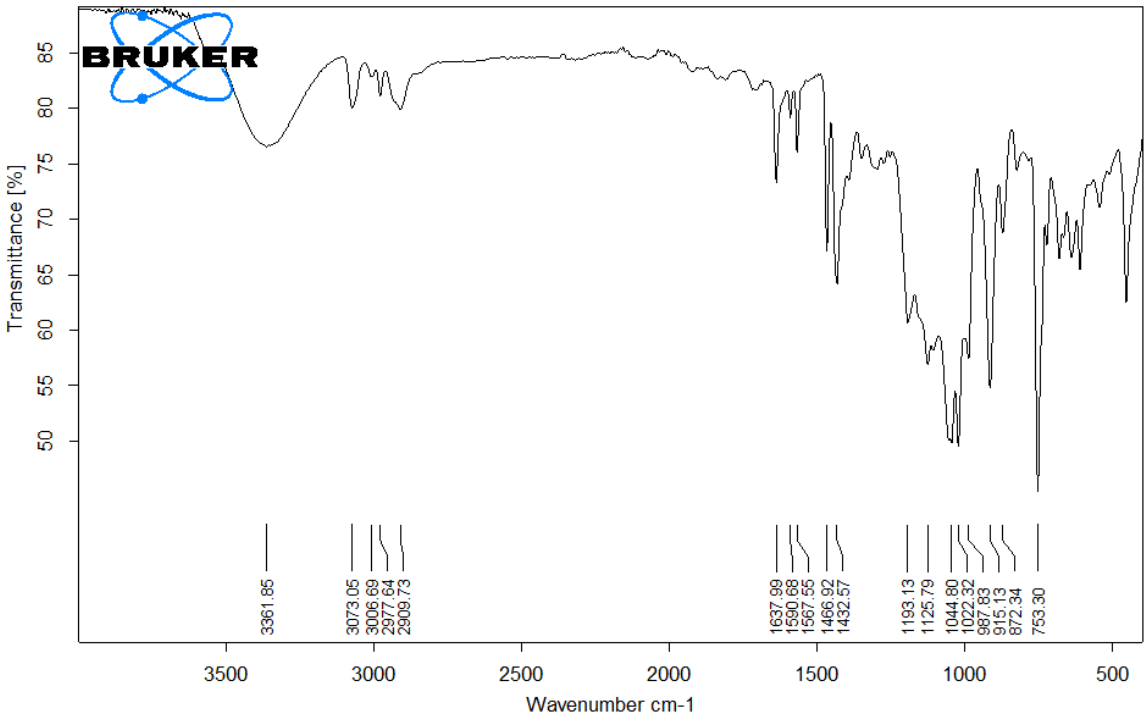

^{1}H NMR 149b

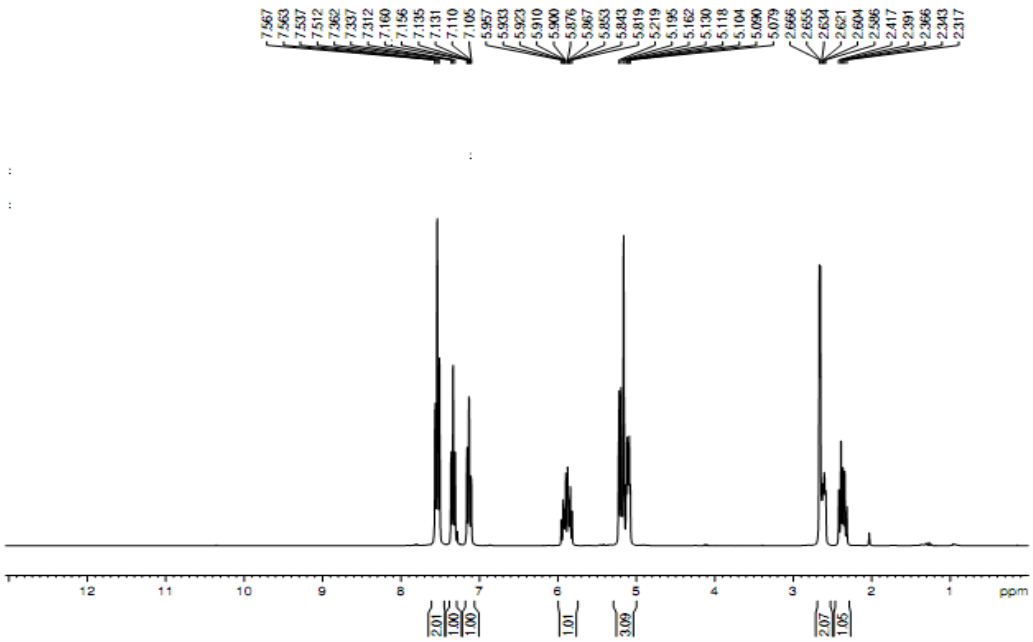

^{13}C NMR 149b

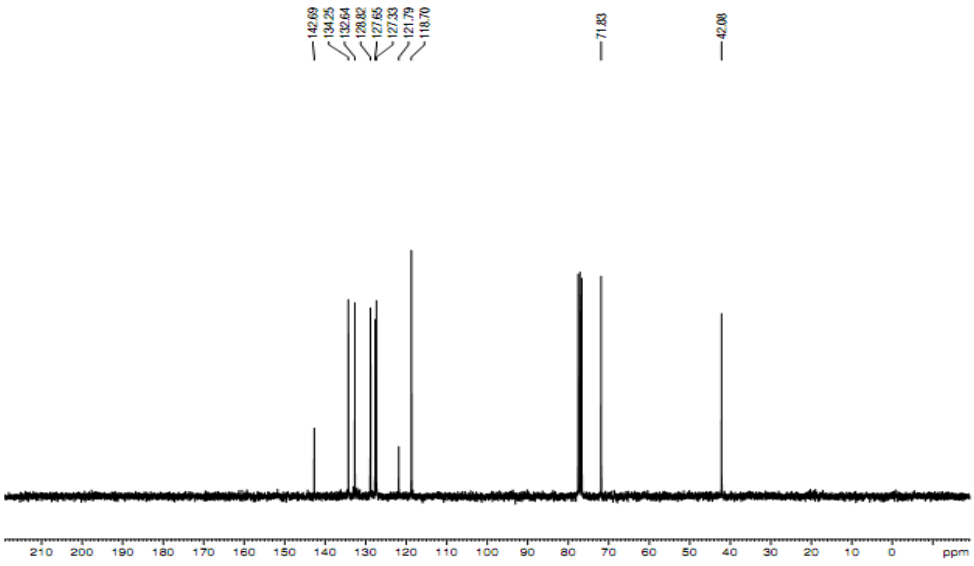

IR 149b

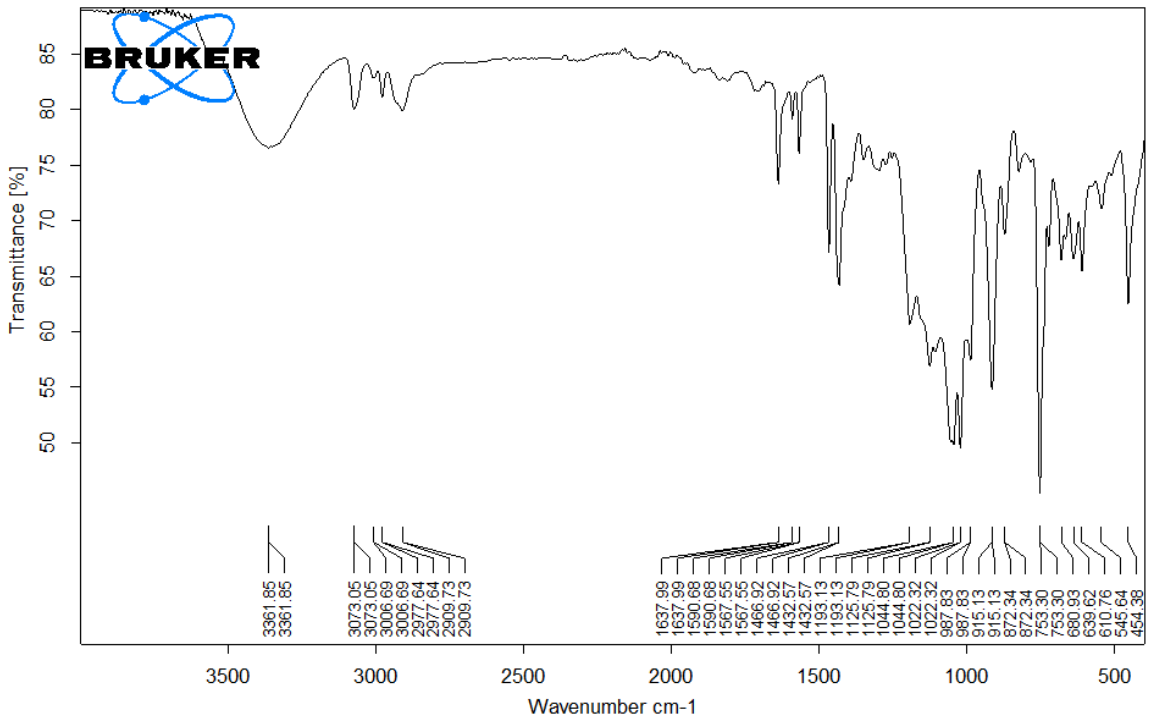

^{1}H NMR 149c

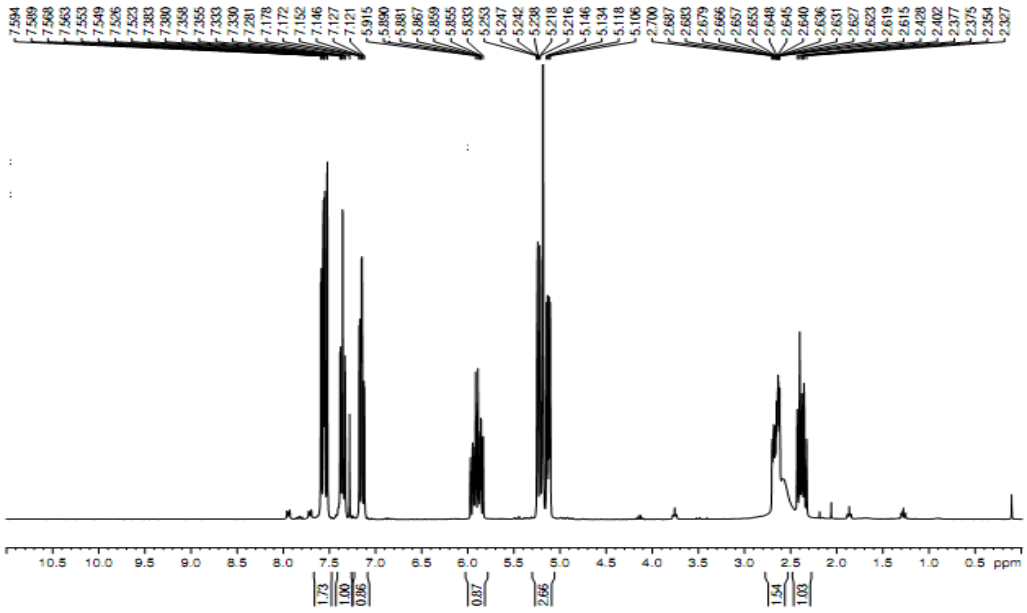

^{13}C NMR 149c

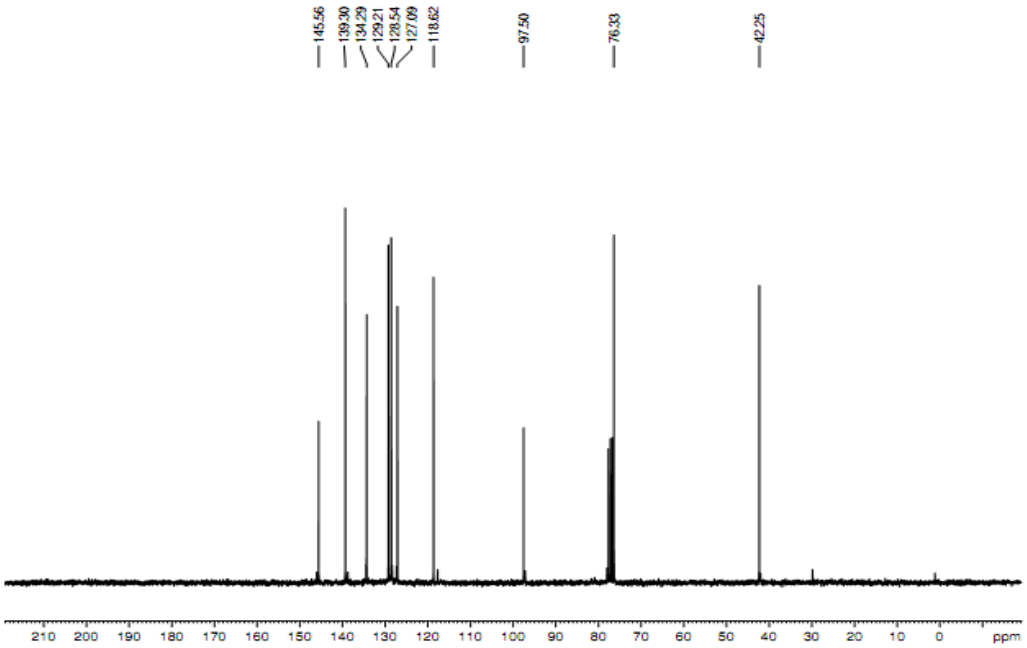

IR 149c

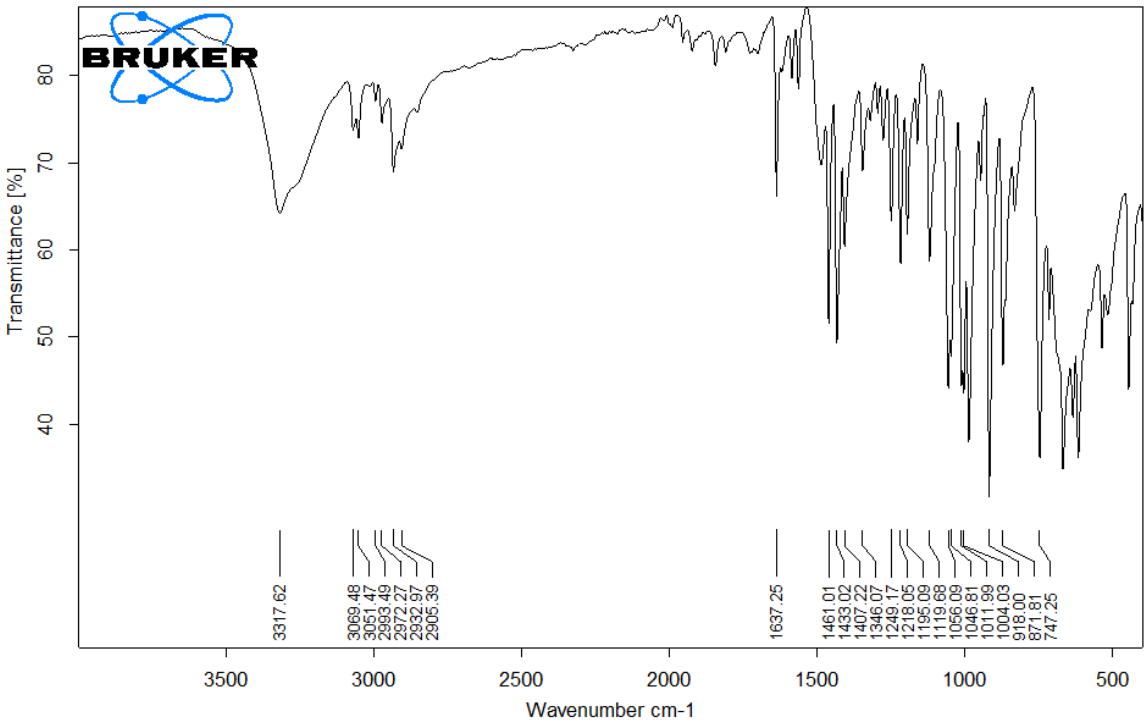

^{1}H NMR 149e

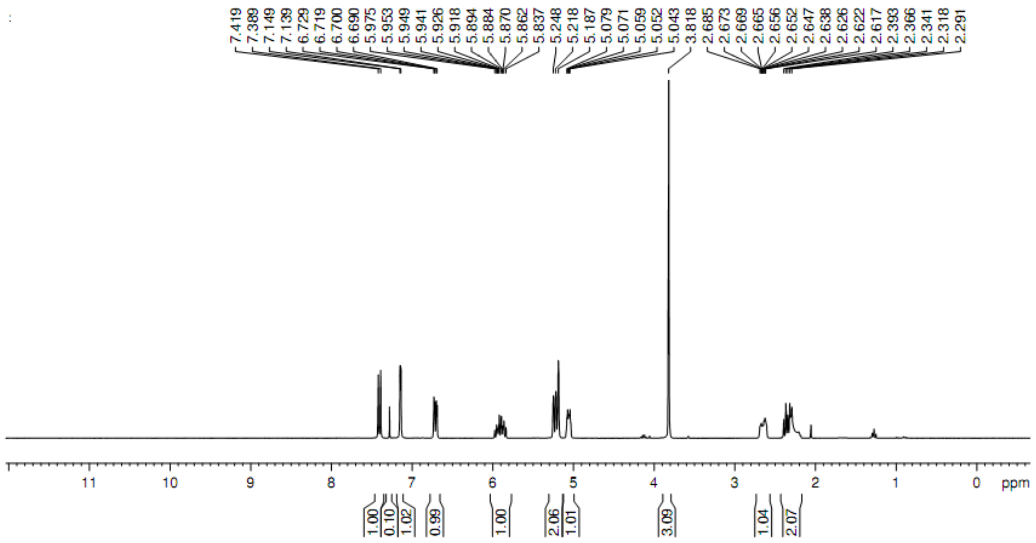

^{13}C NMR 149e

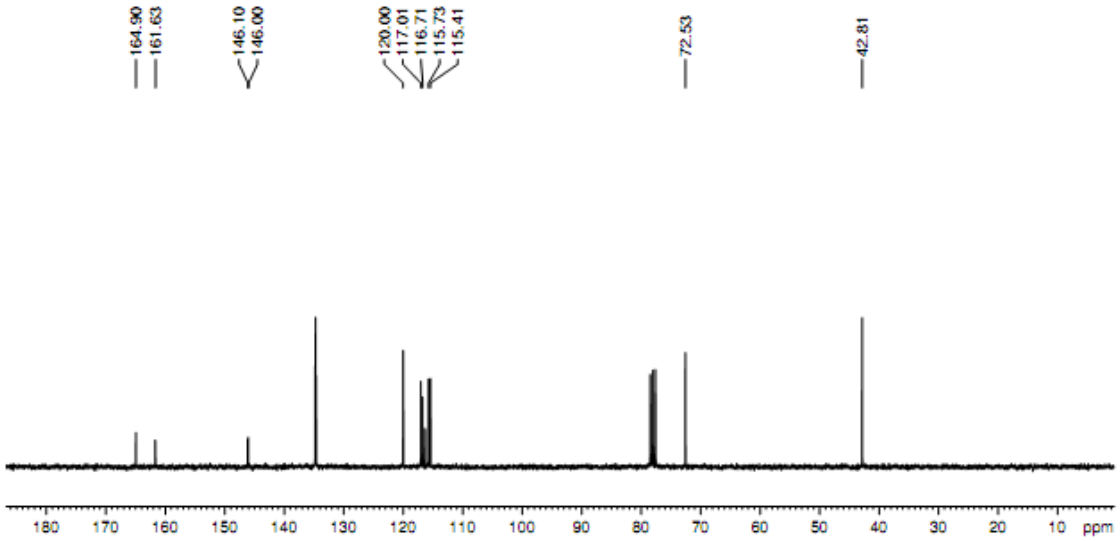

IR 149e

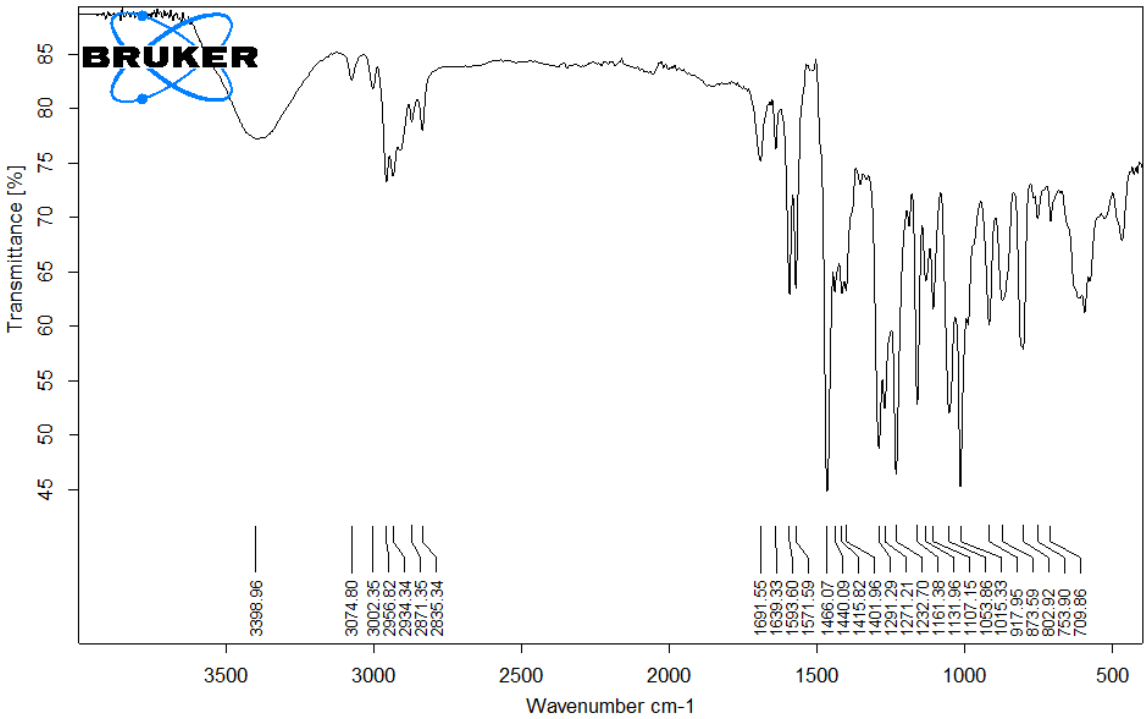

^{1}H NMR 149f

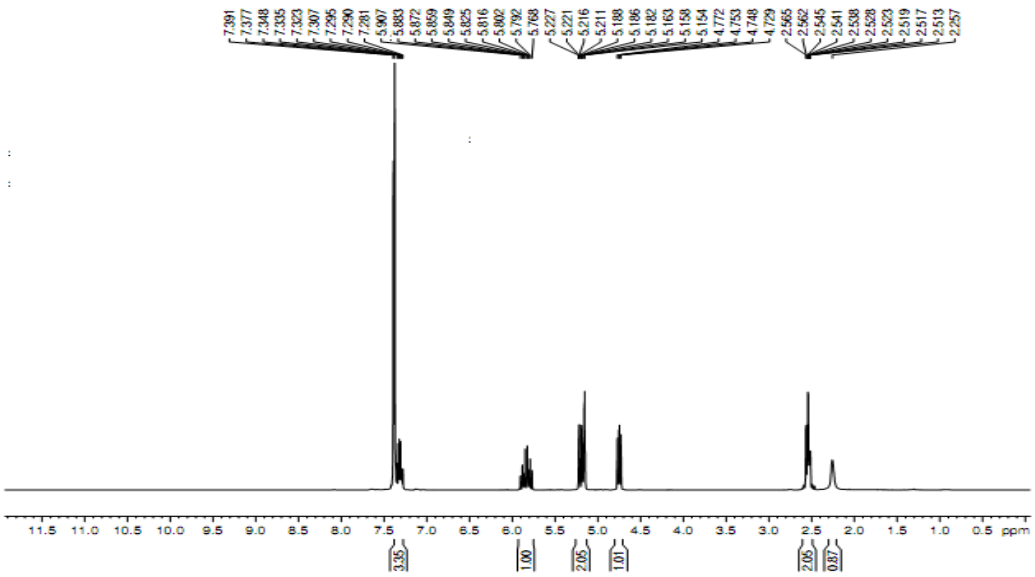

^{13}C NMR 149f

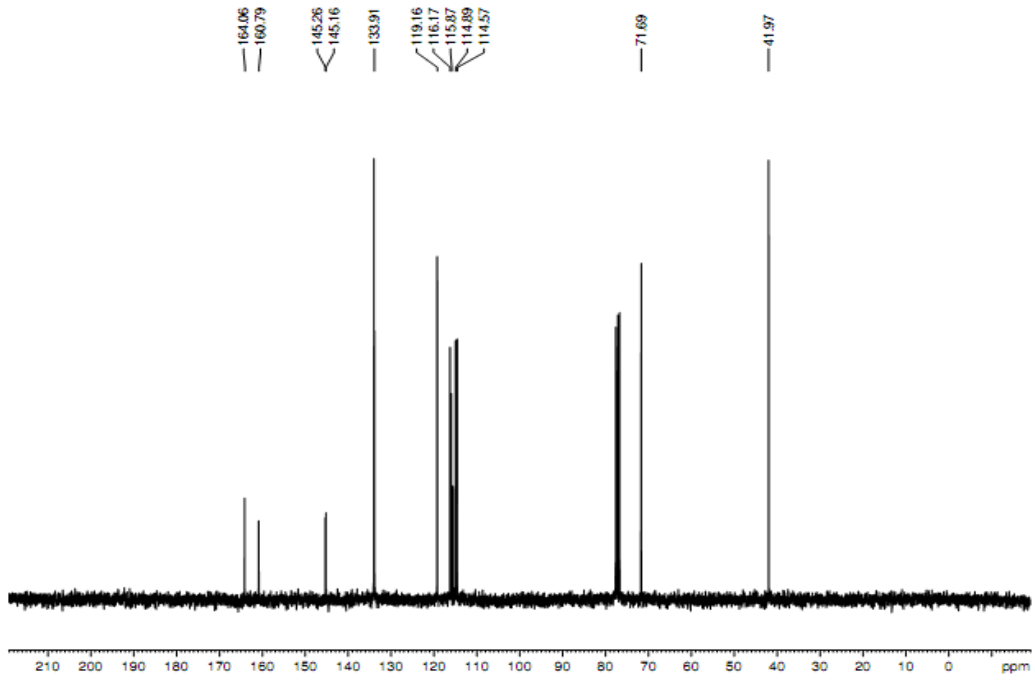

IR 149f

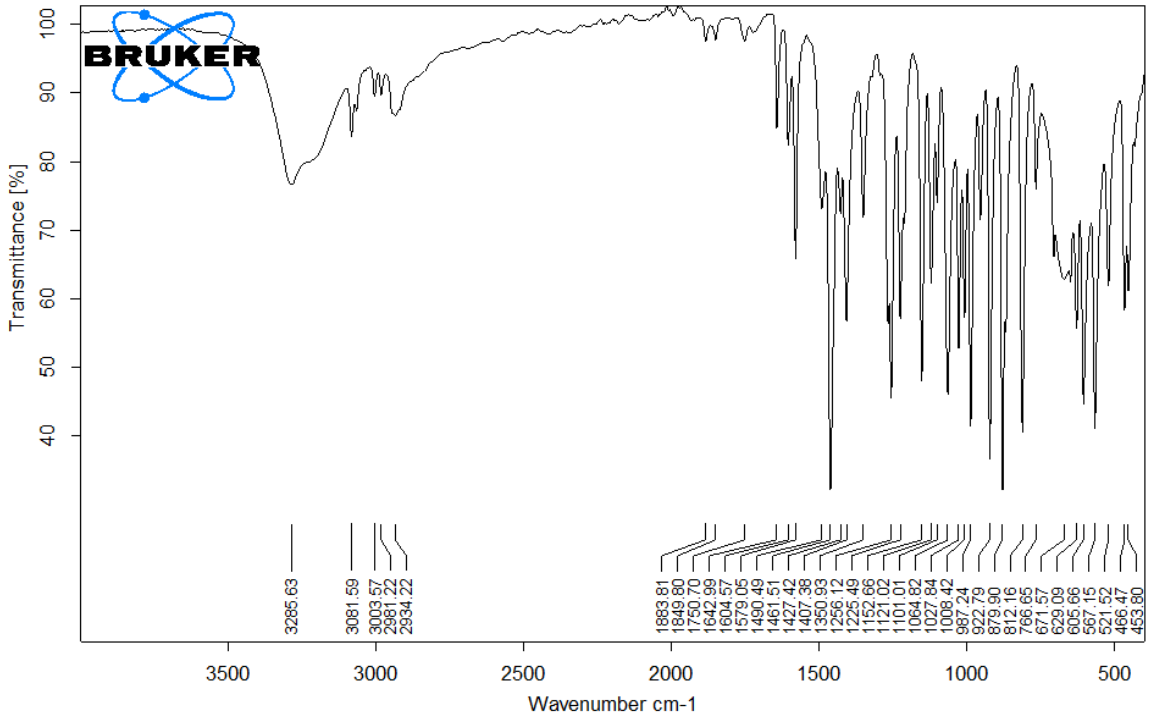

^{1}H NMR 150a

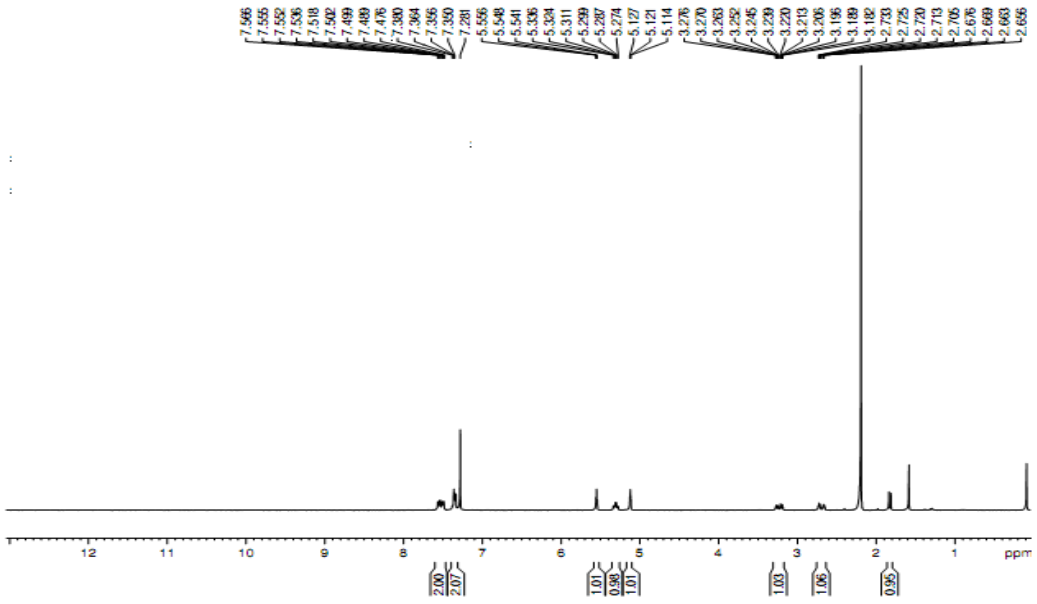

^{13}C NMR 150a

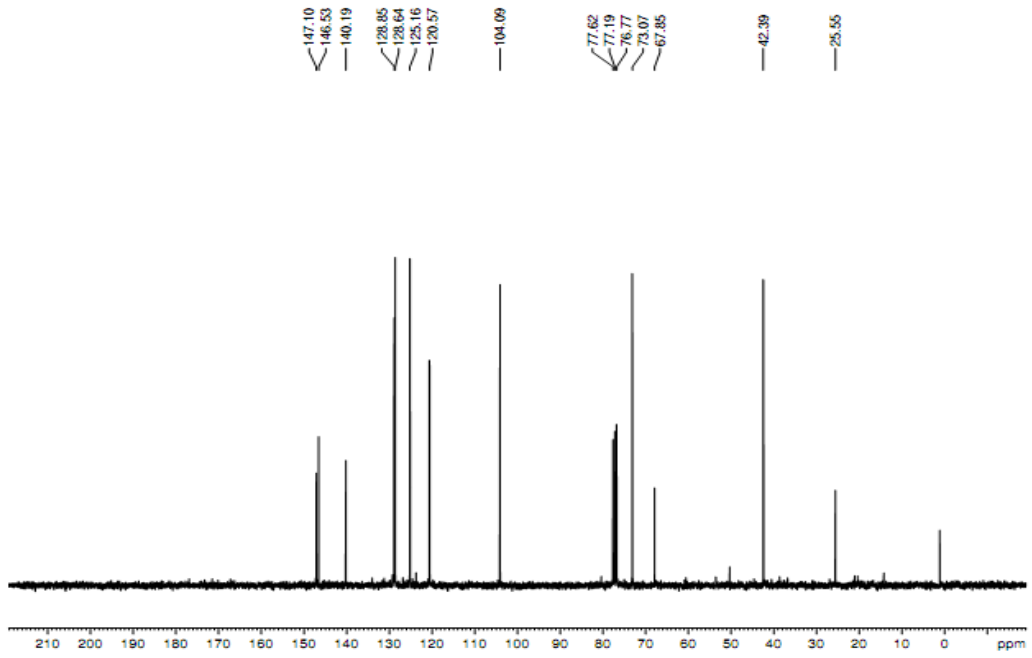

IR 150a

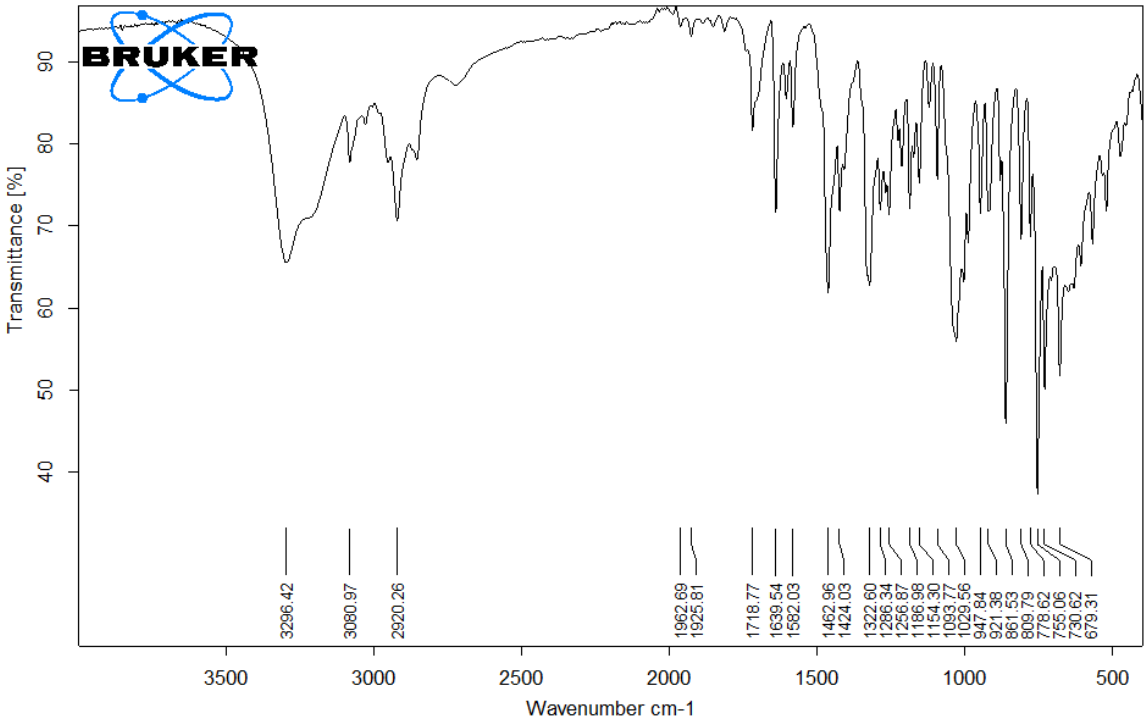

^{1}H NMR 150e

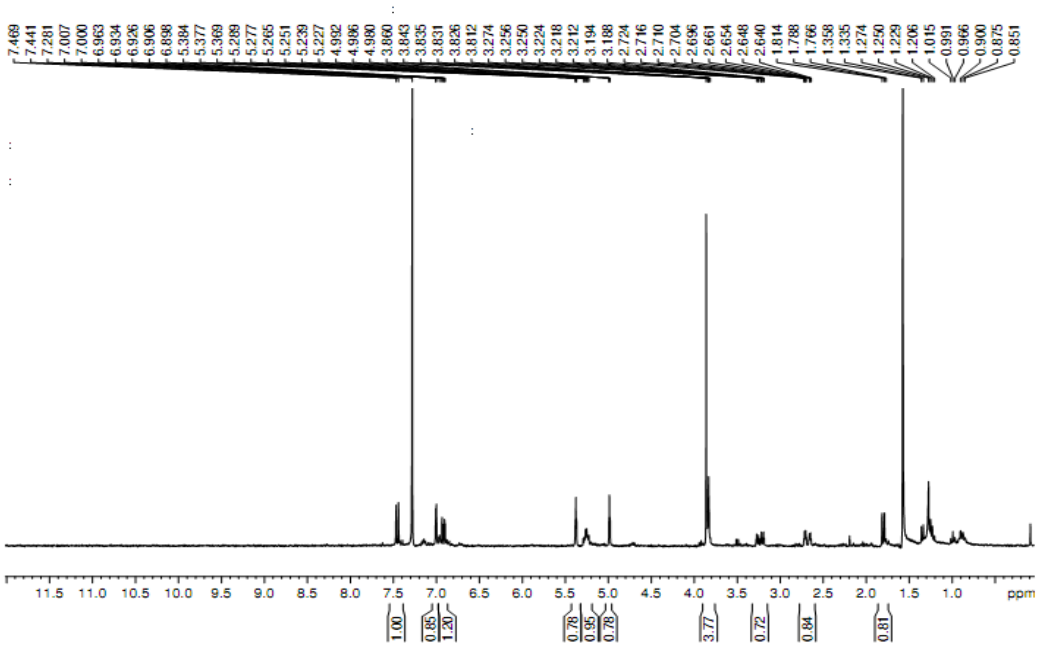

^{13}C NMR 150e

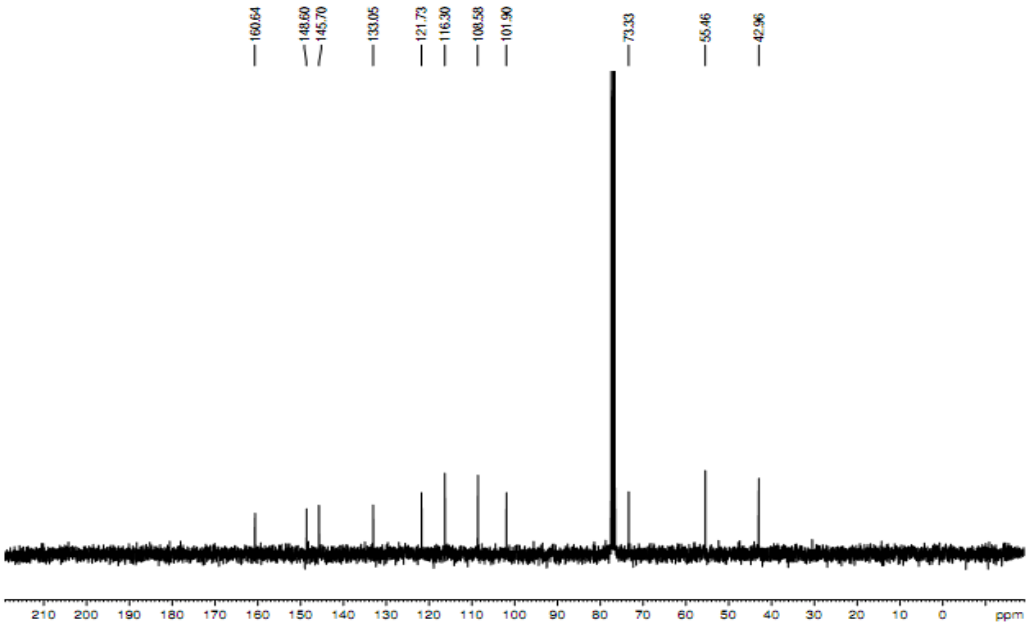

IR 150e

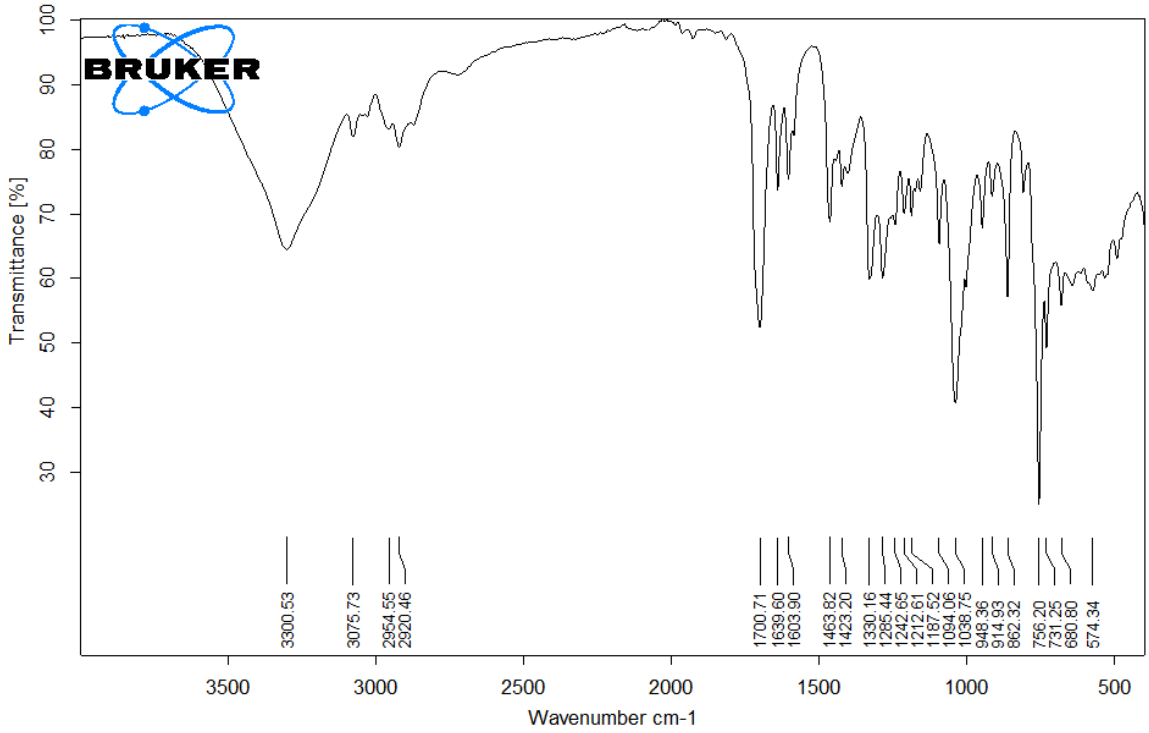

^{1}H NMR 150f

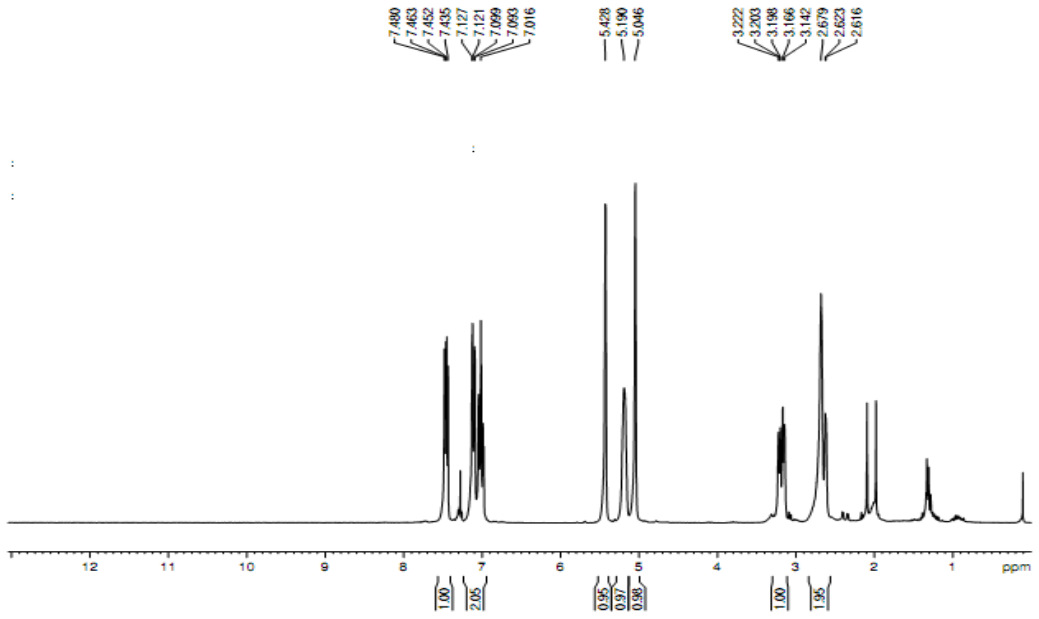

^{13}C NMR 150f

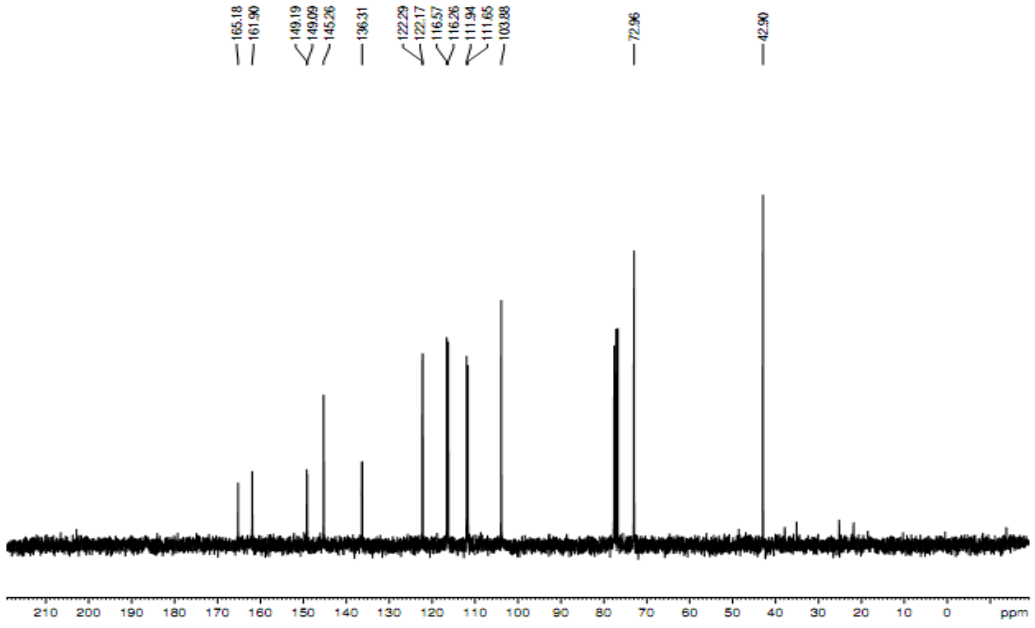

IR 150f

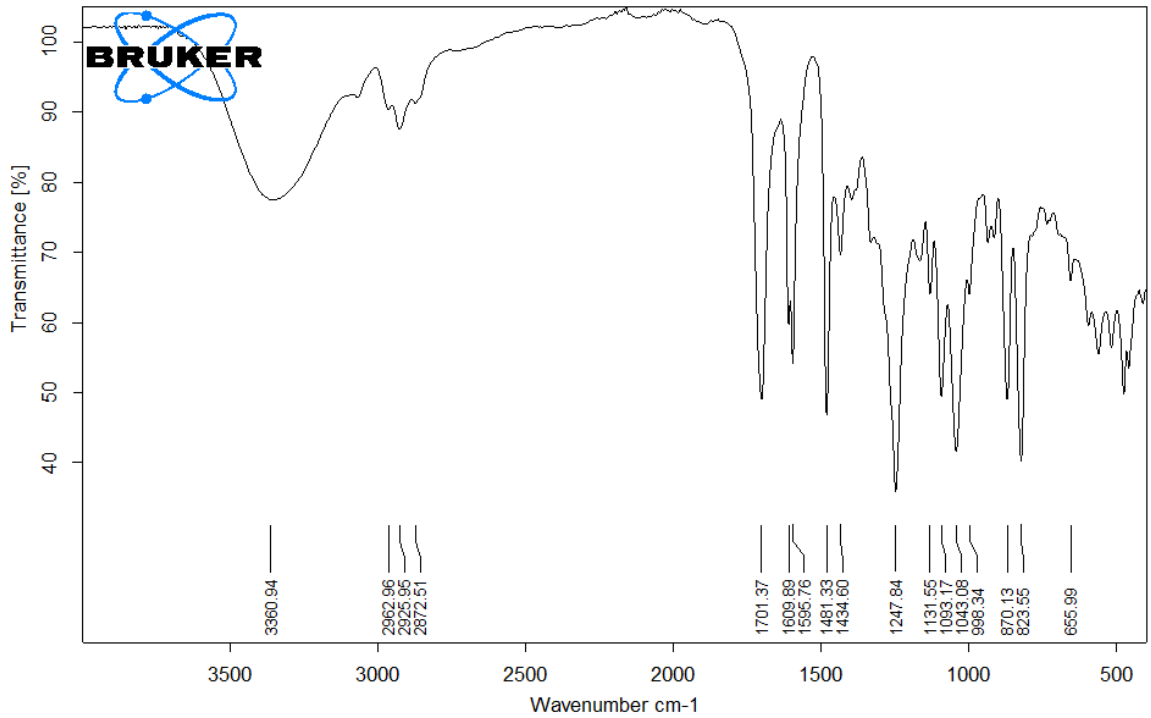

^{1}H NMR 151a

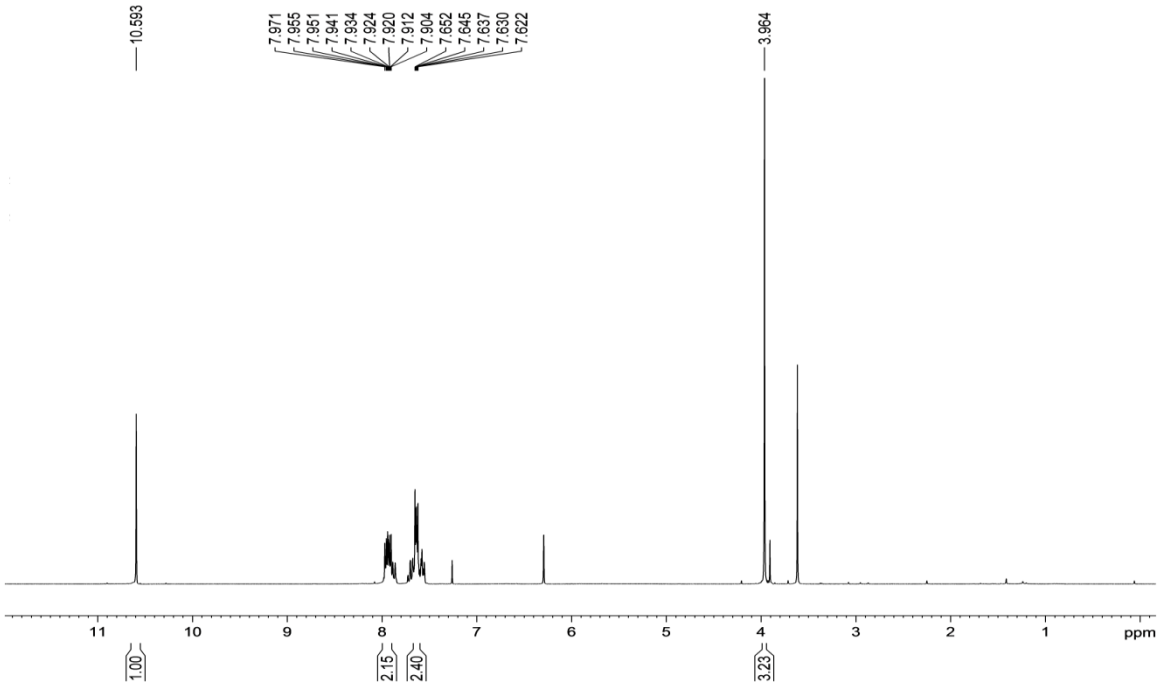

^{13}C NMR 151a

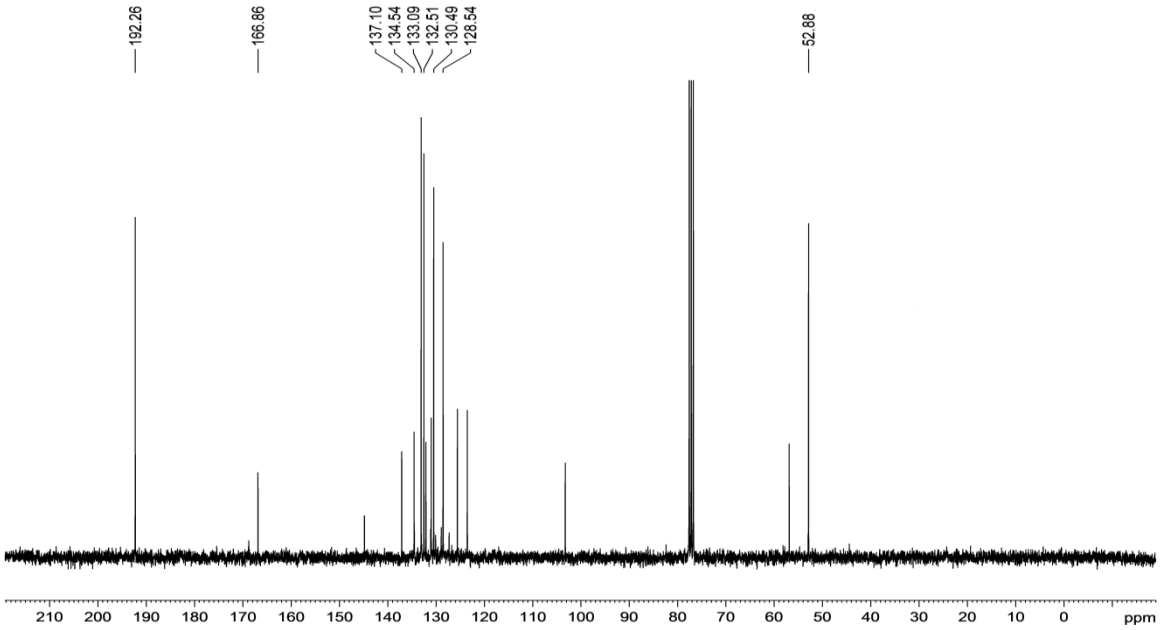

^{1}H NMR 151b

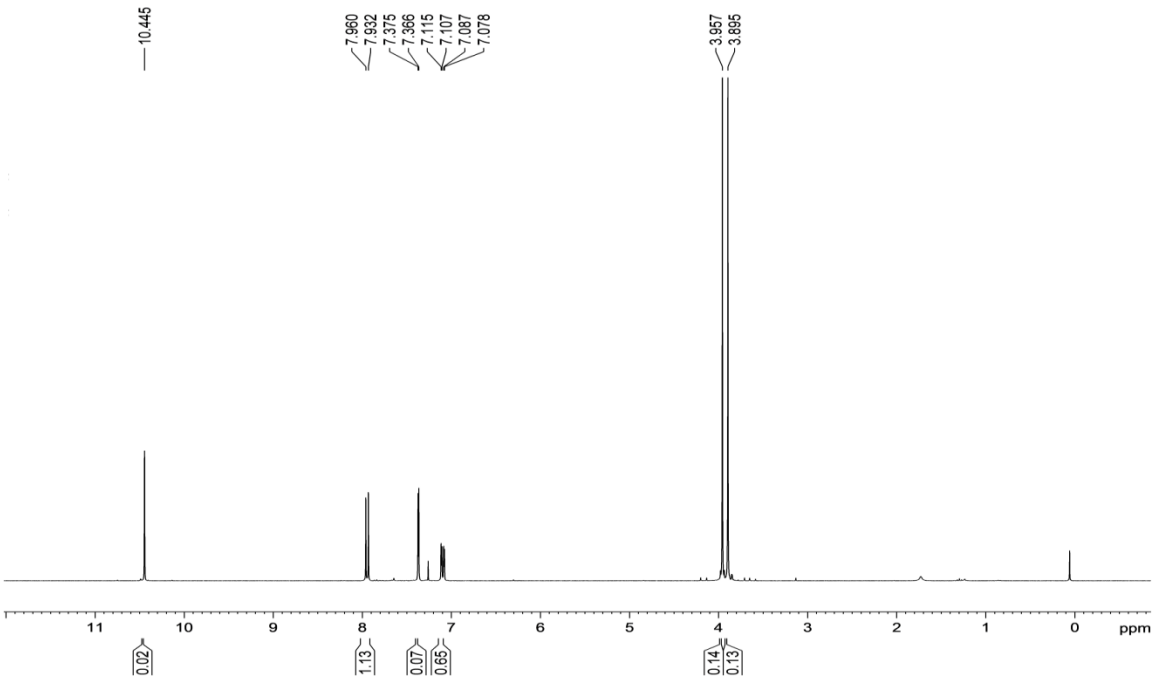

^{13}C NMR 151b

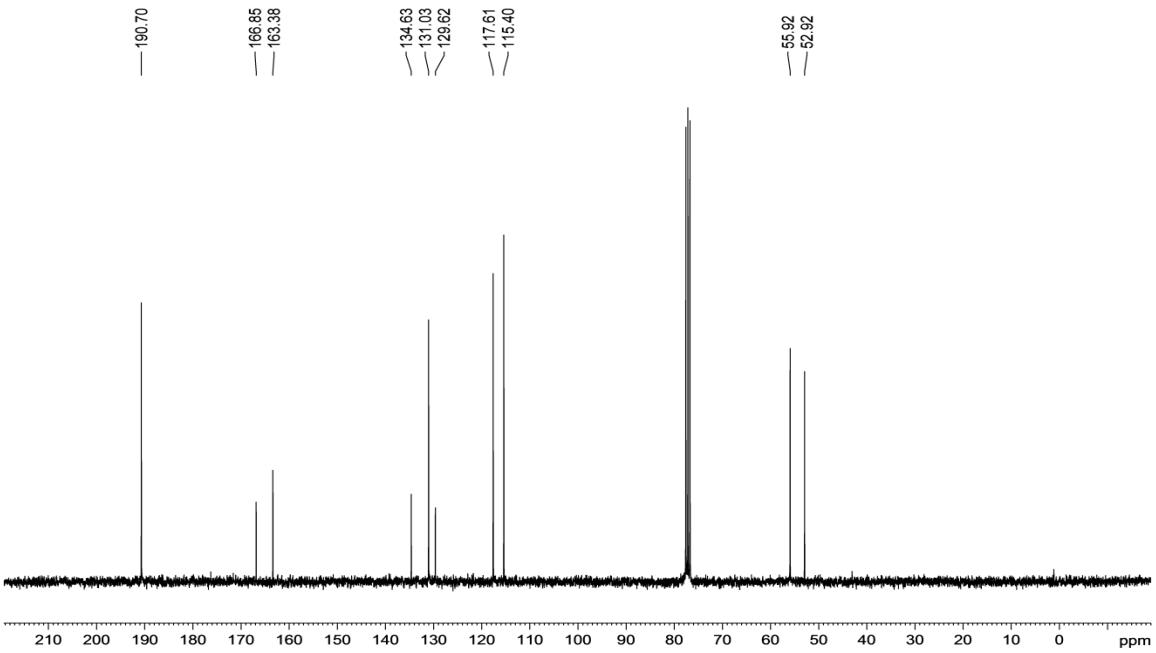

^{1}H NMR 151c

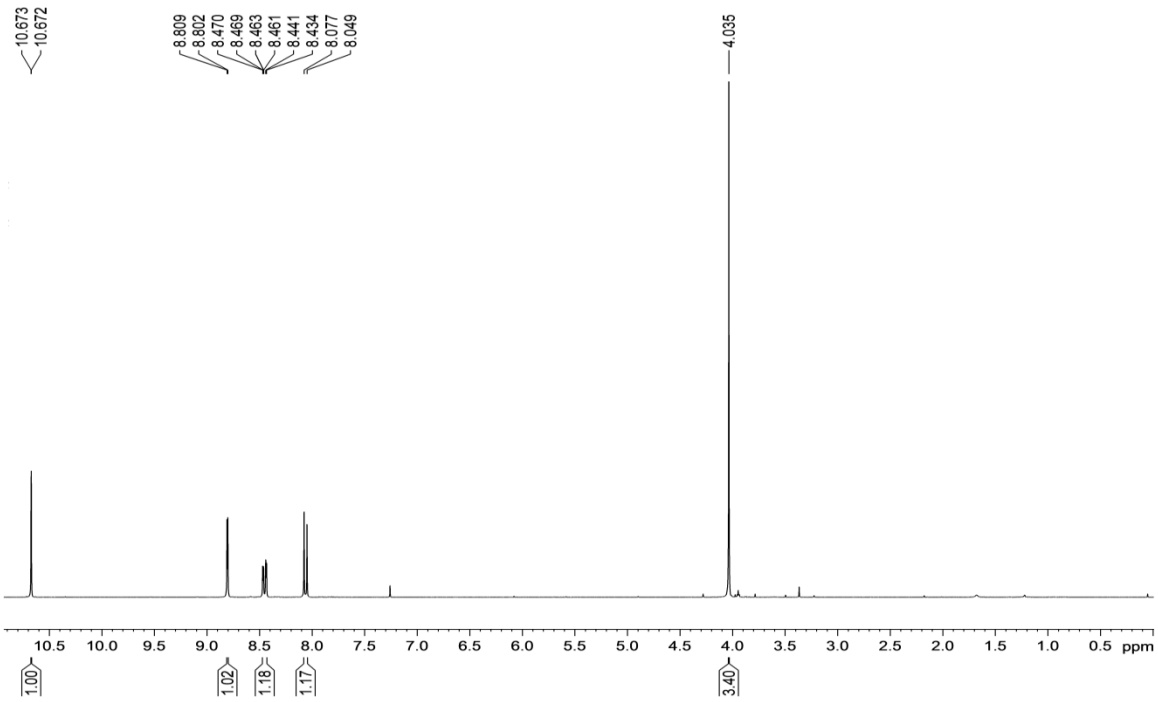

^{13}C NMR 151c

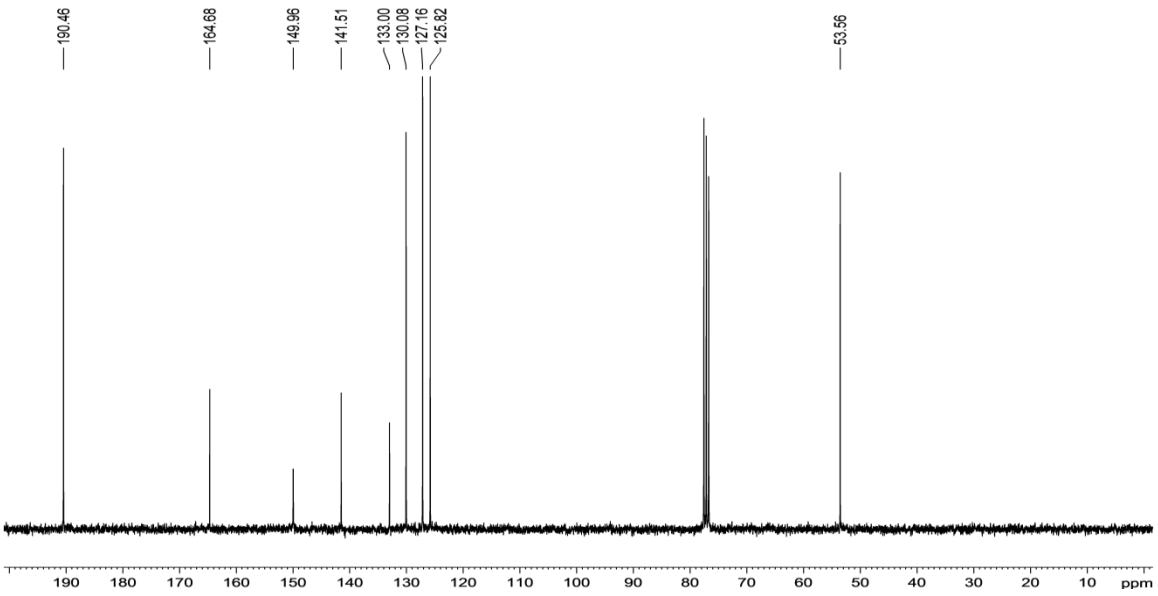

^{1}H NMR 151d

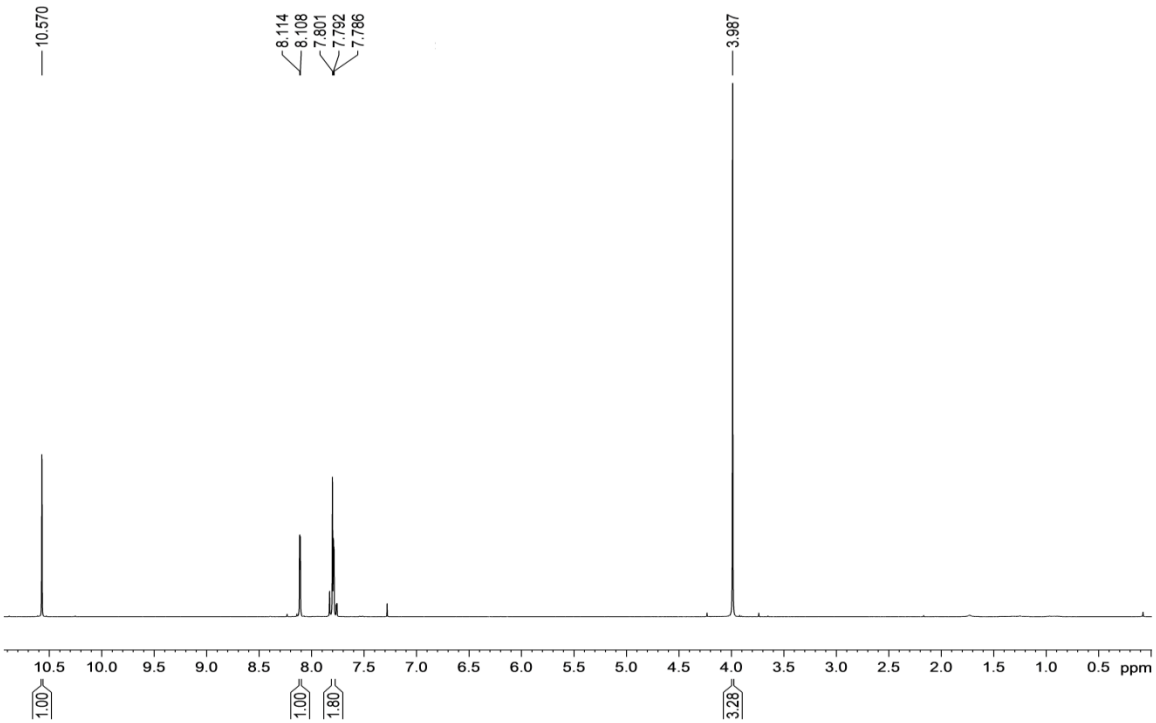

^{13}C NMR 151d

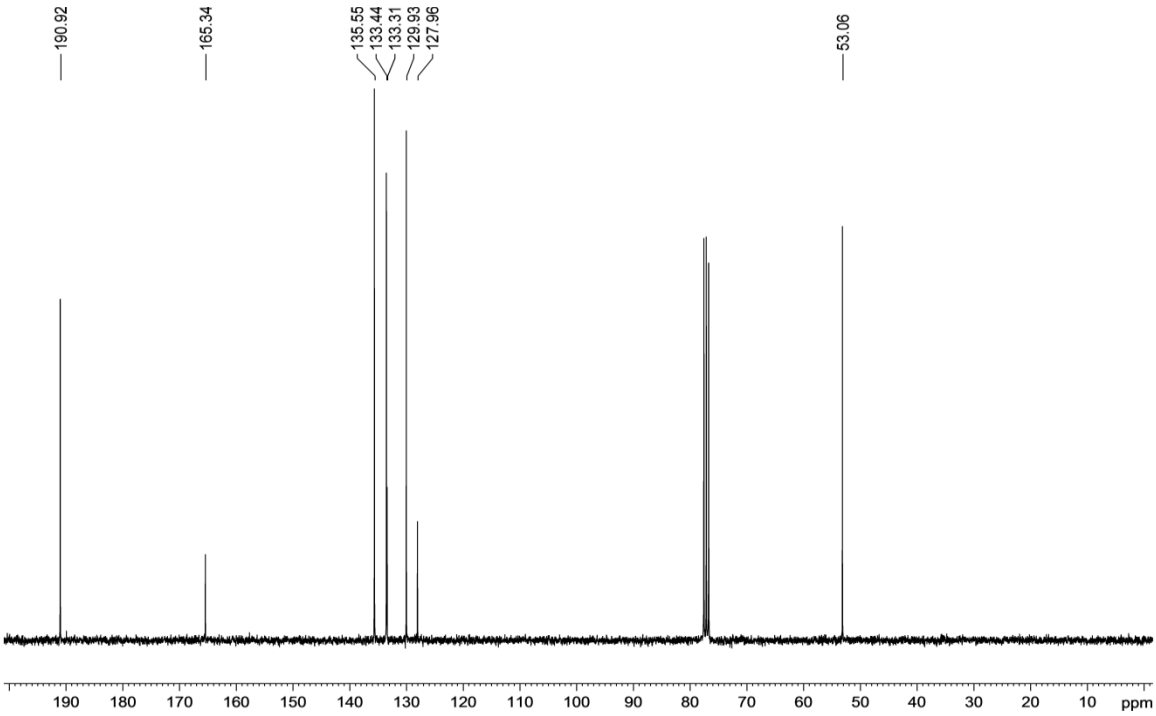

^{1}H NMR 151e

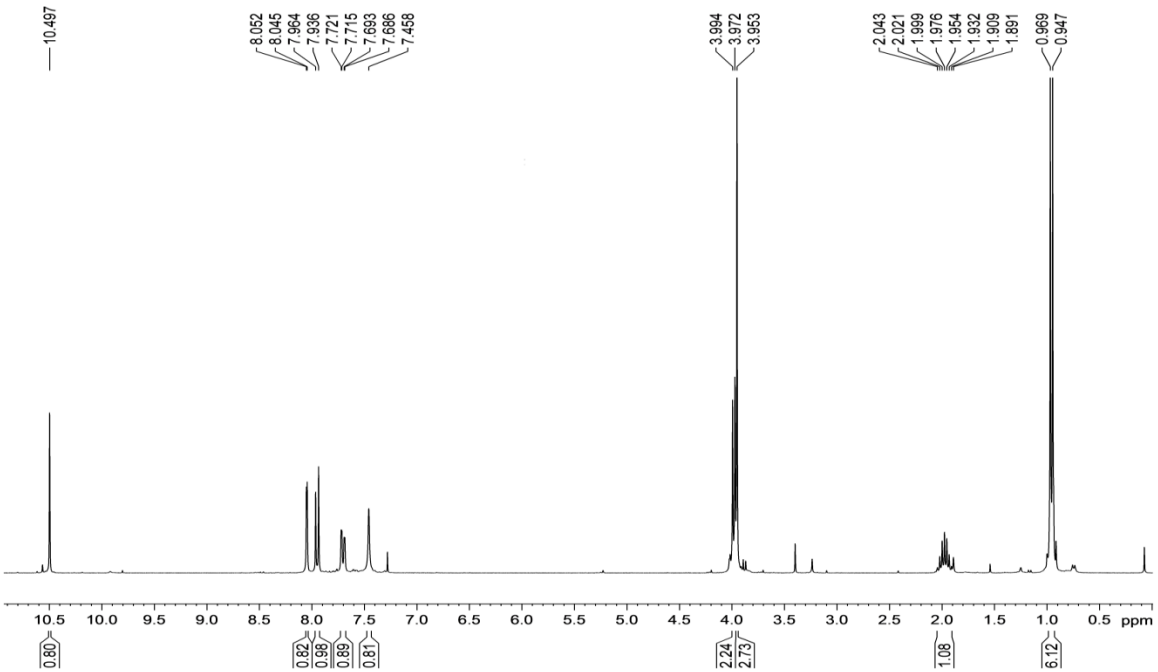

^{13}C NMR 151e

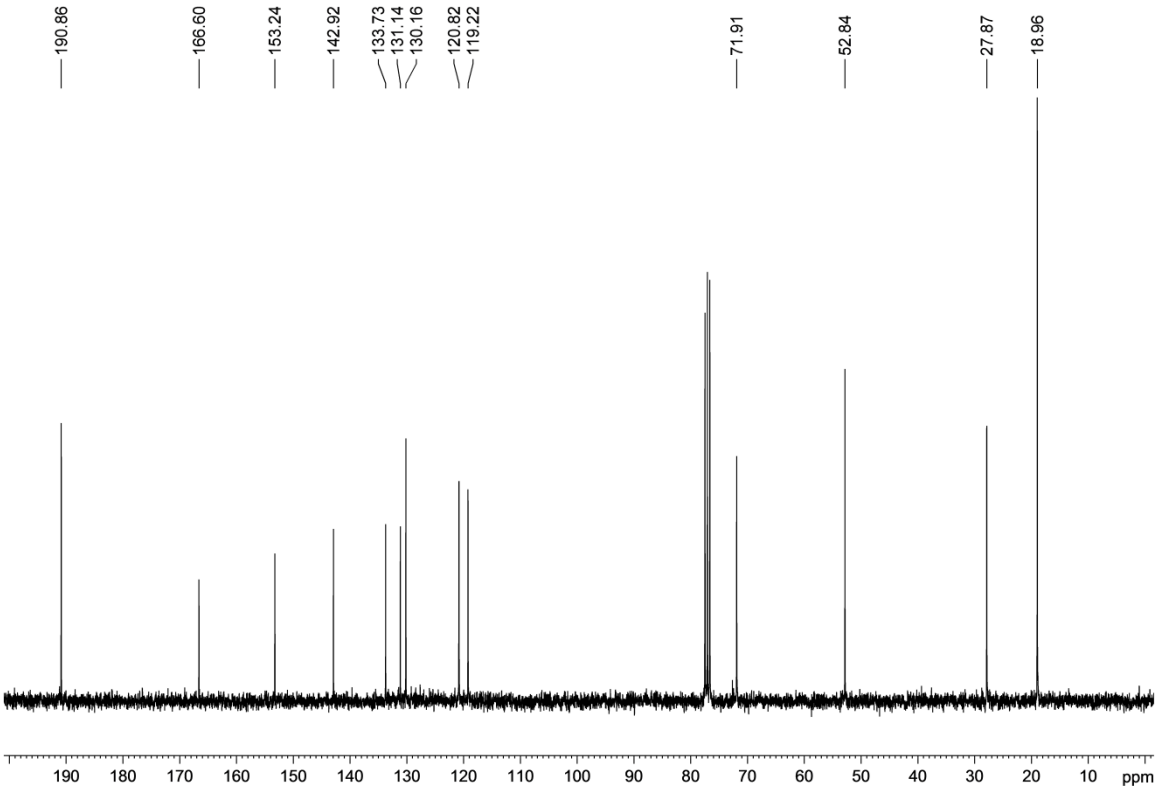

^{1}H NMR 151f

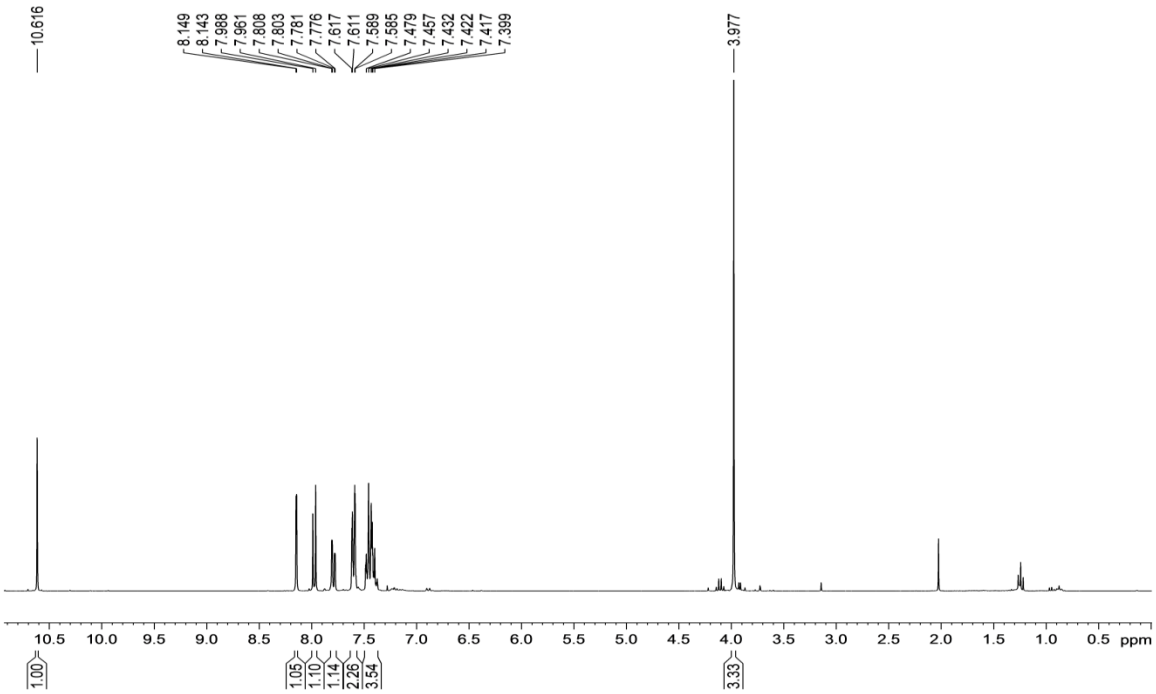

^{13}C NMR 151f

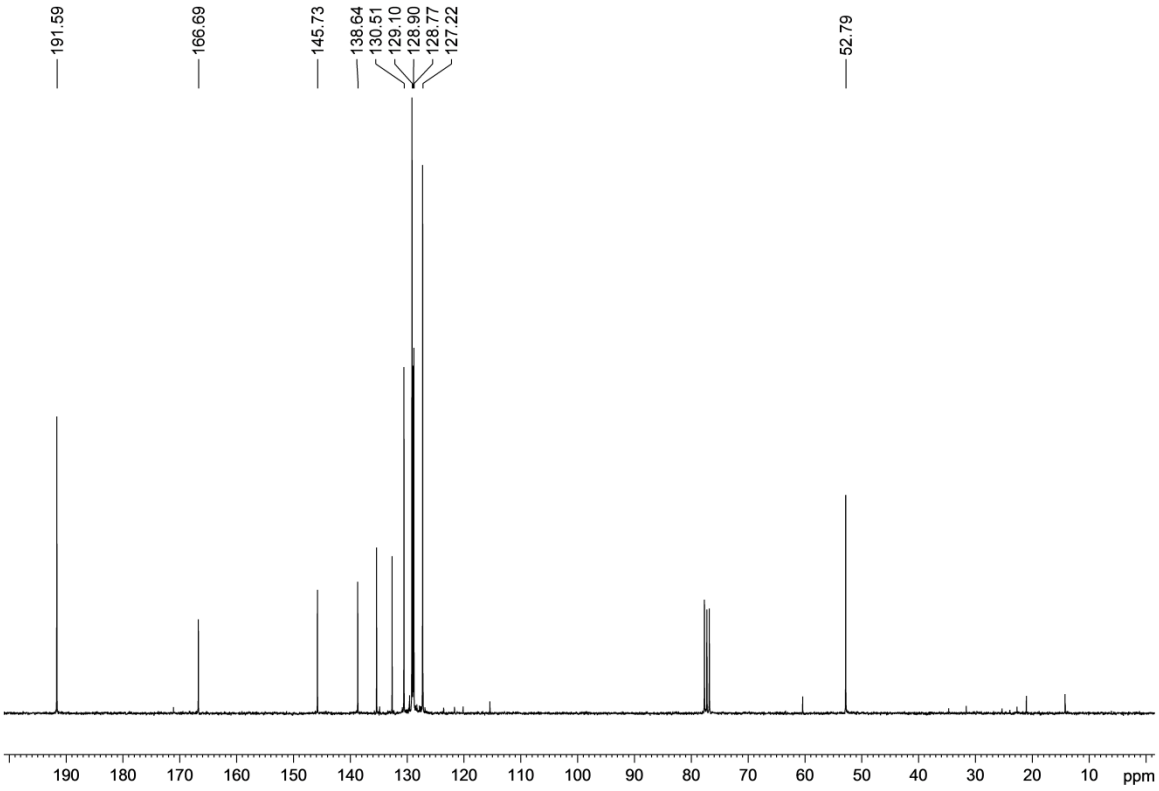

^{1}H NMR 151g

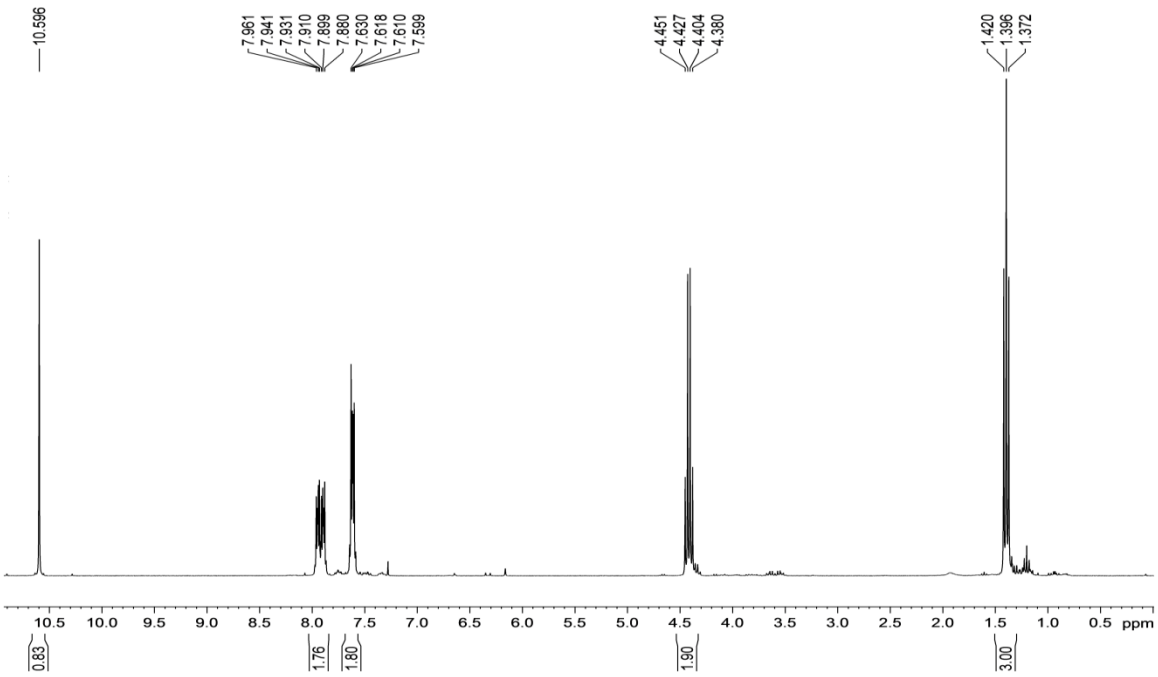

^{13}C NMR 151g

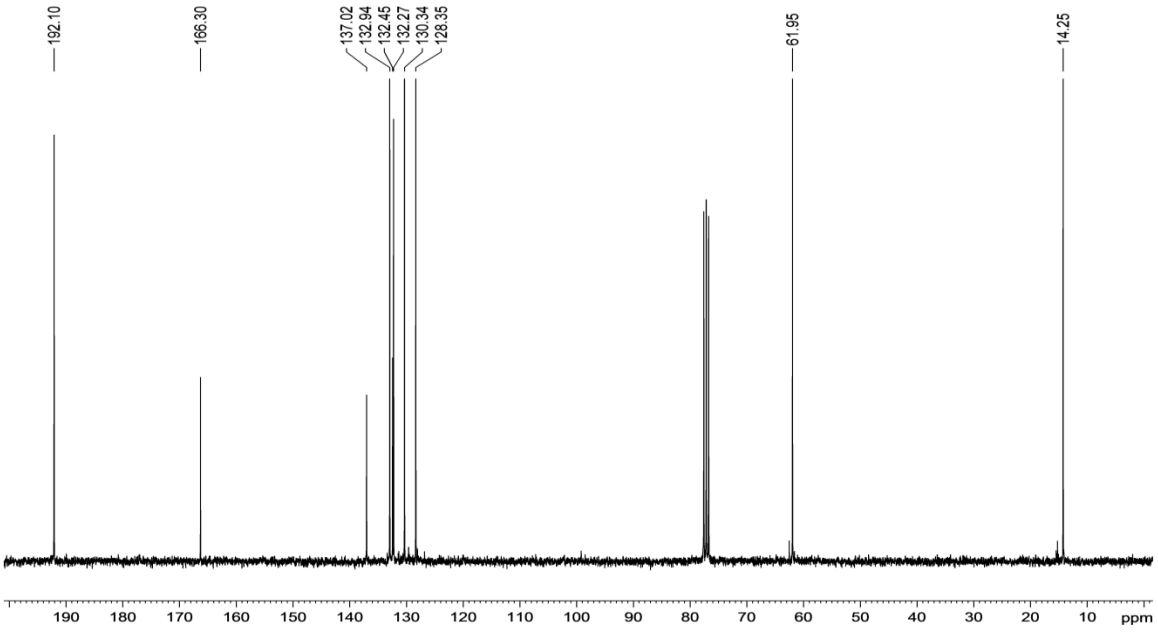

^{1}H NMR 151h

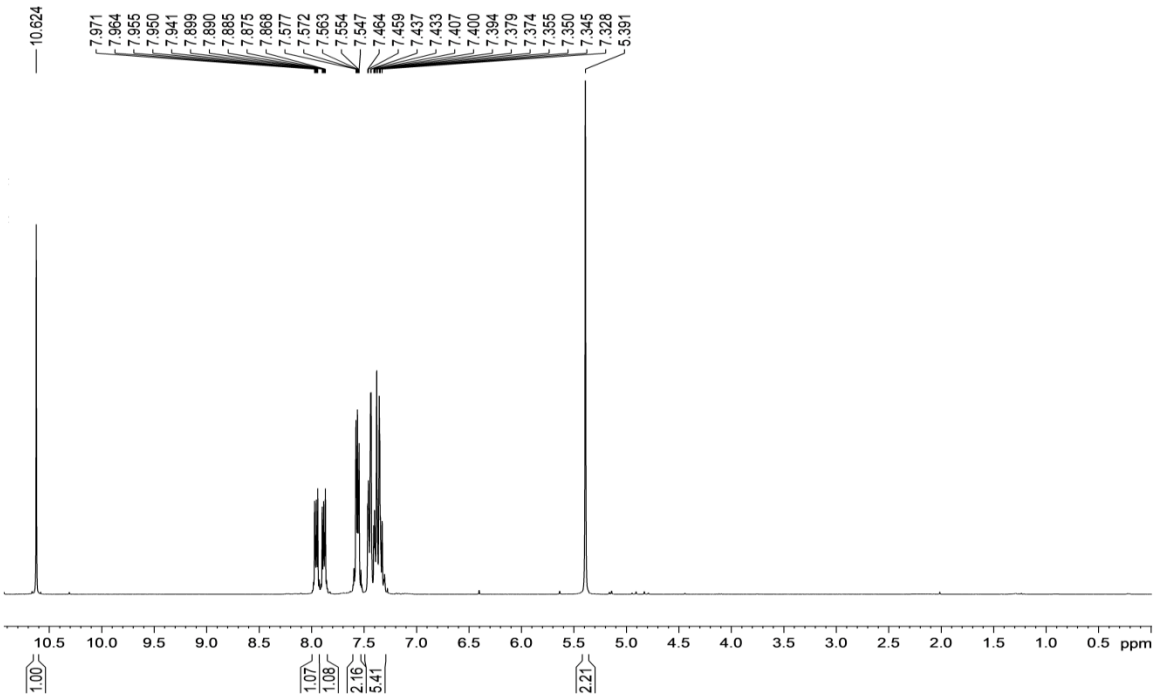

^{13}C NMR 151h

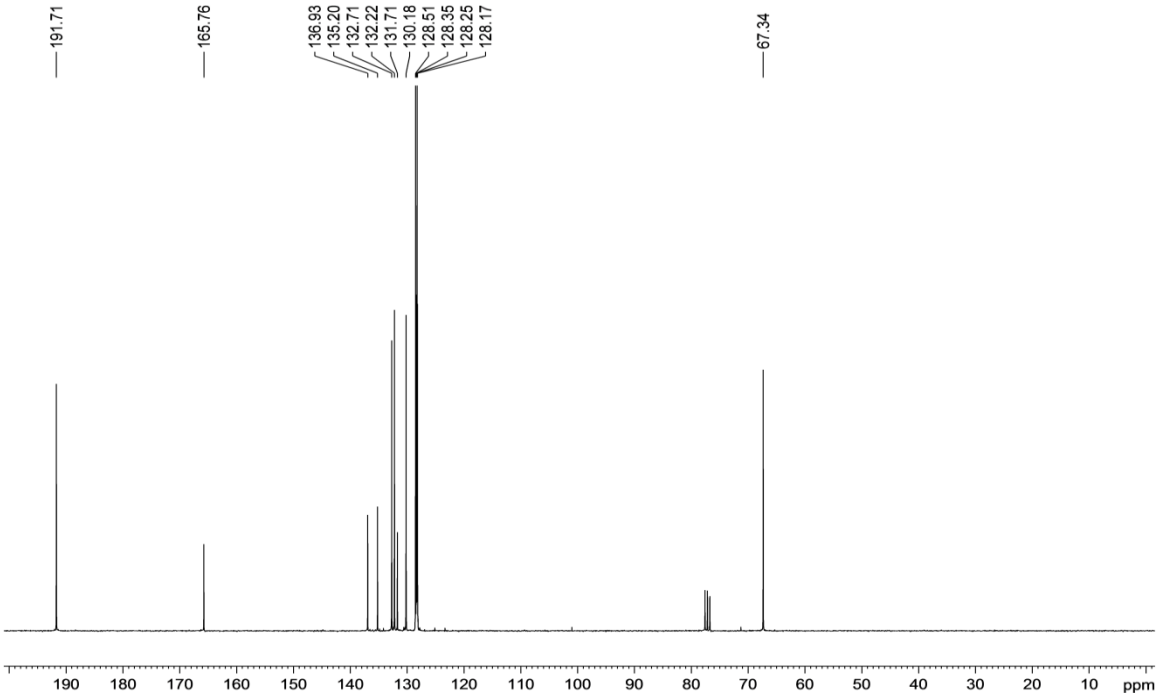

^{1}H NMR 151i

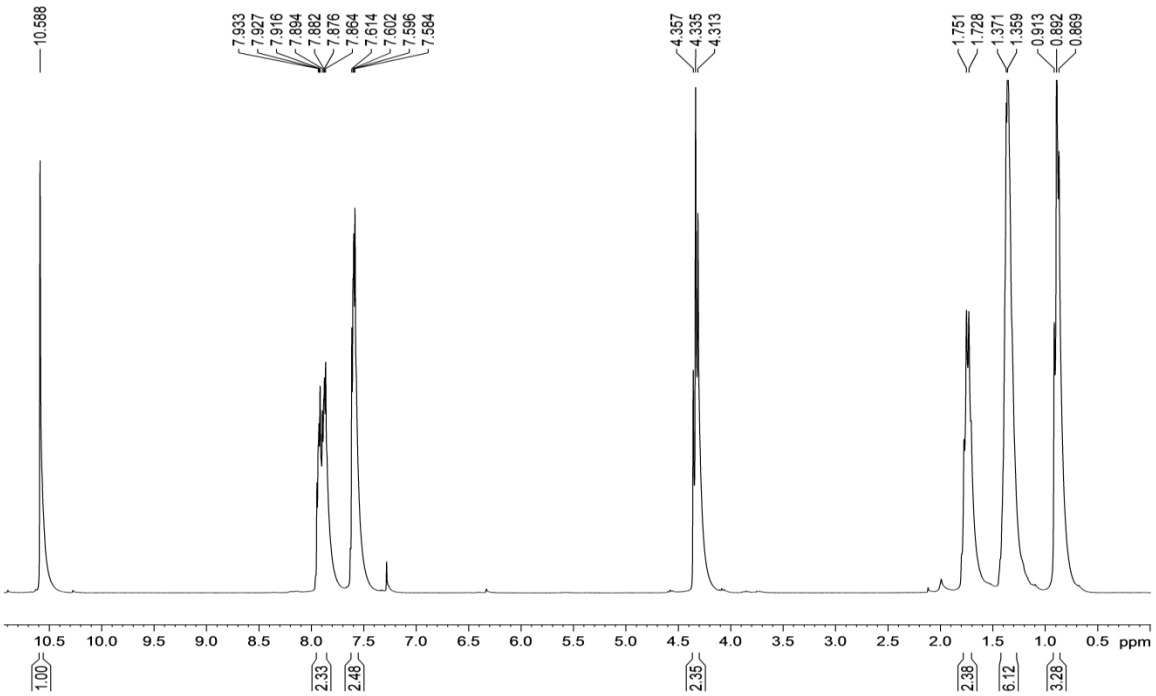

^{13}C NMR 151i

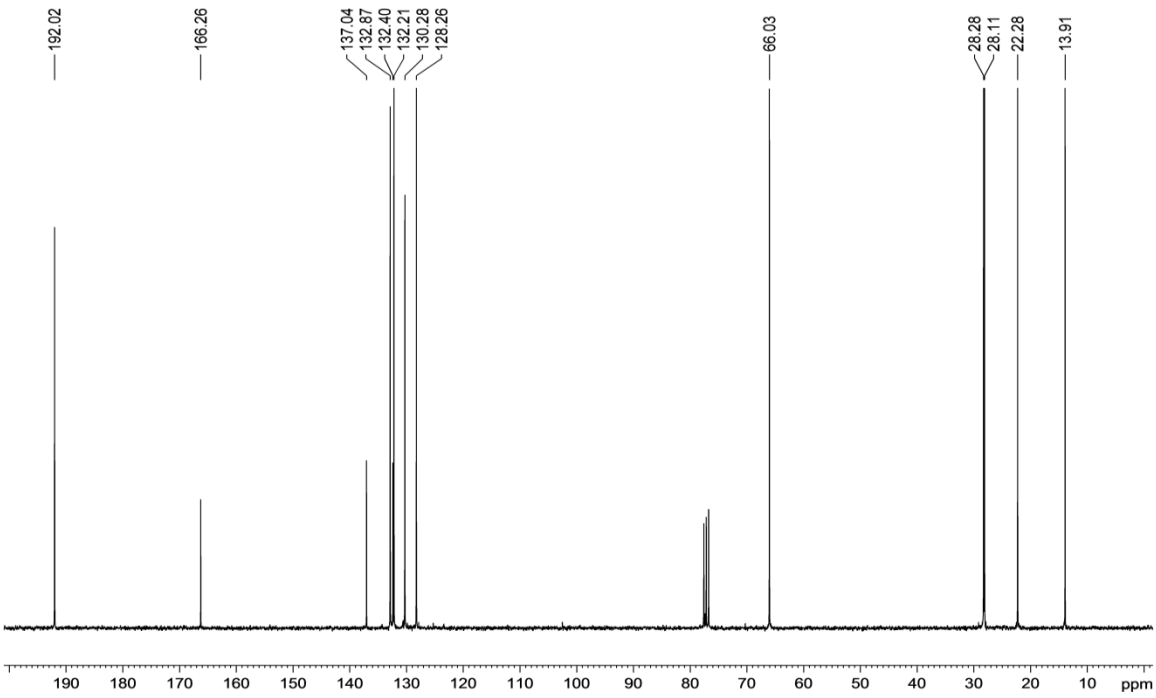

^{1}H NMR 151j

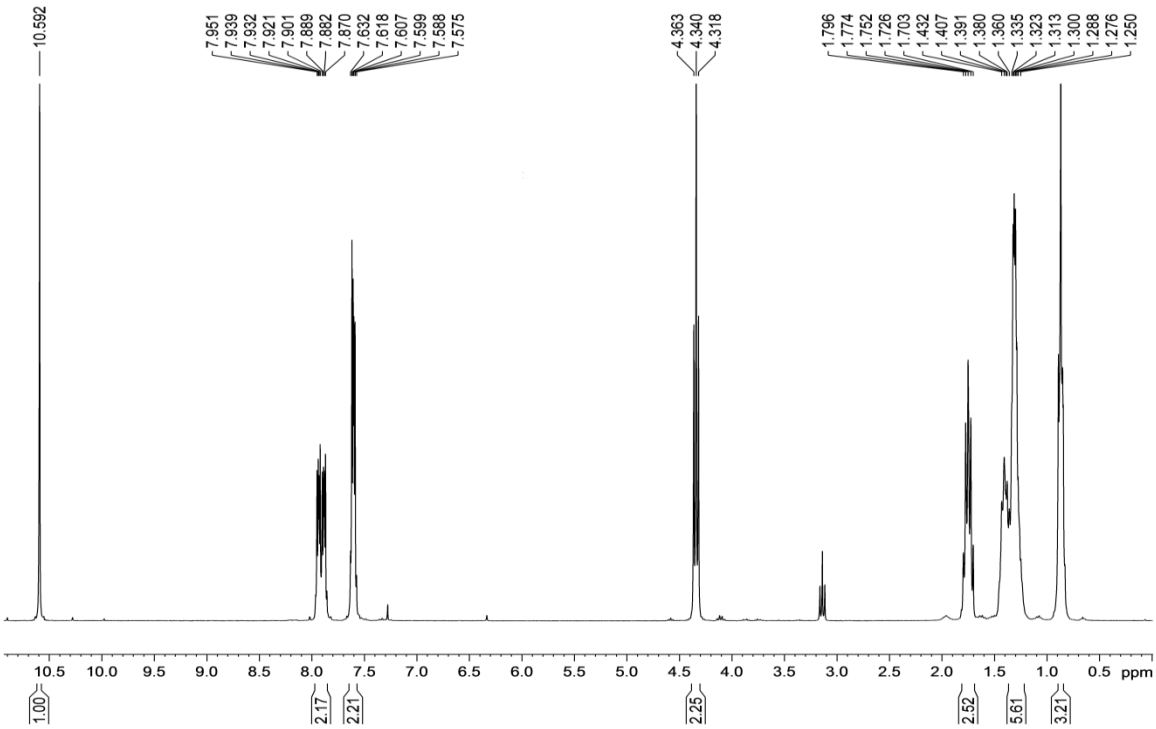

^{13}C NMR 151i

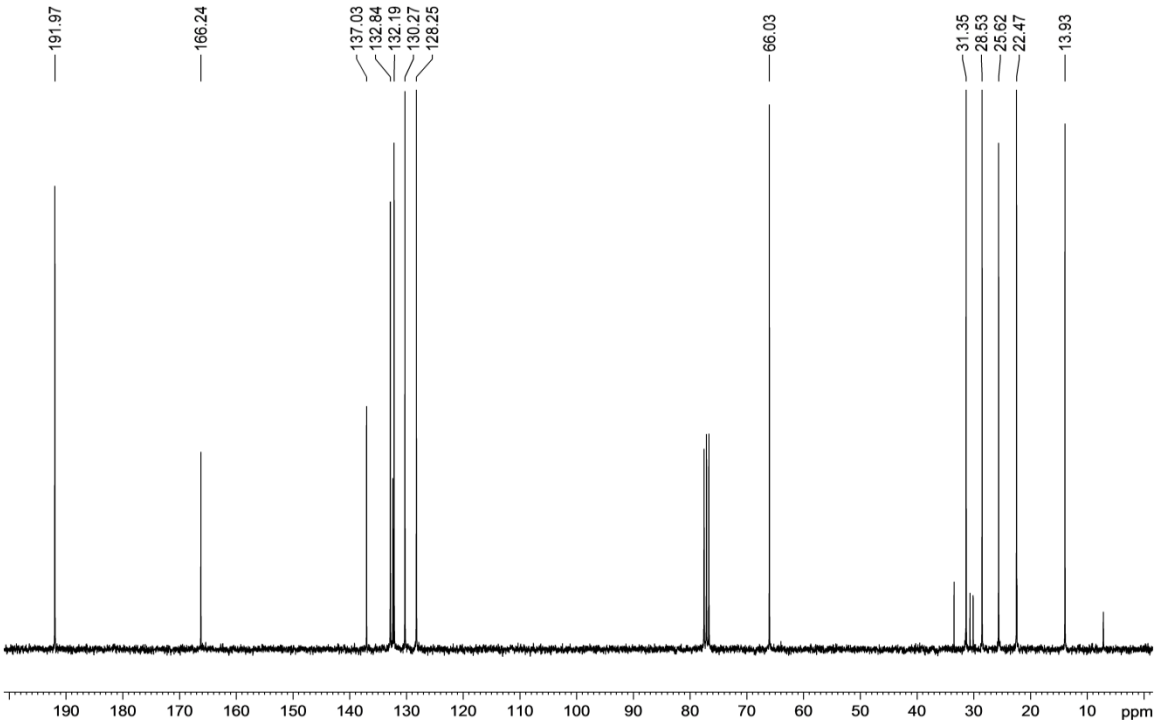

^{1}H NMR 151k

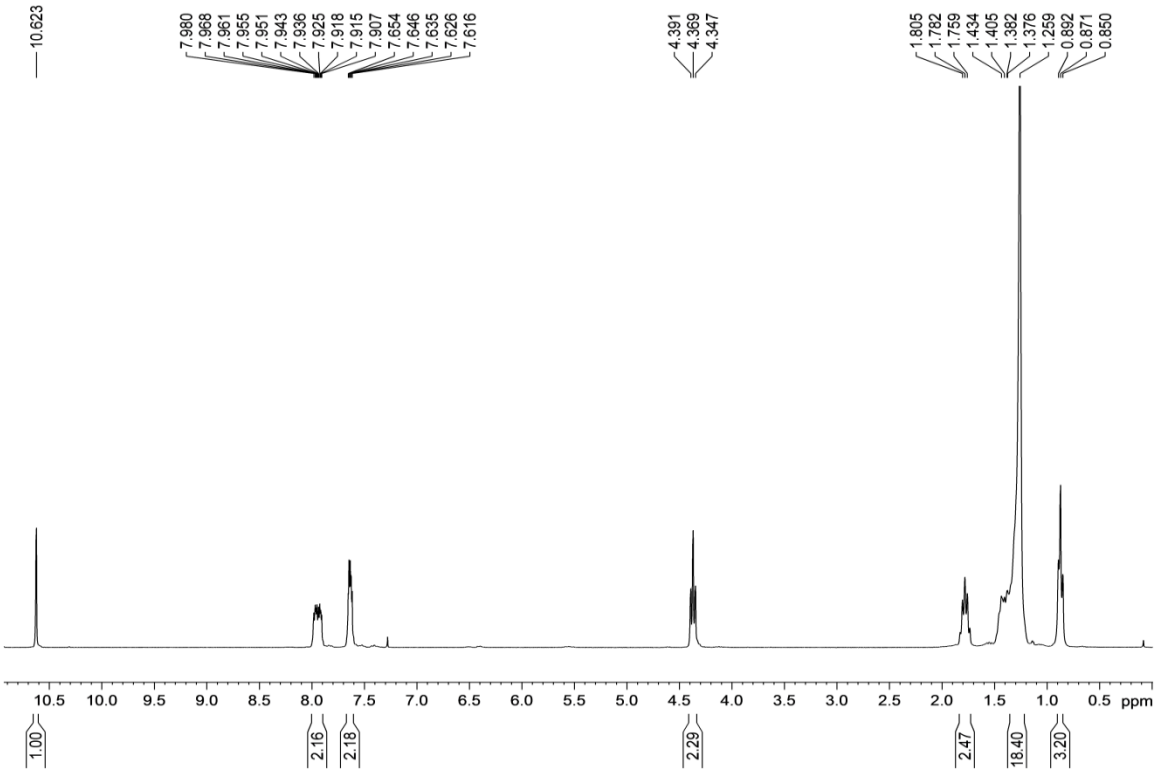

^{13}C NMR 151k

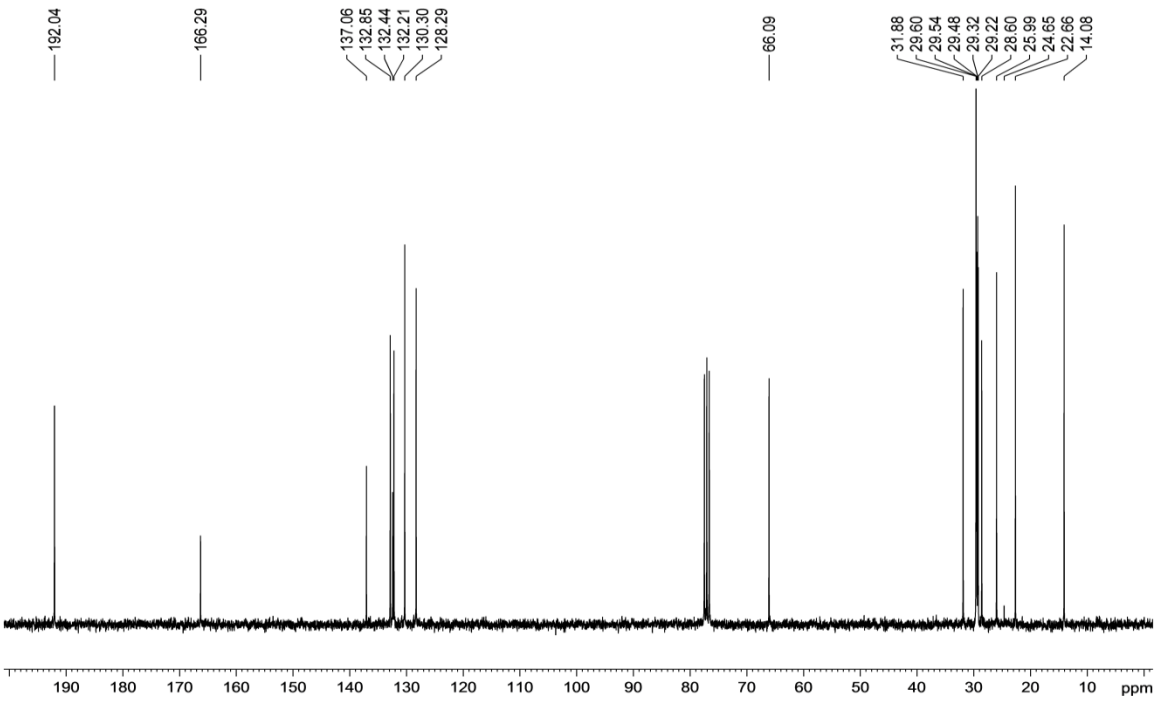

^{1}H NMR 151l

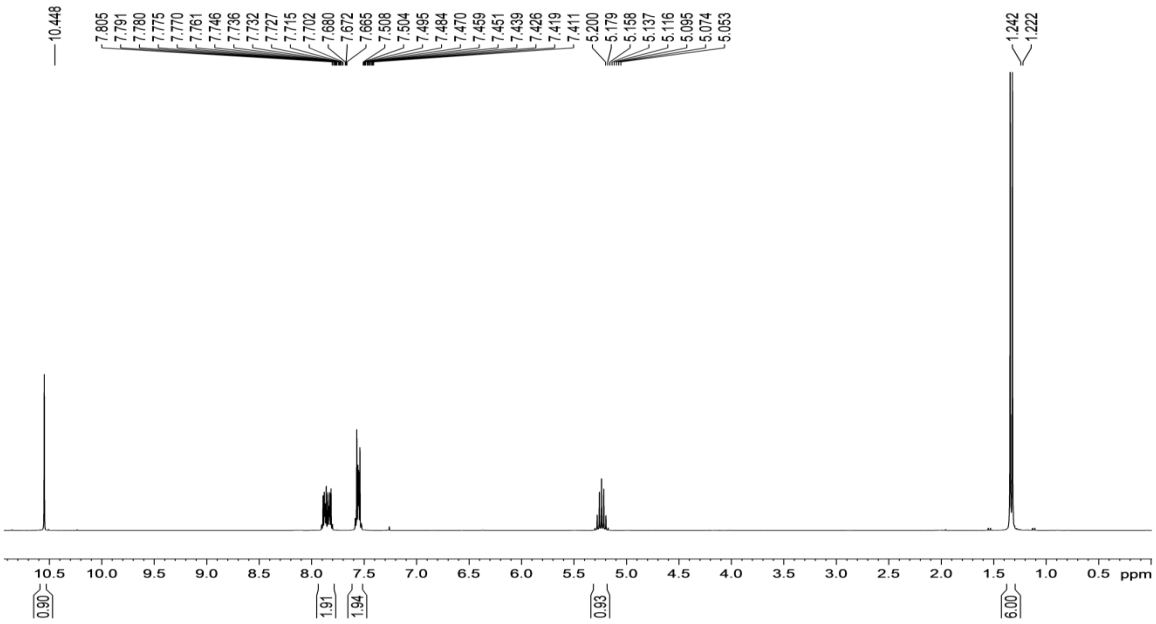

^{13}C NMR 151i

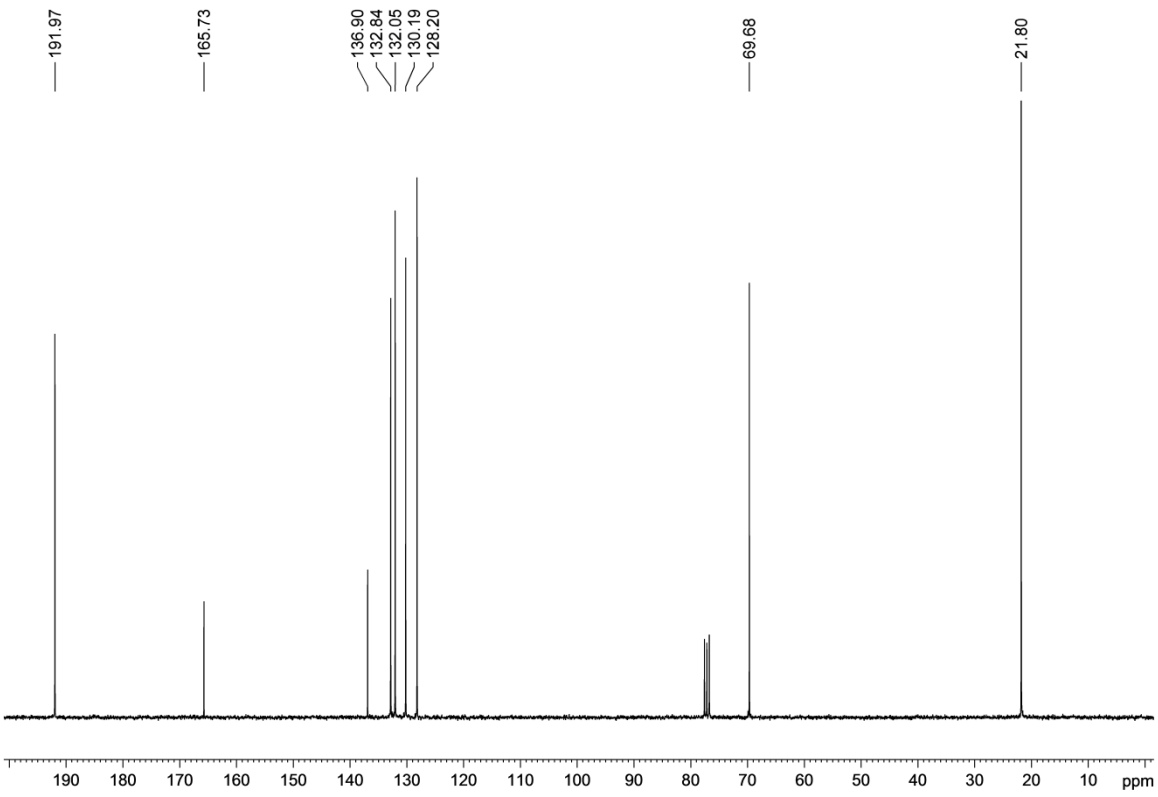

^{1}H NMR 1151m

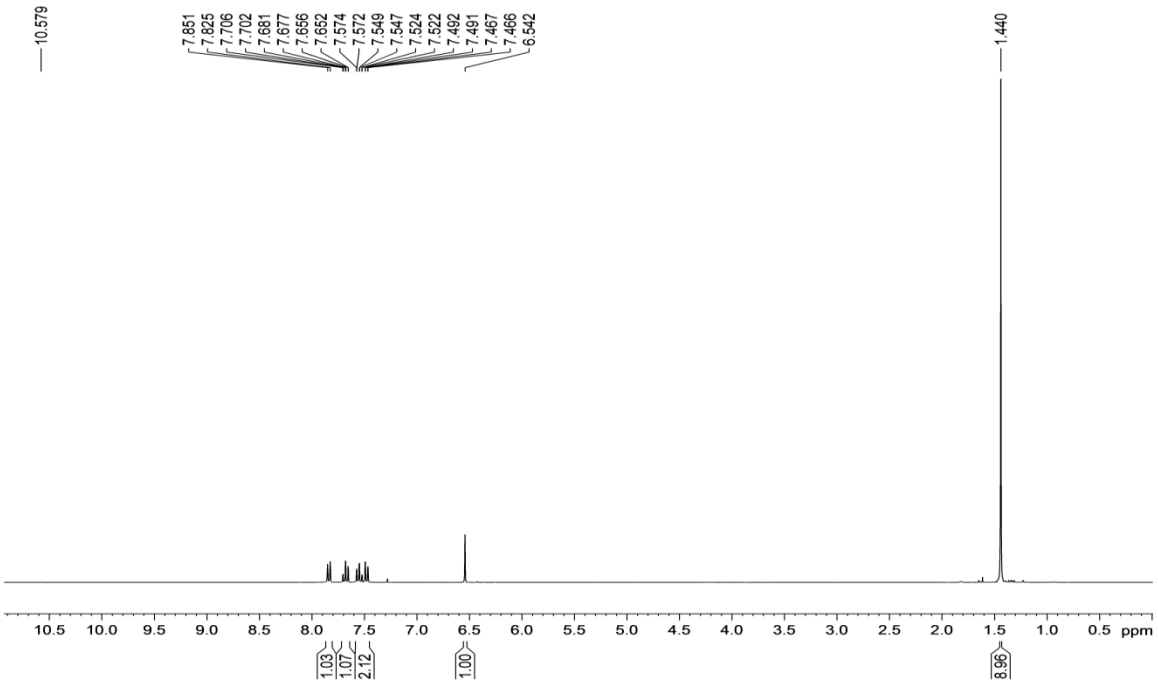

^{13}C NMR 151m

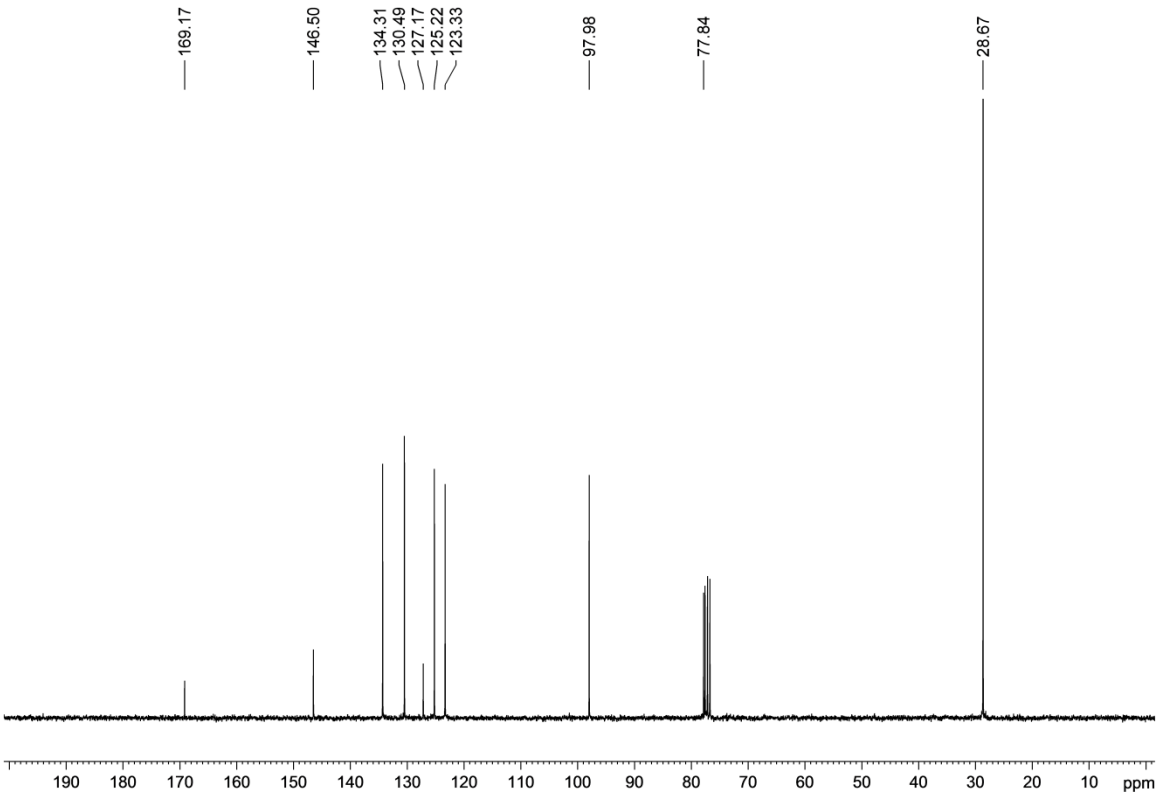

IR 151n

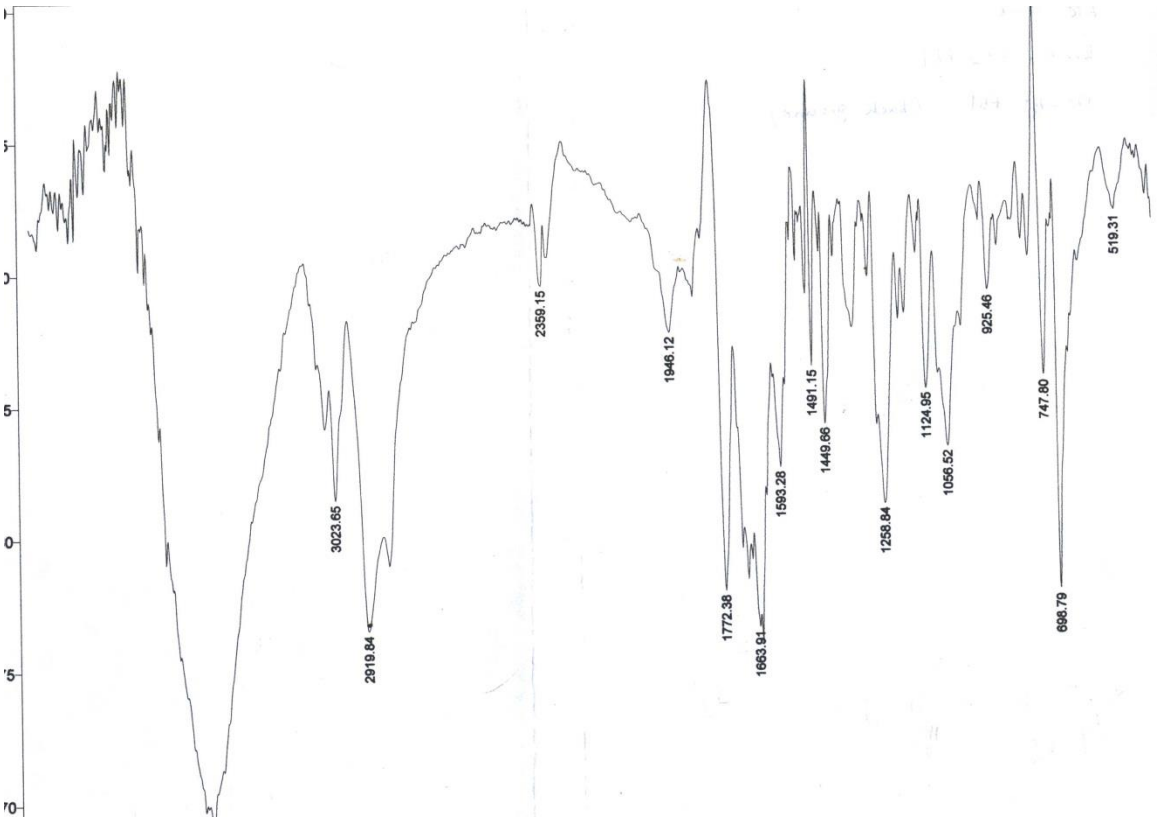
3023.65
2919.84
2359.15
1946.12
1772.38
1663.91
1593.28
1491.15
1449.66
1258.84
1124.95
1056.52
925.46
747.80
698.79
519.31

^{1}H NMR 152a

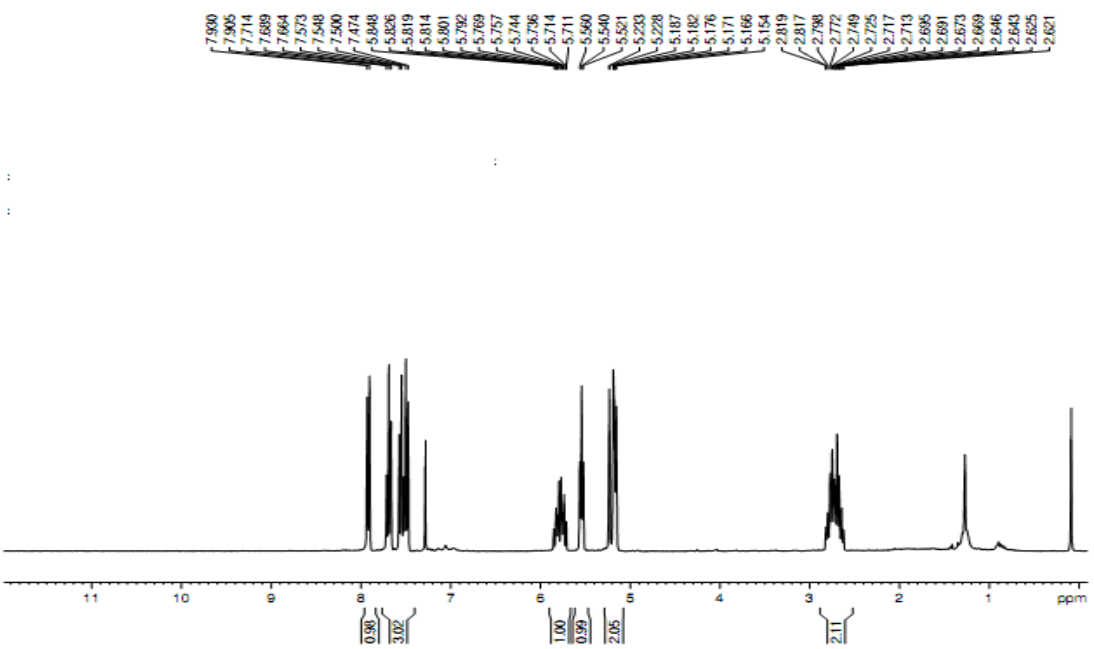

^{13}C NMR 152a

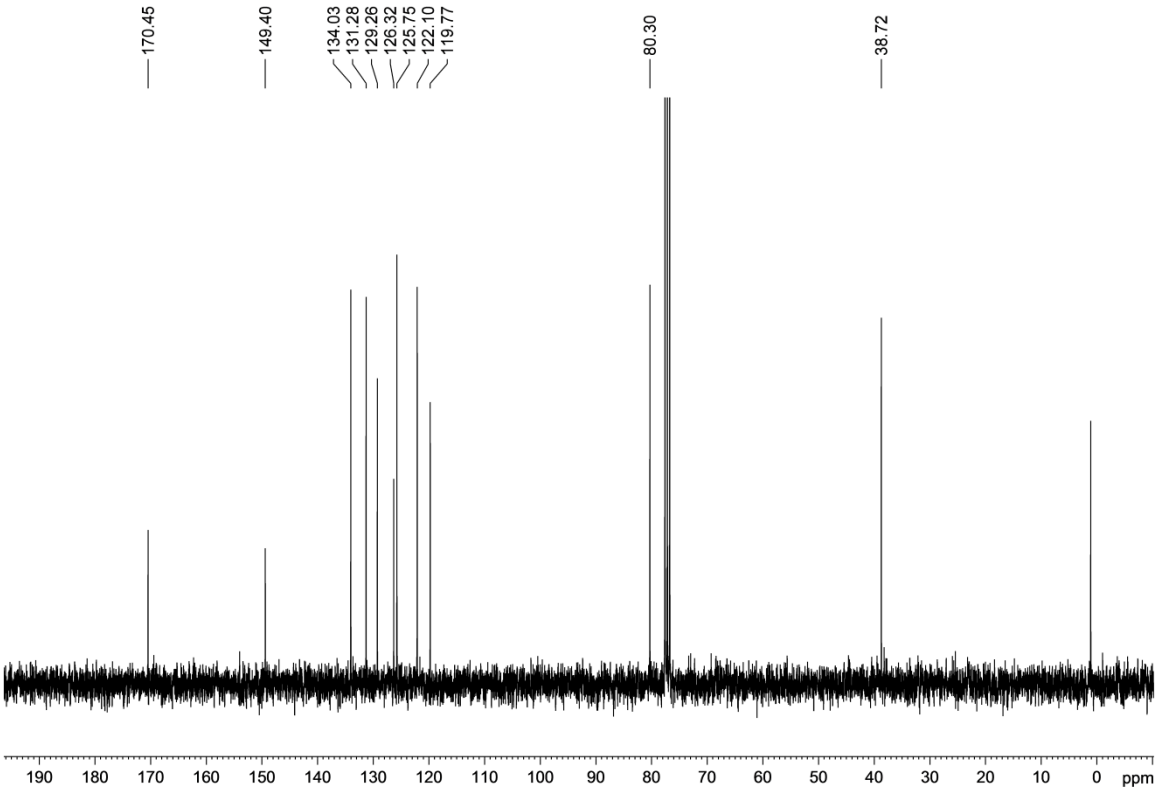

IR 152a

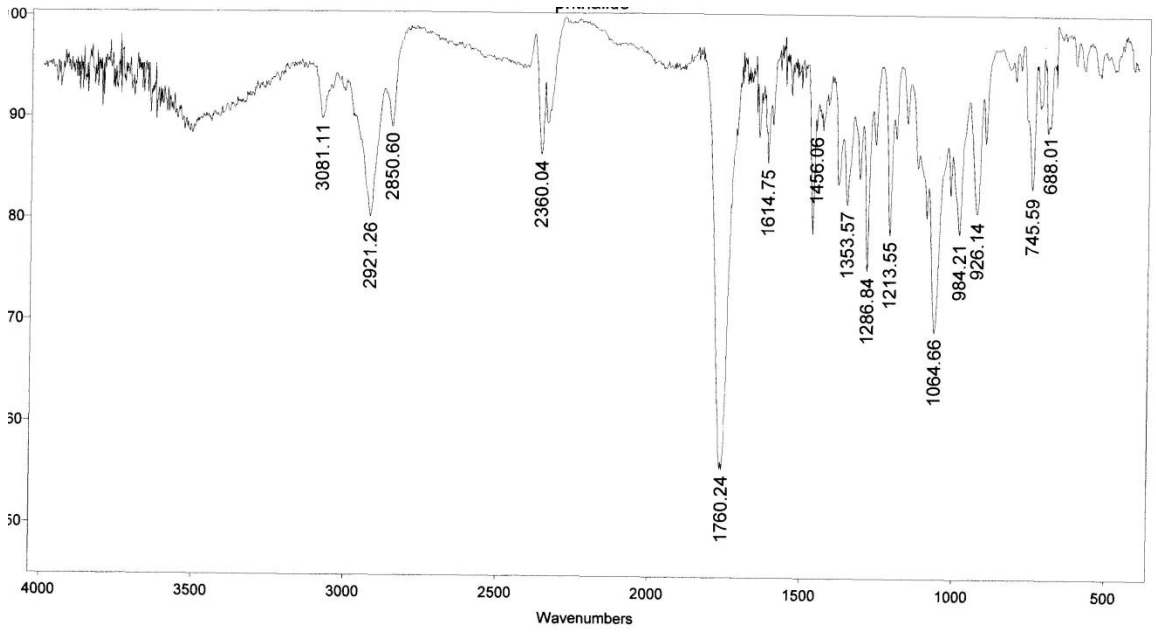
3081.11
2921.26
2850.60
2360.04
1760.24
1614.75
1456.06
1353.57
1286.84
1213.55
1064.66
984.21
926.14
745.59
688.01
4000
3500
3000
2500
2000
1500
1000
500
Wavenumbers

^{1}H NMR 152b

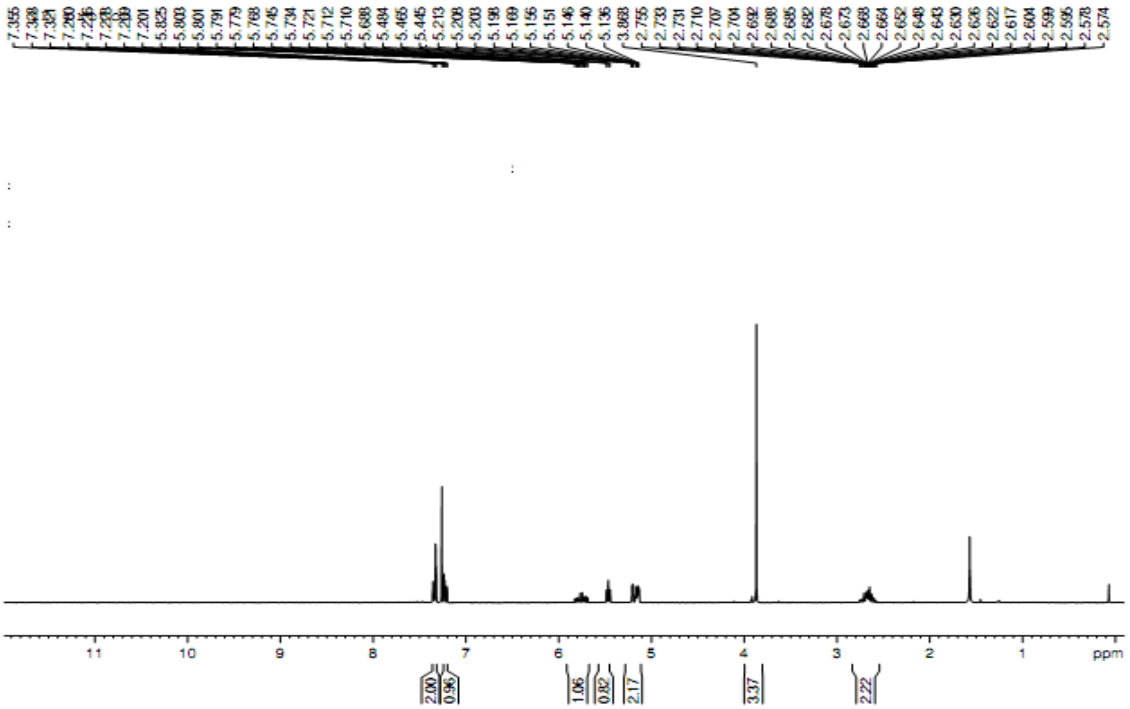

^{13}C NMR 152b

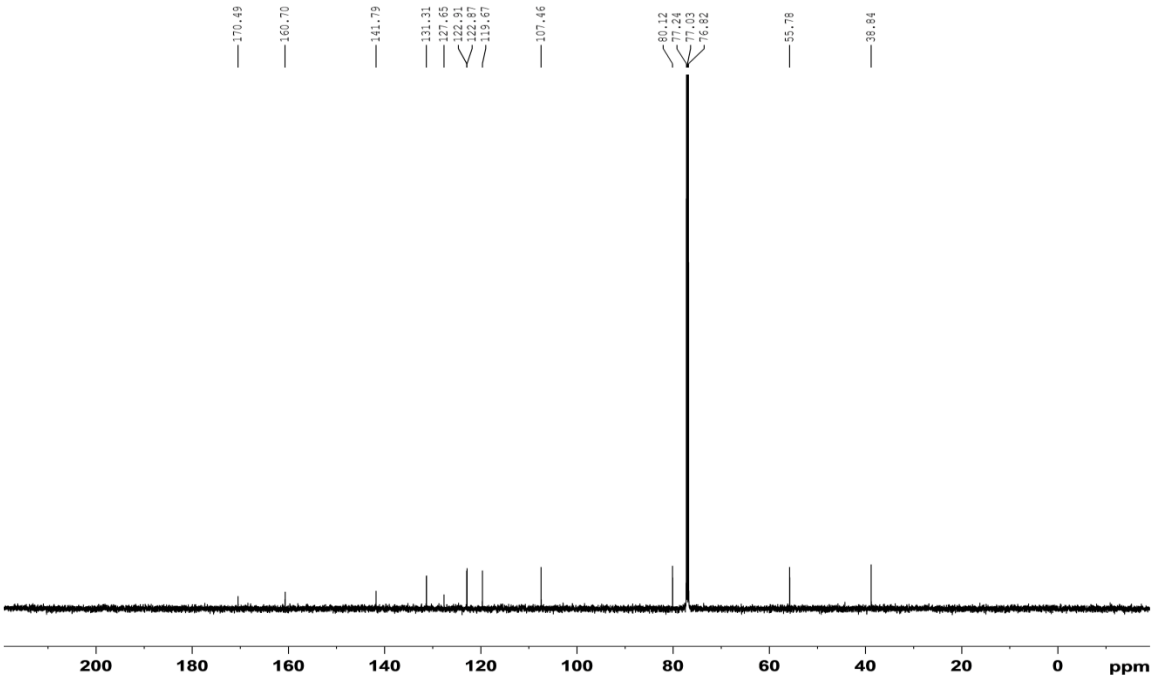

IR 152b

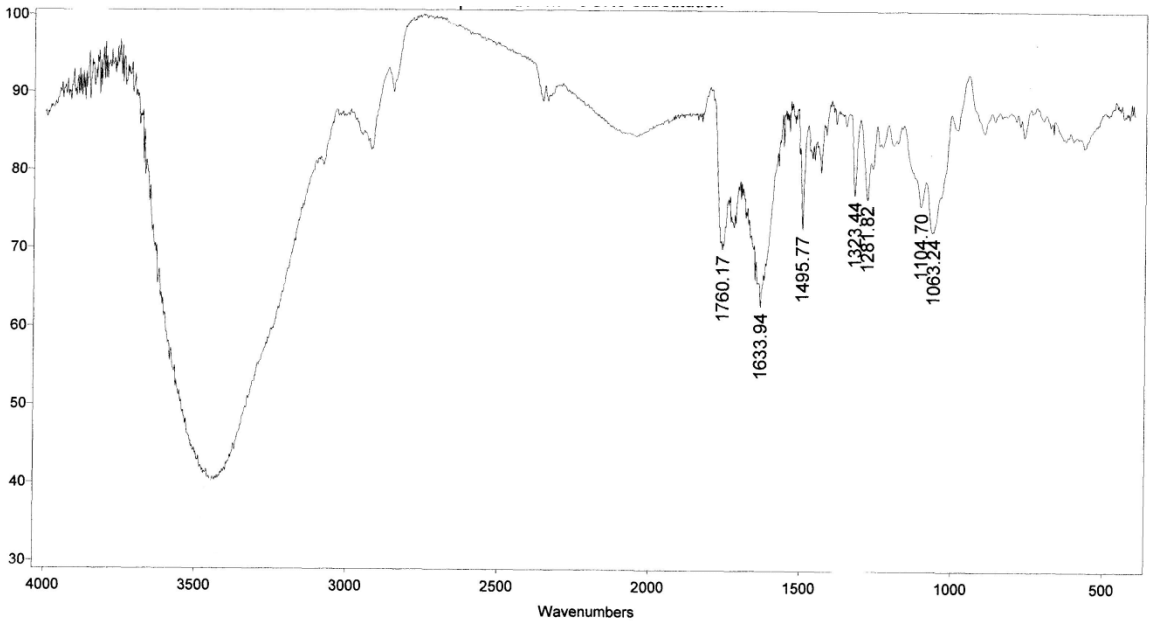
100
90
80
70
60
50
40
30
4000
3500
3000
2500
2000
1500
1000
500
Wavenumbers
1760.17
1633.94
1495.77
1323.44
1281.82
1104.70
1063.24

^{1}H NMR 152c

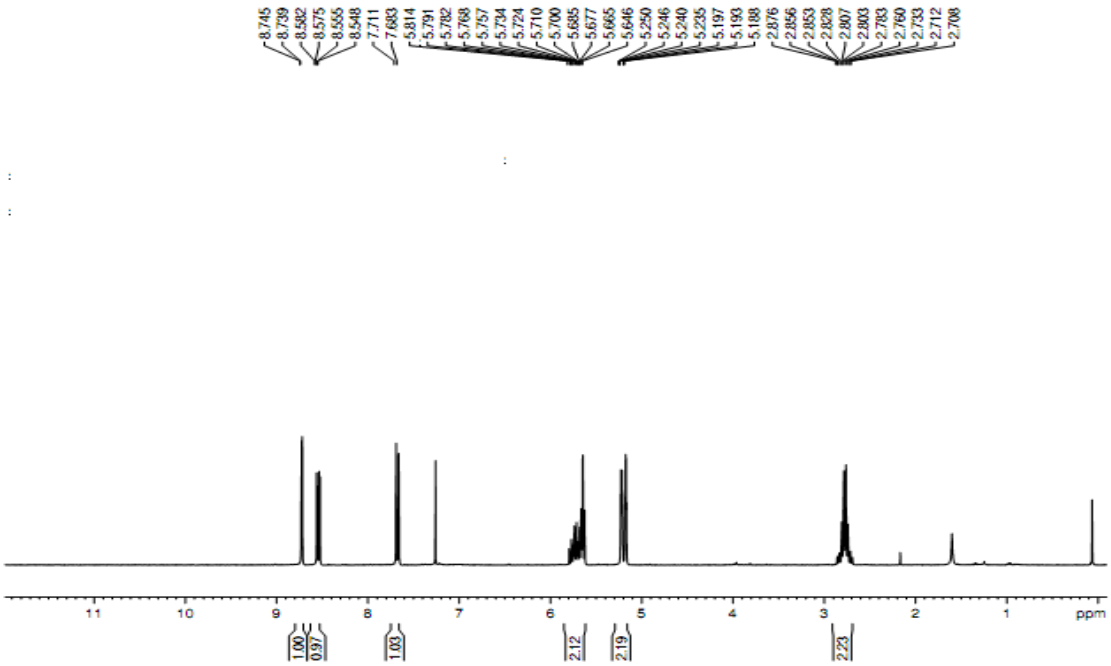

^{13}C NMR 152c

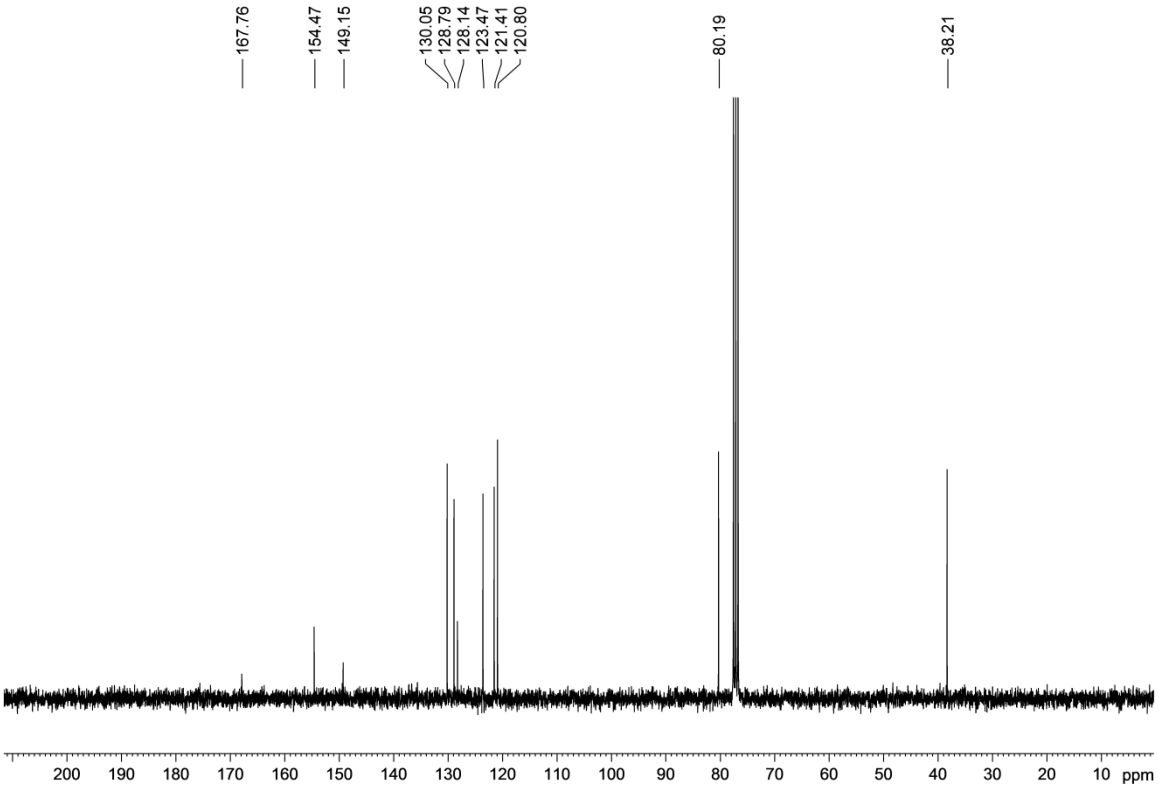

IR 152c

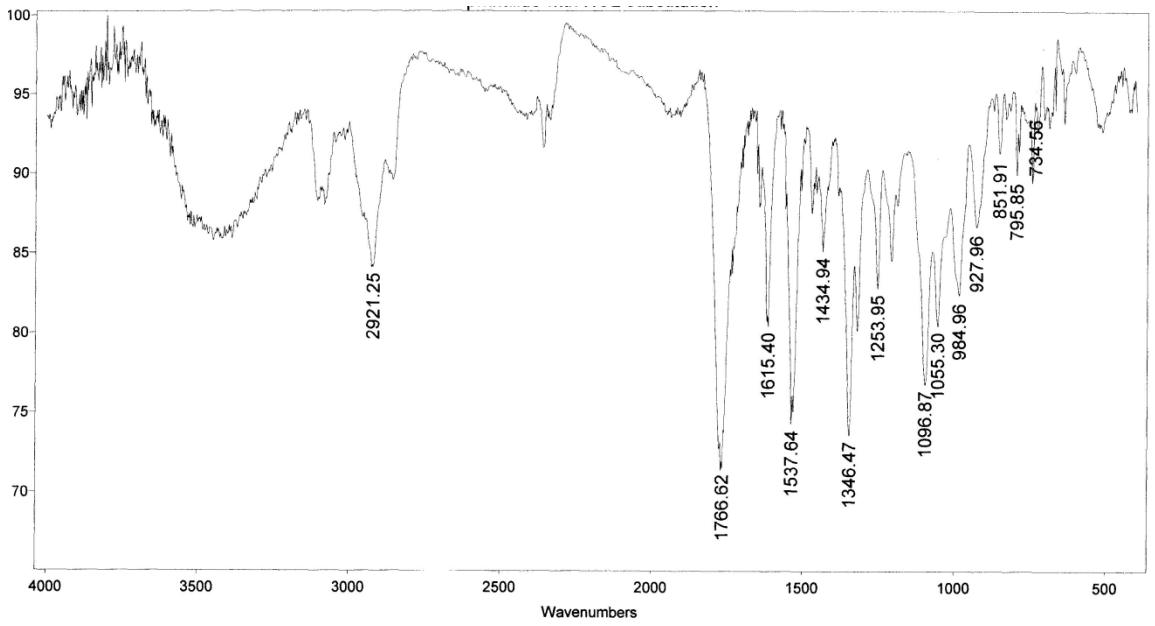
100
95
90
85
80
75
70
2921.25
1766.62
1615.40
1537.64
1434.94
1346.47
1253.95
1096.87
1055.30
984.96
927.96
851.91
795.85
734.56
4000
3500
3000
2500
2000
1500
1000
500
Wavenumbers

^{1}H NMR 152d

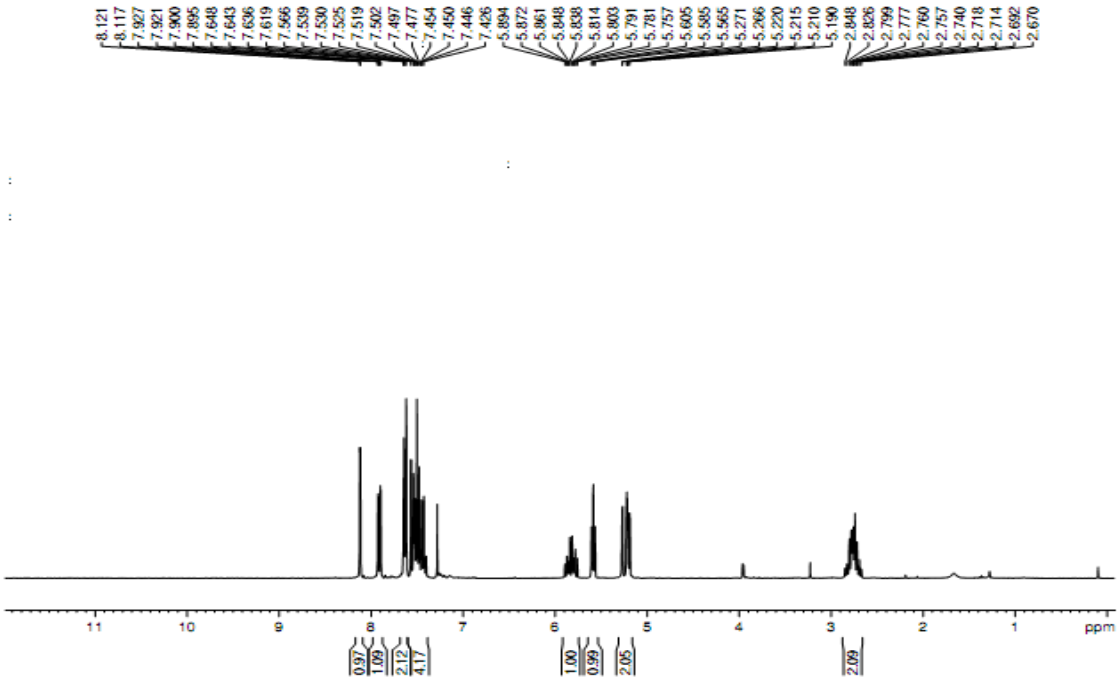

^{13}C NMR 152d

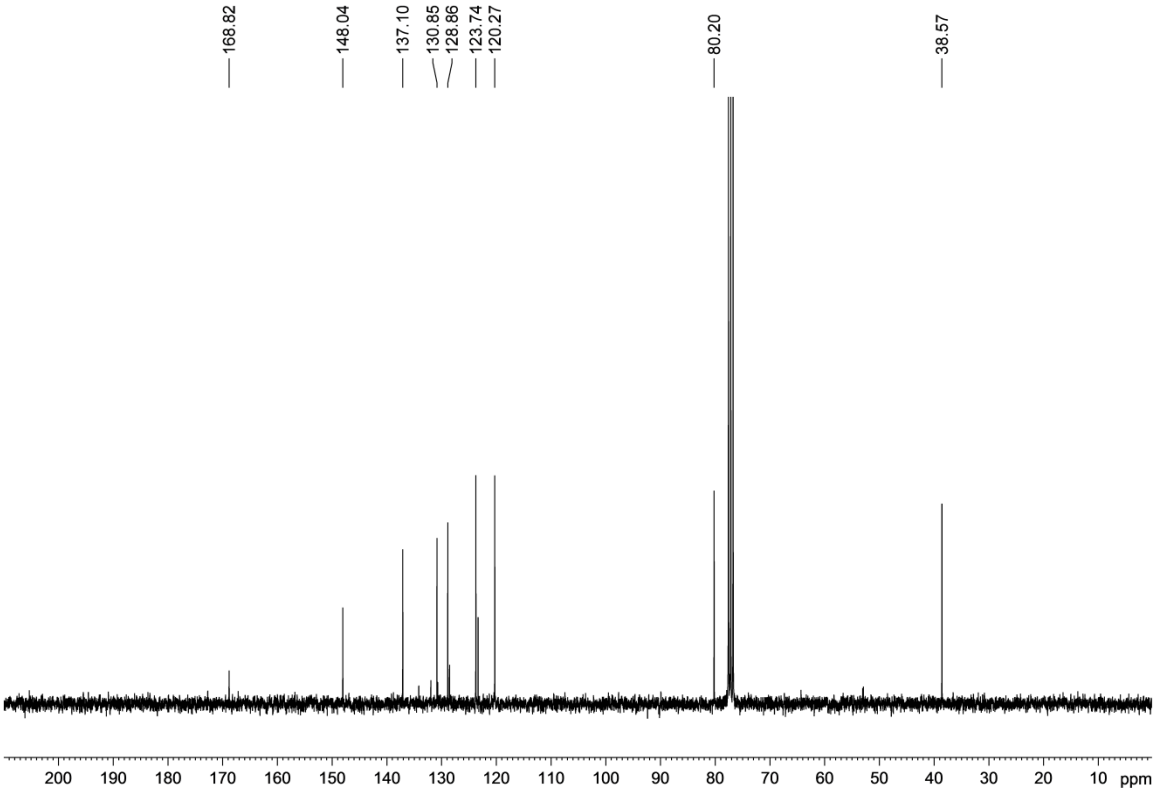

IR 152d

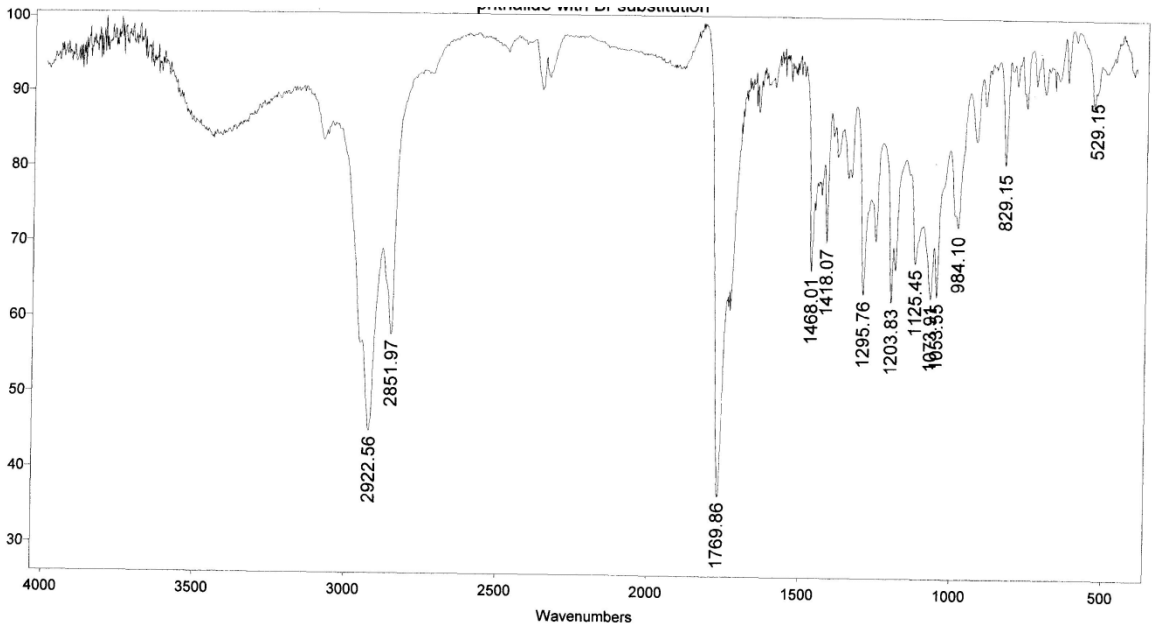
100
90
80
70
60
50
40
30
4000
3500
3000
2500
2000
1500
1000
500
Wavenumbers
2922.56
2851.97
1769.86
1468.01
1418.07
1295.76
1203.83
1125.45
984.10
829.15
529.15

^{1}H NMR 152e

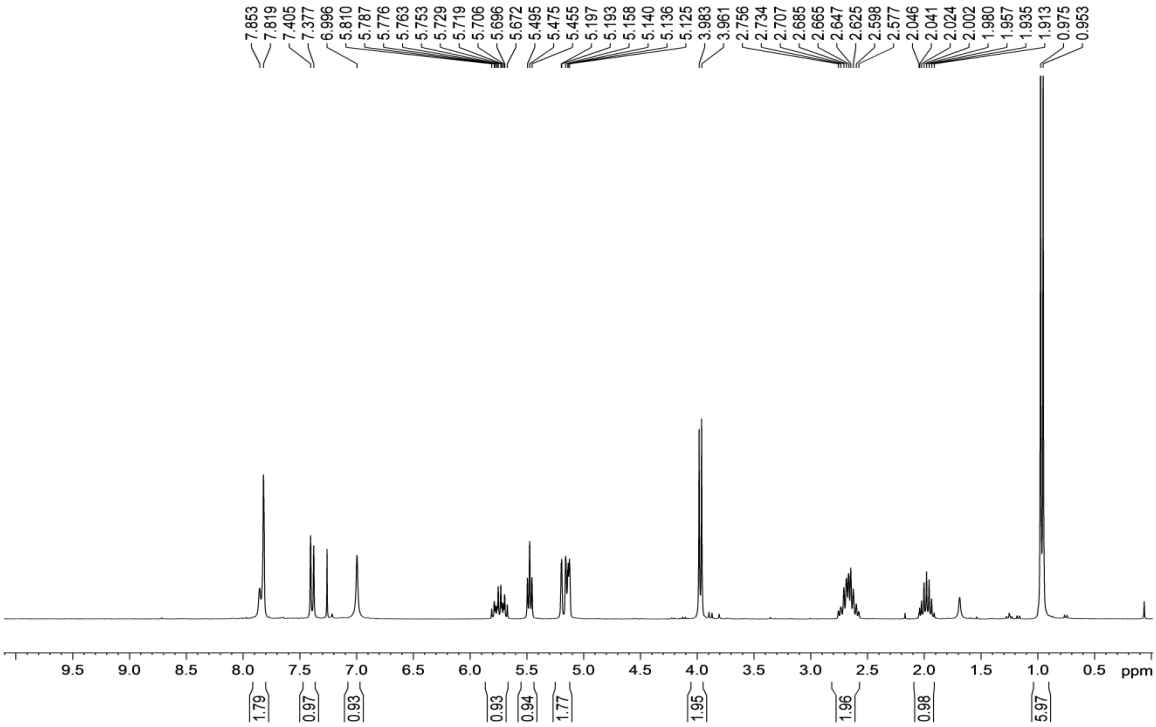

^{13}C NMR 152e

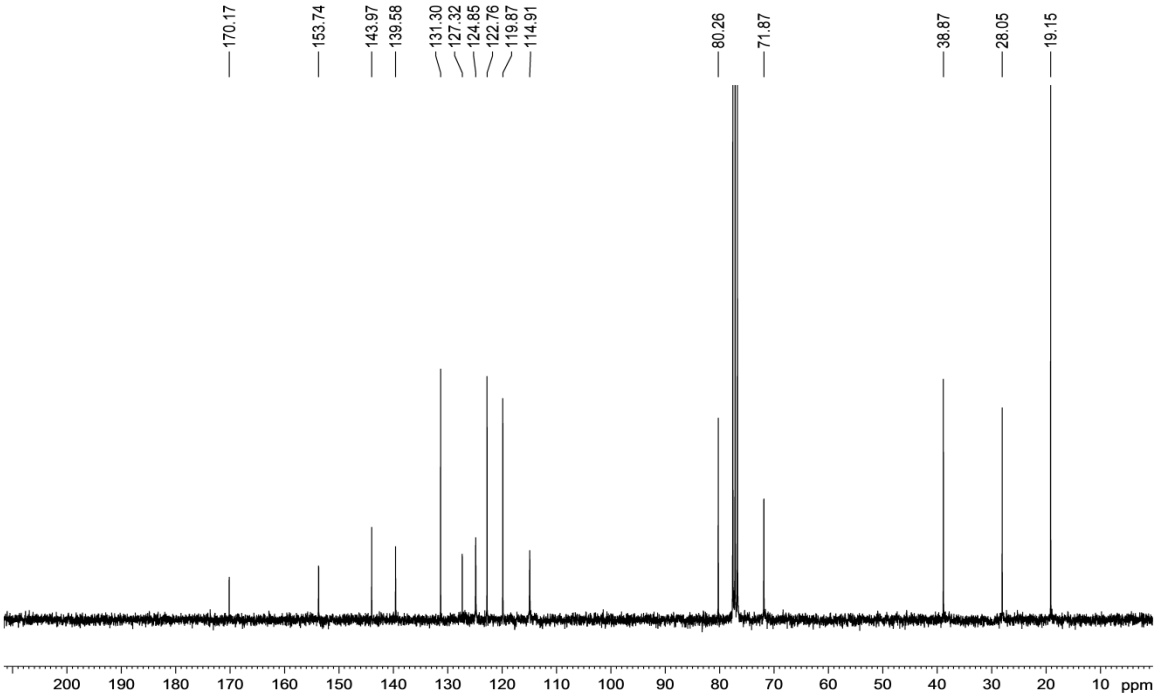

IR 152e

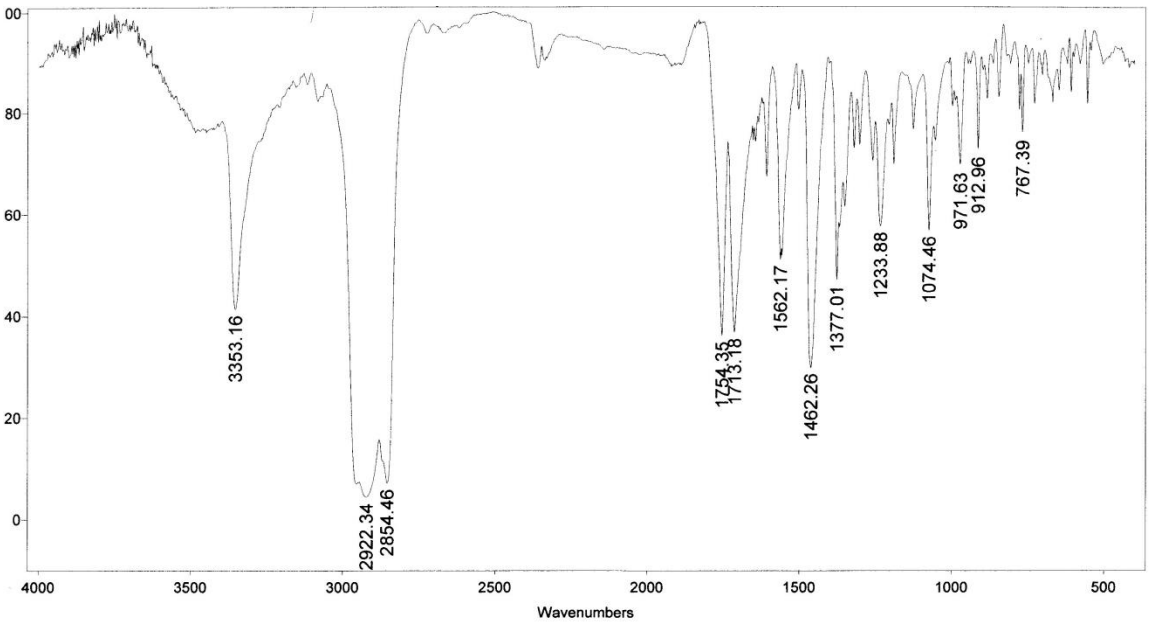
00
80
60
40
20
0
3353.16
2922.34
2854.46
1754.35
1713.18
1562.17
1462.26
1377.01
1233.88
1074.46
971.63
912.96
767.39
4000
3500
3000
2500
2000
1500
1000
500
Wavenumbers

^{1}H NMR 152f

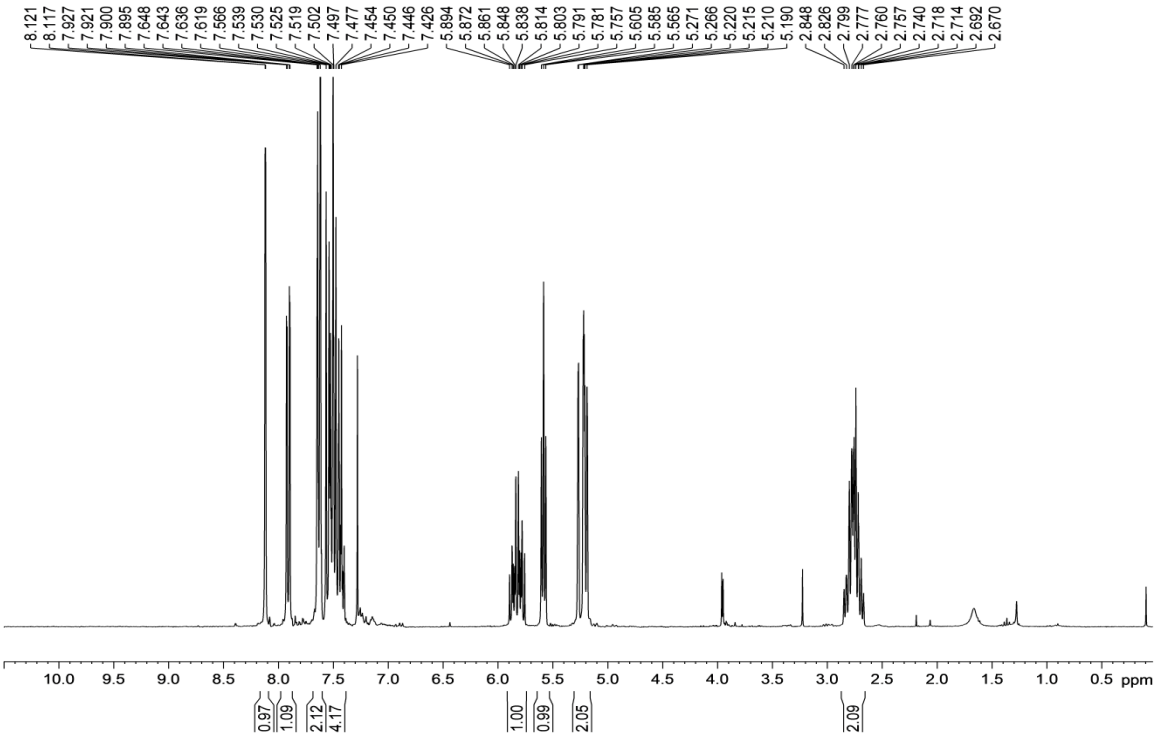

^{13}C NMR 152f

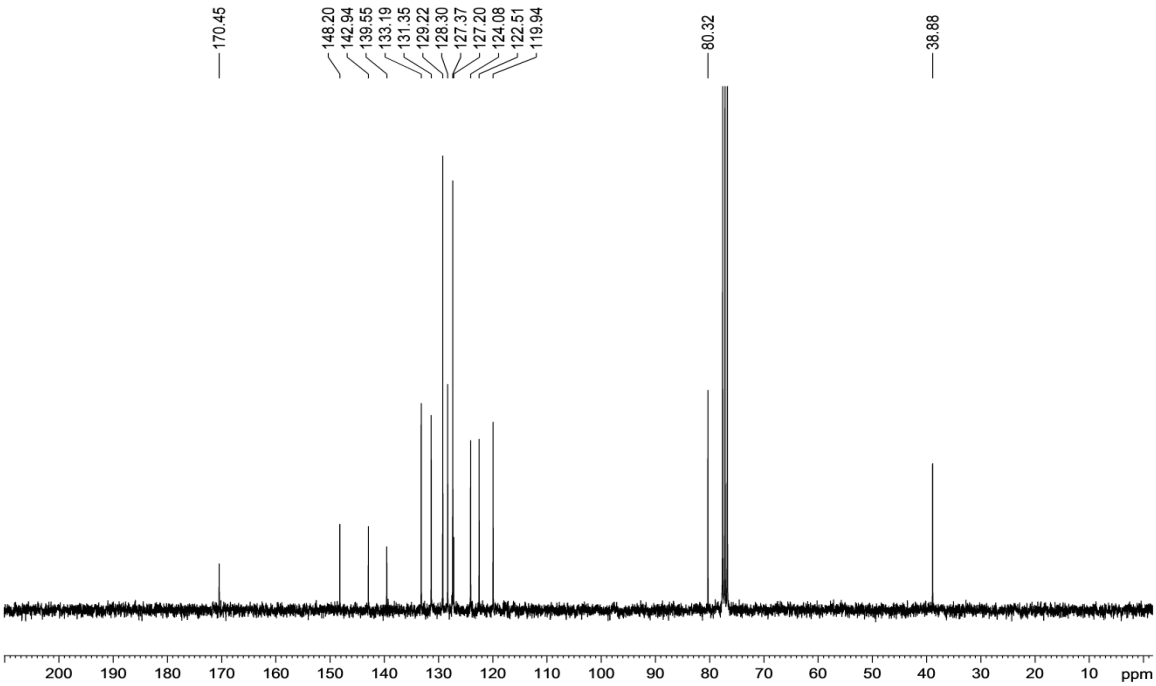

IR 152f

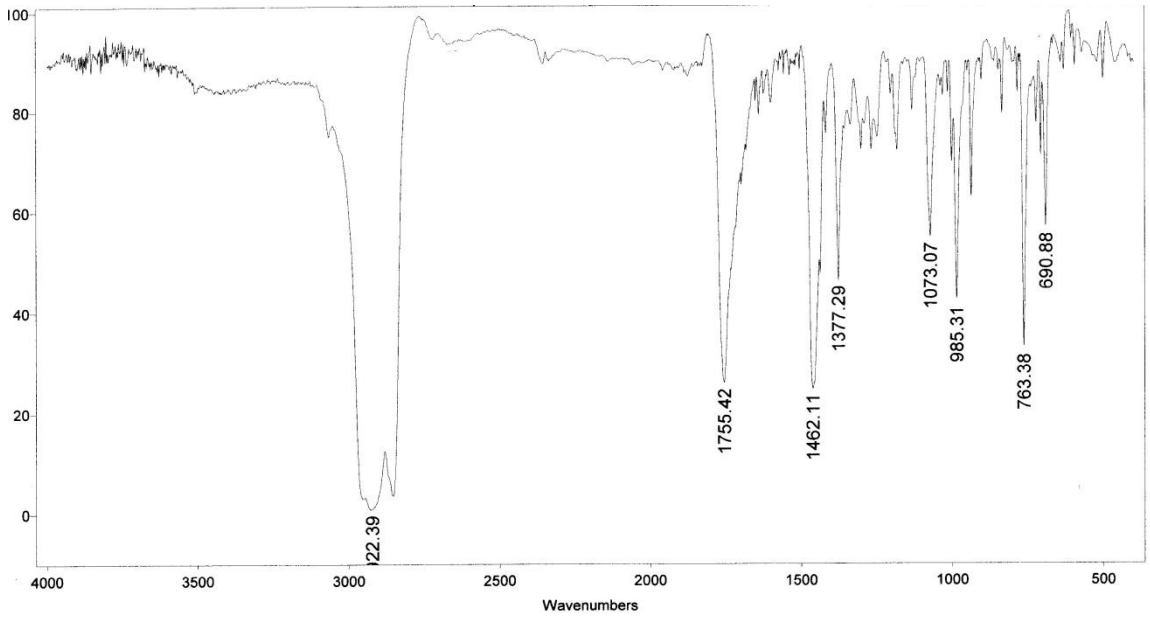
100
80
60
40
20
0
22.39
1755.42
1462.11
1377.29
1073.07
985.31
763.38
690.88
4000
3500
3000
2500
2000
1500
1000
500
Wavenumbers

^{1}H NMR 168•Cl^{-}

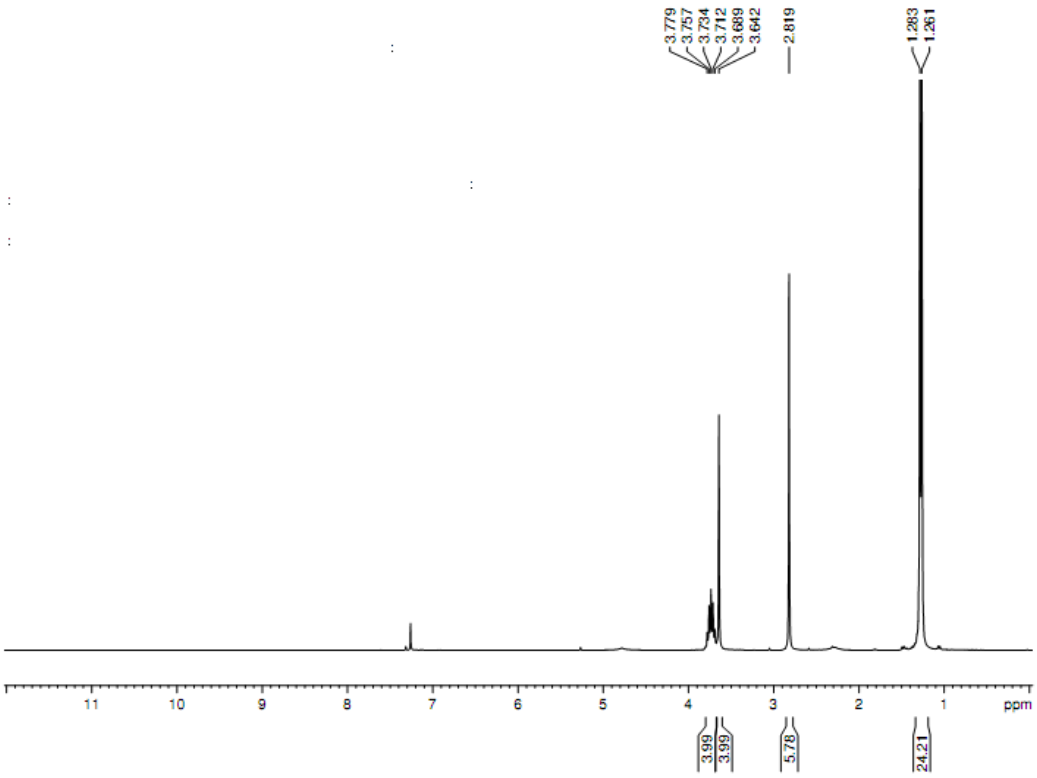

^{13}C NMR 168•Cl^{-}

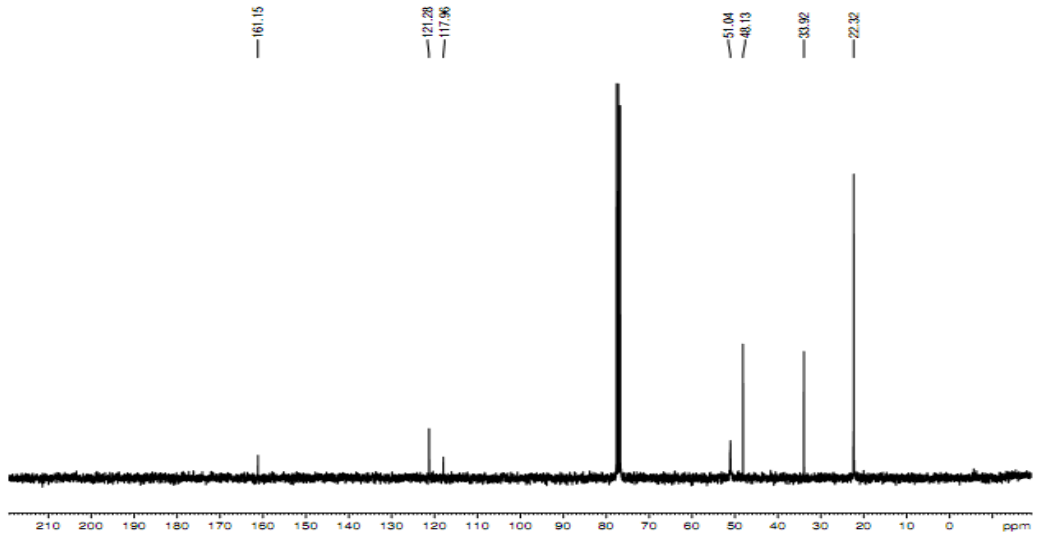

^{15}N NMR 168•Cl^{-}

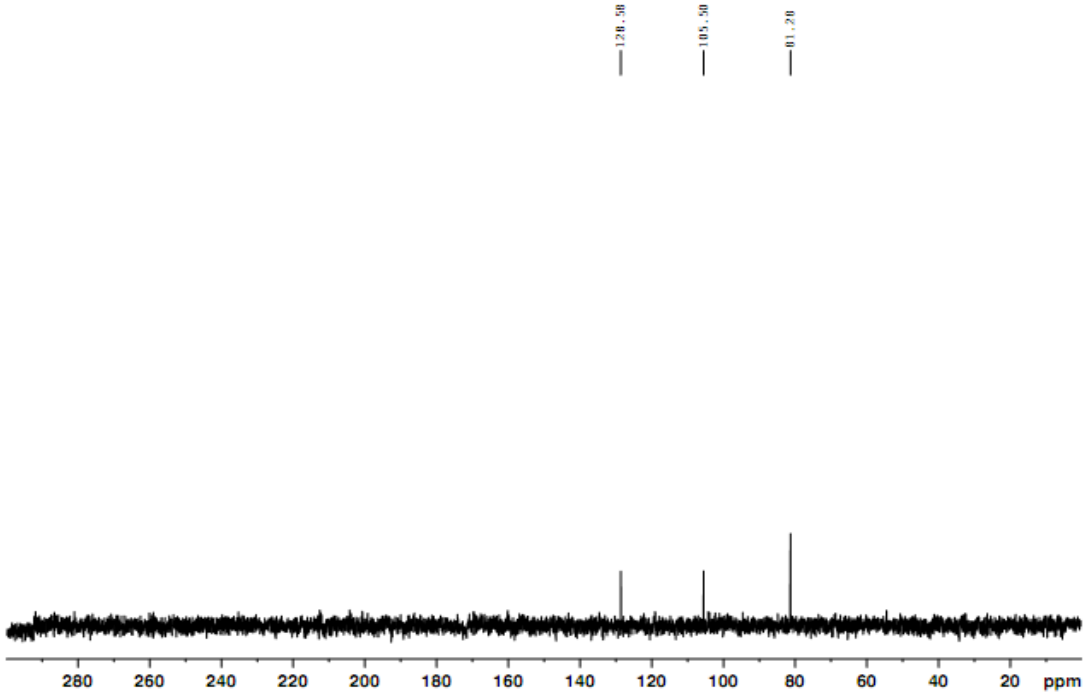

IR 168•Cl⁻

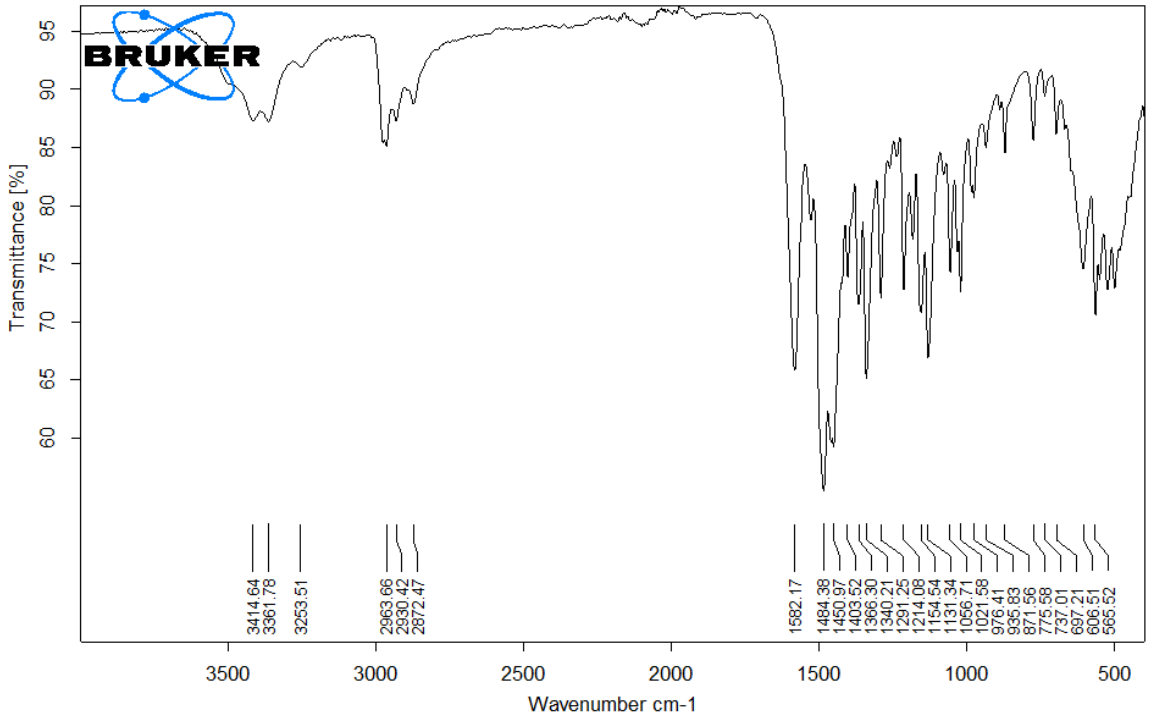
BRUKER
Transmittance [%]
95
90
85
80
75
70
65
60
3414.64
3361.78
3253.51
2963.66
2930.42
2872.47
1582.17
1484.38
1450.97
1403.52
1366.30
1340.21
1291.25
1214.08
1154.54
1131.34
1056.71
1021.58
976.41
935.83
871.56
775.58
737.01
697.21
606.51
565.52
3500
3000
2500
2000
1500
1000
500
Wavenumber cm-1

^{1}H NMR 168•$AuCl_4^-$

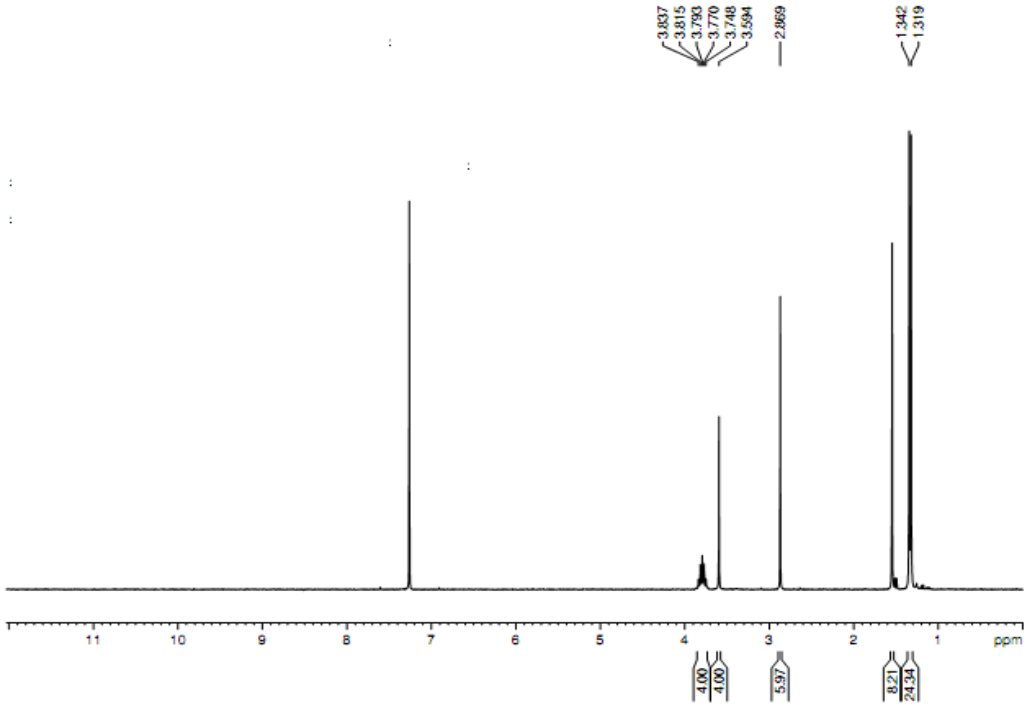

^{13}C NMR 168•$AuCl_4^-$

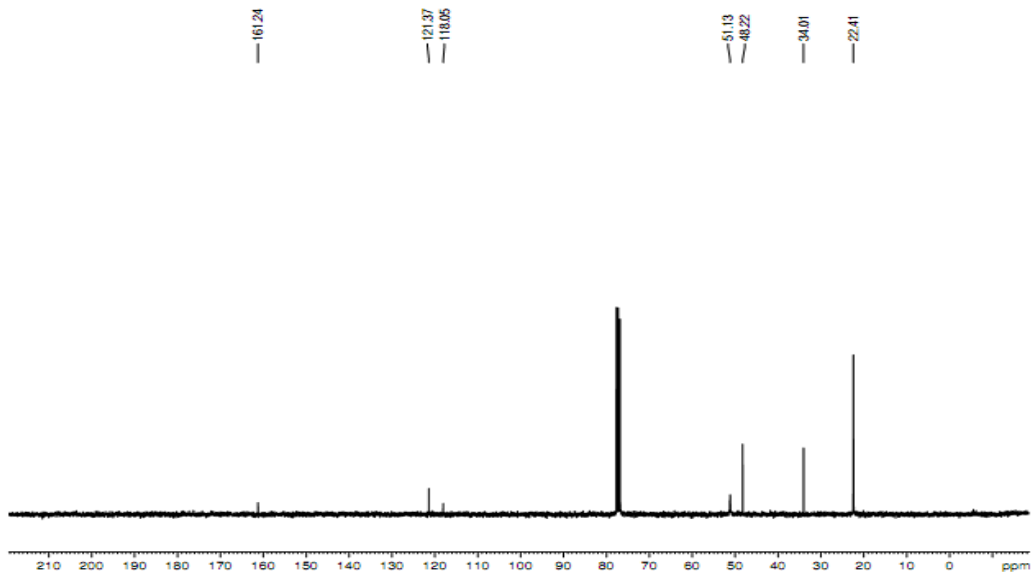

IR 168•$AuCl_4^-$

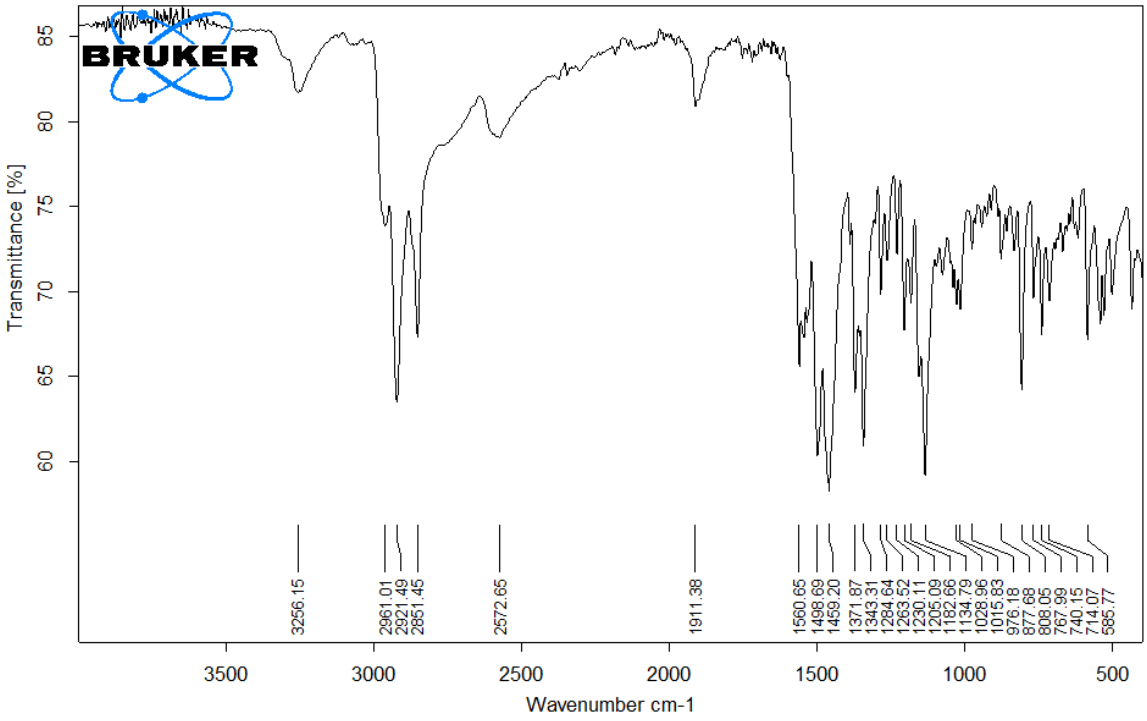
BRUKER
Transmittance [%]
85
80
75
70
65
60
3256.15
2961.01
2921.49
2851.45
2572.65
1911.38
1560.65
1498.69
1459.20
1371.87
1343.31
1284.64
1263.52
1230.11
1205.09
1182.66
1134.79
1028.96
1015.83
976.18
877.68
808.05
767.99
740.15
714.07
585.77
3500
3000
2500
2000
1500
1000
500
Wavenumber cm-1

^{1}H NMR 168•(TFA)$_3$Cl$^-$

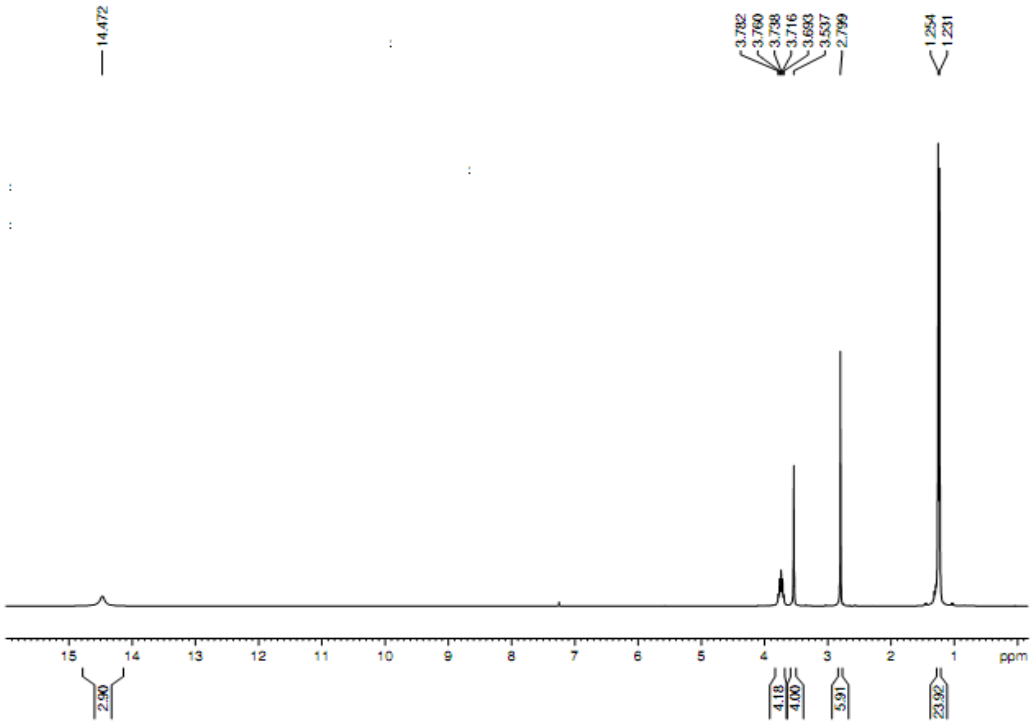

^{13}C NMR 168•(TFA)$_3$Cl$^-$

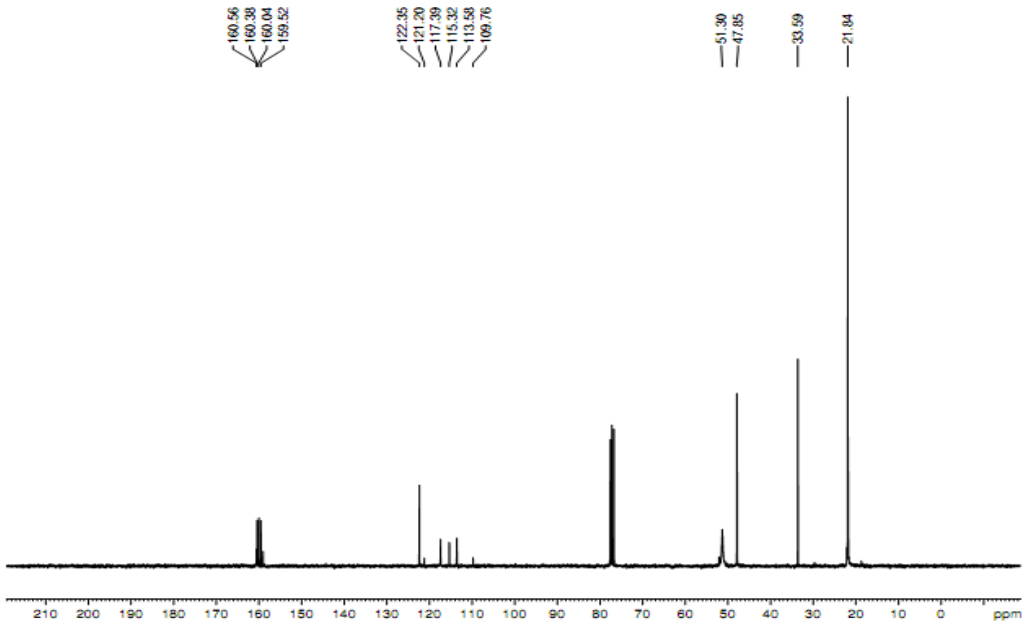

^{15}N NMR 168•$(TFA)_3Cl^-$

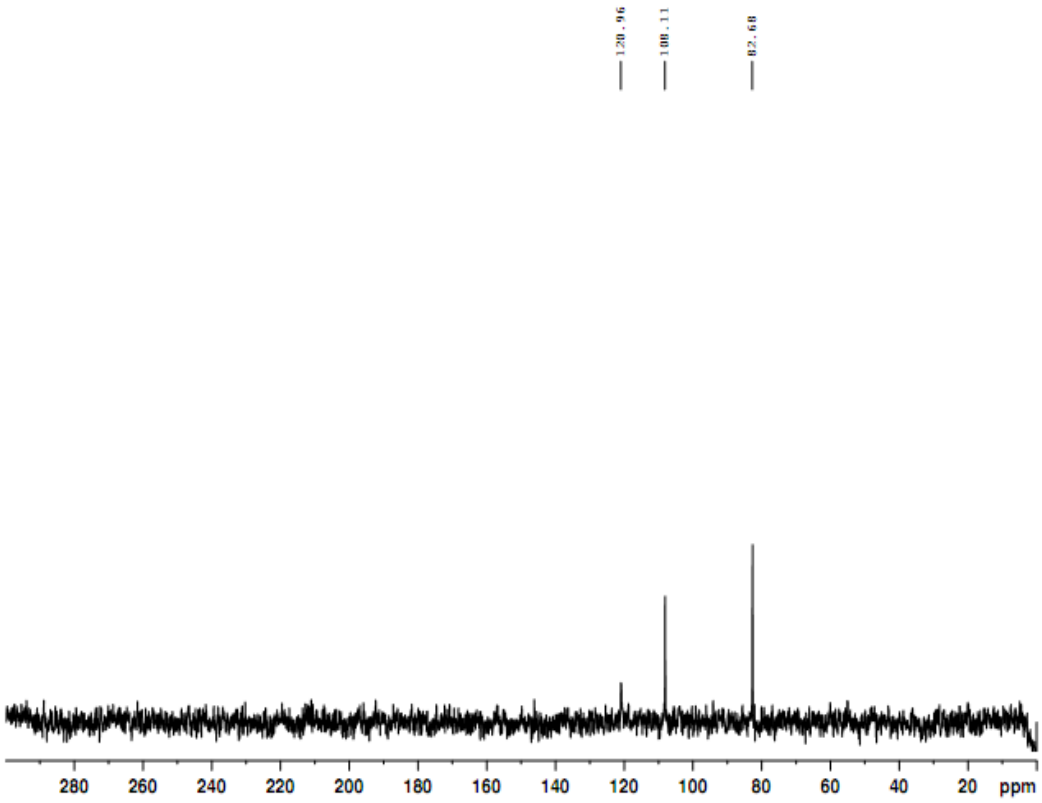

^{1}H NMR 170

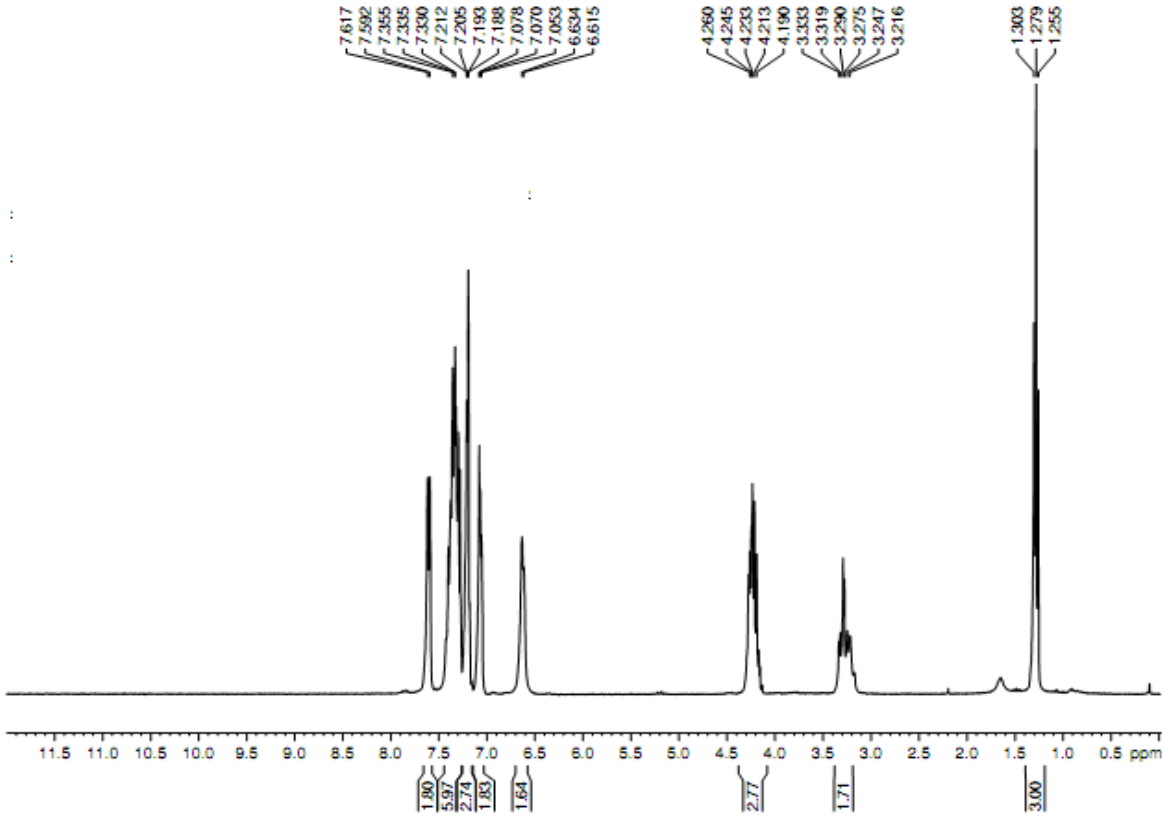

^{13}C NMR 170

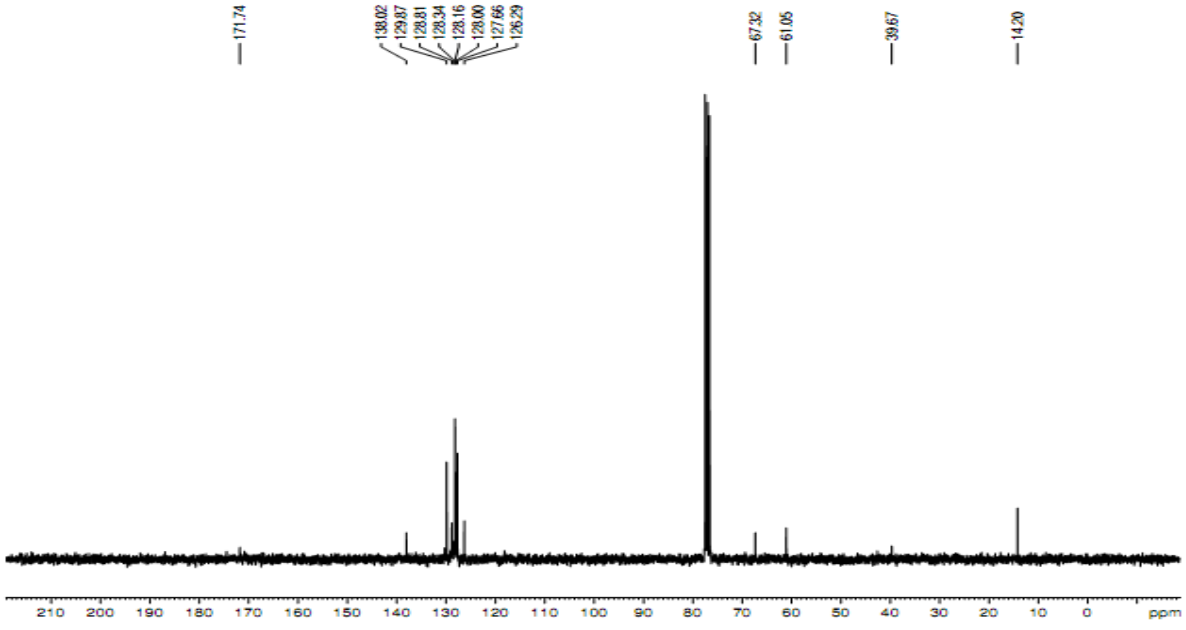

^{1}H NMR 172

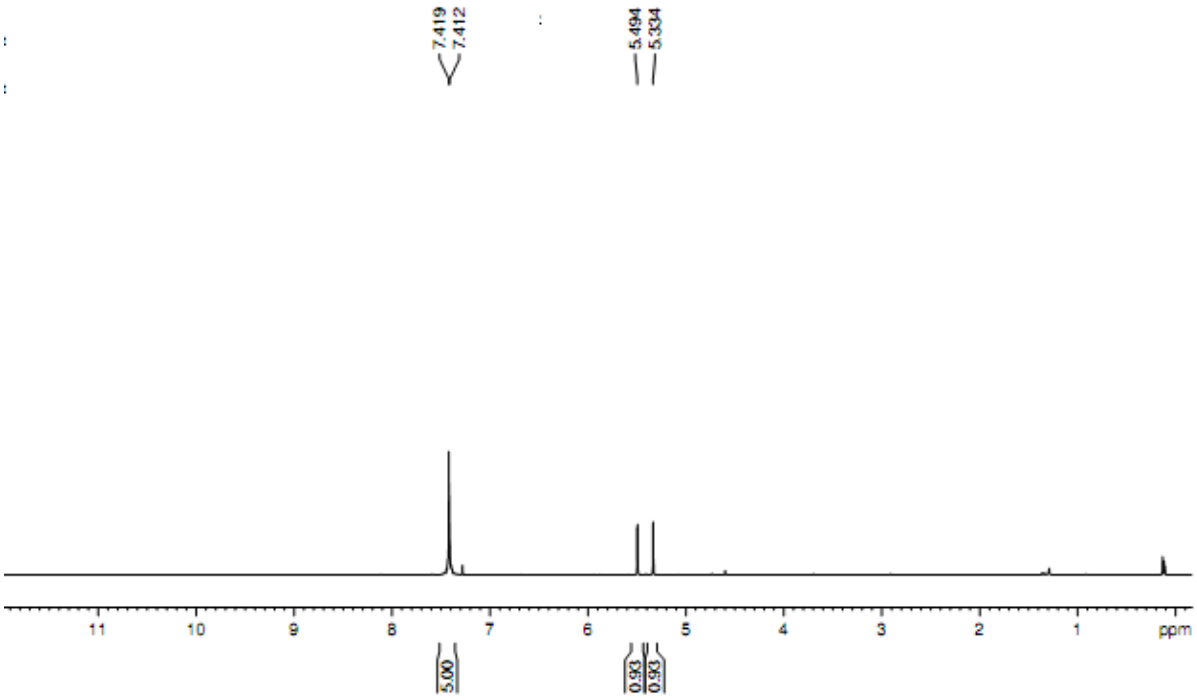

^{19}F NMR 172

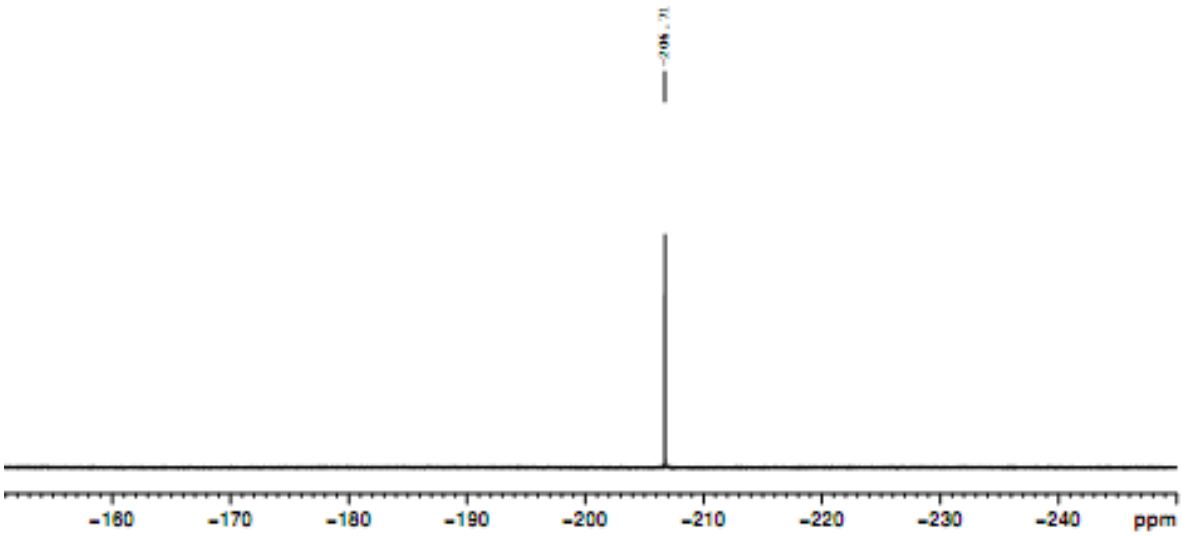

[1]H NMR 173

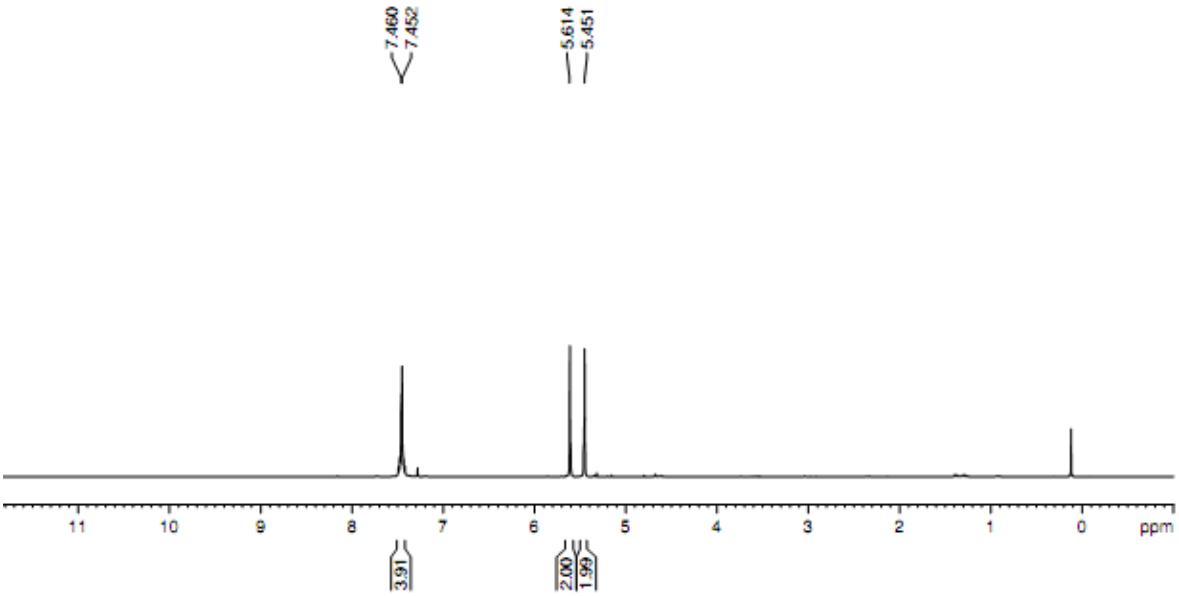

[13]C NMR 173

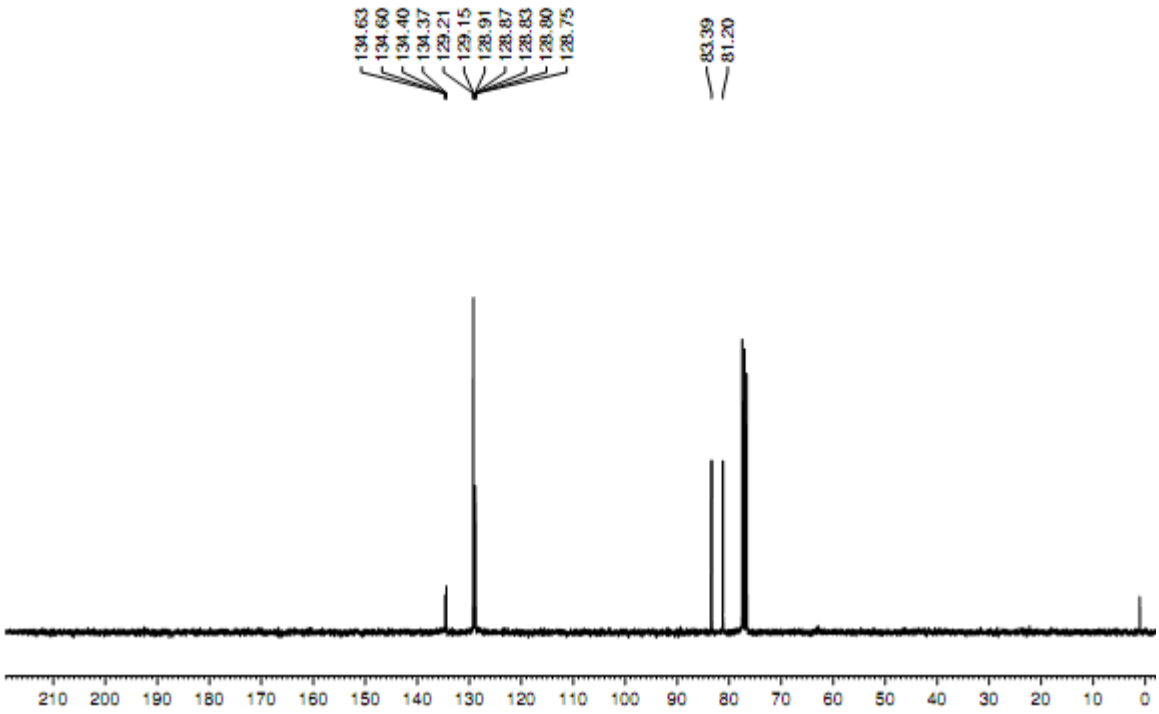

^{19}F NMR 173

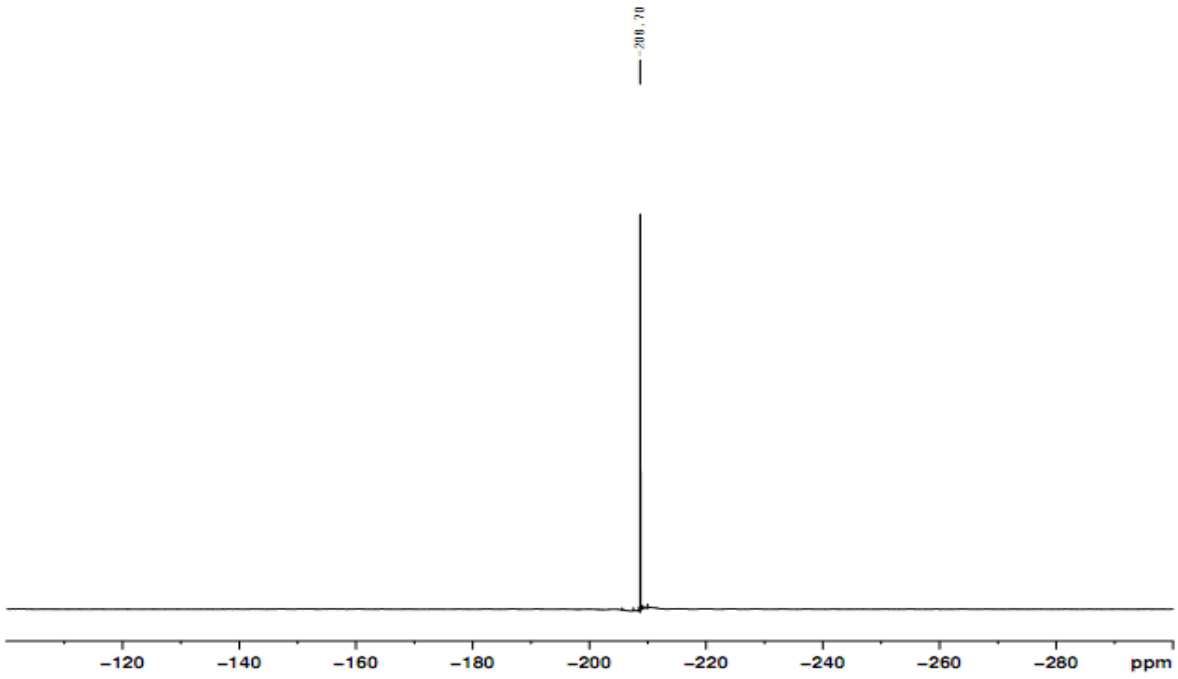

1H NMR 174

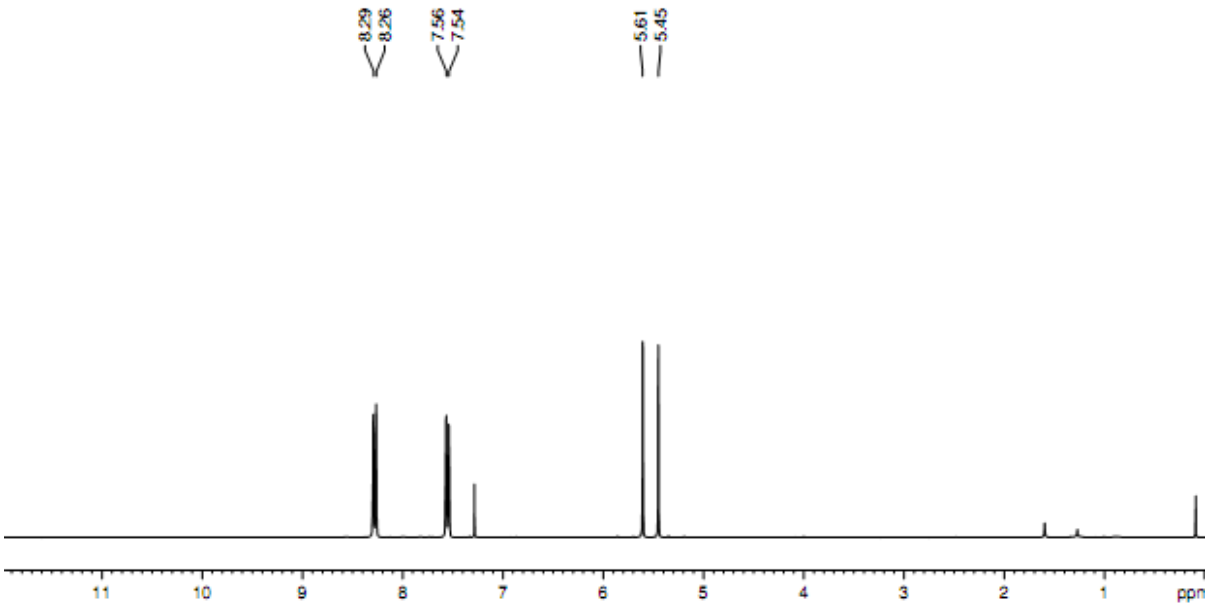

^{13}C NMR 174

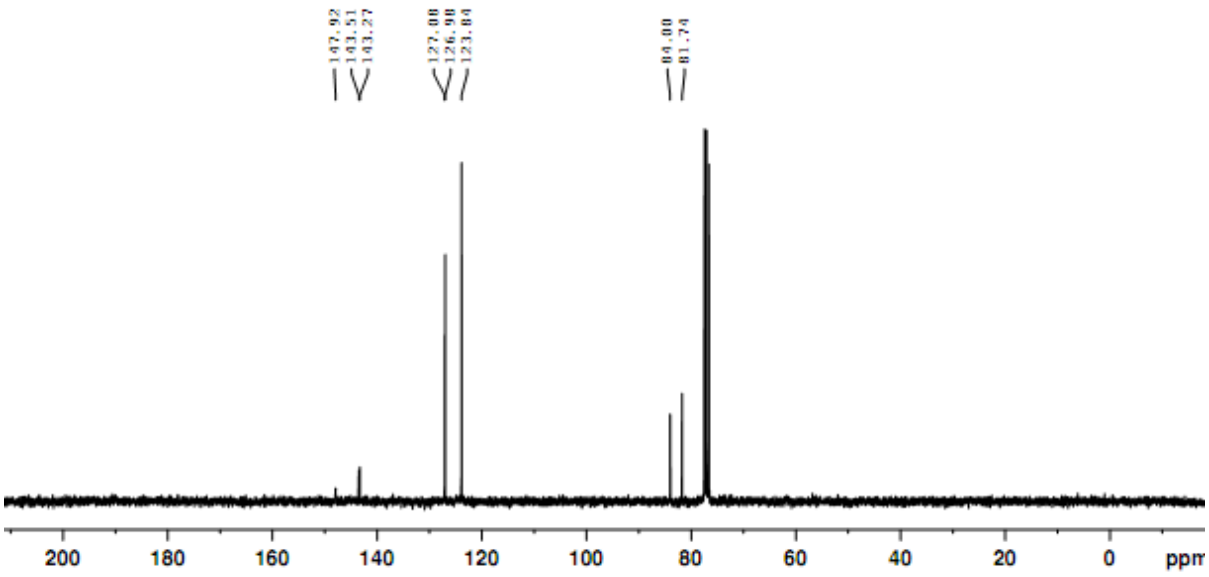

^{19}F NMR 174

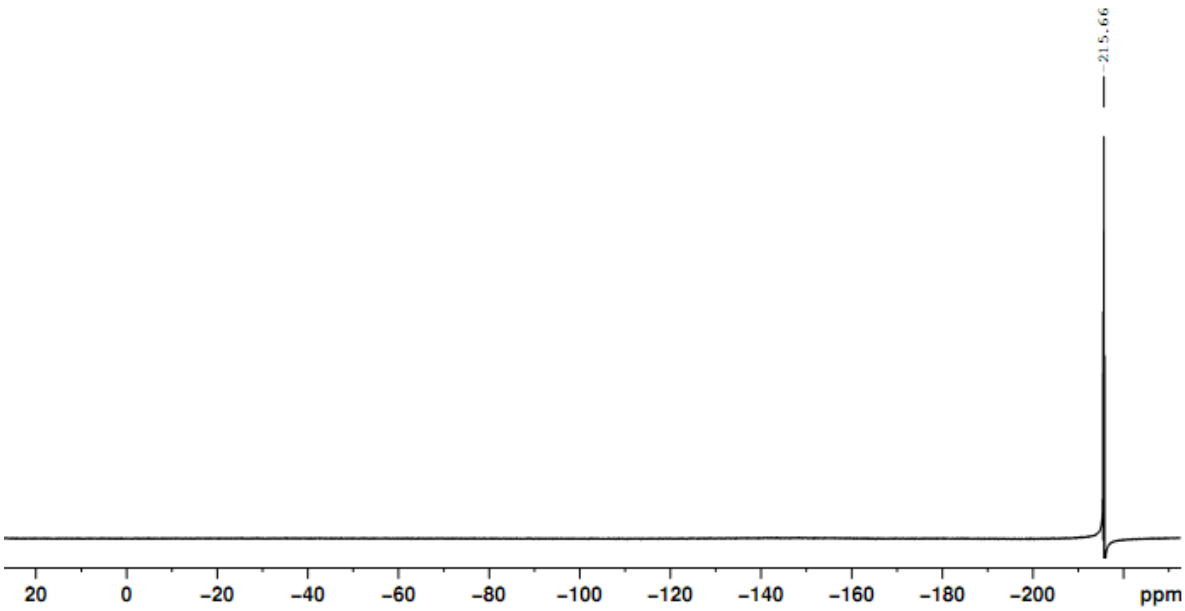

^{1}H NMR 175

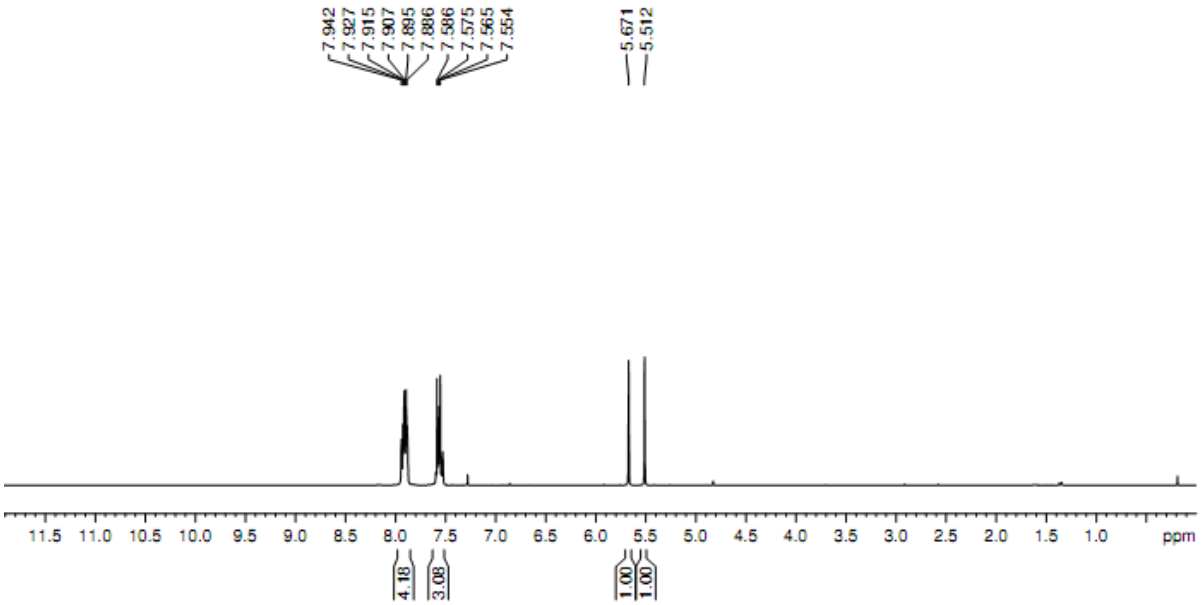

^{13}C NMR 175

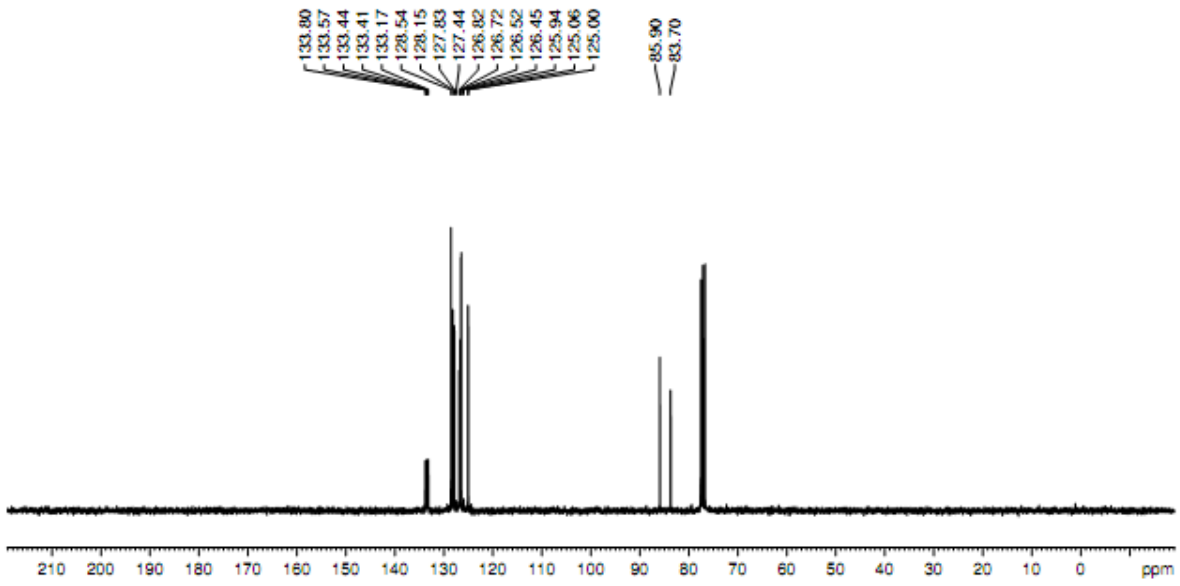

^{19}F NMR 175

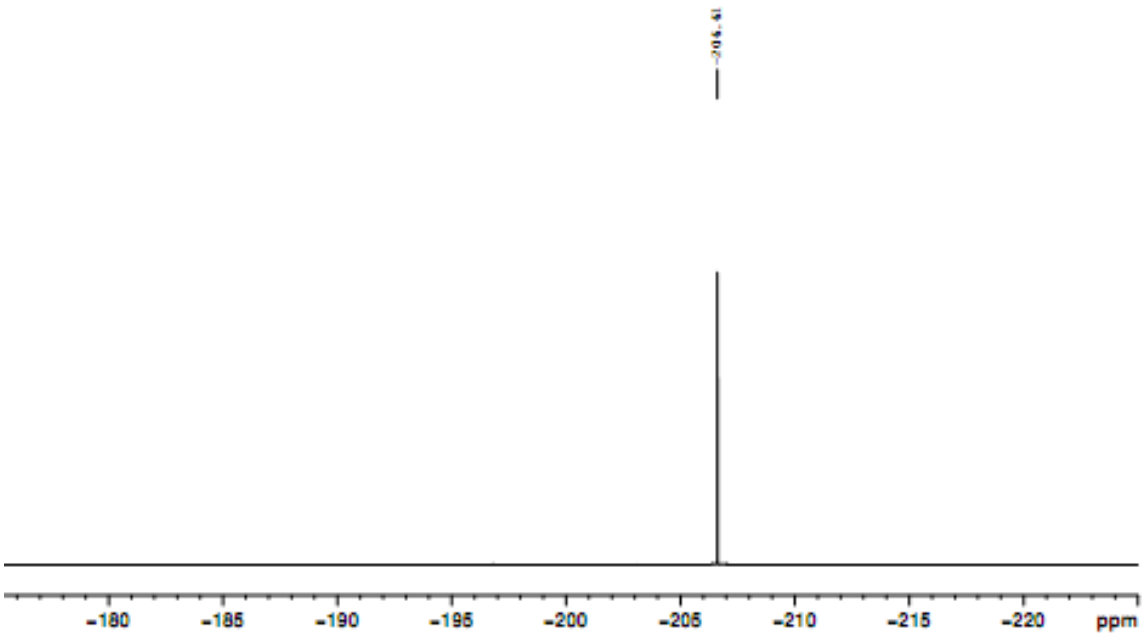

Appendix A. X-ray Crystallographic Data for 168•$AuCl_4^-$.

```
data_rm06495

#
==========================================================================
===== #

_audit_creation_method            'SHELXL-97, manual editing plus
enCIFer'
_audit_creation_date              '19 November 2013'

#
==========================================================================
===== #

_chemical_name_systematic
;
 ?
;
_chemical_name_common             ?
_chemical_melting_point           ?
_chemical_formula_moiety          'C20 H38 N5, Au Cl4'
_chemical_formula_sum             'C20 H38 Au Cl4 N5'
_chemical_formula_weight          687.32

loop_
 _atom_type_symbol
 _atom_type_description
 _atom_type_scat_dispersion_real
 _atom_type_scat_dispersion_imag
 _atom_type_scat_source
 'C'  'C'   0.0033   0.0016
 'International Tables Vol C Tables 4.2.6.8 and 6.1.1.4'
 'H'  'H'   0.0000   0.0000
 'International Tables Vol C Tables 4.2.6.8 and 6.1.1.4'
 'Au'  'Au'  -2.0133   8.8022
 'International Tables Vol C Tables 4.2.6.8 and 6.1.1.4'
 'Cl'  'Cl'   0.1484   0.1585
 'International Tables Vol C Tables 4.2.6.8 and 6.1.1.4'
 'N'  'N'   0.0061   0.0033
 'International Tables Vol C Tables 4.2.6.8 and 6.1.1.4'

_symmetry_cell_setting            Triclinic
_symmetry_space_group_name_H-M    'P -1'
_symmetry_space_group_name_Hall   '-P 1'

loop_
 _symmetry_equiv_pos_as_xyz
 'x, y, z'
 '-x, -y, -z'
```

```
_cell_length_a                    8.9016(6)
_cell_length_b                    12.9340(9)
_cell_length_c                    13.6174(9)
_cell_angle_alpha                 63.626(3)
_cell_angle_beta                  78.563(3)
_cell_angle_gamma                 80.061(3)
_cell_volume                      1370.35(16)
_cell_formula_units_Z             2
_cell_measurement_temperature     150(2)
_cell_measurement_reflns_used     9749
_cell_measurement_theta_min       2.65
_cell_measurement_theta_max       33.45

_exptl_crystal_description        prism
_exptl_crystal_colour             orange
_exptl_crystal_size_max           0.42
_exptl_crystal_size_mid           0.35
_exptl_crystal_size_min           0.28
_exptl_crystal_density_meas       ?
_exptl_crystal_density_diffrn     1.666
_exptl_crystal_density_method     'not measured'
_exptl_crystal_F_000              680
_exptl_absorpt_coefficient_mu     5.774
_exptl_absorpt_correction_type    multi-scan
_exptl_absorpt_correction_T_min   0.1953
_exptl_absorpt_correction_T_max   0.2947
_exptl_absorpt_process_details
;
 SADABS (Sheldrick, 1997)
;

_exptl_special_details
;
 ?
;

_diffrn_ambient_temperature       150(2)
_diffrn_radiation_wavelength      0.71073
_diffrn_radiation_type            MoK\a
_diffrn_radiation_source          'fine-focus sealed tube'
_diffrn_radiation_monochromator   graphite
_diffrn_measurement_device_type   'Bruker X8 Kappa CCD APEX II'
_diffrn_measurement_method        '\f and \w scans'
_diffrn_detector_area_resol_mean  ?
_diffrn_standards_number          ?
_diffrn_standards_interval_count  ?
_diffrn_standards_interval_time   ?
_diffrn_standards_decay_%         ?
_diffrn_reflns_number             34973
_diffrn_reflns_av_R_equivalents   0.0314
_diffrn_reflns_av_sigmaI/netI     0.0220
```

```
_diffrn_reflns_limit_h_min        -11
_diffrn_reflns_limit_h_max        11
_diffrn_reflns_limit_k_min        -16
_diffrn_reflns_limit_k_max        16
_diffrn_reflns_limit_l_min        -17
_diffrn_reflns_limit_l_max        17
_diffrn_reflns_theta_min          3.70
_diffrn_reflns_theta_max          27.48
_reflns_number_total              6230
_reflns_number_gt                 5924
_reflns_threshold_expression      >2sigma(I)

_computing_data_collection        'APEX2 (Bruker, 2006)'
_computing_cell_refinement        'APEX2 '
_computing_data_reduction         'SAINT+ (Bruker, 1997-2005)'
_computing_structure_solution     'SHELXTL (Bruker 2001)'
_computing_structure_refinement   'SHELXTL '
_computing_molecular_graphics     'SHELXTL '
_computing_publication_material   'SHELXTL '

_refine_special_details
;
 Refinement of F^2^ against ALL reflections.  The weighted R-factor
wR and
 goodness of fit S are based on F^2^, conventional R-factors R are
based
 on F, with F set to zero for negative F^2^. The threshold
expression of
 F^2^ > 2sigma(F^2^) is used only for calculating R-factors(gt) etc.
and is
 not relevant to the choice of reflections for refinement.  R-
factors based
 on F^2^ are statistically about twice as large as those based on F,
and R-
 factors based on ALL data will be even larger.
;

_refine_ls_structure_factor_coef  Fsqd
_refine_ls_matrix_type            full
_refine_ls_weighting_scheme       calc
_refine_ls_weighting_details
 'calc w=1/[\s^2^(Fo^2^)+(0.0000P)^2^+2.6768P] where
P=(Fo^2^+2Fc^2^)/3'
_atom_sites_solution_primary      direct
_atom_sites_solution_secondary    difmap
_atom_sites_solution_hydrogens    geom
_refine_ls_hydrogen_treatment     constr
_refine_ls_extinction_method      none
_refine_ls_extinction_coef        ?
_refine_ls_number_reflns          6230
_refine_ls_number_parameters      281
_refine_ls_number_restraints      0
```

```
_refine_ls_R_factor_all          0.0256
_refine_ls_R_factor_gt           0.0233
_refine_ls_wR_factor_ref         0.0513
_refine_ls_wR_factor_gt          0.0499
_refine_ls_goodness_of_fit_ref   1.195
_refine_ls_restrained_S_all      1.195
_refine_ls_shift/su_max          0.001
_refine_ls_shift/su_mean         0.000

loop_
 _atom_site_label
 _atom_site_type_symbol
 _atom_site_fract_x
 _atom_site_fract_y
 _atom_site_fract_z
 _atom_site_U_iso_or_equiv
 _atom_site_adp_type
 _atom_site_occupancy
 _atom_site_symmetry_multiplicity
 _atom_site_calc_flag
 _atom_site_refinement_flags
 _atom_site_disorder_assembly
 _atom_site_disorder_group
N1 N 0.1436(3) 0.7280(2) 0.5409(2) 0.0254(5) Uani 1 1 d . . .
N2 N 0.1987(3) 0.6264(2) 0.7132(2) 0.0239(5) Uani 1 1 d . . .
N3 N 0.1752(3) 0.52856(19) 0.60249(18) 0.0189(5) Uani 1 1 d . . .
N4 N -0.0497(3) 0.31000(19) 0.84480(19) 0.0205(5) Uani 1 1 d . . .
N5 N 0.3052(3) 0.22615(19) 0.68767(19) 0.0203(5) Uani 1 1 d . . .
C1 C 0.1578(3) 0.4201(2) 0.6807(2) 0.0168(5) Uani 1 1 d . . .
C2 C 0.0716(3) 0.3380(2) 0.7672(2) 0.0164(5) Uani 1 1 d . . .
C3 C 0.2041(3) 0.3046(2) 0.7088(2) 0.0165(5) Uani 1 1 d . . .
C8 C 0.2923(4) 0.5373(3) 0.7929(2) 0.0294(7) Uani 1 1 d . . .
H8A H 0.2678 0.4606 0.8066 0.044 Uiso 1 1 calc R . .
H8B H 0.2708 0.5461 0.8623 0.044 Uiso 1 1 calc R . .
H8C H 0.4016 0.5452 0.7633 0.044 Uiso 1 1 calc R . .
C5 C 0.2098(5) 0.7485(3) 0.6870(3) 0.0381(8) Uani 1 1 d . . .
H5A H 0.3186 0.7655 0.6705 0.046 Uiso 1 1 calc R . .
H5B H 0.1574 0.7679 0.7487 0.046 Uiso 1 1 calc R . .
C6 C 0.1286(5) 0.8138(3) 0.5856(3) 0.0375(8) Uani 1 1 d . . .
H6A H 0.0192 0.8369 0.6058 0.045 Uiso 1 1 calc R . .
H6B H 0.1797 0.8837 0.5322 0.045 Uiso 1 1 calc R . .
C12 C -0.0708(4) 0.1869(2) 0.9196(2) 0.0273(6) Uani 1 1 d . . .
H12 H 0.0284 0.1400 0.9106 0.033 Uiso 1 1 calc R . .
C14 C -0.1943(5) 0.1453(3) 0.8864(3) 0.0459(10) Uani 1 1 d . . .
H14A H -0.2940 0.1876 0.8972 0.069 Uiso 1 1 calc R . .
H14B H -0.2001 0.0621 0.9323 0.069 Uiso 1 1 calc R . .
H14C H -0.1682 0.1595 0.8084 0.069 Uiso 1 1 calc R . .
C13 C -0.1053(4) 0.1674(3) 1.0399(2) 0.0298(7) Uani 1 1 d . . .
H13A H -0.0264 0.1989 1.0570 0.045 Uiso 1 1 calc R . .
H13B H -0.1051 0.0841 1.0875 0.045 Uiso 1 1 calc R . .
H13C H -0.2066 0.2067 1.0528 0.045 Uiso 1 1 calc R . .
C18 C 0.4453(3) 0.2683(2) 0.6080(2) 0.0206(5) Uani 1 1 d . . .
```

```
H18 H 0.5143 0.1991 0.6068 0.025 Uiso 1 1 calc R . .
C19 C 0.5326(4) 0.3337(3) 0.6446(3) 0.0300(7) Uani 1 1 d . . .
H19A H 0.4692 0.4041 0.6434 0.045 Uiso 1 1 calc R . .
H19B H 0.6288 0.3550 0.5942 0.045 Uiso 1 1 calc R . .
H19C H 0.5561 0.2842 0.7199 0.045 Uiso 1 1 calc R . .
C20 C 0.4042(4) 0.3417(3) 0.4922(2) 0.0289(6) Uani 1 1 d . . .
H20A H 0.3525 0.2959 0.4702 0.043 Uiso 1 1 calc R . .
H20B H 0.4983 0.3667 0.4404 0.043 Uiso 1 1 calc R . .
H20C H 0.3354 0.4099 0.4912 0.043 Uiso 1 1 calc R . .
C15 C 0.2952(3) 0.1004(2) 0.7537(2) 0.0240(6) Uani 1 1 d . . .
H15 H 0.1919 0.0901 0.8002 0.029 Uiso 1 1 calc R . .
C17 C 0.3045(4) 0.0389(3) 0.6790(3) 0.0330(7) Uani 1 1 d . . .
H17A H 0.2227 0.0738 0.6319 0.050 Uiso 1 1 calc R . .
H17B H 0.2918 -0.0435 0.7248 0.050 Uiso 1 1 calc R . .
H17C H 0.4050 0.0470 0.6325 0.050 Uiso 1 1 calc R . .
C16 C 0.4158(4) 0.0474(3) 0.8317(3) 0.0342(7) Uani 1 1 d . . .
H16A H 0.5187 0.0568 0.7886 0.051 Uiso 1 1 calc R . .
H16B H 0.4039 -0.0353 0.8762 0.051 Uiso 1 1 calc R . .
H16C H 0.4026 0.0864 0.8806 0.051 Uiso 1 1 calc R . .
C9 C -0.1680(3) 0.4026(2) 0.8547(2) 0.0211(5) Uani 1 1 d . . .
H9 H -0.2598 0.3640 0.9049 0.025 Uiso 1 1 calc R . .
C11 C -0.2198(4) 0.4845(3) 0.7435(3) 0.0283(6) Uani 1 1 d . . .
H11A H -0.1329 0.5255 0.6930 0.042 Uiso 1 1 calc R . .
H11B H -0.3030 0.5409 0.7536 0.042 Uiso 1 1 calc R . .
H11C H -0.2570 0.4400 0.7123 0.042 Uiso 1 1 calc R . .
C10 C -0.1106(4) 0.4674(3) 0.9078(3) 0.0307(7) Uani 1 1 d . . .
H10A H -0.0688 0.4115 0.9754 0.046 Uiso 1 1 calc R . .
H10B H -0.1963 0.5174 0.9262 0.046 Uiso 1 1 calc R . .
H10C H -0.0298 0.5150 0.8559 0.046 Uiso 1 1 calc R . .
C7 C 0.0535(4) 0.7479(3) 0.4548(3) 0.0345(7) Uani 1 1 d . . .
H7A H 0.0747 0.6817 0.4356 0.052 Uiso 1 1 calc R . .
H7B H 0.0815 0.8185 0.3891 0.052 Uiso 1 1 calc R . .
H7C H -0.0563 0.7569 0.4817 0.052 Uiso 1 1 calc R . .
C4 C 0.1704(3) 0.6197(2) 0.6215(2) 0.0188(5) Uani 1 1 d . . .
Au1 Au 0.319608(13) 0.194938(10) 0.174595(10) 0.02571(4) Uani 1 1 d
. . .
Cl1 Cl 0.14960(11) 0.05653(7) 0.25099(6) 0.03515(18) Uani 1 1 d . .
.
Cl2 Cl 0.29953(11) 0.21999(8) 0.00097(7) 0.0413(2) Uani 1 1 d . . .
Cl3 Cl 0.49165(10) 0.33118(9) 0.09825(10) 0.0498(2) Uani 1 1 d . . .
Cl4 Cl 0.34029(12) 0.17112(10) 0.34723(8) 0.0523(3) Uani 1 1 d . . .

loop_
 _atom_site_aniso_label
 _atom_site_aniso_U_11
 _atom_site_aniso_U_22
 _atom_site_aniso_U_33
 _atom_site_aniso_U_23
 _atom_site_aniso_U_13
 _atom_site_aniso_U_12
N1 0.0299(14) 0.0128(11) 0.0279(13) -0.0062(10) 0.0004(10) -
0.0004(10)
```

```
N2 0.0281(13) 0.0209(12) 0.0263(12) -0.0140(10) 0.0005(10) -
0.0048(10)
N3 0.0243(12) 0.0127(10) 0.0165(10) -0.0042(9) 0.0008(9) -0.0031(9)
N4 0.0195(12) 0.0138(11) 0.0208(11) -0.0050(9) 0.0059(9) 0.0001(9)
N5 0.0189(12) 0.0115(10) 0.0245(12) -0.0064(9) 0.0077(9) -0.0024(8)
C1 0.0172(13) 0.0171(12) 0.0165(12) -0.0082(10) 0.0001(10) -
0.0021(10)
C2 0.0178(13) 0.0138(12) 0.0157(12) -0.0056(10) -0.0013(10)
0.0003(10)
C3 0.0162(13) 0.0142(12) 0.0174(12) -0.0050(10) 0.0011(10) -
0.0054(10)
C8 0.0299(17) 0.0372(17) 0.0261(15) -0.0174(14) -0.0024(12) -
0.0066(13)
C5 0.048(2) 0.0283(17) 0.047(2) -0.0265(16) 0.0028(16) -0.0095(15)
C6 0.048(2) 0.0161(14) 0.046(2) -0.0165(14) 0.0047(16) -0.0010(14)
C12 0.0305(17) 0.0150(13) 0.0235(14) -0.0022(11) 0.0094(12) -
0.0017(11)
C14 0.079(3) 0.0333(19) 0.0260(16) -0.0111(15) 0.0043(17) -
0.0261(19)
C13 0.0285(17) 0.0302(16) 0.0204(14) -0.0013(12) -0.0010(12) -
0.0068(13)
C18 0.0178(14) 0.0170(13) 0.0227(13) -0.0082(11) 0.0061(10) -
0.0018(10)
C19 0.0204(15) 0.0394(18) 0.0317(16) -0.0177(14) 0.0051(12) -
0.0092(13)
C20 0.0318(17) 0.0314(16) 0.0218(14) -0.0116(13) 0.0058(12) -
0.0089(13)
C15 0.0248(15) 0.0110(12) 0.0285(15) -0.0059(11) 0.0072(12) -
0.0023(11)
C17 0.0390(19) 0.0171(14) 0.0411(18) -0.0117(13) -0.0032(15) -
0.0024(13)
C16 0.045(2) 0.0208(15) 0.0268(16) -0.0043(13) -0.0024(14)
0.0021(14)
C9 0.0166(13) 0.0192(13) 0.0239(13) -0.0096(11) 0.0036(10)
0.0014(10)
C11 0.0247(16) 0.0264(15) 0.0295(15) -0.0100(13) -0.0051(12)
0.0045(12)
C10 0.0305(17) 0.0310(16) 0.0339(17) -0.0201(14) -0.0011(13)
0.0024(13)
C7 0.0346(19) 0.0250(16) 0.0300(16) -0.0007(13) -0.0064(14)
0.0032(13)
C4 0.0152(13) 0.0178(13) 0.0214(13) -0.0089(11) 0.0048(10) -
0.0035(10)
Au1 0.02201(6) 0.02434(6) 0.03697(7) -0.01989(5) -0.00661(5)
0.00450(4)
Cl1 0.0474(5) 0.0288(4) 0.0305(4) -0.0139(3) 0.0009(3) -0.0106(3)
Cl2 0.0431(5) 0.0506(5) 0.0272(4) -0.0109(4) -0.0046(3) -0.0128(4)
Cl3 0.0269(4) 0.0524(5) 0.0858(7) -0.0466(5) 0.0079(4) -0.0125(4)
Cl4 0.0464(6) 0.0831(7) 0.0522(5) -0.0517(6) -0.0142(4) 0.0049(5)

_geom_special_details
;
```

```
 All esds (except the esd in the dihedral angle between two l.s.
planes)
 are estimated using the full covariance matrix.  The cell esds are
taken
 into account individually in the estimation of esds in distances,
angles
 and torsion angles; correlations between esds in cell parameters
are only
 used when they are defined by crystal symmetry.  An approximate
(isotropic)
 treatment of cell esds is used for estimating esds involving l.s.
planes.
;

loop_
 _geom_bond_atom_site_label_1
 _geom_bond_atom_site_label_2
 _geom_bond_distance
 _geom_bond_site_symmetry_2
 _geom_bond_publ_flag
N1 C4 1.359(4) . ?
N1 C7 1.454(4) . ?
N1 C6 1.462(4) . ?
N2 C4 1.363(4) . ?
N2 C8 1.455(4) . ?
N2 C5 1.472(4) . ?
N3 C4 1.307(3) . ?
N3 C1 1.344(3) . ?
N4 C2 1.326(3) . ?
N4 C12 1.481(3) . ?
N4 C9 1.487(3) . ?
N5 C3 1.328(3) . ?
N5 C15 1.477(3) . ?
N5 C18 1.484(3) . ?
C1 C3 1.374(4) . ?
C1 C2 1.384(4) . ?
C2 C3 1.402(4) . ?
C8 H8A 0.9800 . ?
C8 H8B 0.9800 . ?
C8 H8C 0.9800 . ?
C5 C6 1.514(5) . ?
C5 H5A 0.9900 . ?
C5 H5B 0.9900 . ?
C6 H6A 0.9900 . ?
C6 H6B 0.9900 . ?
C12 C13 1.517(4) . ?
C12 C14 1.522(5) . ?
C12 H12 1.0000 . ?
C14 H14A 0.9800 . ?
C14 H14B 0.9800 . ?
C14 H14C 0.9800 . ?
C13 H13A 0.9800 . ?
```

```
C13 H13B 0.9800 . ?
C13 H13C 0.9800 . ?
C18 C20 1.516(4) . ?
C18 C19 1.525(4) . ?
C18 H18 1.0000 . ?
C19 H19A 0.9800 . ?
C19 H19B 0.9800 . ?
C19 H19C 0.9800 . ?
C20 H20A 0.9800 . ?
C20 H20B 0.9800 . ?
C20 H20C 0.9800 . ?
C15 C16 1.517(5) . ?
C15 C17 1.528(4) . ?
C15 H15 1.0000 . ?
C17 H17A 0.9800 . ?
C17 H17B 0.9800 . ?
C17 H17C 0.9800 . ?
C16 H16A 0.9800 . ?
C16 H16B 0.9800 . ?
C16 H16C 0.9800 . ?
C9 C11 1.520(4) . ?
C9 C10 1.523(4) . ?
C9 H9 1.0000 . ?
C11 H11A 0.9800 . ?
C11 H11B 0.9800 . ?
C11 H11C 0.9800 . ?
C10 H10A 0.9800 . ?
C10 H10B 0.9800 . ?
C10 H10C 0.9800 . ?
C7 H7A 0.9800 . ?
C7 H7B 0.9800 . ?
C7 H7C 0.9800 . ?
Au1 Cl4 2.2725(9) . ?
Au1 Cl2 2.2790(8) . ?
Au1 Cl3 2.2812(9) . ?
Au1 Cl1 2.2877(8) . ?

loop_
 _geom_angle_atom_site_label_1
 _geom_angle_atom_site_label_2
 _geom_angle_atom_site_label_3
 _geom_angle
 _geom_angle_site_symmetry_1
 _geom_angle_site_symmetry_3
 _geom_angle_publ_flag
C4 N1 C7 120.7(2) . . ?
C4 N1 C6 109.9(2) . . ?
C7 N1 C6 119.7(3) . . ?
C4 N2 C8 123.4(2) . . ?
C4 N2 C5 109.0(2) . . ?
C8 N2 C5 118.2(3) . . ?
C4 N3 C1 125.2(2) . . ?
```

```
C2 N4 C12 120.4(2) . . ?
C2 N4 C9 119.8(2) . . ?
C12 N4 C9 119.7(2) . . ?
C3 N5 C15 122.1(2) . . ?
C3 N5 C18 117.2(2) . . ?
C15 N5 C18 119.8(2) . . ?
N3 C1 C3 144.8(3) . . ?
N3 C1 C2 151.9(3) . . ?
C3 C1 C2 61.11(18) . . ?
N4 C2 C1 150.9(3) . . ?
N4 C2 C3 149.9(2) . . ?
C1 C2 C3 59.10(18) . . ?
N5 C3 C1 147.3(3) . . ?
N5 C3 C2 152.9(2) . . ?
C1 C3 C2 59.79(19) . . ?
N2 C8 H8A 109.5 . . ?
N2 C8 H8B 109.5 . . ?
H8A C8 H8B 109.5 . . ?
N2 C8 H8C 109.5 . . ?
H8A C8 H8C 109.5 . . ?
H8B C8 H8C 109.5 . . ?
N2 C5 C6 102.8(2) . . ?
N2 C5 H5A 111.2 . . ?
C6 C5 H5A 111.2 . . ?
N2 C5 H5B 111.2 . . ?
C6 C5 H5B 111.2 . . ?
H5A C5 H5B 109.1 . . ?
N1 C6 C5 102.2(2) . . ?
N1 C6 H6A 111.3 . . ?
C5 C6 H6A 111.3 . . ?
N1 C6 H6B 111.3 . . ?
C5 C6 H6B 111.3 . . ?
H6A C6 H6B 109.2 . . ?
N4 C12 C13 111.5(2) . . ?
N4 C12 C14 110.6(3) . . ?
C13 C12 C14 111.9(3) . . ?
N4 C12 H12 107.6 . . ?
C13 C12 H12 107.6 . . ?
C14 C12 H12 107.6 . . ?
C12 C14 H14A 109.5 . . ?
C12 C14 H14B 109.5 . . ?
H14A C14 H14B 109.5 . . ?
C12 C14 H14C 109.5 . . ?
H14A C14 H14C 109.5 . . ?
H14B C14 H14C 109.5 . . ?
C12 C13 H13A 109.5 . . ?
C12 C13 H13B 109.5 . . ?
H13A C13 H13B 109.5 . . ?
C12 C13 H13C 109.5 . . ?
H13A C13 H13C 109.5 . . ?
H13B C13 H13C 109.5 . . ?
N5 C18 C20 110.6(2) . . ?
```

```
N5 C18 C19 111.1(2) . . ?
C20 C18 C19 111.7(2) . . ?
N5 C18 H18 107.7 . . ?
C20 C18 H18 107.7 . . ?
C19 C18 H18 107.7 . . ?
C18 C19 H19A 109.5 . . ?
C18 C19 H19B 109.5 . . ?
H19A C19 H19B 109.5 . . ?
C18 C19 H19C 109.5 . . ?
H19A C19 H19C 109.5 . . ?
H19B C19 H19C 109.5 . . ?
C18 C20 H20A 109.5 . . ?
C18 C20 H20B 109.5 . . ?
H20A C20 H20B 109.5 . . ?
C18 C20 H20C 109.5 . . ?
H20A C20 H20C 109.5 . . ?
H20B C20 H20C 109.5 . . ?
N5 C15 C16 111.3(2) . . ?
N5 C15 C17 111.0(2) . . ?
C16 C15 C17 112.0(3) . . ?
N5 C15 H15 107.4 . . ?
C16 C15 H15 107.4 . . ?
C17 C15 H15 107.4 . . ?
C15 C17 H17A 109.5 . . ?
C15 C17 H17B 109.5 . . ?
H17A C17 H17B 109.5 . . ?
C15 C17 H17C 109.5 . . ?
H17A C17 H17C 109.5 . . ?
H17B C17 H17C 109.5 . . ?
C15 C16 H16A 109.5 . . ?
C15 C16 H16B 109.5 . . ?
H16A C16 H16B 109.5 . . ?
C15 C16 H16C 109.5 . . ?
H16A C16 H16C 109.5 . . ?
H16B C16 H16C 109.5 . . ?
N4 C9 C11 111.4(2) . . ?
N4 C9 C10 111.1(2) . . ?
C11 C9 C10 111.7(2) . . ?
N4 C9 H9 107.5 . . ?
C11 C9 H9 107.5 . . ?
C10 C9 H9 107.5 . . ?
C9 C11 H11A 109.5 . . ?
C9 C11 H11B 109.5 . . ?
H11A C11 H11B 109.5 . . ?
C9 C11 H11C 109.5 . . ?
H11A C11 H11C 109.5 . . ?
H11B C11 H11C 109.5 . . ?
C9 C10 H10A 109.5 . . ?
C9 C10 H10B 109.5 . . ?
H10A C10 H10B 109.5 . . ?
C9 C10 H10C 109.5 . . ?
H10A C10 H10C 109.5 . . ?
```

```
H10B C10 H10C 109.5 . . ?
N1 C7 H7A 109.5 . . ?
N1 C7 H7B 109.5 . . ?
H7A C7 H7B 109.5 . . ?
N1 C7 H7C 109.5 . . ?
H7A C7 H7C 109.5 . . ?
H7B C7 H7C 109.5 . . ?
N3 C4 N1 120.5(2) . . ?
N3 C4 N2 129.4(3) . . ?
N1 C4 N2 110.0(2) . . ?
Cl4 Au1 Cl2 179.62(4) . . ?
Cl4 Au1 Cl3 90.79(4) . . ?
Cl2 Au1 Cl3 88.84(4) . . ?
Cl4 Au1 Cl1 89.31(4) . . ?
Cl2 Au1 Cl1 91.05(3) . . ?
Cl3 Au1 Cl1 179.25(3) . . ?

loop_
 _geom_torsion_atom_site_label_1
 _geom_torsion_atom_site_label_2
 _geom_torsion_atom_site_label_3
 _geom_torsion_atom_site_label_4
 _geom_torsion
 _geom_torsion_site_symmetry_1
 _geom_torsion_site_symmetry_2
 _geom_torsion_site_symmetry_3
 _geom_torsion_site_symmetry_4
 _geom_torsion_publ_flag
C4 N3 C1 C3 -144.8(4) . . . . ?
C4 N3 C1 C2 64.1(6) . . . . ?
C12 N4 C2 C1 -179.1(4) . . . . ?
C9 N4 C2 C1 2.7(6) . . . . ?
C12 N4 C2 C3 6.4(6) . . . . ?
C9 N4 C2 C3 -171.7(4) . . . . ?
N3 C1 C2 N4 -15.3(9) . . . . ?
C3 C1 C2 N4 -176.7(5) . . . . ?
N3 C1 C2 C3 161.4(5) . . . . ?
C15 N5 C3 C1 179.7(4) . . . . ?
C18 N5 C3 C1 10.4(6) . . . . ?
C15 N5 C3 C2 -2.6(7) . . . . ?
C18 N5 C3 C2 -171.9(5) . . . . ?
N3 C1 C3 N5 13.8(8) . . . . ?
C2 C1 C3 N5 178.8(5) . . . . ?
N3 C1 C3 C2 -164.9(5) . . . . ?
N4 C2 C3 N5 -1.7(9) . . . . ?
C1 C2 C3 N5 -178.6(6) . . . . ?
N4 C2 C3 C1 176.8(5) . . . . ?
C4 N2 C5 C6 19.9(3) . . . . ?
C8 N2 C5 C6 167.5(3) . . . . ?
C4 N1 C6 C5 21.2(3) . . . . ?
C7 N1 C6 C5 167.6(3) . . . . ?
N2 C5 C6 N1 -23.8(3) . . . . ?
```

```
C2 N4 C12 C13 130.6(3) . . . . ?
C9 N4 C12 C13 -51.2(4) . . . . ?
C2 N4 C12 C14 -104.2(3) . . . . ?
C9 N4 C12 C14 73.9(3) . . . . ?
C3 N5 C18 C20 -68.2(3) . . . . ?
C15 N5 C18 C20 122.2(3) . . . . ?
C3 N5 C18 C19 56.4(3) . . . . ?
C15 N5 C18 C19 -113.2(3) . . . . ?
C3 N5 C15 C16 -104.9(3) . . . . ?
C18 N5 C15 C16 64.2(3) . . . . ?
C3 N5 C15 C17 129.6(3) . . . . ?
C18 N5 C15 C17 -61.3(3) . . . . ?
C2 N4 C9 C11 49.8(3) . . . . ?
C12 N4 C9 C11 -128.3(3) . . . . ?
C2 N4 C9 C10 -75.4(3) . . . . ?
C12 N4 C9 C10 106.4(3) . . . . ?
C1 N3 C4 N1 -160.4(3) . . . . ?
C1 N3 C4 N2 24.2(5) . . . . ?
C7 N1 C4 N3 28.4(4) . . . . ?
C6 N1 C4 N3 174.4(3) . . . . ?
C7 N1 C4 N2 -155.4(3) . . . . ?
C6 N1 C4 N2 -9.4(3) . . . . ?
C8 N2 C4 N3 23.0(5) . . . . ?
C5 N2 C4 N3 168.5(3) . . . . ?
C8 N2 C4 N1 -152.8(3) . . . . ?
C5 N2 C4 N1 -7.3(3) . . . . ?

_diffrn_measured_fraction_theta_max    0.992
_diffrn_reflns_theta_full              27.48
_diffrn_measured_fraction_theta_full   0.992
_refine_diff_density_max    1.224
_refine_diff_density_min   -1.074
_refine_diff_density_rms    0.095

#===============================================================================
=========#
#      Luis Cunha-Silva @ REQUIMTE & DQB FCUP  *  19/11/2013  *
END        #
#===============================================================================
=========#
```

Appendix B. X-ray Crystallographic Data for 168•$(TFA)_3Cl^-$.

```
data_rm06493

#
================================================================================
===== #

_audit_creation_method            'SHELXL-97, manual editing plus
enCIFer'
_audit_creation_date              '17 December 2013'

#
================================================================================
===== #

_chemical_name_systematic
;
 ?
;
_chemical_name_common             ?
_chemical_melting_point           ?
_chemical_formula_moiety          'C20 H38 N5, 3(C2 H F3 O2), Cl'
_chemical_formula_sum             'C26 H41 Cl F9 N5 O6'
_chemical_formula_weight          726.09

loop_
 _atom_type_symbol
 _atom_type_description
 _atom_type_scat_dispersion_real
 _atom_type_scat_dispersion_imag
 _atom_type_scat_source
 'C'  'C'   0.0033   0.0016
 'International Tables Vol C Tables 4.2.6.8 and 6.1.1.4'
 'H'  'H'   0.0000   0.0000
 'International Tables Vol C Tables 4.2.6.8 and 6.1.1.4'
 'Cl'  'Cl'   0.1484   0.1585
 'International Tables Vol C Tables 4.2.6.8 and 6.1.1.4'
 'F'  'F'   0.0171   0.0103
 'International Tables Vol C Tables 4.2.6.8 and 6.1.1.4'
 'N'  'N'   0.0061   0.0033
 'International Tables Vol C Tables 4.2.6.8 and 6.1.1.4'
 'O'  'O'   0.0106   0.0060
 'International Tables Vol C Tables 4.2.6.8 and 6.1.1.4'

_symmetry_cell_setting            Monoclinic
_symmetry_space_group_name_H-M    'P 21/c'
_symmetry_space_group_name_Hall   '-P 2ybc'

loop_
 _symmetry_equiv_pos_as_xyz
 'x, y, z'
```

```
 '-x, y+1/2, -z+1/2'
 '-x, -y, -z'
 'x, -y-1/2, z-1/2'

_cell_length_a                    16.646(4)
_cell_length_b                    22.121(5)
_cell_length_c                    9.329(2)
_cell_angle_alpha                 90.00
_cell_angle_beta                  90.328(7)
_cell_angle_gamma                 90.00
_cell_volume                      3435.1(14)
_cell_formula_units_Z             4
_cell_measurement_temperature     150(2)
_cell_measurement_reflns_used     1234
_cell_measurement_theta_min       3.24
_cell_measurement_theta_max       24.38

_exptl_crystal_description        plate
_exptl_crystal_colour             colourless
_exptl_crystal_size_max           0.16
_exptl_crystal_size_mid           0.08
_exptl_crystal_size_min           0.04
_exptl_crystal_density_meas       ?
_exptl_crystal_density_diffrn     1.404
_exptl_crystal_density_method     'not measured'
_exptl_crystal_F_000              1512
_exptl_absorpt_coefficient_mu     0.205
_exptl_absorpt_correction_type    multi-scan
_exptl_absorpt_correction_T_min   0.9680
_exptl_absorpt_correction_T_max   0.9919
_exptl_absorpt_process_details
;
 SADABS (Sheldrick, 1997)
;

_exptl_special_details
;
 ?
;

_diffrn_ambient_temperature       150(2)
_diffrn_radiation_wavelength      0.71073
_diffrn_radiation_type            MoK\a
_diffrn_radiation_source          'fine-focus sealed tube'
_diffrn_radiation_monochromator   graphite
_diffrn_measurement_device_type   'Bruker X8 Kappa CCD APEX II'
_diffrn_measurement_method        'omega/phi scans'
_diffrn_detector_area_resol_mean  ?
_diffrn_standards_number          ?
_diffrn_standards_interval_count  ?
_diffrn_standards_interval_time   ?
_diffrn_standards_decay_%         ?
```

```
_diffrn_reflns_number             16450
_diffrn_reflns_av_R_equivalents   0.0860
_diffrn_reflns_av_sigmaI/netI     0.1276
_diffrn_reflns_limit_h_min        -19
_diffrn_reflns_limit_h_max        19
_diffrn_reflns_limit_k_min        -20
_diffrn_reflns_limit_k_max        26
_diffrn_reflns_limit_l_min        -11
_diffrn_reflns_limit_l_max        10
_diffrn_reflns_theta_min          3.68
_diffrn_reflns_theta_max          25.03
_reflns_number_total              5386
_reflns_number_gt                 3445
_reflns_threshold_expression      >2sigma(I)

_computing_data_collection        'APEX2 (Bruker, 2006)'
_computing_cell_refinement        'APEX2 '
_computing_data_reduction         'SAINT+ (Bruker, 1997-2005)'
_computing_structure_solution     'SHELXTL (Bruker 2001)'
_computing_structure_refinement   'SHELXTL '
_computing_molecular_graphics     'SHELXTL '
_computing_publication_material   'SHELXTL '

_refine_special_details
;
 Refinement of F^2^ against ALL reflections.  The weighted R-factor
wR and
 goodness of fit S are based on F^2^, conventional R-factors R are
based
 on F, with F set to zero for negative F^2^. The threshold
expression of
 F^2^ > 2sigma(F^2^) is used only for calculating R-factors(gt) etc.
and is
 not relevant to the choice of reflections for refinement.  R-
factors based
 on F^2^ are statistically about twice as large as those based on F,
and R-
 factors based on ALL data will be even larger.
;

_refine_ls_structure_factor_coef  Fsqd
_refine_ls_matrix_type            full
_refine_ls_weighting_scheme       calc
_refine_ls_weighting_details
 'calc w=1/[\s^2^(Fo^2^)+(0.2000P)^2^+0.0000P] where
P=(Fo^2^+2Fc^2^)/3'
_atom_sites_solution_primary      direct
_atom_sites_solution_secondary    difmap
_atom_sites_solution_hydrogens    geom
_refine_ls_hydrogen_treatment     mixed
_refine_ls_extinction_method      none
_refine_ls_extinction_coef        ?
```

```
_refine_ls_number_reflns          5386
_refine_ls_number_parameters      437
_refine_ls_number_restraints      24
_refine_ls_R_factor_all           0.3472
_refine_ls_R_factor_gt            0.2940
_refine_ls_wR_factor_ref          0.6581
_refine_ls_wR_factor_gt           0.6423
_refine_ls_goodness_of_fit_ref    2.637
_refine_ls_restrained_S_all       2.635
_refine_ls_shift/su_max           0.001
_refine_ls_shift/su_mean          0.000

loop_
 _atom_site_label
 _atom_site_type_symbol
 _atom_site_fract_x
 _atom_site_fract_y
 _atom_site_fract_z
 _atom_site_U_iso_or_equiv
 _atom_site_adp_type
 _atom_site_occupancy
 _atom_site_symmetry_multiplicity
 _atom_site_calc_flag
 _atom_site_refinement_flags
 _atom_site_disorder_assembly
 _atom_site_disorder_group
N1 N 0.6561(10) 0.1829(8) 0.9608(18) 0.051(4) Uani 1 1 d . . .
N3 N 0.5465(10) 0.1129(8) 1.0143(18) 0.051(5) Uani 1 1 d . . .
N2 N 0.5220(12) 0.2033(8) 0.913(2) 0.065(6) Uani 1 1 d . . .
N4 N 0.7510(9) 0.0581(6) 0.7547(17) 0.037(4) Uani 1 1 d . . .
N5 N 0.8614(11) 0.1459(8) 1.0327(18) 0.054(5) Uani 1 1 d U . .
C22 C 1.014(2) 0.1701(11) 0.974(3) 0.101(12) Uani 1 1 d . . .
H22A H 1.0230 0.1934 1.0621 0.152 Uiso 1 1 calc R . .
H22B H 0.9957 0.1973 0.8976 0.152 Uiso 1 1 calc R . .
H22C H 1.0640 0.1504 0.9455 0.152 Uiso 1 1 calc R . .
C18 C 0.876(2) 0.0475(12) 0.594(4) 0.114(12) Uani 1 1 d . . .
H18A H 0.9133 0.0170 0.5585 0.171 Uiso 1 1 calc R . .
H18B H 0.9058 0.0837 0.6234 0.171 Uiso 1 1 calc R . .
H18C H 0.8373 0.0581 0.5187 0.171 Uiso 1 1 calc R . .
C10 C 0.5817(14) 0.0714(11) 1.112(3) 0.070(7) Uani 1 1 d . . .
H10A H 0.6395 0.0792 1.1198 0.104 Uiso 1 1 calc R . .
H10B H 0.5729 0.0300 1.0781 0.104 Uiso 1 1 calc R . .
H10C H 0.5570 0.0763 1.2067 0.104 Uiso 1 1 calc R . .
C7 C 0.5771(19) 0.1650(14) 0.978(3) 0.098(11) Uani 1 1 d . . .
C9 C 0.460(3) 0.1237(11) 1.017(3) 0.115(15) Uani 1 1 d . . .
H9A H 0.4424 0.1305 1.1170 0.138 Uiso 1 1 calc R . .
H9B H 0.4312 0.0874 0.9803 0.138 Uiso 1 1 calc R . .
C8 C 0.4369(15) 0.1766(11) 0.929(3) 0.068(7) Uani 1 1 d . . .
H8A H 0.4001 0.2043 0.9795 0.082 Uiso 1 1 calc R . .
H8B H 0.4132 0.1648 0.8352 0.082 Uiso 1 1 calc R . .
C13 C 0.7528(11) 0.0980(7) 0.8606(18) 0.032(4) Uani 1 1 d . . .
C12 C 0.7116(14) 0.1424(8) 0.948(2) 0.049(6) Uani 1 1 d . . .
```

```
C20 C 0.7967(11) 0.1311(9) 0.9668(18) 0.042(5) Uani 1 1 d . . .
C14 C 0.6769(15) 0.0590(10) 0.639(3) 0.064(7) Uani 1 1 d . . .
H14 H 0.6937 0.0322 0.5583 0.077 Uiso 1 1 calc R . .
C17 C 0.8306(12) 0.0221(8) 0.7242(19) 0.041(5) Uani 1 1 d . . .
H17 H 0.8662 0.0229 0.8109 0.049 Uiso 1 1 calc R . .
C19 C 0.8026(16) -0.0449(9) 0.693(3) 0.070(7) Uani 1 1 d . . .
H19A H 0.7826 -0.0477 0.5938 0.105 Uiso 1 1 calc R . .
H19B H 0.7597 -0.0561 0.7590 0.105 Uiso 1 1 calc R . .
H19C H 0.8482 -0.0725 0.7054 0.105 Uiso 1 1 calc R . .
C15 C 0.6134(18) 0.0212(17) 0.729(3) 0.121(13) Uani 1 1 d . . .
H15A H 0.6049 0.0409 0.8220 0.181 Uiso 1 1 calc R . .
H15B H 0.6338 -0.0198 0.7445 0.181 Uiso 1 1 calc R . .
H15C H 0.5623 0.0194 0.6765 0.181 Uiso 1 1 calc R . .
C21 C 0.9428(14) 0.1170(10) 1.004(2) 0.058(6) Uani 1 1 d U . .
H21 H 0.9365 0.0949 0.9110 0.069 Uiso 1 1 calc R . .
C11 C 0.5328(17) 0.2535(11) 0.826(4) 0.104(12) Uani 1 1 d . . .
H11A H 0.5306 0.2902 0.8847 0.156 Uiso 1 1 calc R . .
H11B H 0.4902 0.2548 0.7532 0.156 Uiso 1 1 calc R . .
H11C H 0.5852 0.2509 0.7791 0.156 Uiso 1 1 calc R . .
C23 C 0.967(2) 0.0756(11) 1.099(2) 0.088(10) Uani 1 1 d . . .
H23A H 0.9246 0.0699 1.1710 0.133 Uiso 1 1 calc R . .
H23B H 1.0161 0.0892 1.1463 0.133 Uiso 1 1 calc R . .
H23C H 0.9765 0.0372 1.0499 0.133 Uiso 1 1 calc R . .
C24 C 0.8542(17) 0.1826(13) 1.172(4) 0.100(11) Uani 1 1 d . . .
H24 H 0.9081 0.1834 1.2199 0.120 Uiso 1 1 calc R . .
C25 C 0.8338(12) 0.2465(8) 1.123(2) 0.046(5) Uani 1 1 d . . .
H25A H 0.7862 0.2455 1.0613 0.069 Uiso 1 1 calc R . .
H25B H 0.8792 0.2634 1.0703 0.069 Uiso 1 1 calc R . .
H25C H 0.8230 0.2718 1.2074 0.069 Uiso 1 1 calc R . .
C26 C 0.795(2) 0.1573(19) 1.274(3) 0.123(13) Uani 1 1 d . . .
H26A H 0.7925 0.1833 1.3586 0.184 Uiso 1 1 calc R . .
H26B H 0.8124 0.1166 1.3027 0.184 Uiso 1 1 calc R . .
H26C H 0.7425 0.1551 1.2277 0.184 Uiso 1 1 calc R . .
C16 C 0.6671(12) 0.1153(9) 0.581(2) 0.045(5) Uani 1 1 d U . .
H16A H 0.6160 0.1170 0.5286 0.068 Uiso 1 1 calc R . .
H16B H 0.7114 0.1238 0.5153 0.068 Uiso 1 1 calc R . .
H16C H 0.6669 0.1456 0.6579 0.068 Uiso 1 1 calc R . .
F1 F 0.0672(16) 0.1048(9) 0.522(3) 0.177(11) Uani 1 1 d . . .
F2 F -0.0172(11) 0.1598(10) 0.4336(17) 0.120(7) Uani 1 1 d . . .
F3 F 0.0220(12) 0.1792(11) 0.6376(16) 0.129(8) Uani 1 1 d . . .
O1 O 0.1587(12) 0.2240(7) 0.539(2) 0.101(8) Uani 1 1 d . . .
H1 H 0.1600 0.2598 0.5095 0.121 Uiso 1 1 calc R . .
O2 O 0.1275(13) 0.1865(6) 0.317(2) 0.097(7) Uani 1 1 d . . .
C2 C 0.1210(17) 0.1933(10) 0.456(2) 0.064(7) Uani 1 1 d . . .
C1 C 0.0468(17) 0.1602(11) 0.527(3) 0.067(7) Uani 1 1 d . . .
F4 F 0.4431(10) 0.1035(7) 0.4020(15) 0.092(5) Uani 1 1 d . . .
F5 F 0.4701(11) 0.1369(9) 0.595(2) 0.136(8) Uani 1 1 d . . .
F6 F 0.3769(13) 0.0825(9) 0.551(3) 0.151(9) Uani 1 1 d . . .
O3 O 0.3434(10) 0.2136(7) 0.5860(18) 0.067(4) Uani 1 1 d . . .
O4 O 0.3323(10) 0.1866(7) 0.3648(18) 0.060(4) Uani 1 1 d . . .
H4 H 0.3693 0.2012 0.3146 0.072 Uiso 1 1 calc R . .
C4 C 0.3535(13) 0.1829(9) 0.480(3) 0.045(5) Uani 1 1 d . . .
```

```
C3 C 0.4113(13) 0.1232(10) 0.525(2) 0.044(5) Uani 1 1 d . . .
F7 F 0.1629(12) 0.0480(6) 0.948(2) 0.120(7) Uani 1 1 d . . .
F8 F 0.2853(14) 0.0393(7) 0.942(2) 0.140(9) Uani 1 1 d . . .
F9 F 0.2295(15) 0.0606(6) 0.7504(17) 0.127(9) Uani 1 1 d . . .
O5 O 0.2527(10) 0.1482(6) 1.0507(13) 0.057(4) Uani 1 1 d . . .
H5 H 0.2088 0.1473 1.0946 0.068 Uiso 1 1 calc R . .
O6 O 0.2363(11) 0.1754(6) 0.8212(16) 0.070(5) Uani 1 1 d . . .
C6 C 0.2403(14) 0.1416(9) 0.922(2) 0.049(5) Uani 1 1 d U . .
C5 C 0.2341(13) 0.0746(9) 0.878(2) 0.049(5) Uani 1 1 d . . .
Cl1 Cl 0.2387(3) 0.23344(16) 0.2049(4) 0.0270(12) Uani 1 1 d . . .

loop_
 _atom_site_aniso_label
 _atom_site_aniso_U_11
 _atom_site_aniso_U_22
 _atom_site_aniso_U_33
 _atom_site_aniso_U_23
 _atom_site_aniso_U_13
 _atom_site_aniso_U_12
N1 0.016(10) 0.075(12) 0.063(11) -0.012(9) 0.000(8) 0.002(9)
N3 0.014(10) 0.073(12) 0.067(11) 0.009(9) -0.004(9) 0.017(8)
N2 0.047(14) 0.061(12) 0.088(13) -0.016(10) -0.031(11) 0.003(10)
N4 0.019(9) 0.025(7) 0.067(10) -0.007(7) -0.024(8) 0.012(6)
N5 0.042(9) 0.058(8) 0.061(8) -0.005(6) -0.007(7) 0.004(7)
C22 0.17(3) 0.071(17) 0.063(16) -0.002(12) -0.074(19) 0.049(18)
C18 0.08(3) 0.070(18) 0.20(3) -0.04(2) 0.01(2) -0.040(16)
C10 0.036(15) 0.105(18) 0.067(14) 0.027(13) -0.025(13) 0.010(12)
C7 0.07(2) 0.11(2) 0.11(2) 0.069(19) -0.020(18) -0.037(18)
C9 0.21(5) 0.043(15) 0.09(2) 0.003(14) 0.09(2) 0.006(19)
C8 0.048(18) 0.082(17) 0.075(15) -0.023(13) 0.032(12) 0.024(13)
C13 0.020(11) 0.035(10) 0.042(10) 0.006(8) 0.004(8) 0.006(8)
C12 0.057(16) 0.033(11) 0.058(12) -0.017(9) -0.015(11) -0.014(10)
C20 0.014(11) 0.082(14) 0.029(10) -0.017(9) -0.008(9) -0.002(9)
C14 0.040(16) 0.074(16) 0.078(15) -0.005(12) 0.019(12) -0.034(12)
C17 0.041(13) 0.036(10) 0.045(10) 0.019(8) 0.008(9) 0.030(9)
C19 0.046(17) 0.051(13) 0.115(19) -0.024(12) 0.039(14) 0.007(11)
C15 0.07(2) 0.18(3) 0.12(2) -0.04(2) -0.029(19) -0.09(2)
C21 0.045(9) 0.065(9) 0.063(9) -0.010(8) -0.003(8) -0.008(8)
C11 0.06(2) 0.057(15) 0.19(3) 0.081(18) 0.05(2) 0.037(14)
C23 0.14(3) 0.067(16) 0.054(14) -0.009(12) -0.047(17) -0.013(16)
C24 0.04(2) 0.10(2) 0.15(3) -0.07(2) -0.02(2) -0.002(15)
C25 0.040(14) 0.050(12) 0.047(11) -0.004(9) -0.026(10) -0.005(9)
C26 0.06(3) 0.23(4) 0.08(2) -0.06(2) 0.033(17) -0.02(2)
C16 0.027(8) 0.048(8) 0.060(8) 0.011(7) -0.008(7) 0.010(7)
F1 0.16(3) 0.077(13) 0.29(3) 0.025(15) 0.10(2) 0.050(14)
F2 0.062(13) 0.22(2) 0.076(10) 0.062(11) 0.017(9) -0.016(12)
F3 0.098(16) 0.25(2) 0.038(8) 0.010(10) 0.021(8) 0.004(14)
O1 0.074(14) 0.064(11) 0.163(18) -0.049(12) -0.063(14) 0.006(10)
O2 0.121(19) 0.040(9) 0.132(16) 0.001(9) 0.070(13) -0.030(9)
C2 0.10(2) 0.056(14) 0.038(12) -0.015(10) 0.013(12) -0.038(13)
C1 0.06(2) 0.070(17) 0.068(17) 0.006(12) -0.022(16) -0.021(13)
F4 0.084(13) 0.110(12) 0.083(10) -0.003(8) 0.013(9) 0.046(10)
```

```
F5 0.068(13) 0.159(17) 0.178(19) -0.037(14) -0.076(14) 0.002(11)
F6 0.077(16) 0.086(12) 0.29(3) 0.058(15) 0.042(17) 0.047(11)
O3 0.045(11) 0.063(9) 0.093(12) -0.010(9) -0.005(9) 0.011(8)
O4 0.051(12) 0.068(11) 0.060(10) -0.010(8) -0.013(8) 0.006(8)
C4 0.038(15) 0.048(12) 0.049(13) -0.006(10) -0.007(11) 0.014(10)
C3 0.022(13) 0.046(12) 0.063(13) 0.001(10) 0.002(11) -0.016(10)
F7 0.110(16) 0.056(9) 0.195(18) -0.018(10) -0.002(14) -0.052(9)
F8 0.17(2) 0.075(10) 0.176(18) -0.022(11) -0.042(16) 0.085(12)
F9 0.25(3) 0.056(9) 0.070(10) -0.029(7) 0.033(12) -0.045(11)
O5 0.091(14) 0.037(7) 0.043(8) -0.023(6) 0.019(8) -0.010(8)
O6 0.100(15) 0.058(9) 0.053(9) 0.001(7) 0.006(9) -0.011(8)
C6 0.051(10) 0.055(9) 0.041(8) 0.007(7) 0.008(7) -0.003(7)
C5 0.039(15) 0.059(14) 0.048(12) 0.004(10) 0.000(10) -0.007(11)
Cl1 0.038(3) 0.021(2) 0.0216(19) 0.0040(15) 0.0044(16) 0.0005(18)

_geom_special_details
;
 All esds (except the esd in the dihedral angle between two l.s.
planes)
 are estimated using the full covariance matrix.  The cell esds are
taken
 into account individually in the estimation of esds in distances,
angles
 and torsion angles; correlations between esds in cell parameters
are only
 used when they are defined by crystal symmetry.  An approximate
(isotropic)
 treatment of cell esds is used for estimating esds involving l.s.
planes.
;

loop_
 _geom_bond_atom_site_label_1
 _geom_bond_atom_site_label_2
 _geom_bond_distance
 _geom_bond_site_symmetry_2
 _geom_bond_publ_flag
N1 C12 1.29(3) . ?
N1 C7 1.38(3) . ?
N3 C7 1.30(3) . ?
N3 C10 1.42(2) . ?
N3 C9 1.47(4) . ?
N2 C7 1.39(3) . ?
N2 C11 1.39(3) . ?
N2 C8 1.54(3) . ?
N4 C13 1.33(2) . ?
N4 C17 1.57(2) . ?
N4 C14 1.64(3) . ?
N5 C20 1.28(2) . ?
N5 C21 1.52(3) . ?
N5 C24 1.54(3) . ?
C22 C21 1.69(4) . ?
```

```
C22 H22A 0.9800 . ?
C22 H22B 0.9800 . ?
C22 H22C 0.9800 . ?
C18 C17 1.54(4) . ?
C18 H18A 0.9800 . ?
C18 H18B 0.9800 . ?
C18 H18C 0.9800 . ?
C10 H10A 0.9800 . ?
C10 H10B 0.9800 . ?
C10 H10C 0.9800 . ?
C9 C8 1.48(4) . ?
C9 H9A 0.9900 . ?
C9 H9B 0.9900 . ?
C8 H8A 0.9900 . ?
C8 H8B 0.9900 . ?
C13 C20 1.43(2) . ?
C13 C12 1.45(3) . ?
C12 C20 1.45(3) . ?
C14 C16 1.37(3) . ?
C14 C15 1.59(4) . ?
C14 H14 1.0000 . ?
C17 C19 1.58(3) . ?
C17 H17 1.0000 . ?
C19 H19A 0.9800 . ?
C19 H19B 0.9800 . ?
C19 H19C 0.9800 . ?
C15 H15A 0.9800 . ?
C15 H15B 0.9800 . ?
C15 H15C 0.9800 . ?
C21 C23 1.34(3) . ?
C21 H21 1.0000 . ?
C11 H11A 0.9800 . ?
C11 H11B 0.9800 . ?
C11 H11C 0.9800 . ?
C23 H23A 0.9800 . ?
C23 H23B 0.9800 . ?
C23 H23C 0.9800 . ?
C24 C26 1.48(4) . ?
C24 C25 1.52(4) . ?
C24 H24 1.0000 . ?
C25 H25A 0.9800 . ?
C25 H25B 0.9800 . ?
C25 H25C 0.9800 . ?
C26 H26A 0.9800 . ?
C26 H26B 0.9800 . ?
C26 H26C 0.9800 . ?
C16 H16A 0.9800 . ?
C16 H16B 0.9800 . ?
C16 H16C 0.9800 . ?
F1 C1 1.27(3) . ?
F2 C1 1.37(3) . ?
F3 C1 1.19(3) . ?
```

```
O1 C2 1.20(2) . ?
O1 H1 0.8400 . ?
O2 C2 1.31(3) . ?
C2 C1 1.59(4) . ?
F4 C3 1.34(3) . ?
F5 C3 1.21(2) . ?
F6 C3 1.10(2) . ?
O3 C4 1.21(2) . ?
O4 C4 1.13(2) . ?
O4 H4 0.8400 . ?
C4 C3 1.69(3) . ?
F7 C5 1.48(3) . ?
F8 C5 1.30(3) . ?
F9 C5 1.23(2) . ?
O5 C6 1.23(2) . ?
O5 H5 0.8400 . ?
O6 C6 1.20(2) . ?
C6 C5 1.54(3) . ?

loop_
 _geom_angle_atom_site_label_1
 _geom_angle_atom_site_label_2
 _geom_angle_atom_site_label_3
 _geom_angle
 _geom_angle_site_symmetry_1
 _geom_angle_site_symmetry_3
 _geom_angle_publ_flag
C12 N1 C7 120(2) . . ?
C7 N3 C10 125(2) . . ?
C7 N3 C9 104(2) . . ?
C10 N3 C9 120(2) . . ?
C7 N2 C11 131(2) . . ?
C7 N2 C8 109(2) . . ?
C11 N2 C8 118.9(19) . . ?
C13 N4 C17 117.2(13) . . ?
C13 N4 C14 119.8(15) . . ?
C17 N4 C14 121.3(15) . . ?
C20 N5 C21 123.7(17) . . ?
C20 N5 C24 118(2) . . ?
C21 N5 C24 116.4(17) . . ?
C21 C22 H22A 109.5 . . ?
C21 C22 H22B 109.5 . . ?
H22A C22 H22B 109.5 . . ?
C21 C22 H22C 109.5 . . ?
H22A C22 H22C 109.5 . . ?
H22B C22 H22C 109.5 . . ?
C17 C18 H18A 109.5 . . ?
C17 C18 H18B 109.5 . . ?
H18A C18 H18B 109.5 . . ?
C17 C18 H18C 109.5 . . ?
H18A C18 H18C 109.5 . . ?
H18B C18 H18C 109.5 . . ?
```

```
N3 C10 H10A 109.5 . . ?
N3 C10 H10B 109.5 . . ?
H10A C10 H10B 109.5 . . ?
N3 C10 H10C 109.5 . . ?
H10A C10 H10C 109.5 . . ?
H10B C10 H10C 109.5 . . ?
N3 C7 N1 131(3) . . ?
N3 C7 N2 113(2) . . ?
N1 C7 N2 114(2) . . ?
N3 C9 C8 112(2) . . ?
N3 C9 H9A 109.3 . . ?
C8 C9 H9A 109.3 . . ?
N3 C9 H9B 109.3 . . ?
C8 C9 H9B 109.3 . . ?
H9A C9 H9B 108.0 . . ?
C9 C8 N2 97(2) . . ?
C9 C8 H8A 112.3 . . ?
N2 C8 H8A 112.3 . . ?
C9 C8 H8B 112.3 . . ?
N2 C8 H8B 112.3 . . ?
H8A C8 H8B 109.9 . . ?
N4 C13 C20 150.1(17) . . ?
N4 C13 C12 149.5(17) . . ?
C20 C13 C12 60.3(13) . . ?
N1 C12 C20 144.0(17) . . ?
N1 C12 C13 149.1(18) . . ?
C20 C12 C13 59.0(14) . . ?
N5 C20 C13 152.8(19) . . ?
N5 C20 C12 146.4(18) . . ?
C13 C20 C12 60.7(12) . . ?
C16 C14 C15 128(2) . . ?
C16 C14 N4 111.1(16) . . ?
C15 C14 N4 98.4(17) . . ?
C16 C14 H14 106.0 . . ?
C15 C14 H14 106.0 . . ?
N4 C14 H14 106.0 . . ?
C18 C17 N4 112.0(17) . . ?
C18 C17 C19 110.0(18) . . ?
N4 C17 C19 105.1(16) . . ?
C18 C17 H17 109.9 . . ?
N4 C17 H17 109.9 . . ?
C19 C17 H17 109.9 . . ?
C17 C19 H19A 109.5 . . ?
C17 C19 H19B 109.5 . . ?
H19A C19 H19B 109.5 . . ?
C17 C19 H19C 109.5 . . ?
H19A C19 H19C 109.5 . . ?
H19B C19 H19C 109.5 . . ?
C14 C15 H15A 109.5 . . ?
C14 C15 H15B 109.5 . . ?
H15A C15 H15B 109.5 . . ?
C14 C15 H15C 109.5 . . ?
```

```
H15A C15 H15C 109.5 . . ?
H15B C15 H15C 109.5 . . ?
C23 C21 N5 115(2) . . ?
C23 C21 C22 112(2) . . ?
N5 C21 C22 111.2(18) . . ?
C23 C21 H21 105.6 . . ?
N5 C21 H21 105.6 . . ?
C22 C21 H21 105.6 . . ?
N2 C11 H11A 109.5 . . ?
N2 C11 H11B 109.5 . . ?
H11A C11 H11B 109.5 . . ?
N2 C11 H11C 109.5 . . ?
H11A C11 H11C 109.5 . . ?
H11B C11 H11C 109.5 . . ?
C21 C23 H23A 109.5 . . ?
C21 C23 H23B 109.5 . . ?
H23A C23 H23B 109.5 . . ?
C21 C23 H23C 109.5 . . ?
H23A C23 H23C 109.5 . . ?
H23B C23 H23C 109.5 . . ?
C26 C24 C25 113(3) . . ?
C26 C24 N5 113(2) . . ?
C25 C24 N5 105(2) . . ?
C26 C24 H24 108.3 . . ?
C25 C24 H24 108.3 . . ?
N5 C24 H24 108.3 . . ?
C24 C25 H25A 109.5 . . ?
C24 C25 H25B 109.5 . . ?
H25A C25 H25B 109.5 . . ?
C24 C25 H25C 109.5 . . ?
H25A C25 H25C 109.5 . . ?
H25B C25 H25C 109.5 . . ?
C24 C26 H26A 109.5 . . ?
C24 C26 H26B 109.5 . . ?
H26A C26 H26B 109.5 . . ?
C24 C26 H26C 109.5 . . ?
H26A C26 H26C 109.5 . . ?
H26B C26 H26C 109.5 . . ?
C14 C16 H16A 109.5 . . ?
C14 C16 H16B 109.5 . . ?
H16A C16 H16B 109.5 . . ?
C14 C16 H16C 109.5 . . ?
H16A C16 H16C 109.5 . . ?
H16B C16 H16C 109.5 . . ?
C2 O1 H1 109.5 . . ?
O1 C2 O2 131(2) . . ?
O1 C2 C1 113(2) . . ?
O2 C2 C1 115.4(19) . . ?
F3 C1 F1 118(3) . . ?
F3 C1 F2 106(3) . . ?
F1 C1 F2 100(2) . . ?
F3 C1 C2 118(2) . . ?
```

```
F1 C1 C2 103(2) . . ?
F2 C1 C2 110(2) . . ?
C4 O4 H4 109.5 . . ?
O4 C4 O3 134(2) . . ?
O4 C4 C3 117.7(19) . . ?
O3 C4 C3 108.7(18) . . ?
F6 C3 F5 120(3) . . ?
F6 C3 F4 98(2) . . ?
F5 C3 F4 103(2) . . ?
F6 C3 C4 114(2) . . ?
F5 C3 C4 113.2(19) . . ?
F4 C3 C4 105.8(17) . . ?
C6 O5 H5 109.5 . . ?
O6 C6 O5 134(2) . . ?
O6 C6 C5 112.8(18) . . ?
O5 C6 C5 112.7(17) . . ?
F9 C5 F8 109(2) . . ?
F9 C5 F7 106.3(18) . . ?
F8 C5 F7 94.8(18) . . ?
F9 C5 C6 120.1(17) . . ?
F8 C5 C6 114.6(18) . . ?
F7 C5 C6 108.7(17) . . ?

loop_
 _geom_torsion_atom_site_label_1
 _geom_torsion_atom_site_label_2
 _geom_torsion_atom_site_label_3
 _geom_torsion_atom_site_label_4
 _geom_torsion
 _geom_torsion_site_symmetry_1
 _geom_torsion_site_symmetry_2
 _geom_torsion_site_symmetry_3
 _geom_torsion_site_symmetry_4
 _geom_torsion_publ_flag
C10 N3 C7 N1 35(5) . . . . ?
C9 N3 C7 N1 179(3) . . . . ?
C10 N3 C7 N2 -163(2) . . . . ?
C9 N3 C7 N2 -19(3) . . . . ?
C12 N1 C7 N3 16(4) . . . . ?
C12 N1 C7 N2 -146(2) . . . . ?
C11 N2 C7 N3 -160(3) . . . . ?
C8 N2 C7 N3 11(4) . . . . ?
C11 N2 C7 N1 5(5) . . . . ?
C8 N2 C7 N1 176(2) . . . . ?
C7 N3 C9 C8 22(3) . . . . ?
C10 N3 C9 C8 168(2) . . . . ?
N3 C9 C8 N2 -15(2) . . . . ?
C7 N2 C8 C9 3(3) . . . . ?
C11 N2 C8 C9 175(2) . . . . ?
C17 N4 C13 C20 7(4) . . . . ?
C14 N4 C13 C20 -158(3) . . . . ?
C17 N4 C13 C12 -178(3) . . . . ?
```

```
C14 N4 C13 C12 17(4) . . . . ?
C7 N1 C12 C20 -156(3) . . . . ?
C7 N1 C12 C13 77(5) . . . . ?
N4 C13 C12 N1 -30(6) . . . . ?
C20 C13 C12 N1 147(4) . . . . ?
N4 C13 C12 C20 -177(3) . . . . ?
C21 N5 C20 C13 -4(5) . . . . ?
C24 N5 C20 C13 -168(4) . . . . ?
C21 N5 C20 C12 -178(3) . . . . ?
C24 N5 C20 C12 17(5) . . . . ?
N4 C13 C20 N5 1(7) . . . . ?
C12 C13 C20 N5 -176(5) . . . . ?
N4 C13 C20 C12 177(3) . . . . ?
N1 C12 C20 N5 26(6) . . . . ?
C13 C12 C20 N5 177(4) . . . . ?
N1 C12 C20 C13 -151(4) . . . . ?
C13 N4 C14 C16 53(3) . . . . ?
C17 N4 C14 C16 -112(2) . . . . ?
C13 N4 C14 C15 -83(2) . . . . ?
C17 N4 C14 C15 112(2) . . . . ?
C13 N4 C17 C18 -101(2) . . . . ?
C14 N4 C17 C18 64(2) . . . . ?
C13 N4 C17 C19 139.2(18) . . . . ?
C14 N4 C17 C19 -55(2) . . . . ?
C20 N5 C21 C23 -102(2) . . . . ?
C24 N5 C21 C23 63(3) . . . . ?
C20 N5 C21 C22 129(2) . . . . ?
C24 N5 C21 C22 -67(2) . . . . ?
C20 N5 C24 C26 49(3) . . . . ?
C21 N5 C24 C26 -117(3) . . . . ?
C20 N5 C24 C25 -75(3) . . . . ?
C21 N5 C24 C25 119(2) . . . . ?
O1 C2 C1 F3 20(4) . . . . ?
O2 C2 C1 F3 -156(3) . . . . ?
O1 C2 C1 F1 -112(3) . . . . ?
O2 C2 C1 F1 73(3) . . . . ?
O1 C2 C1 F2 142(2) . . . . ?
O2 C2 C1 F2 -34(3) . . . . ?
O4 C4 C3 F6 -85(3) . . . . ?
O3 C4 C3 F6 95(3) . . . . ?
O4 C4 C3 F5 133(2) . . . . ?
O3 C4 C3 F5 -47(3) . . . . ?
O4 C4 C3 F4 21(3) . . . . ?
O3 C4 C3 F4 -159.0(19) . . . . ?
O6 C6 C5 F9 3(3) . . . . ?
O5 C6 C5 F9 -173(2) . . . . ?
O6 C6 C5 F8 136(2) . . . . ?
O5 C6 C5 F8 -40(3) . . . . ?
O6 C6 C5 F7 -119(2) . . . . ?
O5 C6 C5 F7 64(2) . . . . ?

_diffrn_measured_fraction_theta_max    0.888
```

```
_diffrn_reflns_theta_full              25.03
_diffrn_measured_fraction_theta_full   0.888
_refine_diff_density_max    0.946
_refine_diff_density_min   -0.921
_refine_diff_density_rms    0.241


#=============================================================================
=========#
#      END        #
#=============================================================================
=========#
```